Phosphorus-functionalised carbyne complexes

Annie Louise Colebatch

A thesis submitted for the degree of Doctor of Philosophy of
The Australian National University

October 2014

Australian National University

Author's declaration

This thesis is an account of the research undertaken between March 2011 and October 2014 at the Research School of Chemistry, The Australian National University. Except where due reference has been made, the work contained in this thesis is my own.

Annie Louise Colebatch

October 2014

Contents

Acknowledgements

The past three and a half years have been an incredible time. Although at times it has been challenging, it has overwhelmingly been so much better than I could have hoped for. I've been so lucky to meet such amazing people and have had so much fun while learning so much. I am so grateful to all the wonderful people who have shown me how enjoyable life can be.

Thank you Tony for giving me this opportunity and being so incredibly supportive throughout my whole time at RSC, you have taught me so much. You have constantly encouraged me and helped me to achieve so much more than I thought I could. You have shown so much confidence in me, and (almost) made me believe it. I couldn't have wished for a kinder, more generous or more brilliant supervisor. And thank you for letting me submit even though I still haven't made $[W_2\{\mu\text{-}(CPN^tBu)_2\}(CO)_4(Tp^*)_2]$!

Thank you to everyone who I have been lucky enough to work with in the Hill group. You have made coming to uni everyday such a pleasure and I have had more fun, more laughs and met more amazing people than I could have ever hoped. And on top of that thank you for the amazing times we've had on our OZOM and ICOMC travels. Thank you to Caitlin, Rong, Lily, Yong-Shen and Jas for being such wonderful friends. You have helped me get through the bad days and brightened the good days, and you've always made me laugh even when chemistry was trying to make me cry. Thank you Ian for helping me fumble through when I started and for setting my morning tea body clock – it's still going strong. Thank you Stephen for the chocopies, the unstuck taps, the sparkling clean lab, and my disco schlenk line. Thank you for the dates Horst. Thank you for your wise wisdom, incredible patience, never-ending biscuits and amazing dance moves Manab and Torsten. Thank you to Jane for being such a fun and super clean lab buddy. Thank you to Richie, Kathy, Kass, Siân, Rowan, Vincent, Tim and Arup for making everyday enjoyable. Thank you to Mark for the endless generosity and all the good times that that has entailed. And of course the Friday lab dancers for helping me make it through, week after week.

Thank you to Martin Bennett for being such a pillar of support throughout my Ph.D. For teaching me so much about chemistry, careers and life, for your guidance and encouragement, and your faith in me. It has meant a lot to me.

Thank you to the RSC community for creating such a wonderful place to work in. All of the friends that I have been lucky to make over my time here, especially to the Barrow group, all the incarnations of the morning tea crew, and everyone at Bramleys, especially Adam and Prue, you've all made life at RSC a lot more enjoyable. Thank you to Mark and Geoff for your confidence in me right from the beginning of my undergraduate years and supporting me throughout the past nine years. I really appreciate you giving me the opportunity to teach, and for helping me to become a better teacher. Tony Willis and Jas for you neverending patience despite my complete incompetence with crystallography. To all the analytical staff Chris, Peta, Viki, Sasha, Anitha and Elizabeth for running all of my samples, good and bad, and helping me solve countless problems.

Thank you to all of my family and friends who have loved and supported me throughout this journey. You have helped keep me balanced. Especially to my parents who created such a loving and encouraging environment, and in this way allowed me to even imagine I could make it to this point in my life. For teaching me to strive to achieve my goals, showing me how to be a good person, and for putting up with me while doing it.

Thank you to Andrew for everything. I could not have gotten through the past three and a half years without you. Thank you for teaching me to be a better person, for helping me find my way when I get lost, for making me smile everyday, and for your never-ending support and love.

Abstract

This thesis describes the study of tungsten complexes bearing phosphorus-functionalised carbyne ligands. The development of two generalised synthetic routes towards phosphinocarbyne complexes is presented. The further functionalisation and derivatisation of these phosphinocarbyne complexes highlights their synthetic versatility.

The bromocarbyne complex [W(≡CBr)(CO)$_2$(Tp*)] was found to undergo a lithium-halogen exchange reaction with butyllithium to generate the lithiated carbyne [W(≡CLi)(CO)$_2$(Tp*)], which reacts in situ with a range of chlorophosphines to provide phosphinocarbyne complexes [W(≡CPRR')(CO)$_2$(Tp*)] (R = Cl, R' = Cl, Cy, Ph, NEt$_2$, N^{i}Pr$_2$; R = Ph, R' = Cl, Ph). Alternatively, [W(≡CBr)(CO)$_2$(Tp*)] reacts with secondary and primary phosphines in the presence of base and a palladium catalyst, yielding phosphinocarbyne complexes [W(≡CPRR')(CO)$_2$(Tp*)] (R = H, R' = Cy, Ph; R = Ph, R' = H, Ph) bearing aryl, alkyl and hydro substituents. Both of these methods represent scalable, one-pot preparations compatible with a variety of phosphorus substituents.

The tertiary phosphinocarbyne complex [W(≡CPPh$_2$)(CO)$_2$(Tp*)] has been found to undergo reactions with a wide range of electrophiles. With most electrophiles (E = O, Se, BH$_3$, Me$^+$, [RhCl$_2$(Cp*)]) addition to the phosphine was observed, yielding [W(≡CPEPh$_2$)(CO)$_2$(Tp*)], and calculations suggest that this preference is steric in origin. The reaction with sulfur provided both the phosphine sulfide [W{≡CP(=S)Ph$_2$}(CO)$_2$(Tp*)] and the η^2-thioacyl complex [W{η^2-SCP(=S)Ph$_2$}(CO)$_2$(Tp*)]. Addition of sulfur to isolated [W{≡CP(=S)Ph$_2$}(CO)$_2$(Tp*)] does not proceed, demonstrating that oxidation of the phosphorus deactivates the tungsten-carbon triple bond towards electrophilic addition, as also observed for the complexes [W(≡CPEPh$_2$)(CO)$_2$(Tp*)] (E = BH$_3$, Me$^+$, AuCl), which similarly failed to react with sulfur. However, [AuCl(SMe$_2$)] was found to add to this site, affording [W{η^2-C(AuCl)P(=S)Ph$_2$}(CO)$_2$(Tp*)]. Addition of AuCl to [W(≡CPPh$_2$)(CO)$_2$(Tp*)] proceeds in a stepwise manner; first at the phosphine, generating [W(≡CPPh$_2$AuCl)(CO)$_2$(Tp*)], and then via coordination to the W≡C bond to provide [W{η^2-C(AuCl)PPh$_2$AuCl}(CO)$_2$(Tp*)]. In the case of HBF$_4$, kinetic protonation at the

phosphine was observed, yielding $[W(\equiv CPHPh_2)(CO)_2(Tp^*)]BF_4$, followed by a rapid rearrangement to the η^2-phosphinocarbene $[W\{\eta^2\text{-}C(H)PPh_2\}(CO)_2(Tp^*)]BF_4$, the thermodynamic product of protonation. Calculations suggest that this isomerisation proceeds via an intermolecular, solvent-mediated proton transfer.

Chlorophosphinocarbyne complexes $[W(\equiv CPClR)(CO)_2(Tp^*)]$ (R = Cl, Cy, Ph, NEt_2, N^iPr_2) bearing halo, alkyl, aryl and amino substituents are accessible via the lithium/halogen exchange protocol. Subsequent nucleophilic substitution of chloride in $[W(\equiv CPClPh)(CO)_2(Tp^*)]$ proceeds with a range of organometallic carbon-based and alkoxy nucleophiles LiMe, LiPh, LiC≡CPh and KOPh, providing access to the further functionalised phosphinocarbyne complexes $[W(\equiv CPPhR)(CO)_2(Tp^*)]$ (R = Me, Ph, C≡CPh, OPh). Reactivity also ensues at the P−Cl bond of the amino-substituted carbyne $[W\{\equiv CPCl(N^iPr_2)\}(CO)_2(Tp^*)]$, in which the chloride could be substituted by LiMe to afford $[W\{\equiv CPMe(N^iPr_2)\}(CO)_2(Tp^*)]$, or abstracted using $AlCl_3$ to afford the phosphenium carbyne salt $[W\{\equiv CP(N^iPr_2)\}(CO)_2(Tp^*)]AlCl_4$, or the phosphirenium derivative $[W\{\equiv CP(N^iPr_2)(CPhCPh)\}(CO)_2(Tp^*)]AlCl_4$ if performed in the presence of diphenylacetylene.

Reduction of chlorophosphinocarbyne complexes with borohydride reducing agents afforded the first examples of terminal secondary phosphinocarbyne complexes $[W(\equiv CPHR)(CO)_2(Tp^*)]$ (R = Cy, Ph). These complexes can also be prepared using a palladium-catalysed phosphination reaction of $[W(\equiv CBr)(CO)_2(Tp^*)]$ with PH_2R. Attempts to generate a secondary amino-substituted phosphinocarbyne via reduction of $[W\{\equiv CPCl(N^iPr_2)\}(CO)_2(Tp^*)]$ with $Li[BHEt_3]$ resulted in a mixture of the desired product $[W\{\equiv CPH(N^iPr_2)\}(CO)_2(Tp^*)]$ and the Et-transfer product $[W\{\equiv CPEt(N^iPr_2)\}(CO)_2(Tp^*)]$. Deprotonation with potassium hydride yielded the extremely sensitive phosphidocarbyne complexes $K[W(CPR)(CO)_2(Tp^*)]$, examples of hereto unknown terminal phosphaisocyanide complexes.

The synthetic strategies developed herein have been extended to the preparation of bi- and trimetallic phosphinocarbyne complexes $[W_2(\mu\text{-}C_2PR)(CO)_4(Tp^*)_2]$ (R = Cl, Cy, Ph) and $[W_3(\mu\text{-}C_3P)(CO)_6(Tp^*)_3]$. These bimetallic phosphinocarbynes undergo a thermal rearrangement to the highly unusual bridging carbyne-tungstaphosphirene species $[W_2\{\mu\text{:}\eta^1\text{-}C;\eta^2\text{-}C,P\text{-}CC(PR)\}(CO)_4(Tp^*)_2]$ (R = Cl, Ph). Electrophilic addition

of $[AuCl(SMe_2)]$ to $[W_2(\mu\text{-}C_2PPh)(CO)_4(Tp^*)_2]$ produced a mixture of mono-, bi- and tri-aurated complexes $[W_2(\mu\text{-}C_2PPhAuCl)(CO)_4(Tp^*)_2]$, $[W_2\{\mu\text{-}(CAuCl)_2PPh\}(CO)_4(Tp^*)_2]$ and $[W_2\{\mu\text{-}(CAuCl)_2PPhAuCl\}(CO)_4(Tp^*)_2]$, demonstrating that, in contrast to the monometallic analogue $[W(\equiv CPPh_2)(CO)_2(Tp^*)]$, the W≡C units of $[W_2(\mu\text{-}C_2PPh)(CO)_4(Tp^*)_2]$ compete more effectively with the phosphine as the preferred sites of electrophilic attack.

Abbreviations and nomenclature

$\{^1H\}$	proton decoupled NMR experiment
Ac	acetyl
Ar	aryl
br	broad
COD	1,5-cyclooctadiene
COE	cyclooctene
Cp	η^5-cyclopentadienyl
Cp*	η^5-pentamethylcyclopentadienyl
Cy	cyclohexyl
DABCO	1,8-diazabicyclo[2.2.2]octane
dba	dibenzylideneacetone
depe	diethylphosphinoethane
DFT	density functional theory
Dipp	2,6-diisopropylphenyl
dme	1,2-dimethoxyethane
dmpe	dimethylphosphinoethane
dppe	diphenylphosphinoethane
EAN	effective atomic number
ECP	electron core potential
ESI	electrospray ionisation
HOMO	highest occupied molecular orbital
IR	infrared
LUMO	lowest unoccupied molecular orbital
$LW_{1/2}$	linewidth at half height
m	medium
Mes	mesityl (2,4,6-trimethylphenyl)
Mes*	supermesityl (2,4,6-tri-*tert*-butylphenyl)
MS	mass spectrometry
m/z	mass/charge
NHC	N-heterocyclic carbene
$^nJ_{AB}$	n-bond coupling constant between nuclei A and B

NMR	nuclear magnetic resonance
OTf	trifluoromethanesulfonate
py	pyridine
pz	pyrazolyl
R	generalised organic group
rac	racemic
s	strong
sh	shoulder
THF	tetrahydrofuran
THT	tetrahydrothiophene
tmeda	*N,N,N′,N′*-tetramethylethylenediamine
Tol	*p*-tolyl
Tp	hydrotris(pyrazol-1-yl)borate
Tp*	hydrotris(3,5-dimethylpyrazol-1-yl)borate
UV/Vis	ultraviolet-visible
vs	very strong
vw	very weak
w	weak
X	halogen
σ^x, λ^y	coordination number x, valence y

CHAPTER 1.

Introduction

CHAPTER 1: Introduction

The chemistry of transition metal carbyne complexes began in 1973 when Fischer reported the first examples of complexes containing a metal-carbon triple bond.[1*] This seminal work was an extension of his prior discovery of the first transition metal carbene complexes less than ten years earlier.[2] Before this time, isolated 'free' carbene and carbyne species were unknown, mentioned only as transient intermediates, but widely employed in organic synthesis.[3-7] Although later research has shown that the synthesis and reactivity of transition metal carbynes bear little resemblance to free carbynes, Fischer's work nevertheless demonstrated the pivotal role transition metals can play in stabilising reactive molecules, which has since been extended to many otherwise unisolable species such as cyclobutadiene and carbon monosulfide.

Fischer's carbene synthesis was initially achieved by nucleophilic attack of methyllithium on a carbonyl ligand of $[W(CO)_6]$. The initial acylate salt that forms can be protonated to generate an unstable hydroxycarbene, which is then esterified by treatment with CH_2N_2 to provide the carbene complex $[W\{=C(OMe)Me\}(CO)_5]$ (Scheme 1.1).[2] In the interim, this approach has been extended to alkyl, alkenyl and alkynyl nucleophiles in addition to a small range of heteroatom nucleophiles including amino, imino and silyl derivatives. However, thiolate, phosphido and arsenido nucleophiles result in carbonyl substitution. The synthetic versatility of the original alkoxycarbenes lies in the facile nucleophilic substitution of the alkoxide by carbon, nitrogen, phosphido, thiolato, selenolato and arsenido groups, greatly broadening the possible range of accessible carbenes. This protocol, with various refinements, has been extended to vanadium, all the elements of groups 6 and 7, iron, cobalt and nickel, and also proceeds in some cases for heterocarbonyl ligands (CS, CNR).

[*] The terms alkylidene/alkylidyne and carbene/carbyne are used interchangeably in the literature, though IUPAC recommends the former. The former reflects the covalency of the group bound to another element, whilst the latter recalls (questionable) parallels with the free species.

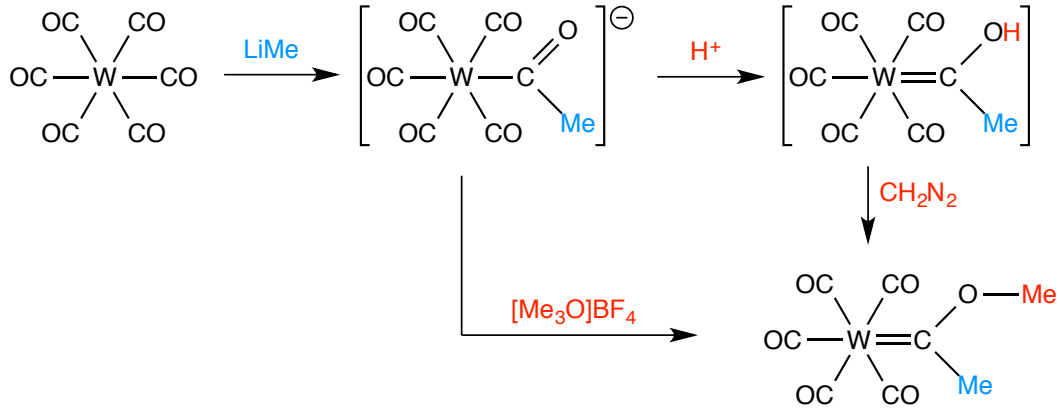

Scheme 1.1. Fischer's synthesis of the first carbene complex.

In an attempt to generate halocarbene complexes, treatment of these alkoxycarbene species with BX_3 instead resulted in abstraction of the alkoxide group to generate the carbyne complexes $[M(\equiv CR)(X)(CO)_4]$ (X = Cl, Br, I; M = Cr, Mo, W; R = Me, Ph) (Scheme 1.2).[1] This route was later modified by Mayr to provide facile, high-yielding syntheses of a range of group six complexes of the form $[M(\equiv CR)(X)(CO)_2(L)_2]$ (X = Cl, Br, O_2CCF_3; M = Cr, Mo, W; R = Me, Ph; L_2 = $(pyridine)_2$, tmeda, bipyridine, dppe, $(PMe_3)_2$, $(CO)(PPh_3)$) through the use of thionyl chloride, phosphine dihalides, phosgene, oxalyl halides or trifluoroacetic anhydride for the direct oxide abstraction from the preliminary acylate intermediate.[8,9] The stability of such derivatives relative to the thermolabile intermediate tetracarbonyl species lies in the mutually compatible facial disposition of three strong π-acceptors, each *trans* to good donor ligands. This approach has since been extended to provide rhenium and iron carbyne complexes.[†]

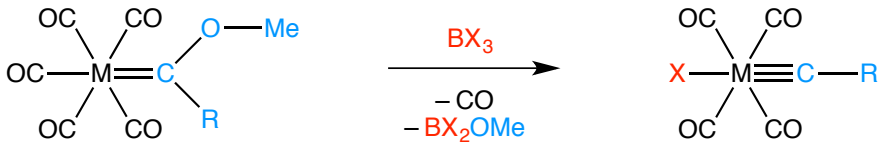

Scheme 1.2. Fischer's synthesis of the first transition metal carbyne complexes (M = Cr, Mo, W; R = Me, Ph; X = Cl, Br, I).

As the first example of metal-carbon triple bonding, these complexes created much excitement and opened up the door to a whole new field of chemistry that would

[†] A caveat of this approach is that for metals towards the right hand side of the periodic table, the higher d-occupancies and lower coordination numbers make the metal centre an increasingly attractive alternative site for electrophilic attack. This is a kinetic issue rather than a reflection on the stability of late transition metal carbynes, for which alternative synthetic strategies have proven effective.

flourish in the years to come.[10-20] Metal-carbon multiple bonding continues to attract much attention in the scientific community,[21-27] as evidenced by the award of the 2005 Nobel Prize to Chauvin, Grubbs and Schrock for the development of the olefin metathesis method in organic synthesis.

The demand for active alkyne metathesis and polymerisation catalysts has driven research towards carbyne complexes bearing organic substituents.[17,22,27,28] In this respect, an extensive body of work featuring M−C multiple bonding emerged which initially appeared distinct to the 'Fischer-type' complexes. Whilst the Fischer protocol begins with low valent metal centres ligated by strong π-acceptors (hence coordinatively saturated and EAN-adherent), Schrock and Wilkinson were exploring the synthesis of high-valent metal homoleptic alkyls employing alkyl groups devoid of β-hydrogen atoms (so-called kinetically stabilised alkyls, CH_3, CH_2Ph, $CH_2{}^tBu$, CH_2SiMe_3). Having averted the usual β-metal-hydride decomposition route, alternative avenues opened up for alkyls bound to highly coordinatively unsaturated metal centres, i.e. through α-H elimination or abstraction. The isolation of $[Ta(=CH{}^tBu)(CH_2{}^tBu)_3]$ from the attempted synthesis of $[Ta(CH_2{}^tBu)_5]$[29] (inspired by Wilkinson's isolation of $[W(CH_3)_6]$),[30] followed by its deprotonation to provide $[Ta(\equiv C{}^tBu)(CH_2{}^tBu)_3][Li(dmp)]$ (dmp = *N,N′*-dimethylpiperazine)[31] presaged an enormous field of 'Schrock-type' carbene and carbyne complexes. This Fischer-Schrock dichotomy survives, yet as complexes between these two extremes emerged (e.g. $[W(\equiv CH)Cl(PMe_3)_4]$ from Schrock,[32] $[Re(=CHPh)(CO)_2(Cp)]$ from Fischer,[33] oxidation of Fischer's $[W(\equiv CPh)Br(CO)_4]$ to Schrock's $[W(\equiv CPh)Br_3(dme)]$,[34] and Roper's low-valent nucleophilic carbynes $[Os(\equiv CR)Cl(CO)(PPh_3)_2]$[35] and carbenes $[Os(=CH_2)Cl(NO)(PPh_3)_2]$),[36] more unified and comprehensive bonding schemes were developed to cover the observed reactivity spectrum (*vide infra*).

As noted, carbynes bearing σ-organyl substituents have dominated the focus of research groups, in part because of the interest in alkyne metathesis, but also because neither the Fischer nor Schrock protocols are well suited to the installation of heteroatom substituents. In the case of the Fischer approach, nucleophilic attack by heteroatom nucleophiles (e.g. RS^-, R_2P^-, R_2As^-) at a carbonyl is disfavoured (with the exception of aminocarbyne syntheses) or the requisite nucleophile is simply not available (e.g. R_2B^-,

R_2Al^-).[‡] For the Schrock protocol, a high degree of coordinative unsaturation is required at the metal centre for the α-elimination/abstraction process to proceed, typically via an α-agostic C−H−M interaction. If the alkyl concerned bears a heteroatom capable of interacting with the metal centre (e.g. MCH_2SR, MCH_2PR_2), then this is likely to compete effectively with the necessary agostic C−H−M interaction.[§]

These synthetic caveats notwithstanding, carbyne complexes bearing heteroatom substituents represent a significant component of the chemistry of carbynes. Indeed the first example [W(≡CSMe)I(CO)$_4$] was reported not long after Fischer's archetype.[38] In the interim, alkoxy carbynes remain rare, whilst amino- and thiolatocarbynes represent by far the largest groups of heteroatom-functionalised carbynes. The virtual absence of phosphorus from this 'quartet' is therefore curious, but may be traced to synthetic hurdles, rather than any reflection on their viability.

Phosphines are ubiquitous in organometallic chemistry and have played vital roles in the development of the field. The organometallic chemistry of unsaturated organophosphorus species has grown enormously over the last two decades, fuelled in part by the demise of the 'double bond rule' and the conceptual link between isolobal 'P' and 'CH' fragments.[39] Nevertheless, simple C_1P_1 ligands that incorporate combinations of metal-carbon multiple bonds and phosphino groups are uncommon. This thesis describes research directed towards the synthesis and reactivity of carbyne complexes bearing phosphorus substituents. An introduction to the bonding of carbyne complexes is first presented, followed by an overview of $MC_1P_1R_n$-type complexes, and some comparisons to work on other pnictogen-functionalised carbyne complexes.

1.1 Bonding in carbyne complexes

As noted above, different groups consider the bonding of carbyne ligands from different perspectives, though a unified description has emerged to accommodate the apparent continuum. One approach is to consider the carbyne ligand as a $[CR]^+$ fragment (CF^+ being isoelectronic with CO and NO^+). The metal-carbon bond in carbyne complexes comprises three components: a triple bond consisting of one σ bond and two orthogonal π bonds. The σ bond can be considered as a dative bond from the lone pair of electrons

[‡] Boryl anions have recently been isolated, but the considerable steric bulk required for their generation makes them unlikely candidates for nucleophilic attack at metal carbonyls.[37]
[§] For an illustrative example of the associated thermodynamics, see Section 2.6.

on the carbyne carbon into an empty d_σ orbital on the metal centre (Figure 1.1(a)). The π bonds arise from retrodonation from the filled metal d_π orbitals into the empty p-type orbitals on the carbon atom (Figure 1.1(b)).

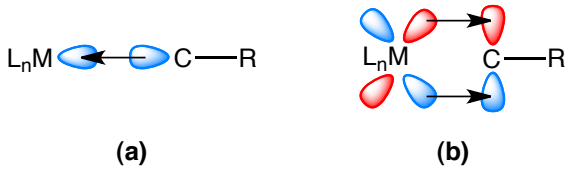

Figure 1.1. Bonding in carbyne complexes is composed of (a) a dative σ bond and (b) two orthogonal retrodative π bonds.

Alternative bonding descriptions appear in the literature in which the *neutral* carbyne fragment CR is considered as a doublet $[(sp)^2p_x^1]$ for Fischer carbynes and a quartet $[(sp)^1p_x^1p_y^1]$ for Schrock carbynes. The net result of these interactions is always a metal-carbon triple bond comprised of one σ and two π bonds, and the extent to which the spin-states of these hypothetical fragments is relevant to the nature of the actual metal-carbon multiple bond is questionable given that, in contrast to NHC chemistry, carbyne ligands are never installed by simple ligand addition. Far more important are the orbital energies of the metal-ligand fragment, how these match with those of the carbyne ligand, and how this determines the character of the resulting M≡C bond. Figure 1.2 below illustrates the π-bonding molecular orbitals for Fischer- and Schrock-type carbynes, focussing on the electron localisation in the resultant complexes, without artificially assigning of electrons to the theoretical ML_n and CR fragments.

Historically, distinctions have been made between Fischer-type and Schrock-type carbynes. Fischer-type carbynes typically contain low-valent metal centres, the π-basicity of which is attenuated by competitive π-acidic CO co-ligands such that the carbyne carbon is comparatively electron poor and prone to attack by nucleophiles.[**] Schrock-type carbynes typically involve higher-valent metal centres, devoid of π-acidic co-ligands such that the carbyne carbon displays nucleophilic character. In reality these are two extreme descriptions that border a spectrum of bonding scenarios. Assignment of complexes into one of these two classes is often not clear-cut and numerous examples of carbyne complexes with ambiphilic character have been described.

[**] Because Fischer-type carbynes typically adhere to the EAN rule, the metal centre is not attacked directly by nucleophiles.

Independent of the notional origin of the electrons involved or spin-states of the hypothetical fragments, the key discriminating factor in the Fischer-Schrock dichotomy is the energy of the orbitals presented by the metal centre. The reactivity of the M−C bond is primarily concerned with nucleophilic or electrophilic attack at the M−C π-bonds. For a given carbyne group, the closer in energy the metal t_{2g}-type orbitals are to the p_x/p_y orbitals of the carbyne fragment, the greater the overlap and the higher the degree of covalency. In the case of Fischer-type metal centres, where interaction with π-acidic co-ligands stabilises the t_{2g}-type orbitals, the energy match (and resulting overlap) is not so favourable such that the bonding combination is substantially metal based, whilst the anti-bonding combination has considerable carbon character (Figure 1.2). Accordingly, in frontier orbital controlled reactions, the carbyne carbon is the preferred site of nucleophilic attack rather than the coordinatively saturated metal centre.

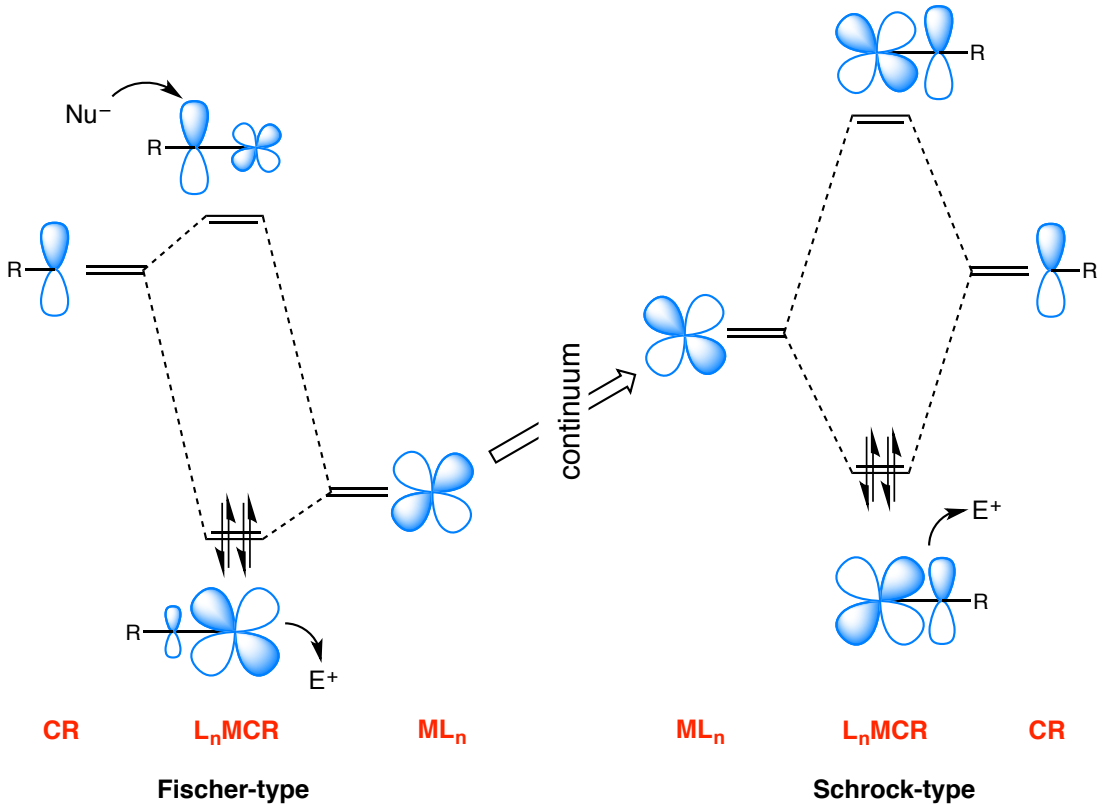

Figure 1.2. Molecular orbital description of π-bonding in Fischer- and Schrock-type carbyne complexes.

In contrast, for metal centres within the Schrock-type regime, the metal orbitals are typically higher in energy (in some cases elevated by π-donor co-ligands) and better matched for effective overlap with the carbyne p_x/p_y orbitals. This leads to greater covalency and increased contributions from carbon to the bonding combination (Figure 1.2). Although this more equitable contribution of both metal and carbon orbitals also applies to the anti-bonding combination, the metal centre, being typically coordinatively unsaturated, presents alternative orbitals for incoming nucleophiles (i.e. ligands). Thus electrophilic attack is encouraged at the carbyne carbon and nucleophilic attack may occur at the metal centre. For higher valent metal centres, direct electrophilic attack at the metal centre may also be precluded based on formal oxidation state limitations. These descriptions should be seen as extremes separated by a continuum that can be populated by tuning the nature of the metal centre (oxidation state, co-ligands, degree of coordinative unsaturation). Thus, for example, simply varying the nature of co-ligands in a classical Fischer-type carbyne may result in activation of the carbyne carbon towards electrophilic attack. Tuning the energies of the metal-based orbitals is the classic approach. The work detailed in this thesis focuses on the alternative approach of tuning the energies of the *ligand*-based orbitals by modifying the nature of the carbyne substituent and studying the effect this has on the chemistry of such complexes.

As noted above, for simple hydrocarbon carbyne substituents the M≡CR π-orbitals are either degenerate (R = H, alkyl, alkynyl) or near degenerate (R = aryl, alkenyl), whereas heteroatom substituents bearing lone pairs may alleviate the π-orbital degeneracy. This is most dramatic in the case of aminocarbynes, for which a 2-azavinylidene canonical description is occasionally invoked (Figure 1.3). Crystal structures of aminocarbynes display trigonal planar nitrogen atoms, and contracted carbon-nitrogen bonds accompanied by elongated carbon-metal bonds. This may in turn be manifest in conformational substituent preferences and an increased *trans* influence and/or *trans* effect. Spectroscopically, aminocarbynes display downfield M≡C ^{13}C NMR shifts and lower ν_{CO} infrared frequencies due to the increased electron density at the metal centre. Chemically, these compounds are considerably less reactive than carbyne complexes bearing hydrocarbon substituents. Given the usual decrease in efficiency for p_π-p_π orbital overlap on descending the main-group elements, it remains to be seen to what extent such factors apply to carbynes bearing heavier pnictogen substituents. This issue will be addressed in the work to follow.

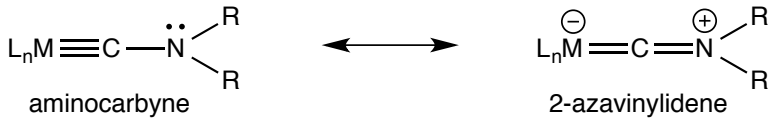

Figure 1.3. Resonance descriptions of aminocarbyne complexes.

Carbyne complexes with a multitude of substituents are known. This project focuses on those bearing phosphorus substituents, a remarkably small subset considering the important role of phosphorus in coordination, organometallic and organic chemistries. The majority of the known phosphorus-functionalised carbyne complexes are phosphoniocarbynes $[M(\equiv CPR_3)(L)_n]$, but examples of a number of other bonding modes exist. An overview of the literature encompassing carbyne complexes bearing phosphorus substituents is detailed below.

1.2 Phosphinocarbyne complexes

To date only three reports exist in the literature describing phosphinocarbyne complexes $[M(\equiv CPR_2)(L)_n]$. Cummins prepared the first examples of phosphinocarbyne complexes $[Mo(\equiv CPClR)(X)_3]$ (X = N^{t}Bu(3,5-$C_6H_3Me_2$); R = Cl, Ph), arising from the synthetic sequence shown in Scheme 1.3,[40,41] as part of a wider study into novel chemistry supported by the sterically congested molybdenum triamide platform.[42-53] Deprotonation of a terminal methylidyne complex using KCH_2Ph gave the potassium dimer $[Mo(\equiv CK)(X)_3]_2$ which undergoes nucleophilic halide substitution reaction with organophosphorus halides to provide phosphinocarbyne products.

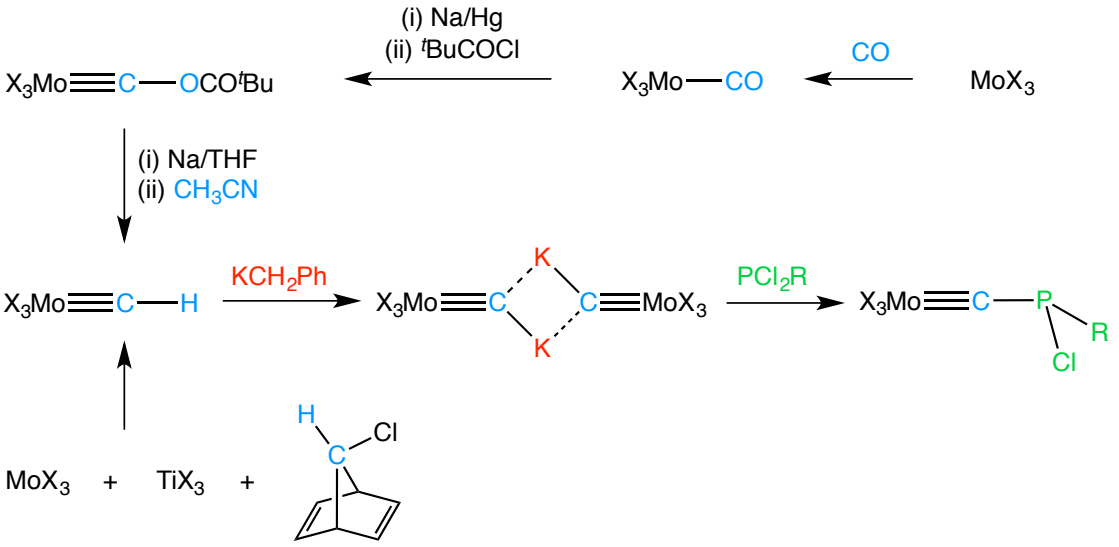

Scheme 1.3. Cummins' synthesis of phosphinocarbyne complexes (X = N^{t}Bu(3,5-$C_6H_3Me_2$); R = Cl, Ph).

Investigations into the reactivity of the phosphinocarbyne complex [Mo(≡CPClPh)$(X)_3$] were undertaken. Reduction with excess sodium amalgam in the presence of a coordinating solvent (Et_2O, THF) gave the dimer [Mo(≡CPPhNa)$(S')_2(X)_3]_2$ (S' = Et_2O, THF) (Scheme 1.4).[40] The crystal structure shows a tight ion pair interaction between phosphorus and sodium. The observed bond lengths favour the phosphidocarbyne formalisation [Mo(≡C−PPh)$(X)_3]^-$, rather than an anionic complex of a phosphaisocyanide [Mo(=C=PPh)$(X)_3]^-$, although there is some suggestion of carbon-phosphorus multiple bonding due to the slightly contracted C−P bond length (1.771(5) Å).

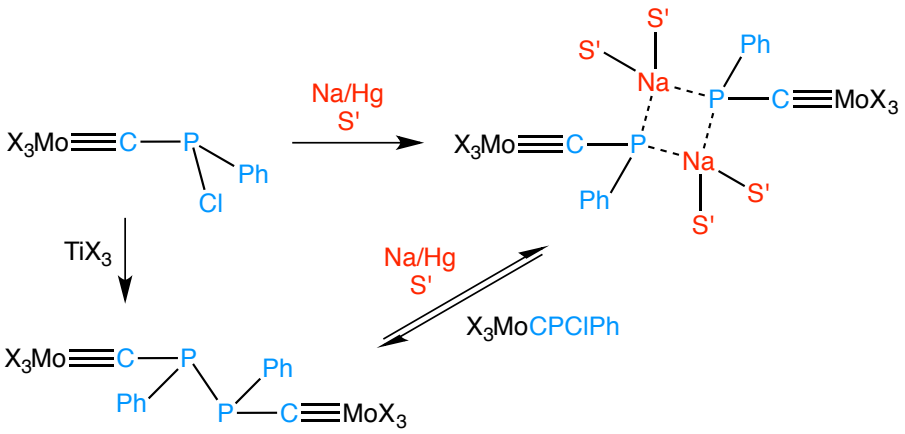

Scheme 1.4. Reactivity of the phosphinocarbyne complex [Mo(≡CPClPh)$(X)_3$] (X = N^{t}Bu(3,5-$C_6H_3Me_2$); S' = Et_2O, THF).

Attempts to synthesise a neutral phosphaisocyanide complex [Mo(CPPh)(X)$_3$] led instead to the phosphinocarbyne dimer [Mo$_2$(μ-CPPh)$_2$(X)$_6$] (Scheme 1.4), either via chlorine abstraction from [Mo(≡CPClPh)(X)$_3$] or reaction of [Mo(≡CPClPh)(X)$_3$] with the phosphido complex [Mo(≡CPPhNa)(S')$_2$(X)$_3$]$_2$.[40] The dimer [Mo$_2$(μ-CPPh)$_2$(X)$_6$] could be cleaved by reduction with sodium amalgam to regenerate the phosphido species [Mo(≡CPPhNa)(S')$_2$(X)$_3$]$_2$. DFT studies on the hypothetical model [Mo(CPPh)(NH$_2$)$_3$]$^-$ reveal a degree of C−P multiple bond character and predict a chemical shift (δ_P 132) close to the limiting value of δ_P 126.1 observed in the presence of ion-pair disrupting 12-crown-4.[40] It may therefore be concluded that the ligand does indeed show some phosphaisocyanide character, but that it is the exceptionally electron-rich nature of the 'MoX$_3^-$' group that is responsible for the activation of the C−P bond, a feature that underpins the activation of CO earlier in the synthetic sequence. Thus, whilst entirely unequivocal examples of terminal phosphaisocyanides remain elusive, it may be anticipated that if these emerge based on less π-basic metal centres, more pronounced phosphaisocyanide character will become evident.

The single other example of a phosphinocarbyne complex, [Mo(≡CPPh$_2$)(CO)$_2$(Tp*)],[54] also utilised nucleophilic halide substitution to install the phosphorus-carbon bond, but in a shorter synthetic sequence (Scheme 1.5). The one-pot procedure involved a lithium-halogen exchange reaction of Lalor's bromocarbyne complex [Mo(≡CBr)(CO)$_2$(Tp*)][55] with ^{n}BuLi to generate the nucleophilic lithiocarbyne complex [Mo(≡CLi)(CO)$_2$(Tp*)] for use, in situ, with a range of electrophiles. As in Cummins' work, addition of the corresponding phosphine halide afforded the phosphinocarbyne complex. Interestingly, synthesis of [Mo(≡CPPh$_2$)(CO)$_2$(Tp*)] via nucleophilic substitution rather than electrophilic substitution was unsuccessful. Treatment of [Mo(≡CBr)(CO)$_2$(Tp*)] with LiPPh$_2$ did not result in the desired phosphinocarbyne, and the only identifiable product from the reaction was the benzylidyne complex [Mo(≡CPh)(CO)$_2$(Tp*)]. No subsequent investigations into the chemistry of this or Cummins' phosphinocarbynes have been reported.

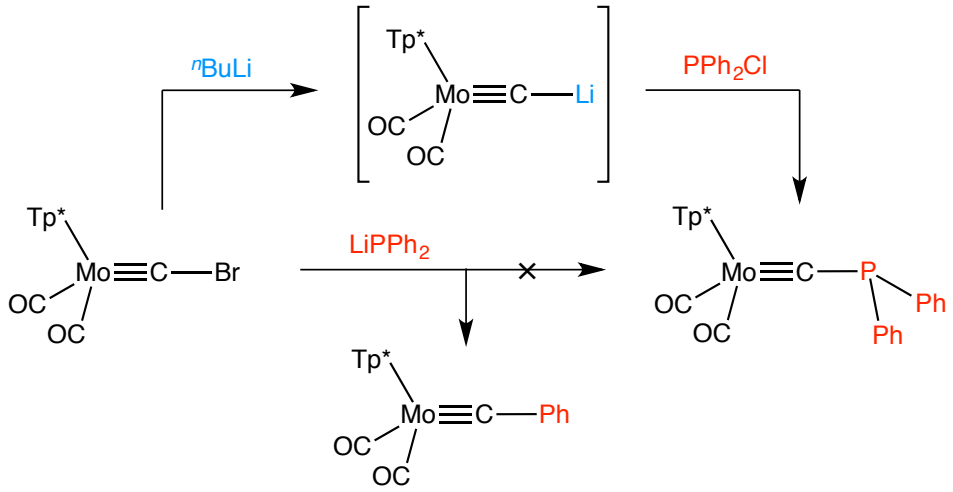

Scheme 1.5. Phosphinocarbyne synthesis via lithium-halogen exchange.

1.3 Other phosphorus-functionalised carbyne complexes

In contrast to aminocarbynes, which constitute by far the largest class of nitrogen-functionalised carbynes, phosphinocarbynes are rare, while the more prevalent examples of phosphorus-functionalised carbyne complexes are those based on exotic phosphorus variants. The literature hosts reports of a number of other phosphorus-functionalised carbyne systems, the most common being phosphoniocarbynes $[M(\equiv CPR_3)(L)_n]$. There are a couple of one-off examples,[56-61] along with more comprehensive studies by Templeton,[62-67] Weber,[68-72] and Sundermeyer and Li.[73-79] A summary of this chemistry is given below.

The first example of a phosphorus-functionalised carbyne was that of Schrock and co-workers in 1984. In an attempt to oxidise the methylidyne species $[W(\equiv CH)Cl(PMe_3)_4]$ to $[W(\equiv CH)Cl_3(PMe_3)_3]$ using $AlCl_3$ and C_2Cl_6, the dimeric phosphoniocarbyne complex $[W(\equiv CPMe_3)Cl_2(PMe_3)_2]_2[AlCl_4]_2$ was obtained (Scheme 1.6).[58] The mechanism of formation remains unclear, and no further studies have been undertaken.

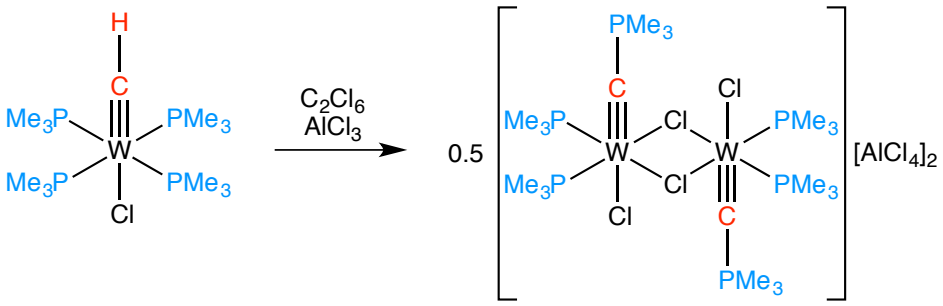

Scheme 1.6. Schrock's phosphoniocarbyne synthesis.

A novel strategy utilised by Hillhouse and co-workers to access phosphoniocarbynes involved cleavage of carbon suboxide O=C=C=C=O and triphenylphosphoranylidene ketene Ph_3P=C=C=O.[59-61] Reaction of $[WCl_2(PMePh_2)_4]$ with carbon suboxide cleaves one of the C=C bonds providing a CO and a CCO ligand (Scheme 1.7). Subsequent $PMePh_2$ migration to the CCO ligand affords the η^2-ketenyl complex $[W\{C,C':\eta^2\text{-}C(O)CPMePh_2\}Cl(CO)(PMePh_2)_2]$. This complex is thermally unstable and loses CO over two days at 35°C to give a phosphoniocarbyne complex $[W(\equiv CPMePh_2)Cl_2(CO)(PMePh_2)_2]$. This reaction appears irreversible, as addition of carbon monoxide (1 atm) to $[W(\equiv CPMePh_2)Cl_2(CO)(PMePh_2)_2]$ does not regenerate $[W\{C,C':\eta^2\text{-}C(O)CPMePh_2\}Cl(CO)(PMePh_2)_2]$, though carbonyl-carbyne coupling to form ketenyl ligands is common in other systems.[80] The related PPh_3 analogue $[W(\equiv CPPh_3)Cl_2(CO)(PMePh_2)_2]$ was obtained from the direct reaction of $[WCl_2(PMePh_2)_4]$ with Ph_3P=C=C=O at 35°C. Unfortunately, this exciting sequential cleavage of CO does not appear to be a general strategy to access phosphorus-substituted carbynes, as no further reports of such reactivity have been published, despite extensive studies on the coordination chemistry of R_3P=C=C=O.[81,82]

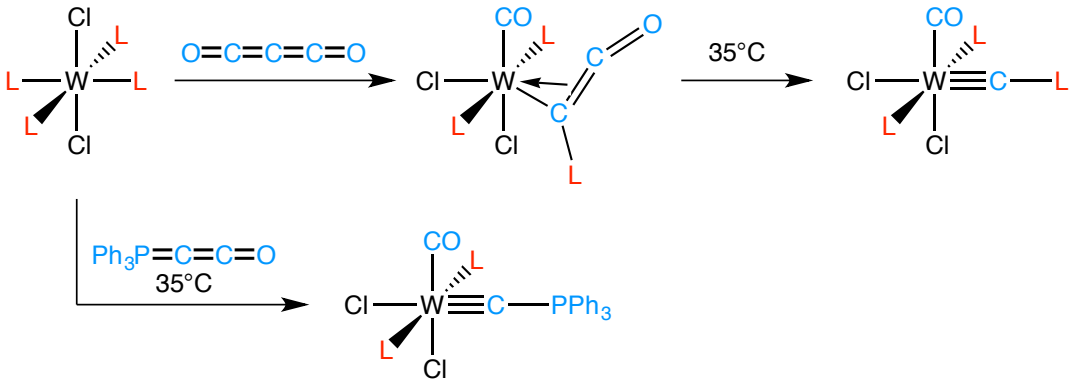

Scheme 1.7. Synthesis of phosphoniocarbynes through cleavage of carbon suboxide and triphenylphosphoranylidene ketene (L = $PMePh_2$).

Templeton and co-workers have utilised nucleophilic substitution to access cationic phosphoniocarbynes $[W(\equiv CPR_3)(CO)_2(Tp^*)]PF_6$ bearing a range of R groups (R_3 = Me_3, Et_3, Cy_3, Ph_3, Me_2Ph).[62,66] Treatment of the chlorocarbyne $[W(\equiv CCl)(CO)_2(Tp^*)]$ or the thiocarbyne $[W(\equiv CSMe)(CO)_2(Tp^*)]$ with the requisite phosphine in the presence of MPF_6 (M = NH_4, K) provides the corresponding phosphoniocarbyne as the hexafluorophosphate salt (Scheme 1.8).

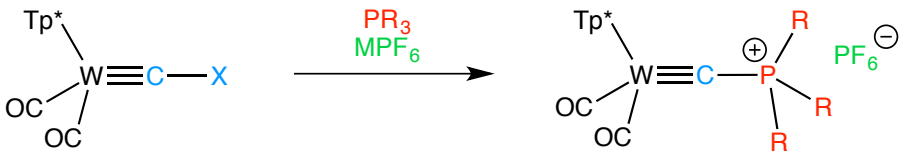

Scheme 1.8. Templeton's synthesis of phosphoniocarbynes by nucleophilic displacement of chloride or SMe^- by phosphine (X = Cl, M = K, R_3 = Cy_3, Ph_3, Me_2Ph; X = SMe, M = NH_4, R = Me, Et).

Templeton has demonstrated the reactivity of these complexes with a broad range of nucleophiles.[62-67] These reactions proceed via nucleophilic attack at the carbyne carbon, or at the carbonyl co-ligand, in some cases followed by rearrangement often involving loss of the phosphine. A particularly interesting example is the reaction of $[W(\equiv CPR_3)(CO)_2(Tp^*)]PF_6$ with aryloxide nucleophiles KOC_6H_4R'-4 (R_3 = Ph_3, Me_2Ph; R' = H, Me, OMe, CN, Cl, NO_2).[67] When the aryloxide employed is electron-rich (R' = H, Me, OMe), the phosphonium moiety is substituted to yield aryloxycarbynes $[W(\equiv COC_6H_4R\text{-}4')(CO)_2(Tp^*)]$. When electron-poor aryloxides (R' = CN, Cl, NO_2) were used, a mixture of products resulted due to the weaker nucleophilicity of the aryloxide. As well as the aryloxycarbyne, phosphoranylideneketene complexes $[W\{O(4\text{-}C_6H_4R')\}\{C,C':\eta^2\text{-}C(O)CPR_3\}(CO)(Tp^*)]$ were produced. This results from attack of the aryloxide nucleophile at the metal centre accompanied by coupling of the carbyne moiety with one of the carbonyl ligands. In contrast, the reaction of $[W(\equiv CPPh_3)(CO)_2(Tp^*)]PF_6$ with $Li[BHEt_3]$ proceeds initially by nucleophilic attack at a carbonyl co-ligand to generate a transient formyl complex which rearranges to a labile phosphoniomethylidene followed by extrusion of phosphine to afford the parent methylidyne complex $[W(\equiv CH)(CO)_2(Tp^*)]$.[64]

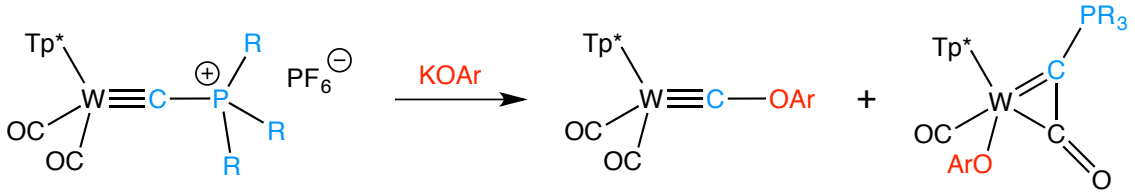

Scheme 1.9. Reactivity of phosphoniocarbyne complexes with aryloxide nucleophiles (PR_3 = PPh_3, PMe_2Ph; Ar = 4-C_6H_4R'; R' = H, Me, OMe, CN, Cl, NO_2).

Weber has comprehensively studied the chemistry of the novel tungsten and molybdenum phosphaalkenylcarbyne complexes [M{≡CP=C(NR$_2$)$_2$}(CO)$_2$(Tp*)] (M = Mo, W; R = Me, Et) along with their arsenic analogues.[68-72] Reaction of the chlorocarbyne [M(≡CCl)(CO)$_2$(Tp*)] with Me$_3$SiP=C(NR$_2$)$_2$ eliminates SiClMe$_3$ to generate the phosphaalkenylcarbyne (Scheme 1.10). A crystallographic study of the tungsten tetraethyl example confirmed the structure as a phosphaalkenyl-functionalised carbyne. The WCPC spine is bent at phosphorus so as to present a nucleophilic lone pair. A range of electrophiles were shown to add to the phosphorus, although in the case of protonation a rearrangement to the metallaphosphirene complex ensues, the only example of reactivity at the M≡C bond among this work. Addition of 'AuCl' (from [AuCl(CO)]) proceeds not once but twice to afford the trimetallic species [M{≡CP(AuCl)$_2$C(NMe$_2$)$_2$}(CO)$_2$(Tp*)]. These complexes can also be oxidised by air or pressurised O$_2$ to form the only examples of phosphinate-functionalised carbyne complexes [M{≡CPO$_2$C(NR$_2$)$_2$}(CO)$_2$(Tp*)].

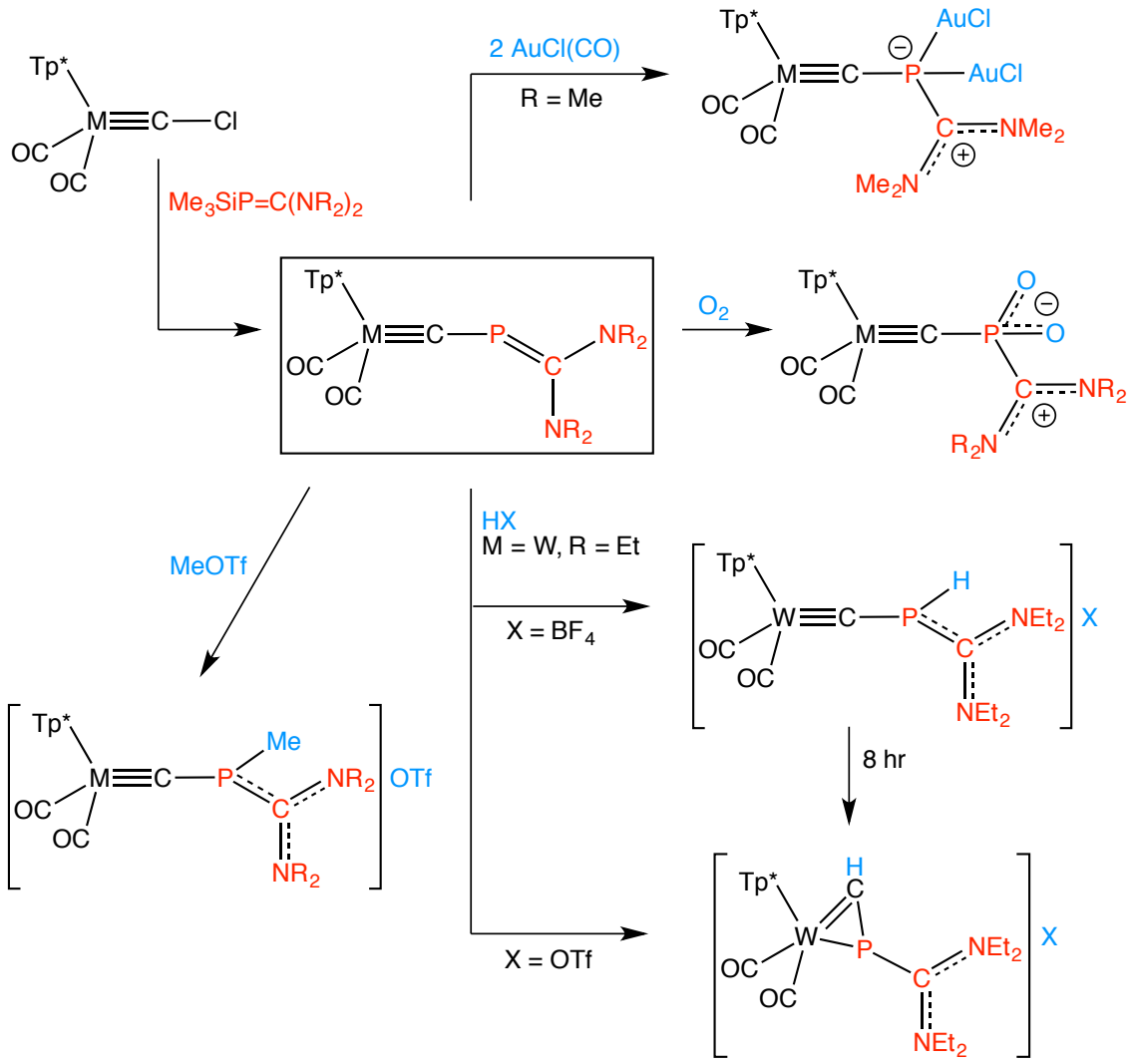

Scheme 1.10. Weber's synthesis of phosphaalkenylcarbyne complexes and subsequent reactivity (M = Mo, W; R = Me, Et).

A single example of a phosphonatocarbyne complex, [Mo{≡CP(=O)(OEt)$_2$}(CO)$_2$(Tp*)], has been reported to arise via palladium-catalysed C−P bond formation using a halocarbyne complex[54] in place of more conventional aryl halides.[83-85] Treatment of the bromocarbyne [Mo(≡CBr)(CO)$_2$(Tp*)] with HP(=O)(OEt)$_2$ and NEt$_3$ in the presence of 5 mol% [Pd(PPh$_3$)$_4$] generates the phosphonatocarbyne in 64% yield (Scheme 1.11). The reaction is believed to proceed via oxidative addition of Pd(0) to the C−Br bond, nucleophilic substitution of the bromide by P(=O)(OEt)$_2$, then reductive elimination of the product.

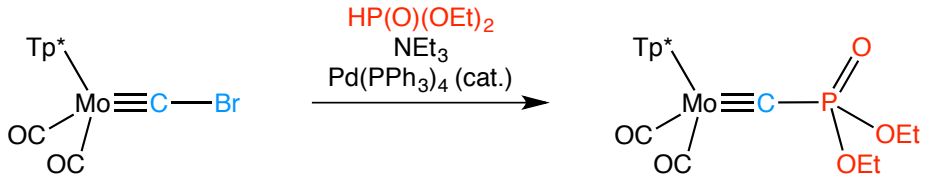

Scheme 1.11. Palladium-catalysed synthesis of a phosphonatocarbyne complex.

Following Schmidbaur's demonstration that binuclear phosphoniocarbyne complexes arise from transylidation reactions involving phosphorus ylides and $TiCl_4$,[56] Li and Sundermeyer published a number of reports of d^0 phosphoniocarbyne complexes of tungsten, rhenium, niobium and tantalum (Figure 1.4).[73-79] These complexes might also be described by a heteroallenic $M{=}C{=}PR_3$ canonical form, in addition to the zwitterionic phosphinocarbyne resonance depiction $^{-}M{\equiv}C{-}PR_3^{+}$ (shown below in Figure 1.4). As with Schmidbaur's approach, the syntheses of these complexes proceeds via transylidation reactions of $R_3P{=}CH_2$ with a metal halide precursor, eliminating $[R_3PCH_3]X$ and forming both $CHPR_3$ and CPR_3 ligands.

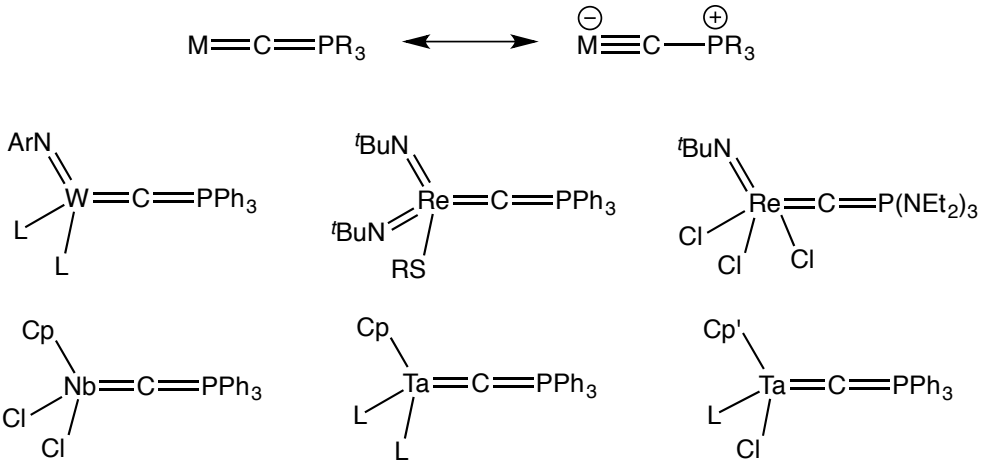

Figure 1.4. Resonance descriptions of MCP bonding in Li and Sundermeyer's complexes (Ar = 2,6-$C_6H_3{}^{i}Pr_2$, 2,4,6-$C_6H_2Me_3$; R = ^{t}Bu, adamantyl; L = $CHPPh_3$; Cp' = Cp, Cp*).

As is evident from these examples, a broad range of synthetic pathways for the installation of phosphorus substituents on carbyne ligands exists. However, most of these studies represent isolated syntheses or cover a fairly narrow scope of complexes and their analogues. The unpredictability of some of these results highlights current

limitations in our understanding of the reactivity of phosphorus substituted carbyne complexes, calling for further research into this area.

1.4 Other $MC_1P_1R_n$ systems

To understand the chemistry of phosphorus-functionalised carbyne complexes, it is pertinent to consider the chemistry of other $MC_1P_1R_n$ systems beyond that of transition metal carbyne complexes. A selection of relevant $MC_1P_1R_n$ chemistry is given here, focusing on previous work on cyaphide and phosphaisocyanide species, as well as an overview of phosphorus-functionalised carbene complexes.

1.4.1 Cyaphide complexes

The simplest conceivable carbon-phosphorus ligand is cyaphide, 'CP'. Although cyanide $C{\equiv}N^-$ is commonly encountered both as a free salt and as a ligand complexed to transition metals, the phosphorus analogue cyaphide $C{\equiv}P^-$ is extremely rare.[86] The first report of a terminal cyaphide ligand was that of Angelici and co-workers from the reaction of *trans*-[Pt{η^1-C(X)=PMes*}(X)$(PEt_3)_2$] (X = Cl, Br; Mes* = 2,4,6-$C_6H_2{}^tBu_3$) with [Pd$(PEt_3)_4$]. This reaction produced *trans*-[Pd(Mes*)(X)$(PEt_3)_2$] and a second species which was postulated to be *trans*-[Pt(C≡P)(X)$(PEt_3)_2$] (Scheme 1.12).[87,88] This complex was observed by in situ ^{31}P NMR spectroscopy of the reaction mixture which showed a triplet at δ_P 68.0 (J_{PP} 9.16 Hz), straddled by platinum-195 satellites showing a relatively small coupling constant (J_{PtP} 303 Hz), suggesting a two-bond *cis*-platinum-phosphorus interaction. Attempts to isolate this species led to decomposition but it could be trapped by addition of [Pt$(PEt_3)_4$] to afford the first binuclear bridging cyaphide complex [Pt_2(μ:η^1-*C*;η^2-*C,P*-C≡P)X$(PEt_3)_4$]. The bonding mode, atypical of cyanide bridging, was confirmed by a single crystal X-ray diffraction study which showed η^1-C coordination to one platinum, η^2-C≡P coordination to a second platinum and no Pt−Pt interaction. The carbon-phosphorus distance (1.666(6) Å) is similar to that seen in η^2-coordinated phosphaalkynes.[89]

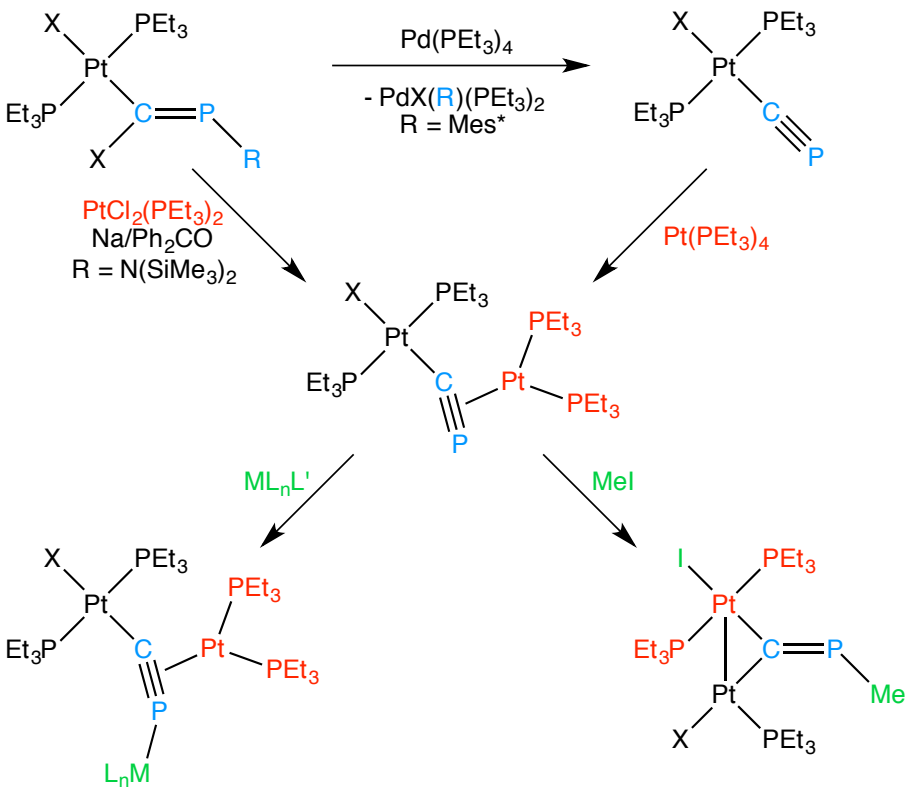

Scheme 1.12. Angelici's synthesis of platinum cyaphide complexes (R = Mes*, $N(SiMe_3)_2$; X = Cl, Br; ML_nL' = $[W(CO)_5(THF)]$, $[PtCl_2(PEt_3)_2]$).

This bridging cyaphide complex $[Pt_2(\mu{:}\eta^1\text{-}C;\eta^2\text{-}C,P\text{-}C{\equiv}P)X(PEt_3)_4]$ has also been prepared by the reduction of *trans*-$[Pt\{\eta^1\text{-}C(Cl){=}PN(SiMe_3)_2\}Cl(PEt_3)_2]$ with sodium/benzophenone in the presence of $[PtCl_2(PEt_3)_2]$ (Scheme 1.12).[90] This reduction appears to be specific to the PEt_3 co-ligand set as no reaction was observed using $[PtCl_2(PPh_3)_2]$, $[PtCl_2(PCy_3)_2]$, $[PtCl_2(P^iPr_3)_2]$ or $[PtCl_2(depe)]$. This complex is able to coordinate a third metal centre via the phosphorus atom, as shown in the synthesis of $[Pt_2\{\mu{:}\eta^1\text{-}C;\eta^1\text{-}P;\eta^2\text{-}C,P\text{-}C{\equiv}P(ML_n)\}Cl(PEt_3)_4]$ (ML_n = $PtCl_2(PEt_3)$, $W(CO)_5$).[90] Interestingly, X-ray crystallography showed very little deviation in the cyaphide ligand upon complexation of a third metal centre. The nucleophilicity of this phosphorus was also exploited in a reaction with methyl iodide. In this case, rearrangement of the C≡PMe ligand occurs to give a bridging phosphaisocyanide ligand $[Pt_2(\mu{:}\eta^1\text{-}C{=}PMe)ClI(PEt_3)_3]$.[90] The mechanism for this transformation was established using sequential Me^+ and I^- addition using MeOTf and NaI. Initial methylation at the phosphorus occurs, followed by iodide addition to platinum, then elimination of PEt_3 and an accompanying rearrangement to the bridging complex. Unfortunately, this

intriguing transformation again appears to be very limited in scope as alkylation attempts using other alkylating and arylating agents were largely unsuccessful.

The first example of an isolated complex containing a terminal cyaphide ligand came as recently as 2006.[91] Grützmacher and co-workers devised a synthesis of a ligated C≡P ligand from the triphenylsilylphosphaalkyne $Ph_3SiC{\equiv}P$. This phosphaalkyne could not be isolated but could be obtained in situ via double dehydrohalogenation of $Ph_3SiCH_2PCl_2$ using DABCO (1,8-diazabicyclo[2.2.2]octane). The presence of AgOTf is required in the dehydrohalogenation reaction to scavenge chloride from the liberated [HDABCO]Cl as it was suspected that chloride was aiding the decomposition of $Ph_3SiC{\equiv}P$ to produce Ph_3SiCl. Coordination of $Ph_3SiC{\equiv}P$ to $[RuH(dppe)_2]OTf$ yielded the phosphaalkyne complex $[RuH(P{\equiv}CSiPh_3)(dppe)_2]OTf$ in over 80% yield. At this stage, abstraction of the silyl group using fluoride sources did not proceed cleanly, impeded by nucleophilic attack of fluoride at the phosphorus atom of the phosphaalkyne ligand. Attempted desilylation with alkoxide and hydroxide reagents was also complicated by nucleophilic attack at phosphorus. Excitingly, when sodium phenoxide was used as the desilylating agent the desired cyaphide complex $[RuH(C{\equiv}P)(dppe)_2]$ was obtained in 71% yield (Scheme 1.13).

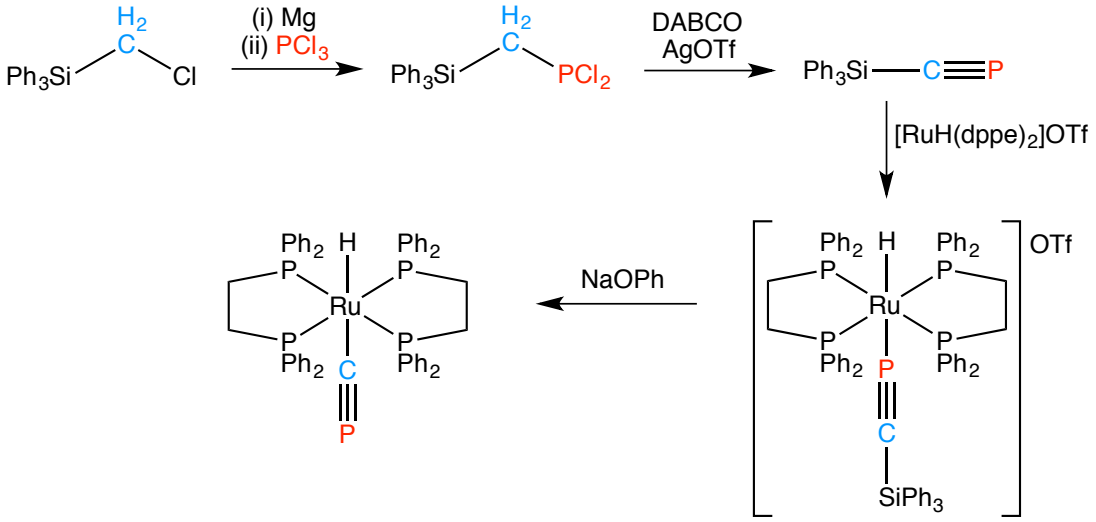

Scheme 1.13. Grützmacher's synthesis of the first isolated terminal cyaphide complex.

The cyaphide ligand was characterised by a broad peak at δ_P 165.0 (THF-d_8) and a multiplet at δ_C 287.1 in the $^{13}C\{^1H\}$ NMR spectrum. The C≡P stretching frequency was

identified in the infrared spectrum at 1228 cm^{-1} at considerably lower frequency than those of alkyl-substituted phosphaalkynes (ν_{CP} > 1500 cm^{-1}). The identity of [RuH(C≡P)(dppe)$_2$] was confirmed crystallographically. The long carbon-phosphorus bond (1.573(2) Å) was attributed to retrodonation from ruthenium into the cyaphide π* orbitals.

Recently, the second example of an isolable terminal cyaphide complex was reported by Crossley and co-workers.[92] This work extended Grützmacher's strategy, wherein the hydride ligand was replaced by a σ-alkynyl ligand, to produce alkynyl cyaphide complexes in which the cyaphide ligand is incorporated in a conjugated π system. Chloride abstraction from [RuCl(C≡CR)(dppe)$_2$] (R = CO_2Me, 4-C_6H_4OMe) by silver triflate and addition of P≡$CSiMe_3$ gave the cationic σ-phosphaalkyne complex [Ru(η^1-P≡$CSiMe_3$)(C≡CR)(dppe)$_2$]$^+$. Desilylation using potassium *tert*-butoxide effected the rearrangement to the C-coordinated cyaphide species [Ru(C≡P)(C≡CR)(dppe)$_2$] (Scheme 1.14).

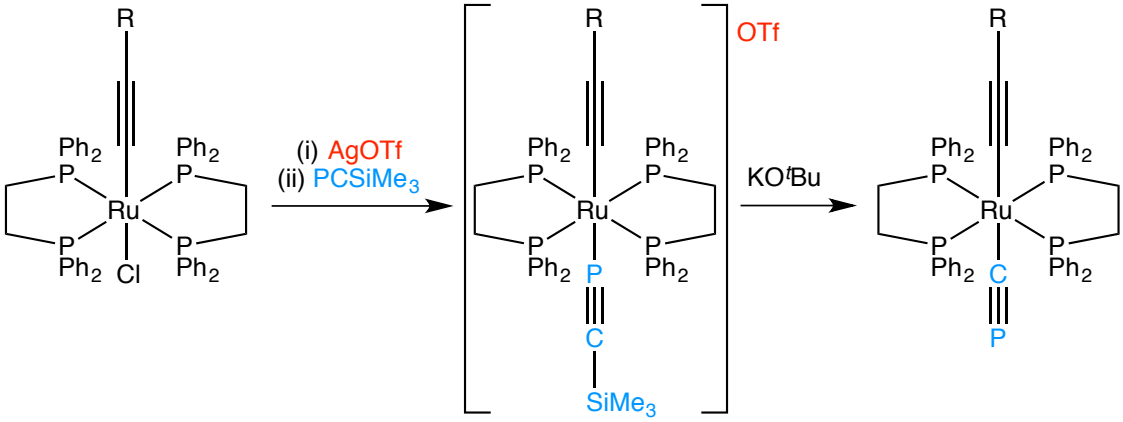

Scheme 1.14. Crossley's synthesis of alkynyl cyaphide complexes (R = CO_2Me, 4-C_6H_4OMe).

The presence of the cyaphide and alkynyl ligands was supported by C≡P and C≡C stretching frequencies in the infrared spectra at ν_{CP} 1255, ν_{CC} 2040 cm^{-1} (R = CO_2Me) and ν_{CP} 1261, ν_{CC} 2032 cm^{-1} (R = 4-C_6H_4OMe), shifted to higher frequency than that of the hydride complex (ν_{CP} 1228 cm^{-1}).[91] A crystallographic study of the *para*-methoxyphenyl derivative indicated a shorter C−P bond (1.544(4) Å) and slightly longer Ru−C bond (2.065(4) Å) than [RuH(C≡P)(dppe)$_2$]. This reflects the decreased retrodonation from ruthenium into the cyaphide π* orbitals as a result of the competing

π-acidic alkynyl ligand. UV/Vis spectroscopy revealed both complexes possessed strong ligand-ligand π (C≡P/C≡C) → π* (dppe) charge transfer absorptions around 250 nm.

Attempts by Russell and co-workers to generate molybdenum cyaphide complexes using analogous nucleophilic desilylation procedures to those employed in ruthenium chemistry have been largely unsuccessful. The formation of $[Mo(C{\equiv}P)(P{\equiv}CSiMe_3)(dppe)_2]^-$ was proposed based on ^{31}P NMR data (δ_P 197.8, multiplet), but further characterisation is required.[93]

Russo and co-workers have analysed a series of phosphaalkynes, cyaphide and cyaphide complexes computationally through DFT studies.[94] These calculations confirmed that the carbon-phosphorus bond in free CP^-, *trans*-$[PtCl(C{\equiv}P)(PMe_3)_2]$ and $[RuH(C{\equiv}P)(dppe)_2]$ is a formal triple bond through natural bond orbital (NBO), electron localisation function (ELF) and atoms in molecules (AIM) approaches. However, in the case of the bridging cyaphide complex $[Pt_2(\mu\text{-}C{\equiv}P)Cl(PMe_3)_4]$ the phosphorus-carbon bond order can be described as either a double or triple bond depending on the analysis in question and the basis set used. This is not surprising as π-coordination of $Pt(PMe_3)_2$ to the C≡P bond should result in a decrease in the bond order, as observed for conventional phosphaalkynes.

1.4.2 Phosphaisocyanide complexes

Akin to the analogy between cyanide CN^- and cyaphide CP^-, phosphaisocyanides C≡P−R are much rarer than their nitrogen based analogues isocyanides C≡N−R (Figure 1.5). While both cyanides and isocyanides are well known species, the same cannot be said in the case of phosphorus. Phosphaalkynes, which may in many cases be isolated as free molecules, have been extensively researched, yet phosphaisocyanides are extremely rare. A review detailing previous efforts towards the preparation of phosphaisocyanides and their complexes has been published,[95] and only selected illustrative examples will be included here.

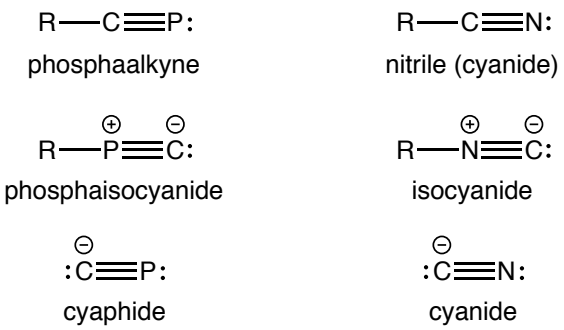

Figure 1.5. Compounds featuring C−P and C−N triple bonds.

A free phosphaisocyanide (also referred to a an isophosphaalkyne or a phosphaisonitriles) has yet to be isolated. Efforts to obtain phosphaisocyanides have mainly involved α-elimination of lithium halides from the corresponding phosphaalkenylidene carbenoids (Scheme 1.15).[95] No phosphaisocyanides have been isolated or observed using these routes, although they have been proposed as intermediates in the decomposition process. This decomposition tends to lead to phosphaalkynes, but in some cases C−H activation of the R group is observed.[96-102]

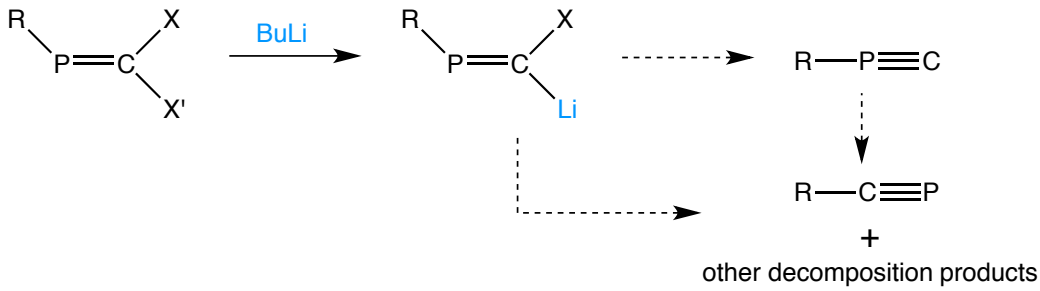

Scheme 1.15. Generalised route used in attempted syntheses of phosphaisocyanides (R = Mes*, 2,4,6-$C_6H_2(C_5H_{11})_3$; X = Cl, Br; X' = H, Cl, Br).

A true terminally ligated phosphaisocyanide is also unknown, the closest example being the phosphidocarbyne complex [Mo(≡CPPhNa)(S')$_2$(X)$_3$]$_2$ (X = N^{t}Bu(3,5-$C_6H_3Me_2$); S' = Et_2O, THF) prepared by Cummins (Scheme 1.4).[40] This species contains the desired atom connectivity. However, inspection of the bond lengths found in the crystal structure reveal that the Mo−C) distance of 1.762(5) Å is consistent with a molybdenum-carbon triple bond, and the C−P distance of 1.771(5) Å is consistent with a carbon-phosphorus single bond, such that the bonding localisation is best described as Mo≡C−P (Figure 1.6 (a)), rather than the desired Mo=C=P (b). Similarly, the

complexes synthesised by Weber [M{CPC(NR_2)$_2$}(CO)$_2$(Tp*)] (M = Mo, W; R = Me, Et) were found to be best represented by the phosphaalkenylcarbyne resonance description M≡C−P=C(NR_2)$_2$ (c) rather than a zwitterionic phosphaisocyanide resonance description M=C=P−C(NR_2)$_2$ (d).[68]

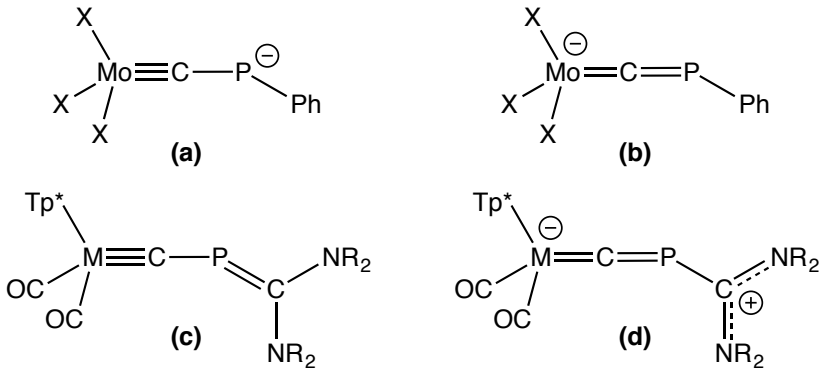

Figure 1.6. Resonance descriptions of [M(CPR)(L)$_n$] complexes (X = N^{t}Bu(3,5-$C_6H_3Me_2$); M = Mo, W; R = Me, Et).

Although no true terminal phosphaisocyanide complexes are known, bridging phosphaisocyanide ligands have been reported for platinum and iron. The first examples, discussed above, were reported by Angelici through the oxidative addition of [Pt{C(X)=PMes*}X(PEt_3)$_2$] to [Pt(PEt_3)$_4$] to afford [Pt_2(μ-C=PMes*)X_2(PEt_3)$_3$] (X = Cl, Br) (Scheme 1.16).[87,88,103-105] The X-ray structure revealed that the phosphaisocyanide ligand is asymmetrically positioned between the two platinum centres with Pt−C bond lengths of 1.86(1) and 2.107(9) Å. The P−C bond length of 1.67(10) Å is typical of a phosphorus-carbon double bond, although the low precision of the structural model does not allow for definitive categorisation. Unfortunately, limitations to this methodology (the metal centre, availability of the dichlorophosphaalkene starting material and the extreme steric bulk required for the substituent) have restricted its applicability. Angelici has also prepared a platinum phosphaisocyanide complex through alkylation of a bridging cyaphide species (Scheme 1.16), as discussed in Section 1.4.1.[90]

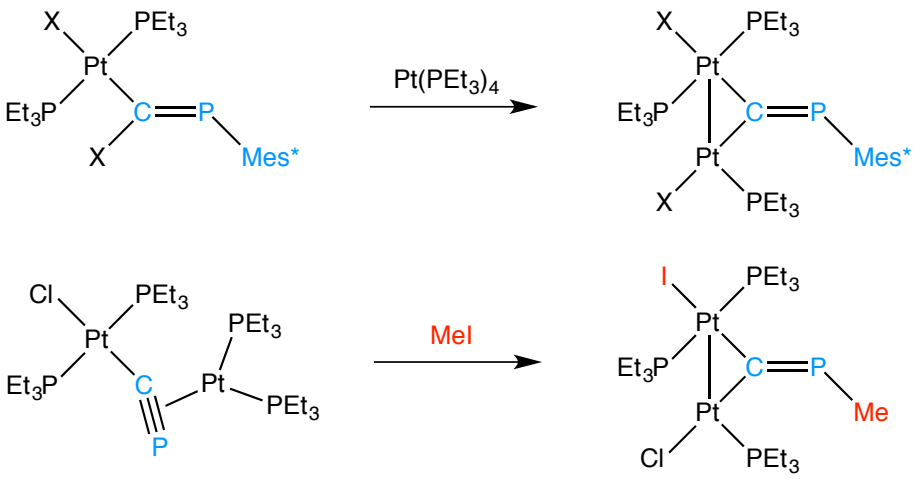

Scheme 1.16. Synthesis of bridging phosphaisocyanide complexes (X = Cl, Br).

Iron bridging phosphaisocyanide complexes have been prepared by addition of silylphosphines PH(Ar)($SiMe_3$) to [Fe_2(μ-CSMe)(μ-CO)$(CO)_2(Cp)_2$]OTf in the presence of base (DBU) to give [Fe_2(μ-C=PAr)(μ-CO)$(CO)_2(Cp)_2$] (Ar = 2,4,6-$C_6H_2R_3$; R = Me, ^{i}Pr, ^{t}Bu, CF_3) (Scheme 1.17).[106,107] The crystal structure of the mesityl derivative showed that the phosphaisocyanide ligand is close to symmetrically positioned between the two metal centres (Fe−C 1.954(16), 1.927(15)Å; Fe−C−P 147.2(10), 129.7(9)°). The phosphorus-carbon distance (1.683(17) Å) is consistent with a double bond and the angle at phosphorus is indicative of the development of a lone pair, as is also often observed for electron rich bridging isocyanide ligands. Unfortunately, this method also appears fairly limited in the scope of substituents, requiring very bulky aryl substituents. Using the smaller phosphine PH(^{t}Bu)($SiMe_3$) in the reaction led to the bridging phosphinocarbyne complex [Fe_2{μ-CPH(^{t}Bu)}(μ-SMe)$(CO)_2(Cp)_2$] (Scheme 1.17).[108]

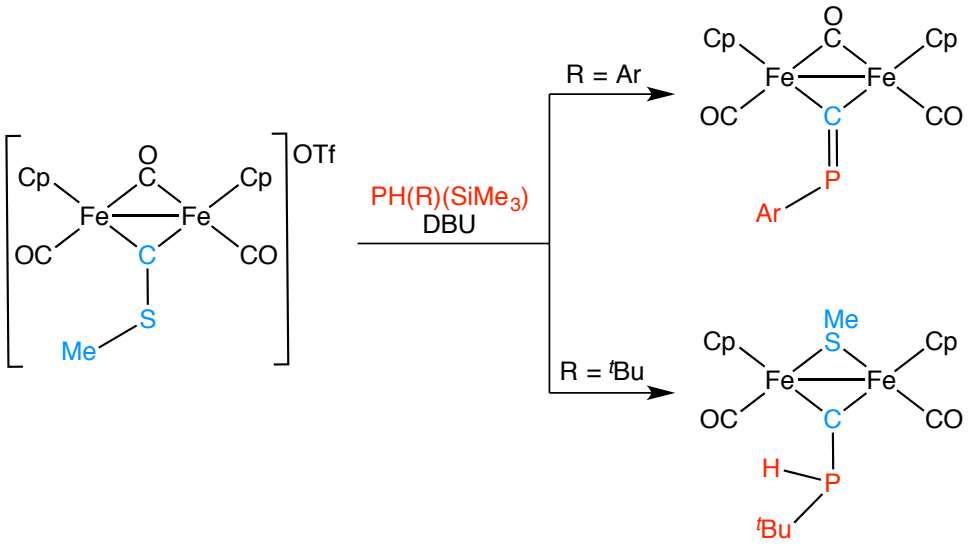

Scheme 1.17. Synthesis of a bridging diiron phosphaisocyanide complex (Ar = 2,4,6-$C_6H_2R_3$; R = Me, ^{i}Pr, ^{t}Bu, CF_3).

These ligated phosphaisocyanides display nucleophilicity at phosphorus and can coordinate to metal complexes to form μ^3-C=PR complexes (Scheme 1.18).[107] Oxidation with elemental sulfur or selenium forms the corresponding phosphine sulfide or selenide, while treatment with methyl triflate leads to the phosphonium salt [Fe_2(μ-C=PMeMes)(μ-CO)$(CO)_2(Cp)_2$]OTf.[108]

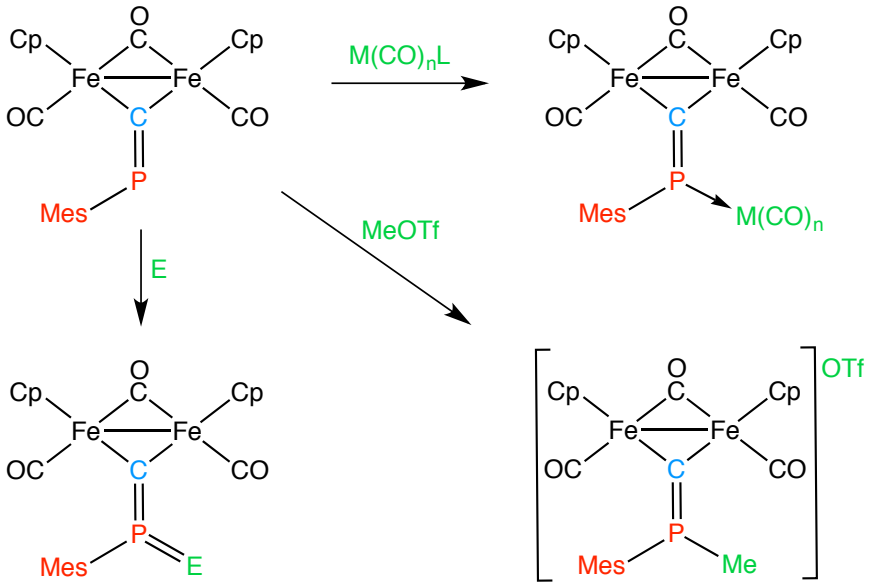

Scheme 1.18. Electrophilic additions to [Fe_2(μ-C=PMes)(μ-CO)$(CO)_2(Cp)_2$] ($M(CO)_nL$ = [$Cr(CO)_5$(COE)], [$Fe_2(CO)_9$]; E = S, Se).

1.4.3 Phosphorus-functionalised carbene complexes

Although phosphorus-functionalised carbyne complexes are fairly uncommon, carbene complexes bearing phosphorus substituents are better known,[109-112] with a large, albeit recent, portion of these based on phosphorus(V) chelates.[110-112] Most relevant to the work contained in this thesis is the chemistry of phosphinocarbene complexes,[109] and to a lesser extent that of phosphoniocarbenes. Accordingly, selected illustrative highlights are presented here.

Examples of η^1-phosphinocarbene complexes are scarce, although η^2-phosphinocarbene complexes are more commonly encountered,[113-125] – for example, through addition of a PR_2 unit to the M≡C bond of carbyne complexes,[115,116,126] or the cyclometallation of alkylphosphines[118] – and further complexes of this type will be described in Section 2.6. Initial attempts to synthesise η^1-phosphinocarbene complexes by Fischer led to the isolation of $[W\{=C(NEt_2)PMePh\}(CO)_4L]$ (L = CO, PHMePh) in very low yields (3 – 4%). These carbene complexes arose from nucleophilic attack of K[PMePh] on the carbyne carbon atom of $[W(\equiv CNEt_2)(CO)_5]BF_4$, with the major product $[W_2\{\mu\text{-}(CNEt_2)_2\}(CO)_{10}]$ being that resulting from reductive coupling of two carbyne moieties (Scheme 1.19).[113]

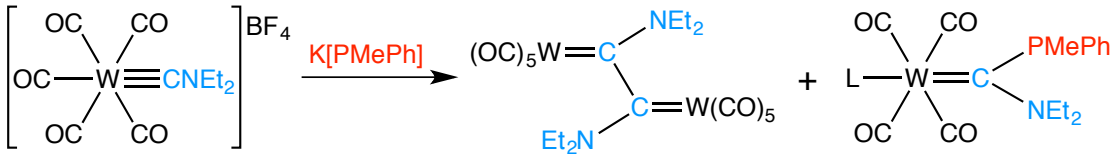

Scheme 1.19. Fischer's preparation of the first phosphinocarbene complexes (L = CO, PHMePh).

Mehrkhodavandi and co-workers found that nucleophilic attack of $K[PPh_2]$ upon the α-carbon of the isocyanide salt $[Fe\{C\equiv N(CH_2)_3PPh_2\}(CO)(Cp)]BF_4$, followed by protonation, gave the cationic η^1-phosphinocarbene $[Fe\{=C(PPh_2)NH(CH_2)_3PPh_2\}(CO)(Cp)]^+$ (Scheme 1.20).[127] Unfortunately, spontaneous $PHPh_2$ extrusion occurs to regenerate the isocyanide precursor. Recently, Schrock and co-workers utilised alkene metathesis to prepare the high oxidation state molybdenum η^1-phosphinocarbene complex $[Mo(=CHPPh_2)(=NDipp)\{O(C_6HPh_4\text{-}2,3,5,6)\}\{N(C(Me)CH)_2\}]$ from $[Mo(=CH_2)(=NDipp)\{O(C_6HPh_4\text{-}2,3,5,6)\}\{N(C(Me)CH)_2\}]$ and diphenylvinylphosphine.[128]

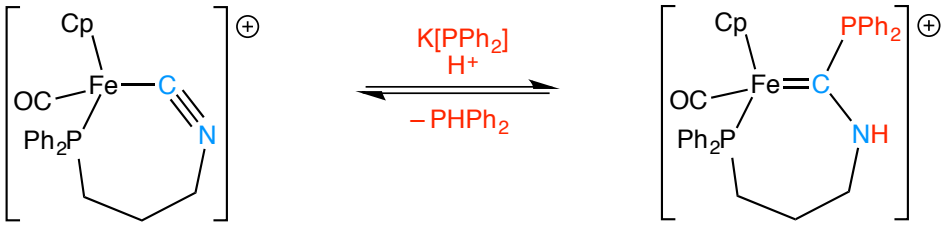

Scheme 1.20. Synthesis of an iron phosphinocarbene cation.

Unlike phosphinocarbynes, phosphinocarbenes can be prepared in their free state (i.e. R_2PCR).[109,129] Indeed the first carbene to be isolated in the free state was $(^iPr_2N)_2PCSiMe_3$, prepared by thermolysis of the corresponding α-diazophosphine $(^iPr_2N)_2PC(=N)SiMe_3$, predating the enormous growth in NHC chemistry.[130] Bertrand and co-workers have demonstrated that rhodium η^1-phosphinocarbene complexes $[Rh\{=C(C_6H_3(CF_3)_2\text{-}2,6)P(N^iPr_2)_2\}Cl(L_2)]$ (L_2 = COD, norbornadiene) can be generated through complexation of the free ligand $(^iPr_2N)_2PC\{C_6H_3(CF_3)_2\text{-}2,6\}$ by an appropriate metal precursor (Scheme 1.21).[131] Although the conceptual simplicity of this methodology makes it very attractive, the availability of stable free phosphinocarbenes is a severe limitation, requiring considerable steric encumbrance or captodative substituent combinations to impart sufficient stability – both factors that may in principle compromise the subsequent coordination chemistry.[129]

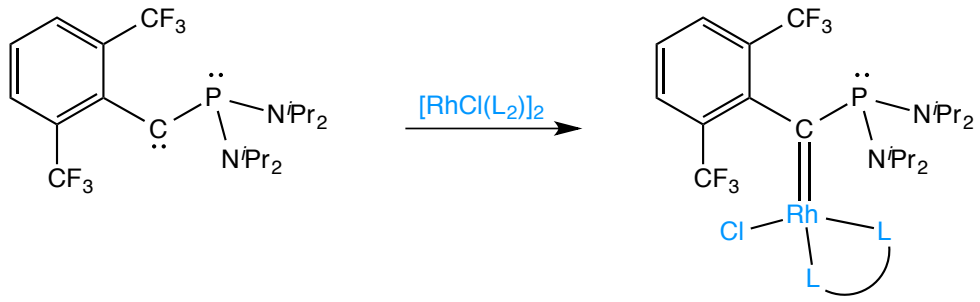

Scheme 1.21. Bertrand's synthesis of phosphinocarbene complexes by ligation of a free phosphinocarbene (L_2 = COD, norbornadiene).

Lugan and co-workers have extended their studies of cationic manganese carbynes to deliver phosphinocarbene complexes through the deprotonation of phosphoniocarbenes.[132,133] The reaction of $[Mn(\equiv CR)(CO)_2(Cp)]BX_4$ (R = Me, Ph; X = Cl, Ph) with primary and secondary phosphines gave the thermolabile phosphoniocarbenes $[Mn\{=C(R)PHR'R''\}(CO)_2(Cp)]BX_4$ (R' = R'' = Ph, N^iPr_2; R' = Me,

R" = Ph; R' = H, R" = Mes), which can be deprotonated to yield phosphinocarbene complexes [Mn{=C(Ph)PRR'}(CO)$_2$(Cp)] (Scheme 1.22). Again, the stability of the resultant phosphoniocarbenes is limited; the transient phosphinocarbenes [Mn{=C(Ph)PRR'}(CO)$_2$(Cp)] (R = R' = Ph, N^{i}Pr$_2$; R = Me, R' = Ph) rapidly isomerise to the η^3-phosphinoketene complexes [Mn{η^2-C(O)C(Ph)PRR'}(CO)(Cp)], resulting from CO insertion into the Mn=C bond. Use of a mesityl substituent at phosphorus conferred kinetic stability upon these species, enabling isolation of the η^1-phosphinocarbenes [Mn{=C(R)PHMes}(CO)$_2$(Cp)] (R = Me, Ph), which nevertheless rearrange within hours (1.5 hours R = Me, 36 hours R = Ph) to give a mixture of η^3-phosphinoketene and η^1-phosphaalkene [Mn{η^1-P(Mes)=CHR}(CO)$_2$(Cp)] products.

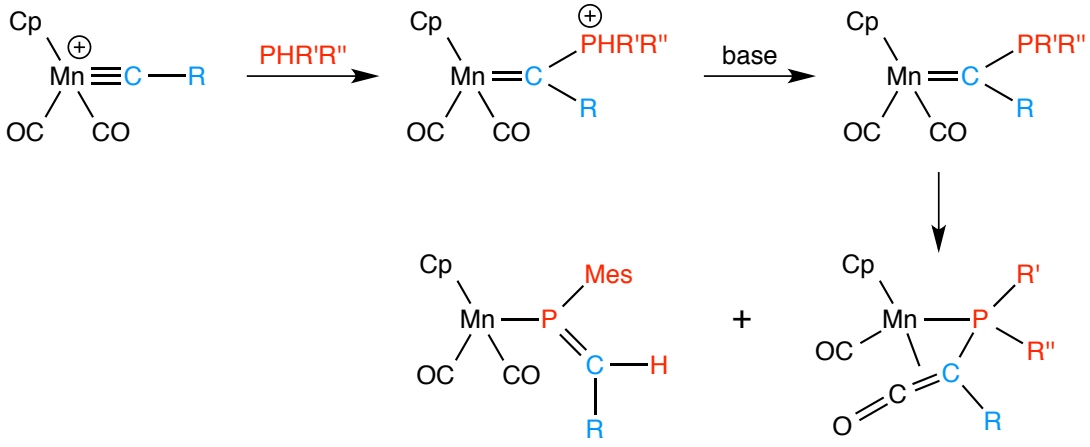

Scheme 1.22. Lugan's preparation of phosphinocarbene complexes (R = Me, Ph; R' = R" = Ph, N^{i}Pr$_2$; R' = Me, R" = Ph; R' = H, R" = Mes; base = NEt$_3$, DBU).

As has been seen, the instability and lack of widely applicable synthetic routes has severely hampered progress in the area of η^1-phosphinocarbene complexes. In contrast, η^1-phosphoniocarbene complexes are often stable and can be prepared in a relatively straightforward manner by nucleophilic addition of phosphines to carbyne complexes. Phosphoniocarbene complexes of group 6 and 7 metals have been prepared via this route, representative examples of which are outlined in Scheme 1.23.[134-136] Addition of phosphines to [W(≡CX)(CO)$_2$(Tp*)] (X = Cl, SMe) generates phosphoniocarbynes [W(≡CPR$_3$)(CO)$_2$(Tp*)]$^+$ (see Section 1.3), but interestingly, when R = Me the phosphoniocarbyne formed actually exists in equilibrium with the di(phosphonio)carbene cation [W{=C(PMe$_3$)$_2$}(CO)$_2$(Tp*)]$^+$, and addition of PMe$_3$ or

methyl iodide can be used to favour formation of the carbene or carbyne species, respectively.[62]

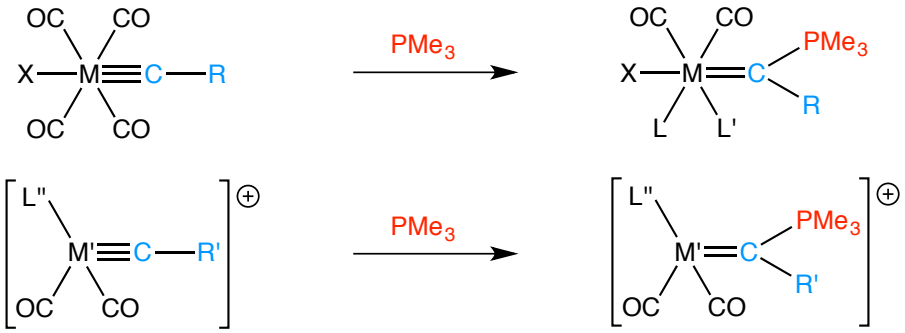

Scheme 1.23. Synthesis of phosphoniocarbene complexes via phosphine addition to carbynes (M = Cr, L = L' = CO; M = Mo, L = CO, L' = PMe_3; M = W, L = L' = PMe_3; X = Cl, Br, I; R = Me, Ph, CH_2Ph, Tol, Mes, $SiPh_3$; M' = Cr, L'' = C_6H_6, 1,4-$C_6H_4Me_2$, 1,3,5-$C_6H_3Me_3$, R = Ph; M' = W, L'' = Tp*, R' = PMe_3; M' = Mn, Re, L'' = Cp, R' = Ph).

Piers and co-workers found that protonation of the ruthenium carbido complexes [Ru(≡C)Cl_2(PR_3)(NHC)] (R_3 = Cy_3, $EtCy_2$, $MeCy_2$, $(C_5H_9)_3$, $^iPr_3$, Et^iPr_2, Me^iPr_2; NHC = $C(NR'CH_2)_2$, R' = Mes, Dipp, 2,6-$C_6H_3Et_2$) triggers phosphine migration to the carbido ligand, yielding phosphoniocarbene salts [Ru(=CHPR_3)Cl_2(NHC)]BX_4 (X = F, C_6F_5) (Scheme 1.24).[137-140] If HCl is used, [Ru(=CHPR_3)Cl_3(NHC)] forms, from which chloride abstraction with $B(C_6F_5)_3$ provides the corresponding $BCl(C_6F_5)_3^-$ salt.[138,140] The 14-electron complexes [Ru(=CHPR_3)Cl_2(NHC)]$^+$ are very active alkene metathesis catalysts as the presence of the requisite vacant coodination site *cis* to the carbene ligand circumvents the dissociative initiation step required by more conventional Grubbs-type mediators.

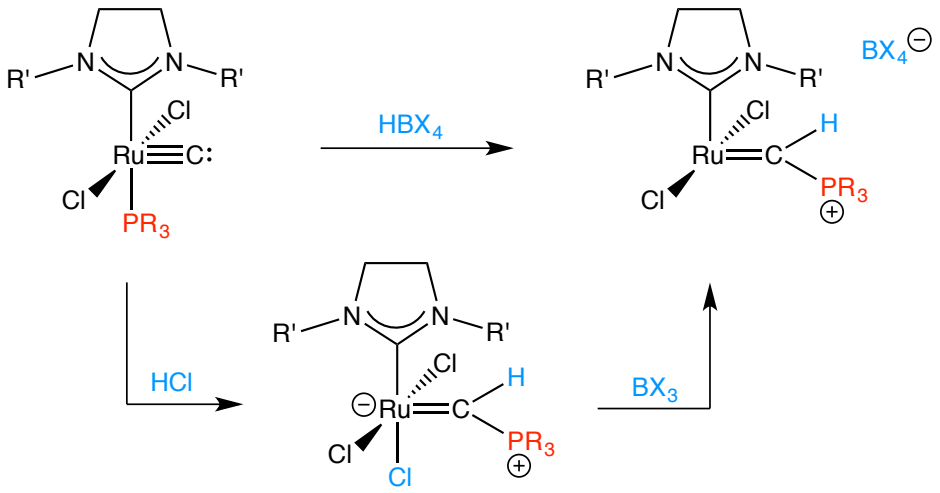

Scheme 1.24. Piers' synthesis of ruthenium phosphoniocarbene complexes (R_3 = Cy_3, $EtCy_2$, $MeCy_2$, $(C_5H_9)_3$, $^iPr_3$, Et^iPr_2, Me^iPr_2; R' = Mes, Dipp, 2,6-$C_6H_3Et_2$; X = F, Cl, C_6F_5).

1.5 Comparisons to other group 15 substituted carbyne complexes

Aminocarbyne complexes have been well studied in comparison to their heavier group 15 analogues, with a range of synthetic routes known for their preparation. The two most general approaches to aminocarbyne complexes involve either conventional Fischer alkoxide abstraction from amino(alkoxy)carbenes or oxide abstraction from carbamoylate precursors.[141-144] Alternatively, isocyanides coordinated to electron-rich metal centres may be activated towards electrophilic attack at nitrogen,[145] provided the metal centre itself does not present a site for electrophilic attack.[146,147] This latter approach mirror's Angelici's synthesis of thiolatocarbynes via alkylation of electron rich thiocarbonyl ligands[38,148] and was developed extensively by the Chatt-Richards-Pombeiro groups.[12,13,149-156]

Fischer demonstrated that the alkoxide abstraction protocol could be extended to the preparation of amino-functionalised chromium and tungsten carbyne complexes $[M(\equiv CNR_2)X(CO)_4]$ (M = Cr, W; R = Me, Et; X = Cl, Br, I) via reaction of the corresponding ethoxy(amino)carbene complexes $[M\{=C(OEt)(NR_2)\}(CO)_5]$ with boron trihalides (Scheme 1.25).[141,142] Alternatively, thionyl chloride was found to effect oxide abstraction from the carbamoylate salt $Li[W\{C(O)NEt_2\}(CO)_5]$, providing the aminocarbyne $[W(\equiv CNEt_2)Cl(CO)_4]$.[143] Variation of the Lewis acids used (BX_3, X_2PPh_3, $(CF_3CO)_2O$) has enabled preparation of a range of mononuclear chromium, molybdenum, tungsten and iron aminocarbyne complexes.[144,157-163]

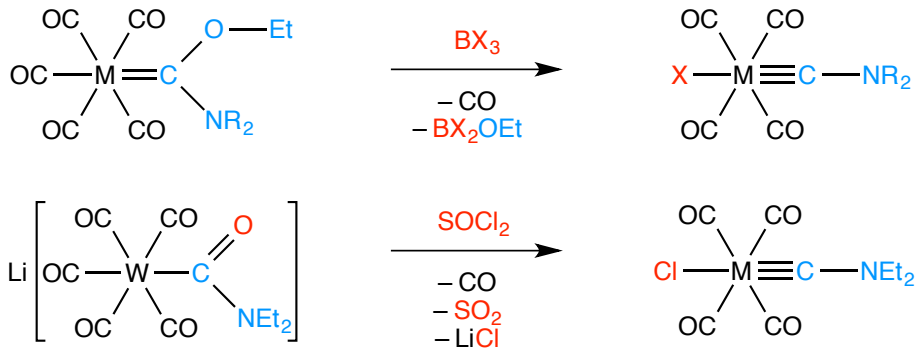

Scheme 1.25. Fischer's syntheses of aminocarbyne complexes via alkoxide or oxide abstraction (M = Cr, W; R = Me, Et; X = Cl, Br, I).

Isocyanides ligated to electron-rich metal centres may be activated towards β-electrophilic attack, and protonation or alkylation occurs at the nitrogen atom to provide aminocarbyne complexes (Scheme 1.26).[12,149-156,164,165] This strategy was utilised to access the first examples of primary aminocarbynes $[Re(\equiv CNH_2)Cl(dppe)_2]X$ (X = Cl, BF_4) via protonation of the parent isocyanide complex $[Re(C\equiv NH)Cl(dppe)_2]$.[12,155,156] This methodology has led to rare examples of bis(carbyne) complexes such as $[W(\equiv CNHMe)_2(dppe)_2]^{2+}$.[166-169] Bis(aminocarbyne) complexes can undergo carbyne-carbyne coupling reactions to afford η^2-di(amino)acetylene complexes,[167,170] and coupling of aminocarbyne ligands has been induced by protonation,[171-173] nucleophilic addition[166,169,174] or oxidative addition.[166,169]

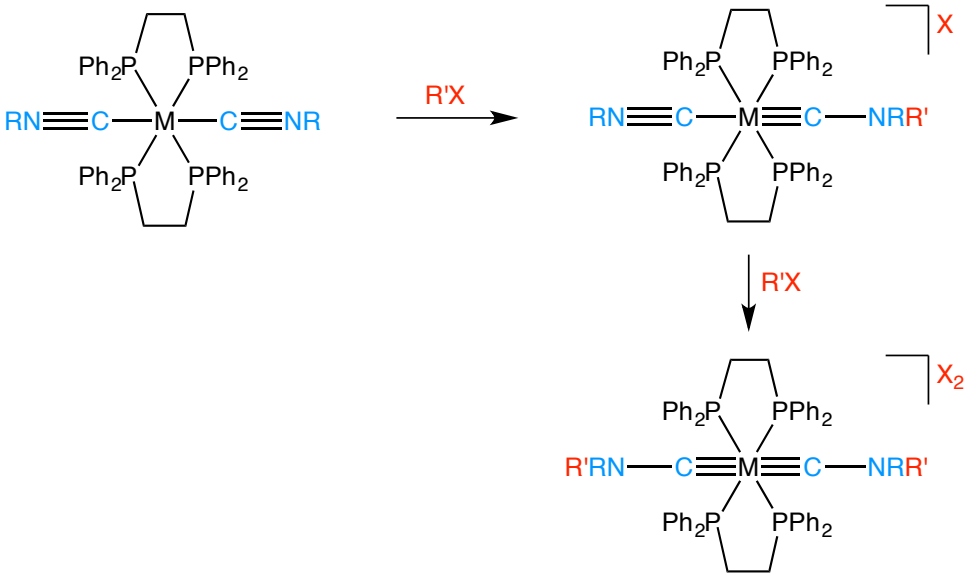

Scheme 1.26. Illustrative examples of protonation and alkylation of electron-rich isocyanide complexes to yield aminocarbynes (M = Mo, W; R = Me, ^{t}Bu; R' = H, Me, Et; X = HBF_4, HSO_4, FSO_3).

Filippou and co-workers have comprehensively studied the chemistry of group 6 aminocarbyne complexes, incorporating both Lewis acid-assisted oxide abstraction[157,158] and β-alkylation of activated isocyanide[147,172,173,175-178] methodologies to install aminocarbyne functionalities, of which some representative examples are depicted in Scheme 1.27. Oxide abstraction using oxalyl halides affords aminocarbyne complexes, which can be further derivatised through replacement of the carbonyl and halide co-ligands with a variety of ligands (e.g. picoline, CN^{t}Bu, Cp).[157,158] Alkylation of zero-valent molybdenum and tungsten isocyanide complexes generates aminocarbyne ligands, and this process has been undertaken with a variety of metal environments and co-ligands.[147,172,173,175-178] Extensive studies have shown that a wide variety of ligand substitution reactions are possible for these classes of compounds, allowing incorporation of phosphine, phosphite, picoline, halo, isocyanide and carbonyl ligands as well as multidentate ligands such as dithiolate, cyclopentadienyl and tris(pyrazoyl)borate derivatives.[168,179-188]

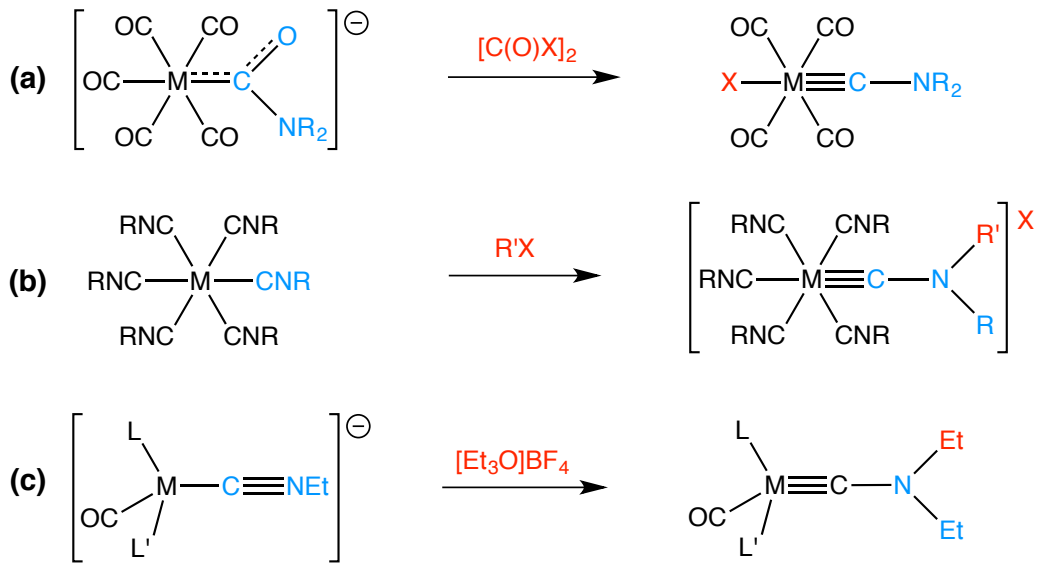

Scheme 1.27. Illustrative examples of Filippou's aminocarbyne syntheses utilising (a) oxide abstraction (M = Cr, W; R = ^{i}Pr, Cy; X = Cl, Br); (b) alkylation of a coordinated isocyanide (M = Mo, W); (c) alkylation of a coordinated isocyanide (M = Mo, W; L = Cp, Cp*, Tp*; L' = CO, CNEt).

The attempted synthesis of chlorocarbene complexes, in failing, set the stage for the development of the new area of carbyne chemistry.[1] In the interim, halocarbene ligands have been isolated and studied.[189] Amongst these, the use of phosgene iminium salts has proven useful in accessing haloamino carbenes, and the reaction of $Na_2[Cr(CO)_5]$ with $[Me_2N{=}CCl_2]Cl$ to afford the complex $[Cr\{{=}CCl(NMe_2)\}(CO)_5]$[190] is particularly noteworthy as the thermally induced rearrangement to the aminocarbyne $[Cr(\equiv CNMe_2)Cl(CO)_4]$ has been demonstrated.[191]

Iminocarbynes, $[M\{\equiv C{-}N{=}C(Ph)R\}(CO)_5]BF_4$ (M = Cr, W; R = NMe_2, ^{t}Bu) and $[Mn\{\equiv C{-}N{=}CR_2\}(CO)(L)(Cp)]BF_4$ (L = CO; R_2 = Ph_2, $(C_6H_4)_2O$, $^{t}Bu_2$; L = $PTol_3$; R_2 = Ph_2) have been described by Helmut Fischer, and in contrast to Weber's phospha- and arsaalkenyl examples, there is definitive evidence for the delocalisation of the π system along the essentially linear MCNC spine.[192,193] Whilst phosphoniocarbynes are comparatively well-known, ammoniocarbynes $[M(\equiv CNR_3)(L)_n]$ remain unknown, although azolium examples have been obtained from the reaction of $[Mo(\equiv CBr)(CO)_2(Tp^*)]$ with a range of nitrogen heterocycles (Scheme 1.28).[194] The reaction of the same halocarbyne precursor with monobasic dialkylamines provides an alternative route to aminocarbynes (Scheme 1.28).[194] However, this methodology fails

when extended to the attempted synthesis of [Mo(≡CPPh$_2$)(CO)$_2$(Tp*)] using LiPPh$_2$ (Scheme 1.5).[54]

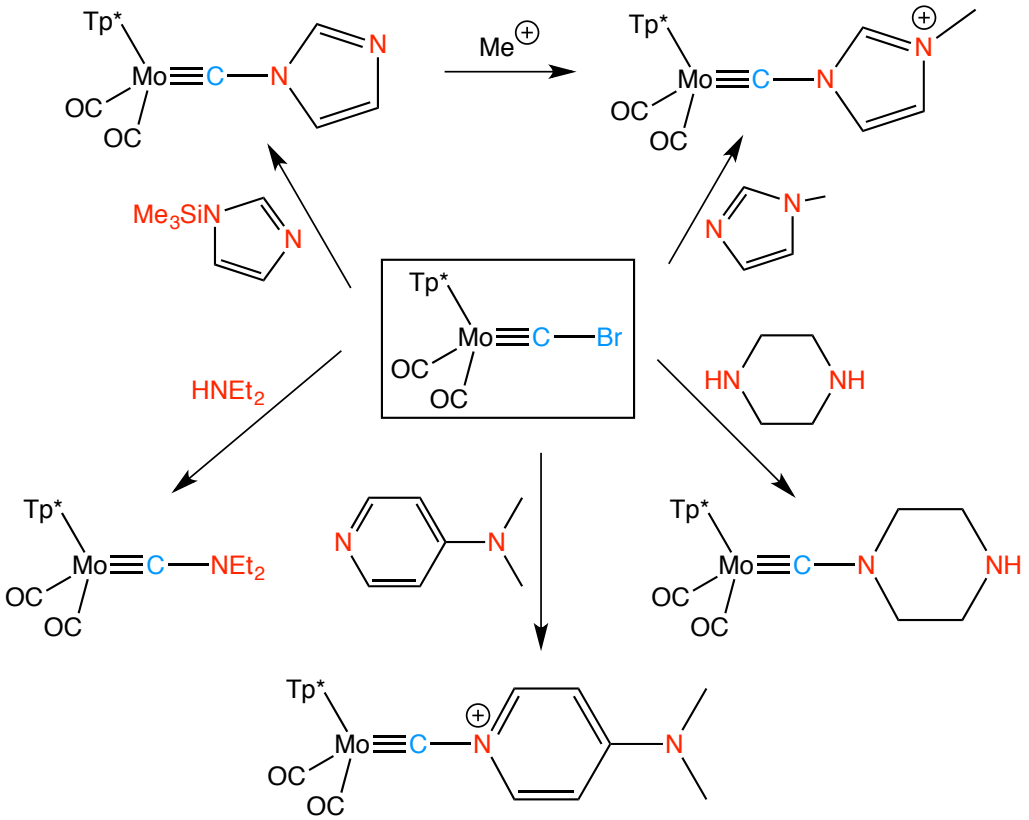

Scheme 1.28. Syntheses of azolium- and aminocarbyne complexes via nucleophilic displacement of bromide from [Mo(≡CBr)(CO)$_2$(Tp*)].

Whilst aminocarbyne chemistry is a mature field, for the heavier pnictogens there are no examples of antimony or bismuth carbyne complexes. However, Weber and co-workers have extended their work on phosphaalkenylcarbyne complexes to synthesise a variety of arsenic substituted carbyne complexes. Applying the same methodology used for phosphorus, arsaalkenylcarbyne complexes [M{≡CAs=C(NMe$_2$)$_2$}(CO)$_2$(Tp*)] (M = Mo, W) were prepared via reaction of the chlorocarbynes [M(≡CCl)(CO)$_2$(Tp*)] with the silylarsaalkene Me$_3$SiAs=C(NMe$_2$)$_2$ (Scheme 1.29).[71] The carbyne resonances (δ_C 349.7 (M = Mo), 329.1 (M = W)) are more deshielded than the corresponding phosphaalkenylcarbyne complexes (δ_C 337.5 (M = Mo), 318.3 (M = W)).[68] The tungsten-carbon distance (1.825(9) Å) in the crystal structure is consistent with a triple bond, confirming the carbyne-arsaalkene bonding description.

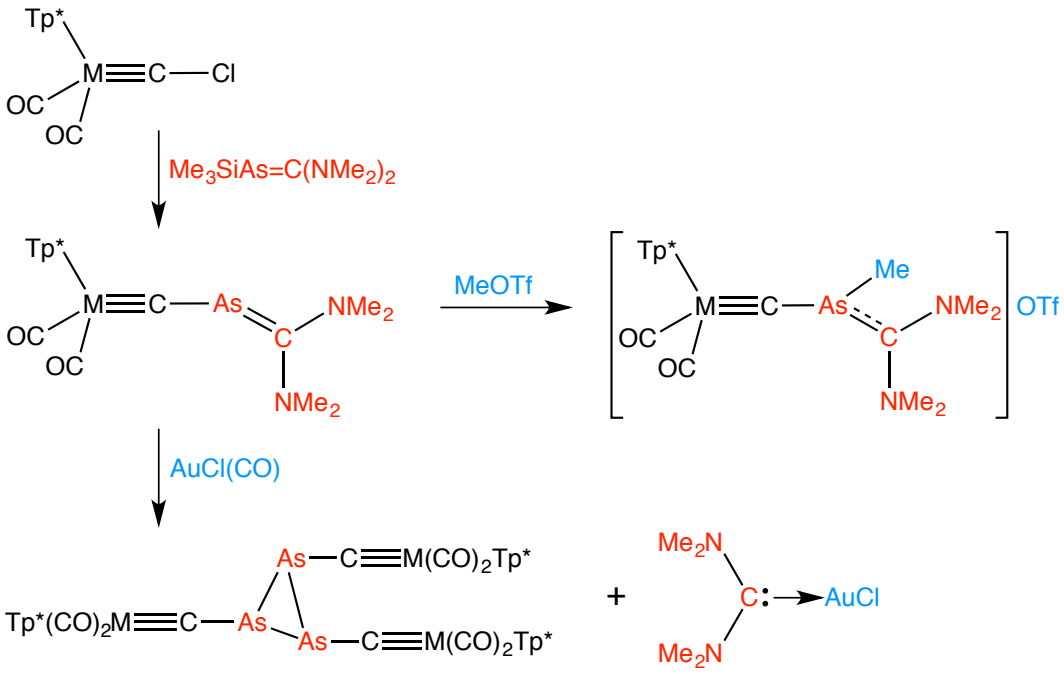

Scheme 1.29. Weber's synthesis of arsenic substituted carbyne complexes (M = Mo, W).

Alkylation with methyl triflate at −100°C demonstrated the nucleophilic character at arsenic, providing the salt $[M\{\equiv CAs(Me)C(NMe_2)_2\}(CO)_2(Tp^*)]OTf$ (Scheme 1.29).[71] Attempts to harness this nucleophilicity to form a gold complex via reaction with [AuCl(CO)] proceeded very differently to the phosphorus analogue, which was found to coordinate two molecules of AuCl to give $[M\{\equiv CP(AuCl)_2C(NMe_2)_2\}(CO)_2(Tp^*)]$. In the arsenic case, the AuCl moiety acts as a carbene abstracting agent to form $[AuCl\{C(NMe_2)_2\}]$, and consequential coupling of three '$M(\equiv CAs)(CO)_2(Tp^*)$' moieties occurs to form the fascinating cyclic triarsine $[M_3(\mu\text{-}CAs)_3(CO)_6(Tp^*)_3]$ (Scheme 1.29). A shift to higher frequency is observed in the IR spectra of $[M_3(\mu\text{-}CAs)_3(CO)_6(Tp^*)_3]$ (ν_{CO} 1987, 1909 cm^{-1} (M = Mo), ν_{CO} 1972, 1887 cm^{-1} (M = W)) in comparison to the starting material (ν_{CO} 1947, 1863 cm^{-1} (M = Mo), ν_{CO} 1936, 1848 cm^{-1} (M = W)), reflecting the increased π-acceptor capacity of the C_3As_3 bridging ligand.

1.6 Summary

The preceding discussion serves to highlight the relatively unexplored field of phosphorus-functionalised carbyne complexes, which stand in stark contrast to aminocarbynes, which are amongst the most stable carbyne complexes encountered. Apart from the exotic examples provided by Weber, simple carbynes of the form $[M(\equiv CPR_2)(L)_n]$ are exceedingly rare and very little is known about their potential reactivity. Furthermore, of these it is only Cummins' complexes $[Mo(\equiv CPClR)\{N^tBu(3,5\text{-}C_6H_2Me_3)\}_3]$ (R = Cl, Ph) that bear potentially reactive phosphorus substituents (chloride) to allow further modification of the phosphino group. The work to be described in this thesis addresses the synthesis and reactivity of the first phosphinocarbyne complexes of tungsten, beginning first with tertiary phosphine examples (Chapter 2), followed by an exploration of phosphinocarbyne complexes bearing chemically reactive substituents at phosphorus (Chapters 3 and 4), and ending with investigations into polymetallic phosphinocarbyne complexes (Chapter 5).

CHAPTER 2.

Tertiary phosphinocarbyne complexes

CHAPTER 2: Tertiary phosphinocarbyne complexes

2.1 The starting material [W(≡CBr)(CO)$_2$(Tp*)]

The starting material used for this project is the bromocarbyne complex [W(≡CBr)(CO)$_2$(Tp*)] (**1**). The molybdenum analogue was first reported by Lalor and co-workers in 1983 from the reaction of NEt$_4$[Mo(CO)$_3$(Tp*)] with [IPh$_2$]$^+$ in bromoform.[195] It was not until 1995 that this was developed into a preparative scale synthesis, this time using the redox reaction of NEt$_4$[M(CO)$_3$(Tp*)] (M = Mo, W) with arene diazonium salts [ArN≡N]BF$_4$ in bromoform.[55] Following Lalor's original syntheses, the development of lithium-halogen exchange protocols called for procedural refinements (Chapter 7) that now afford the complex conveniently on a large scale (40 g [W(CO)$_6$], 28% yield) (Scheme 2.1).[196]

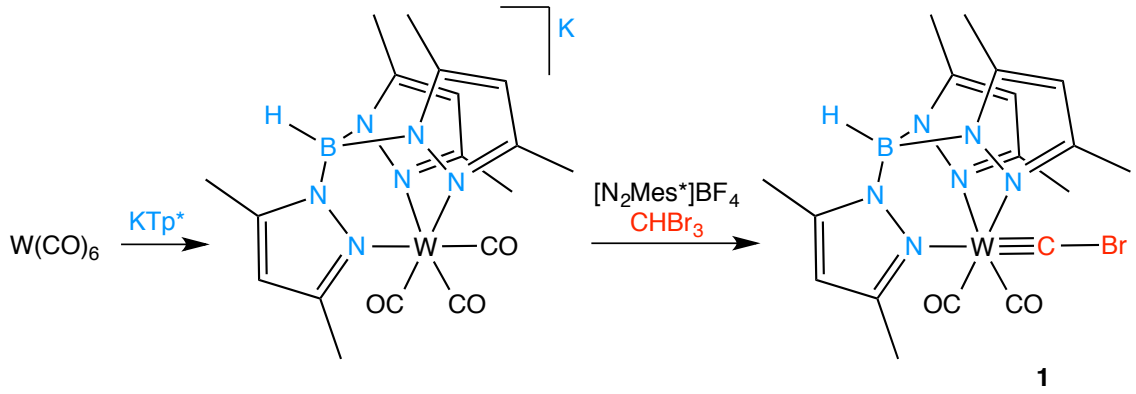

Scheme 2.1. Synthesis of the bromocarbyne starting material.

The hydrotris(3,5-dimethylpyrazol-1-yl)borato ligand (Tp*) is a facially capping tridentate ligand with a very large Tolman cone angle of 224° (*cf.* Tp 184°).[197] In this chemistry Tp* serves as a spectator ligand, and the stability afforded to the metal centre by such a sterically encumbered ligand makes much of this work possible. The steric profile of Tp* is crucial to Lalor's synthesis of **1**. If the reaction is carried out with the smaller Tp ligand or with the larger hydrotris{3-(4-tolyl)pyrazol-1-yl}borate then the carbonyl substitution aryldiazenido product [M(N$_2$R)(CO)$_2$(L)] is formed.[55]

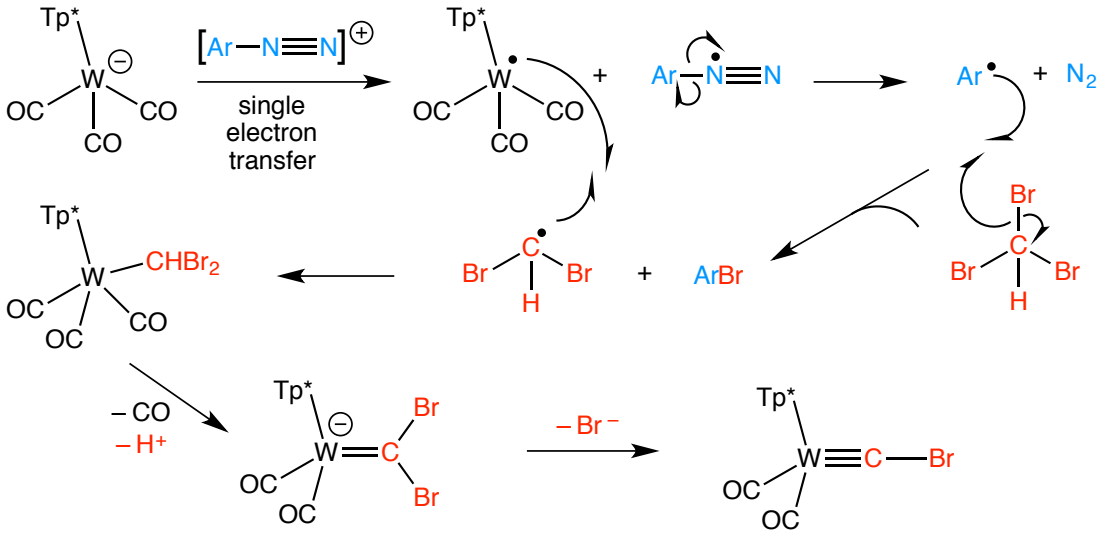

Figure 2.1. Proposed mechanism for bromocarbyne formation.

The reaction mechanism proposed by Lalor involves a radical reaction, as outlined in Figure 2.1. The key initial step is believed to be an outer-sphere single electron transfer to generate the 17 valence electron radical '$W(CO)_3(Tp^*)^{\bullet}$', which has been isolated in separate studies using ferrocenium as the oxidant in an innocuous solvent.[198] When the metal centre is less shielded (e.g. Cp, Tp), electrophilic attack ensues directly at the metal centre. In bromoform, however, the formation of the dibromomethyl radical is presumed to be followed by W–C bond formation. At this stage, a further recurrent feature of the Tp* ligand comes into play, so-called 'octahedral enforcement', which disfavours the 7-coordinate dibromomethyl complex relative to the 6-coordinate bromocarbyne product which arises via spontaneous dehydrobromination.

The halide in halocarbyne complexes $[M(\equiv CX)(CO)_2(Tp^*)]$ (M = Mo, W; X = Cl, Br) can be displaced by nucleophiles to provide a range of functionalised carbyne complexes. This has been demonstrated for groups 14,[199,200] 15,[66,68,194] 16[66,68,194,201,202] and transition metals,[203] representative examples of which are detailed in Scheme 2.2.

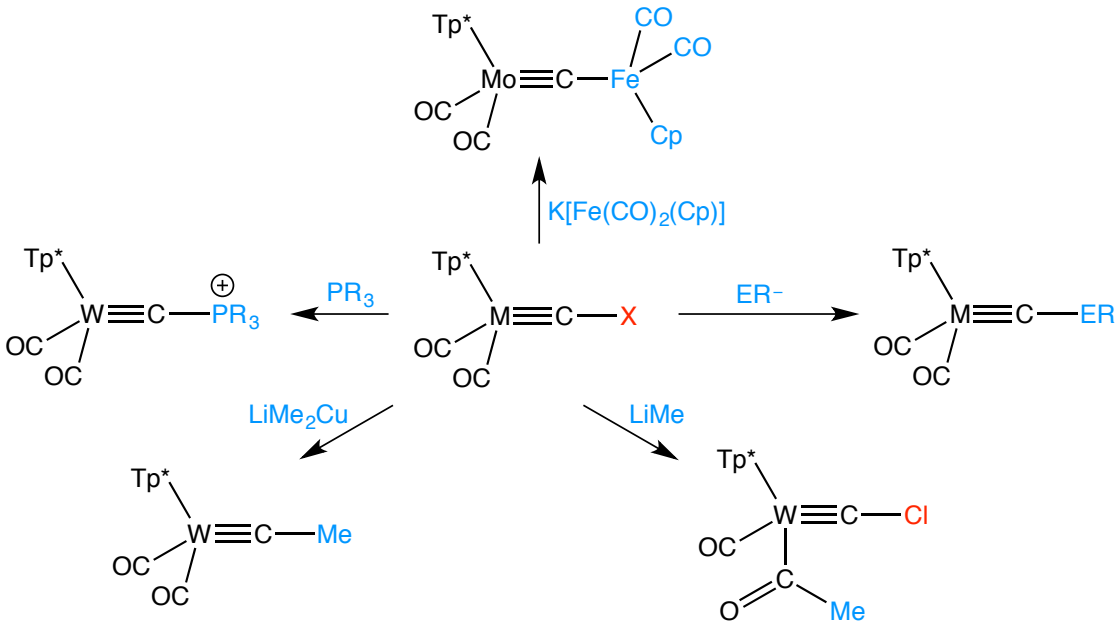

Scheme 2.2. Illustrative examples of nucleophilic displacement from halocarbynes (M = Mo, W; E = O, S, Se).

Carbynes bearing chalcogen substituents have been prepared by displacement of chloride from $[M(\equiv CX)(CO)_2(Tp^*)]$ by various anionic nucleophiles such as aryloxides,[66] aryl- and alkylsulfides,[201] phenylselenide[201] and alkynylselenolates,[202] or E^{2-} (E = S, Se, Te).[201] A bimetallic carbido complex has been similarly prepared using $K[Fe(CO)_2(Cp)]$ as the nucleophile to afford $[Mo\{\equiv CFe(CO)_2(Cp)\}(CO)_2(Tp^*)]$.[203] Neutral amines and phosphines have been used to synthesise cationic ammonio-[194] and phosphoniocarbynes.[66] Attempted direct substitution of chloride from $[W(\equiv CCl)(CO)_2(Tp^*)]$ (M = Mo, W) by methyllithium resulted in methylation at a carbonyl ligand to form the acyl anion $[W(\equiv CCl)\{C(=O)Me\}(CO)(Tp^*)]^-$. However, utilising $LiMe_2Cu$ in place of methyllithium provided the chloride substitution product $[W(\equiv CMe)(CO)_2(Tp^*)]$.[199] Although in this case the desired methylcarbyne was obtained using an alternative methylating agent, this result demonstrates the limited applicability of nucleophilic substitution reactions.

2.2 Synthesis of phosphinocarbyne complexes via the lithiocarbyne approach

In 2001 Templeton and co-workers reported the in situ generation of the lithiocarbyne complex $[W(\equiv CLi)(CO)_2(Tp^*)]$ and demonstrated the synthetic promise of this complex in electrophilic substitution reactions (Scheme 2.3).[64] Prior to this, the same group had

implicated the transient intermediacy of the anions $[M(\equiv C)(CO)_2(Tp^*)]^-$ (M = Mo, W) and their conjugate acids in the fluoride-mediated protodesilylation of silylcarbynes, leading to the non-classical bridging vinylidene complexes $[M_2(\mu\text{-}CCH_2)(CO)_4(Tp^*)_2]$.[65] However, the long and low-yielding synthesis of the precursor $[W(\equiv CH)(CO)_2(Tp^*)]$, in conjunction with its propensity to dimerise irreversibly to the non-classical vinylidene-bridged complex, deterred widespread use of this protocol.

Subsequently, Hill and co-workers developed a one-step synthesis of the lithiocarbyne complex via a lithium-halogen exchange reaction of **1** and ^{n}BuLi.[196] This reaction is performed in THF at −78°C to minimise side-reactions of the lithiocarbyne with other components of the reaction mixture, a number of which have been identified.[204] The lithiocarbyne $[M(\equiv CLi)(CO)_2(Tp^*)]$ (M = Mo, W) has been found to react with the liberated ^{n}BuBr, generating $[M(\equiv C^nBu)(CO)_2(Tp^*)]$. The presence of proton sources (trace H_2O, or under strictly anhydrous conditions, ^{n}BuBr) within the reaction mixture leads to $[M(\equiv CH)(CO)_2(Tp^*)]$, which can rearrange to the non-classical vinylidene-bridged dimer $[M_2(\mu\text{-}CCH_2)(CO)_4(Tp^*)_2]$. In the reaction of $[Mo(\equiv CLi)(CO)_2(Tp^*)]$ with *N,N*-dimethylthiocarbamoyl, the dimeric carbyne complex $[Mo_2(\mu\text{-}C_2)(CO)_4(Tp^*)_2]$ was identified as a side product of the reaction, albeit in trace amounts.[204] This was proposed to eventuate from an outer-sphere single-electron transfer reaction between *N,N*-dimethylthiocarbamoyl and the lithiocarbyne, generating $[Mo(\equiv C)(CO)_2(Tp^*)]^\bullet$ which subsequently dimerises to form $[Mo_2(\mu\text{-}C_2)(CO)_4(Tp^*)_2]$.

Although the lithiocarbyne itself is thermally unstable, in situ treatment with electrophiles has provided thermally stable derivatives functionalised with group 11 – 17 elements as well as transition metals.[54,64,194,196,204-209] Prior to the work contained in this thesis, the only reported phosphorus-functionalised carbyne prepared via this approach was the molybdenum phosphinocarbyne complex $[Mo(\equiv CPPh_2)(CO)_2(Tp^*)]$, depicted in Scheme 1.5,[54] and no discussion of its reactivity has followed. This project expands upon the previously developed methodology to provide novel phosphorus substituted carbyne complexes, some examples of which have been recently published.[210]

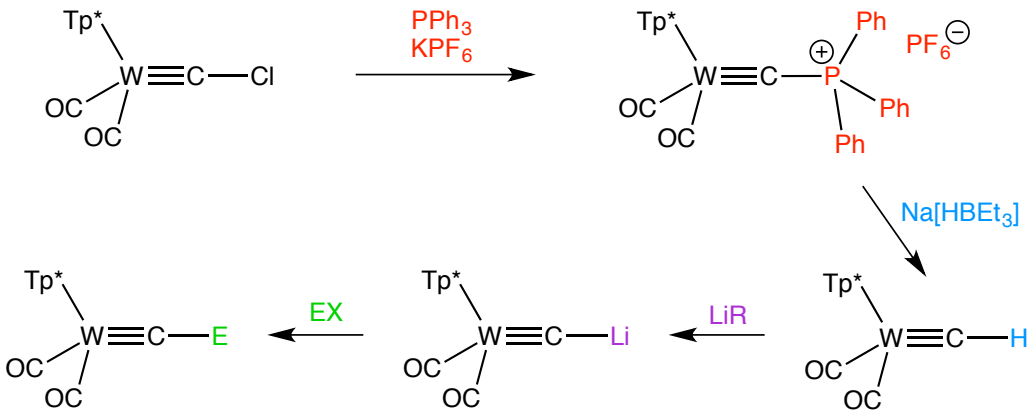

Scheme 2.3. Templeton's synthesis of the lithiocarbyne complex [W(≡CLi)(CO)$_2$(Tp*)] and subsequent electrophilic substitution (R = ^{n}Bu, ^{t}Bu, N^{i}Pr$_2$; EX = MeI, Me$_3$SiOTf, I$_2$, PhCOBr, PhCOPh then H$_2$O, PhCHO then H$_2$O).

To more generally explore the chemistry of phosphorus-functionalised carbynes, the tungsten carbyne precursor was considered in favour of the molybdenum analogue for two reasons. Firstly, the rates of ligand substitution/modification typically decrease down a group such that intermediates or products of limited stability might be expected to be more amenable to study. Secondly, the most useful feature of tungsten (*cf.* molybdenum) is the observation of ^{183}W satellites in the NMR spectra of such complexes (^{183}W: $I = {}^1/_2$, 14.3% natural abundance).* Although often not reported in the literature,† potentially informative data are available for ^{183}W–^{31}P and ^{183}W–^{13}C couplings, which will prove useful in the work to be described. Tungsten carbyne complexes typically show $^1J_{WC}$ coupling constants in the range of 140 – 300 Hz.[10,21] In contrast, data for $^2J_{WP}$ couplings are somewhat sparse, reflecting the scarcity of phosphorus-functionalised organometallic C$_1$ ligands for comparison. Much of the carbyne chemistry in the literature to date has focussed on group 6 species, and in this context little difference in reactivity has been observed between molybdenum and tungsten.

Extending the lithiocarbyne protocol from molybdenum to tungsten allowed the phosphinocarbyne complex [W(≡CPPh$_2$)(CO)$_2$(Tp*)] (**2**) to be prepared in 90% yield

* Molybdenum has two spin active isotopes, ^{95}Mo (15.9%) and ^{97}Mo (9.6%). However, both are quadrupolar ($I = {}^5/_2$) and hence less useful.

† The low abundance of ^{183}W results in low intensity satellites (ca. 7% of primary resonance), the detection of which calls for high signal/noise measurements, which are often foregone.

(Scheme 2.4). Treatment of [W(≡CBr)(CO)$_2$(Tp*)] (**1**) with one equivalent of ^{n}BuLi in THF at −78°C generated the lithiocarbyne [W(≡CLi)(CO)$_2$(Tp*)]. This species was not isolated but was treated at low temperature with chlorodiphenylphosphine. Following work-up and chromatography the phosphinocarbyne **2** was isolated as an air- and moisture-stable orange powder.‡

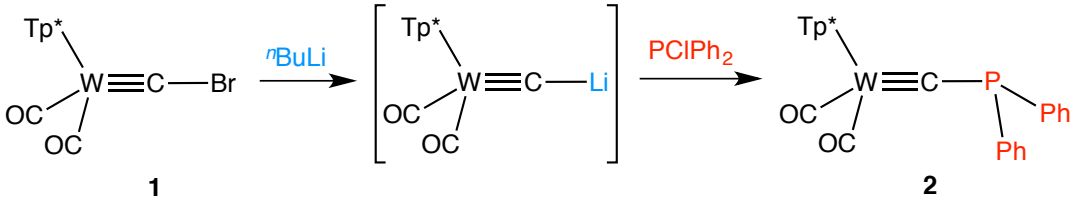

Scheme 2.4. Synthesis of [W(≡CPPh$_2$)(CO)$_2$(Tp*)] (**2**) via the lithiocarbyne.

Many of the spectroscopic features for complexes of this series are typified in the data for **2**, and as such will be discussed in detail here. Complex **2** is manifest in the ^{31}P{^{1}H} NMR spectrum as a singlet at δ_P 32.0 straddled by ^{183}W satellites ($^2J_{WP}$ 69.0 Hz), close to the reported value for the molybdenum analogue (δ_P 35.5).[54] As will become apparent, this $^2J_{WP}$ magnitude is indicative of a three-coordinate phosphinocarbyne complex of this type, and provides valuable information for the formulation of such species.

The ^{1}H NMR spectrum, shown in Figure 2.2, includes resonances attributable to the phenyl protons in the aromatic region. The methine Tp* resonances appear as singlets at 5.85 and 5.74 ppm, integrating for 2 H and 1 H, respectively, while singlets due to the Tp* methyl groups are found at 2.38 (3 H), 2.37 (6 H), 2.31 (3 H) and 2.26 ppm (6 H). In the ^{1}H (and ^{13}C{^{1}H}) NMR spectra the Tp* peaks appear in a 2:1 ratio that is typical of complexes of the form [M(≡CX)(CO)$_2$(Tp*)] where X is non-stereogenic. The spectroscopic data are consistent with **2** possessing time-averaged C_S symmetry in solution, with an internal mirror plane running along the N−W≡C axis, bisecting the two carbonyl ligands and the two phenyl groups of the phosphine (Figure 2.3 below). This leads to two of the pyrazolyl rings being equivalent (out of plane) and one non-equivalent pyrazolyl ring in the plane, in agreement with the NMR spectra.

‡ Under the conditions of its synthesis, subsequent reaction of **2** with the ^{n}BuBr lithium-halogen exchange side product does not occur, in contrast to the reaction with MeI to be described later.

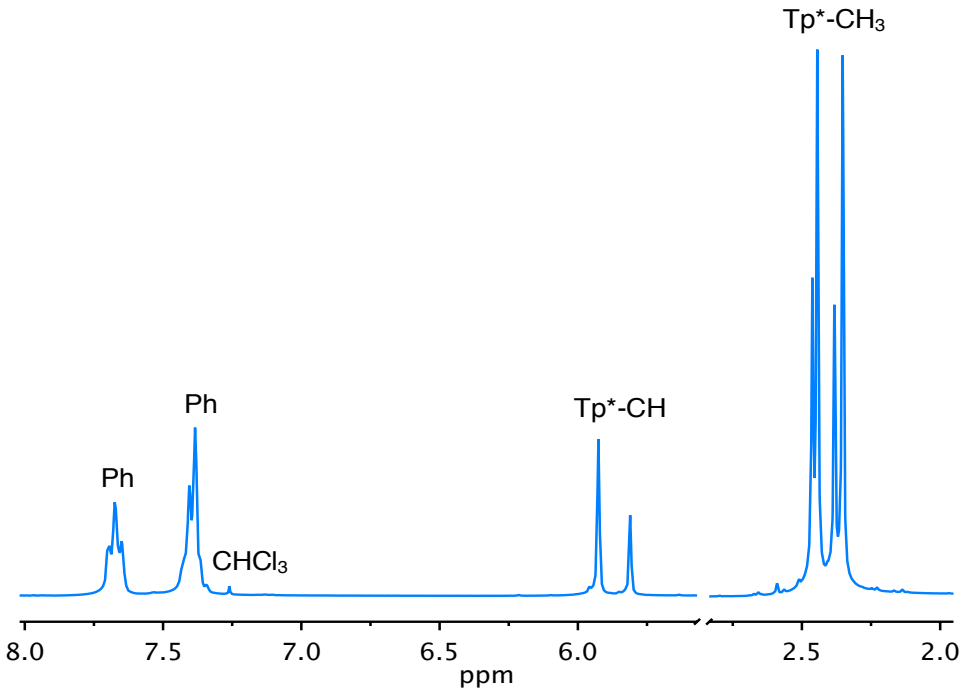

Figure 2.2. ^{1}H NMR spectrum of **2** demonstrating the typical spectroscopic signatures of [W(≡CPPh$_2$)(CO)$_2$(Tp*)] and related compounds, particularly the 2:1 ratio of the Tp* resonances.

The most diagnostic resonance in the ^{13}C{^{1}H} NMR spectrum is the low-field carbyne carbon resonance which appears as a doublet with tungsten satellites at δ_C 292.6 due to coupling to phosphorus ($^{1}J_{PC}$ 74.5 Hz) and tungsten ($^{1}J_{WC}$ 187.9 Hz) (*cf.* [Mo(≡CPPh$_2$)(CO)$_2$(Tp*)] δ_C 309.0, $^{1}J_{PC}$ 84.3 Hz).[54] The δ_C(M≡C) chemical shift values of carbyne complexes ligated by poly(pyrazolyl)borates fall within the wide range of δ_C 183.2 – 360.4, reflecting the diversity of substituents at the carbyne.[21] However, when the carbyne ligand bridges two metal centres the carbyne resonance can occur at a much lower field.[209,211] The lithiocarbyne complex [W(≡CLi)(CO)$_2$(Tp*)] is the most dramatic example of this (δ_C 556).[64] Although this might appear counter-intuitive based on inductive effects, the paramagnetic contribution to the chemical shift is expected to dominate. The carbyne resonances for both the molybdenum and tungsten phosphinocarbynes [M(≡CPPh$_2$)(CO)$_2$(Tp*)] fall significantly downfield from that of the aminocarbyne [Mo(≡CNEt$_2$)(CO)$_2$(Tp*)] (δ_C 251.9),[194] which is shifted to high-field as a consequence of substantial contributions from the 2-azavinylidene resonance form, a consideration that is evidently not significant for the heavier phosphinocarbyne congeners.

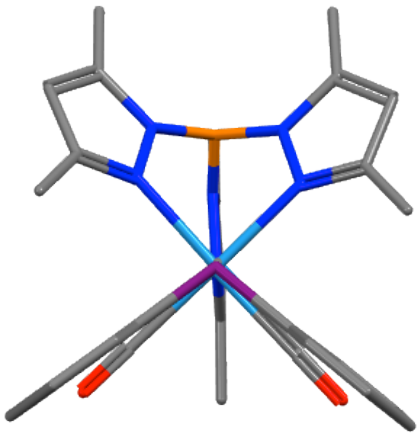

Figure 2.3. Depiction of the mirror plane in **2**.

The observed $^{1}J_{WC}$ coupling falls within the reported range for other poly(pyrazolyl)borate tungsten carbyne complexes of 160 – 250 Hz.[21] The magnitude of internuclear scalar coupling in part reflects the degree of '*s*-character' in the bonding since *s* orbitals have finite nuclear penetration (*cf. p*, *d* and *f* orbitals). Thus, for *sp*-hybridised carbon, large couplings are to be expected. Organic carbyne complexes of the form [W(≡CR)(CO)$_2$(Tp*)] have $^{1}J_{WC}$ in the somewhat narrow range of 183 – 198 Hz, whilst the aminocarbynes [W(≡CNREt)(CO)$_2$(Tp*)] (R = Me, Et) give rise to a larger $^{1}J_{WC}$ value of 208 Hz.[21] There is no obvious correlation between δ_C and $^{1}J_{WC}$.

The mirror plane through the complex renders the two carbonyl ligands chemically equivalent. They give rise to a singlet at δ_C 225.3 with tungsten satellites ($^{1}J_{WC}$ 168.9 Hz). In this work, the chemical shifts and coupling constants for the carbonyl co-ligands in complexes of the type [W(≡CPR$_n$)(CO)$_2$(Tp*)] have been found to be relatively insensitive to changes in the phosphorus substituent.

The remaining peaks in the $^{13}C\{^{1}H\}$ NMR spectrum are within the typical ranges and call for little comment. The heterocyclic pyrazolyl peaks resonate at δ_C 152.6 (1 C), 152.2 (2 C), 145.3 (1 C) and 144.6 (2 C) for the $C^{3,5}$ nuclei, and at δ_C 106.8 (1 C) and 106.6 (2 C) for the C^{4} methine nuclei. Again the 2:1 ratio of the Tp* environments is apparent. The methyl groups appear as singlets in the expected region, with peaks at δ_C 16.6 (2 C), 15.3 (1 C), 12.9 (2 C) and 12.7 (1 C). The presence of the phenyl groups is evidenced by peaks in the aromatic region at δ_C 136.5 – 128.5. Coupling to phosphorus is observed for $C^{1,2,3,5,6}$ nuclei in the phenyl groups, and whilst C^{1} (δ_C 136.5, $^{1}J_{PC}$ 9.4

Hz) and C^4 (δ_C 128.6, singlet) are readily identified, unequivocal identification of the $C^{2,6}$ and $C^{3,5}$ resonances is not possible due to the comparable coupling values.

Characterisation of **2** included electrospray ionisation mass spectrometry, which was recorded using acetonitrile as the matrix. The spectrum contains peaks due to $[M]^+$ (*m/z* 734.7), $[M - 2CO + MeCN]^+$ (*m/z* 619.8) and $[M - 2CO + H]^+$ (*m/z* 679.5). Adducts containing H^+, Na^+, K^+ and MeCN are commonly observed in the mass spectra of these types of complexes. The high resolution mass spectrum contained a $[M + H]^+$ peak at *m/z* 735.2006 in close agreement with the calculated *m/z* value of 735.2005 ($C_{30}H_{33}{}^{11}BN_6O_2P^{184}W$). Peaks due to cleavage of the phosphine substituent or of the entire $CPPh_2$ unit were not observed under these conditions.

The infrared spectrum contains identifiable bands for the BH and CO stretches. The ν_{BH} absorption appears as a weak band at 2550 cm^{-1} (THF). Little variation in this frequency is seen between complexes, as has been noted for other carbyne complexes bearing poly(pyrazolyl)borate ligands, because of the steric and electronic isolation of the B−H bond from reactive sites within the molecules, which also renders it insensitive to solid state effects.[21] In CH_2Cl_2 solution, two CO absorptions are seen for **2** at 1982 and 1891 cm^{-1}, corresponding to the symmetric A_1 mode and antisymmetric B_2 mode, respectively.[21] In THF, this splits into two pairs of absorptions: 1981 and 1893 cm^{-1} (strong) and 2000 and 1914 cm^{-1} (weak) (Figure 2.4). The solid state (Nujol) infrared spectrum contains three pairs of carbonyl absorptions: 1974 and 1883 cm^{-1} (strong), 2001 and 1912 cm^{-1} (medium), and 1957 and 1858 cm^{-1} (weak). These three sets of peaks may correspond to rotational isomerism about the C−P bond, or it may be a consequence of solid state effects causing splitting of the bands.[212] The presence of rotamers is supported by the appearance of two pairs of ν_{CO} absorption bands in the solution IR spectrum in THF, as in this case solid state effects cannot be invoked to explain the presence of more than two ν_{CO} bands. The carbonyl bands of $[Mo(\equiv CNEt_2)(CO)_2(Tp^*)]$ occur at 1938 and 1843 cm^{-1} (Nujol),[194] whereas for $[Mo(\equiv CPPh_2)(CO)_2(Tp^*)]$ these bands are shifted to higher frequency by 50 cm^{-1} (Nujol: 1988, 1901 cm^{-1}),[54] similar to what is seen for **2**. This demonstrates the absence of significant vinylidene contributions in phosphinocarbynes, in contrast to aminocarbynes, which exhibit lower ν_{CO} frequencies resulting from the increased

electron density at the metal centre that accompanies the 2-azavinylidene resonance contributions.

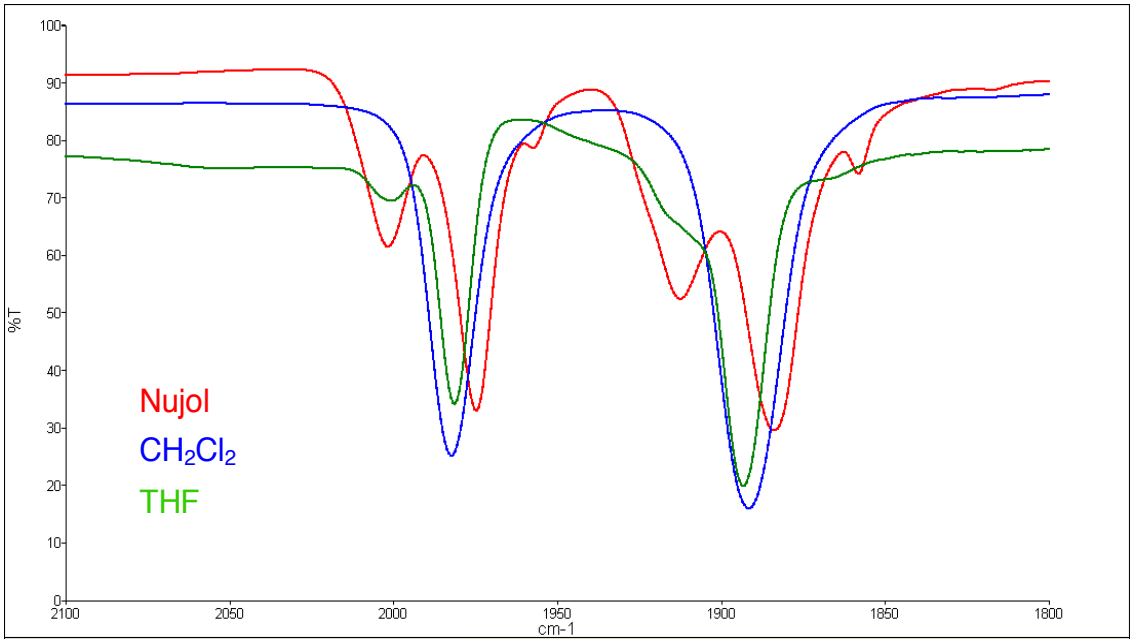

Figure 2.4. Carbonyl absorption region of the infrared spectra of **2** in different media.

Calculations[§] carried out on **2** by Dr Manab Sharma identified three rotational isomers, the free energies of which lie within 10 kJ/mol of each other (Figure 2.5). The existence of these three rotational isomers with very similar energies is consistent with the data obtained.[**] That is, rotational isomers are present but interconvert readily on the NMR timescale as the energy differences between the isomers is very small.

[§] For details of calculations see Appendix.
[**] Calculated vibrational frequencies in the gas phase (uncorrected) do not correspond to those obtained experimentally.

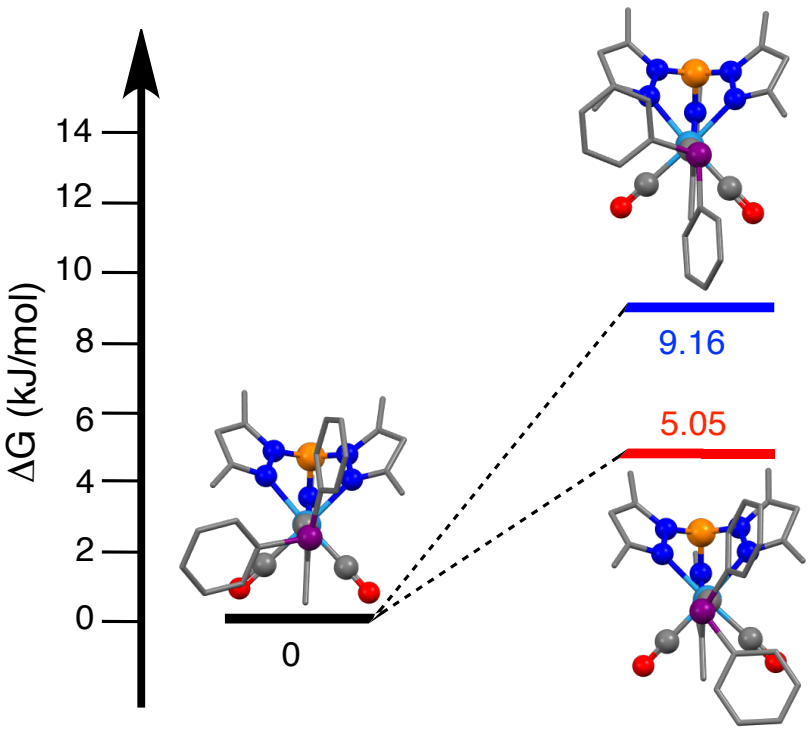

Figure 2.5. Calculated orientations about the WCP spine of **2** and their relative free energies in the gas phase. Conformations depicted looking down the PCWN axis.

The $\nu_{W\equiv C}$ stretching band is not unambiguously identifiable in the IR spectra of carbyne complexes obtained in this project. Through comparison with the IR spectrum of [W(NO)(CO)$_2$(Tp*)], a medium-weak absorption at 1099 cm^{-1} was attributed to the W≡C bond in [W(≡CBr)(CO)$_2$(Tp*)]. However, absorptions associated with the PPh$_2$ moiety in the same region make it difficult to identify the $\nu_{W\equiv C}$ vibrational mode of **2**. For the series *trans*-[M(≡CR)(X)(CO)$_4$] (R = Me, Ph; X = Cl, Br, I, Re(CO)$_5$; M = Cr, Mo, W) the M≡C stretching frequencies fall within the range 1380 – 1250 cm^{-1}.[10] However, the M≡C stretch is generally not reported for carbyne complexes, perhaps due to the difficulty identifying it in the spectra of such complexes. Additionally, such modes may in principle be coupled to other vibrations, e.g. δ_s(CH$_3$) for the complex *trans*-[W(≡CCH$_3$)Br(CO)$_4$], further clouding detailed analysis.

The structure of **2** was confirmed by X-ray crystallography (Figure 2.6), and the structural features were found to conform to those seen for the molybdenum analogue.[54] The molecular structure clearly demonstrates the trigonal pyramidal geometry at the phosphorus centre (C1−P1−C41 101.52(12)°, C1−P1−C51 106.02(12)°, C41−P1−C51

104.32(12)°), in contrast to aminocarbynes in which significant $p_\pi(N)$-$p_\pi(C)$ overlap leads to a trigonal planar nitrogen centre (2-azavinylidene resonance structure, Figure 1.1).[194] This is exemplified by the angle sum about nitrogen in the analogous aminocarbyne complex [Mo(≡CNEt$_2$)(CO)$_2$(Tp*)] of 360°,[194] whereas the angle sum about phosphorus in **2** is 311.9°, similar to that found for the alkynylphosphine Ph$_2$PC≡CMe (304.0°),[213] and the molybdenum analogue [Mo(≡CPPh$_2$)(CO)$_2$(Tp*)] (312.0°).[54] Interestingly, the geometry obtained in the crystal structure does not correspond to the lowest energy conformer calculated, but rather the second lowest (Figure 2.5). However, the energy difference between this orientation and the global minimum conformation is only 5.05 kJ/mol, which would be easily overcome by the energy of the crystal lattice.

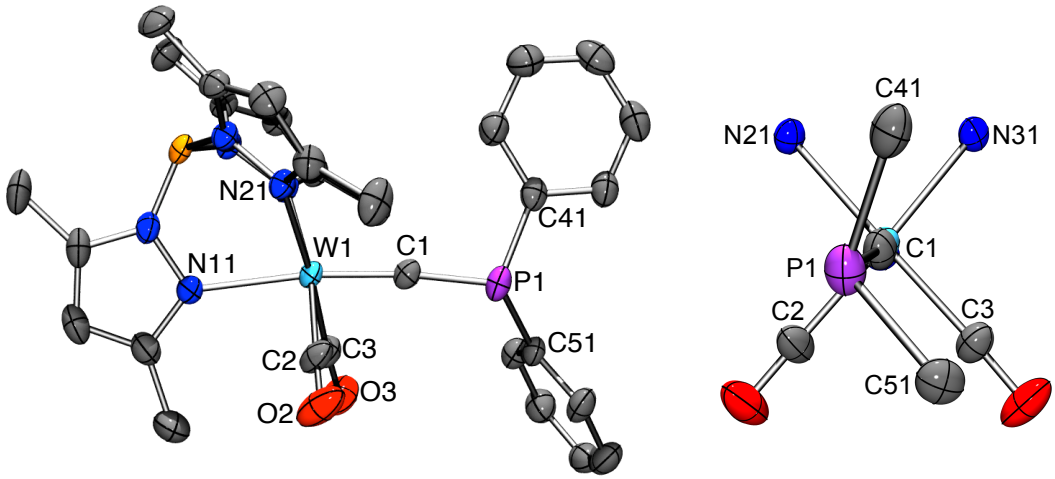

Figure 2.6. Full view (left) and simplified view (right) of the molecular structure of **2** in a crystal (50% displacement ellipsoids, hydrogen atoms omitted). Selected bond lengths (Å) and angles (°): W1−C1 1.827(2), C1−P1 1.783(3), P1−C41 1.833(3), P1−C51 1.829(3), W1−C1−P1 166.62(15), C1−P1−C41 101.52(12), C1−P1−C51 106.02(12), C41−P1−C51 104.32(12).

Some general features of [W(≡CX)(CO)$_2$(Tp*)] structures are apparent here. The geometry about tungsten is distorted octahedral. The N−W−N angles (81.18 – 82.35°) are contracted from the idealised 90° due to the chelation constraints of the tridentate Tp* ligand. The W1−C1−P1 angle of 166.62(15)° deviates slightly from linearity as seen in other complexes of this type.[21] This bending is generally attributed to crystal packing forces.[214] The W1−N11 bond *trans* to the carbyne is significantly longer

(2.319(2) Å) than the W1−N21 (2.208(2) Å) and W1−N31 (2.206(2) Å) bonds *trans* to the carbonyl ligands, demonstrating the strong *trans* influence of the carbyne ligand. The W≡C bond length of 1.827(2) Å falls within the reported range for other poly(pyrazolyl)borate ligated carbyne complexes of molybdenum and tungsten[††] of 1.76 – 1.90 Å.[21] Variation of the carbyne substituent produces fluctuations of the metal-carbon bond length within this range. Most notably, aminocarbynes typically display marginally longer M≡C bond lengths consistent with the 2-azavinylidene canonical description. These features are common to tungsten carbyne complexes of this type and as such need not be discussed further in most cases.

2.3 Synthesis of phosphinocarbyne complexes via palladium-catalysed phosphination

The use of palladium-catalysed P−C bond forming reactions for the preparation of phosphines is well established. Much research has been undertaken to broaden the scope of these reactions such that it now encompasses alkenyl halides,[215] aryl halides and pseudohalides with primary phosphines,[83,216] secondary phosphines,[83,216,217] triarylphosphines,[218] H-phosphinate esters and H-phosphonate diesters,[219] among others. This methodology has even been extended to halocarbynes on one occasion; [Mo(≡CBr)(CO)$_2$(Tp*)] has been shown to undergo a palladium-catalysed reaction with diethylphosphinic acid (HP(=O)(OEt)$_2$) to afford the phosphonitocarbyne complex [Mo{≡CP(=O)(OEt)$_2$}(CO)$_2$(Tp*)] in 64% yield (Scheme 2.5).[54]

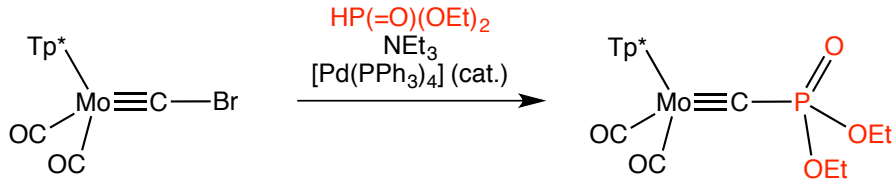

Scheme 2.5. Palladium-catalysed synthesis of [Mo{≡CP(=O)(OEt)$_2$}(CO)$_2$(Tp*)].

This methodology appeared to offer a promising approach to developing an alternative general synthetic route to phosphorus-functionalised carbyne complexes. Upon heating a toluene solution of the tungsten bromocarbyne **1** with diphenylphosphine and

[††] For comparative purposes, it should be noted that molybdenum and tungsten have comparable covalent radii due to the lanthanoid contraction.

triethylamine, in the presence of $[Pd(PPh_3)_4]$ (5 mol%), to 80°C for one hour, infrared and NMR spectroscopic analysis indicated the formation of **2** as the major product (Scheme 2.6).

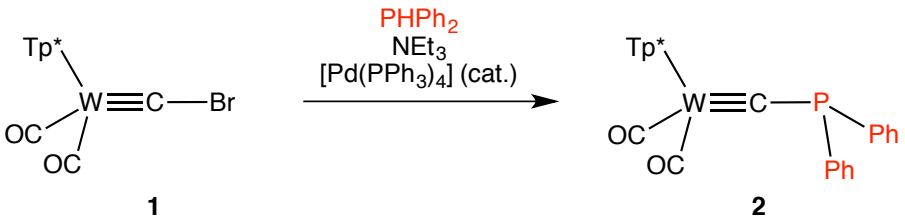

1 **2**

Scheme 2.6. Synthesis of **2** via palladium-mediated P−C bond formation.

The success of this reaction demonstrates the utility of transition metal catalysis as a means of affording functionalised carbyne complexes. More detailed investigations into the synthesis of phosphinocarbyne complexes via palladium-catalysed phosphination reactions can be found in Section 4.2.3.

2.4 Attempted synthesis of phosphinocarbyne complexes via a stannylcarbyne complex

A third route to phosphorus-functionalised carbyne complexes was explored within the scope of this project. The lithiocarbyne route, whilst effective for the synthesis of **2**, does have limitations.[204] The lithiocarbyne endures only at low temperature and needs to be generated freshly for each reaction. The reaction must be carried out under scrupulously anhydrous conditions, otherwise proton scavenging by the lithiocarbynes $[M(\equiv CLi)(CO)_2(Tp^*)]$ (M = Mo, W) leads to formation of the methylidynes $[M(\equiv CH)(CO)_2(Tp^*)]$. Additionally, in some cases side reactions occur in which the liberated ^{n}butyl bromide or the THF solvent act as competitive electrophiles, resulting in $[M(\equiv C^nBu)(CO)_2(Tp^*)]$ or the THF ring-opened complex $[M\{\equiv C(CH_2)_4OH\}(CO)_2(Tp^*)]$.[220] In this work, reactions with phosphorus-based electrophiles have not led to identifiable formation of $[W(\equiv C^nBu)(CO)_2(Tp^*)]$ or $[W\{\equiv C(CH_2)_4OH\}(CO)_2(Tp^*)]$ as side-products, but this possibility should not be disregarded when utilising the lithiocarbyne route. The problems encountered in this work with the lithiocarbyne and palladium-mediated routes were primarily associated with purification of the desired product, and are detailed in the relevant sections.

In light of these issues, the viability of the stannylcarbyne complex [W(≡CSnMe$_3$)(CO)$_2$(Tp*)] as a precursor for the synthesis of phosphorus-functionalised carbyne complexes was explored. Inspired by the success of alkynylstannanes in transmetallation reactions,[221] this stannylcarbyne complex has been used to synthesise functionalised carbyne complexes by a gold-catalysed tandem transmetallation (Scheme 2.7).[211]

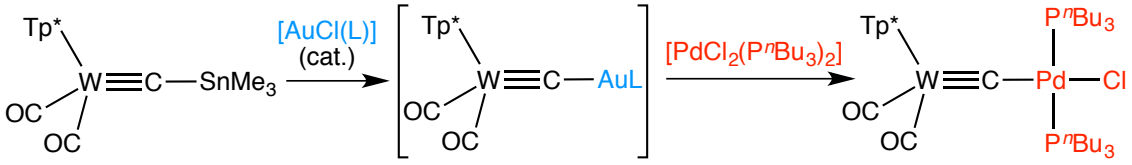

Scheme 2.7. Synthesis of a palladium carbido complex via the catalytic tandem transmetallation of a stannylcarbyne complex (L = AsPh$_3$, SMe$_2$).

A THF solution containing the stannylcarbyne complex [W(≡CSnMe$_3$)(CO)$_2$(Tp*)] and a catalytic amount of [AuCl(AsPh$_3$)] (7 mol%) was treated with PClPh$_2$ and the mixture was stirred overnight. The infrared spectrum revealed complete consumption of the stannylcarbyne and appearance of a number of new species. The ^{31}P{^{1}H} NMR spectrum likewise contained multiple peaks, but no evidence of the desired product **2** was seen in either the NMR or the IR spectra (Scheme 2.8).

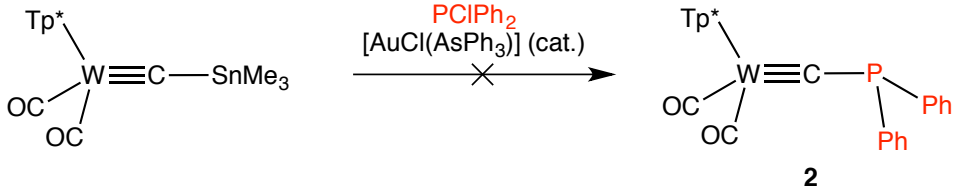

2

Scheme 2.8. Attempted synthesis of **2** via gold-catalysed electrophilic substitution of a stannylcarbyne complex.

Despite the failure of this reaction, the successful synthesis of **2** was achieved via both the lithiocarbyne method and via palladium-catalysed phosphination. With expedient access to this tungsten phosphinocarbyne complex, a detailed exploration of its reactivity was undertaken, the results of which are described in the following sections of this Chapter. Investigations into the synthesis and reactivity of other phosphinocarbyne complexes are presented in Chapters 3, 4 and 5.

2.5 Reactions with electrophiles

The complex **2** is attractive chemically because there are a number of potential sites available for functionalisation: the phosphine substituent, the carbyne carbon atom, the metal centre or the tungsten-carbyne bond. Reactions with electrophiles were carried out to probe the reactivity of **2** and identify preferential sites of reactivity.

2.5.1 Synthesis of [W(≡CPMePh$_2$)(CO)$_2$(Tp*)]I

Templeton and co-workers have synthesised a series of phosphoniocarbyne complexes [W(≡CPR$_3$)(CO)$_2$(Tp*)]PF$_6$ (R$_3$ = Me$_3$, Et$_3$, Cy$_3$, Ph$_3$, Me$_2$Ph) by treating the thiocarbyne [W(≡CSMe)(CO)$_2$(Tp*)] with excess PR$_3$ and NH$_4$PF$_6$,[62] or by treating the chlorocarbyne [W(≡CCl)(CO)$_2$(Tp*)] with PR$_3$ and KPF$_6$ (Scheme 1.8).[66] Transformation of **2** into a phosphoniocarbyne complex should be possible via simple P-alkylation. The provision of a platform for comparison in Templeton's complexes rendered this an obvious place to begin investigations.

Treatment of **2** with methyl iodide affords the methyldiphenylphosphoniocarbyne salt [W(≡CPMePh$_2$)(CO)$_2$(Tp*)]I ([**3**]I) (Scheme 2.9). The ^{31}P{^{1}H} NMR spectrum of [**3**]I contains a singlet with ^{183}W satellites at δ_P 12.2 showing a tungsten-phosphorus coupling of $^2J_{WP}$ 161.6 Hz, comparable to those observed for Templeton's complexes (e.g. [W(≡CPMe$_3$)(CO)$_2$(Tp*)]PF$_6$ δ_P 16.7, $^2J_{WP}$ 147 Hz).[62] Interestingly, the carbyne carbon atom appears in the ^{13}C{^{1}H} NMR spectrum as a singlet straddled by ^{183}W satellites at δ_C 242.8 with $^1J_{WC}$ 206.2 Hz. The absence of resolvable $^1J_{PC}$ coupling seems counter-intuitive, but is consistent with what is observed for other phosphoniocarbynes,[58,61,62,66,73,76,79] with the exception of [W(≡CPCy$_3$)(CO)$_2$(Tp*)]PF$_6$, [Re(≡CPPh$_3$)(SR)(N^{t}Bu)$_2$] (R = adamantyl, ^{t}Bu) and [TaCl(≡CPPh$_3$)(CHPPh$_3$)(Cp*)] which display very small carbon-phosphorus coupling constants between 7.5 and 15 Hz.[66,74,77,78]

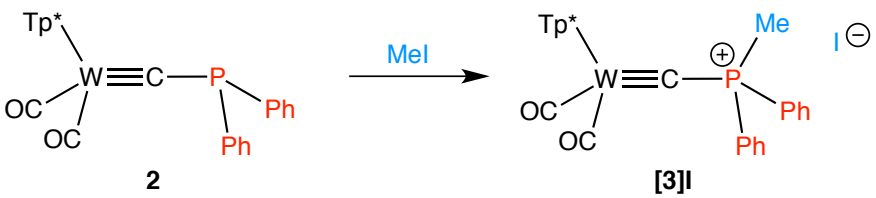

2 **[3]I**

Scheme 2.9. Synthesis of [W(≡CPMePh$_2$)(CO)$_2$(Tp*)]I ([**3**]I).

It seems somewhat puzzling that, in comparing [**3**]I to **2**, we observe a significant increase in $^{2}J_{WP}$ (69.0 to 161.6 Hz), a significant decrease in $^{1}J_{PC}$ (74.5 to ca. 0 Hz), and only a small increase in $^{1}J_{WC}$ (187.9 Hz to 206.2 Hz). It might be expected that the factors that dominate such coupling constants would be similar in all three cases. Typically, the increased coordination number at phosphorus in [**3**]I would be expected to lead to a decrease in the coupling constants because of the reduced *s* orbital contribution to the relevant bonds,[222,223] as seen for $^{1}J_{PC}$. One possible explanation for the attendant counter-intuitive *increase* in the magnitude of $^{2}J_{WP}$ could be the sign of the coupling. If the $^{2}J_{WP}$ coupling were negative (whilst $^{1}J_{PC}$ was positive), a reduction in the coupling would cause an increase in the absolute value, as was observed. Attempts to measure the sign of the $^{2}J_{WP}$ coupling experimentally were thwarted by the extremely low sensitivity of ^{183}W, and no reports of the sign of $^{2}J_{WP}$ couplings could be found in the literature. In the absence of a definitive rationalisation as to the origin of the observed divergence in magnitude, it can be noted that this is a recurrent phenomenon encountered throughout the work to follow.

2.5.2 Synthesis of [W(≡CPPh$_2$·BH$_3$)(CO)$_2$(Tp*)]

Phosphine-borane adducts are commonly used reagents in synthetic chemistry.[224,225] This synergistic relationship stems from the use of phosphines to stabilise boranes, and in turn boranes serve as useful protecting groups for phosphines. Inspired by the work of Miyoshi and co-workers in their synthesis of the metallated phosphine-borane adducts [Fe(PHPh·BR$_3$)(CO)$_2$(Cp)] (R = H, Cl),[226] it was envisaged that addition of borane to **2** might follow a similar path. However, Stone and co-workers have shown that BH$_3$·THF will add to the M≡C bond of more conventional carbyne complexes [W(≡CR)(CO)$_2$(L)] (R = Me, Ph, Tol; L = Cp, Cp*) to form the dimeric species [W$_2${μ-C(R)B(H)CH$_2$R}(CO)$_4$(L)$_2$] (Scheme 2.10).[227,228]

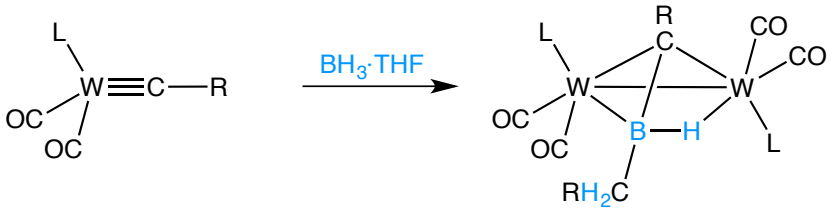

Scheme 2.10. Stone's hydroboration of carbyne complexes (L = Cp, Cp*; R = Me, Ph, Tol).

Wadepohl and co-workers found that the hydroboration of group 6 carbyne complexes charted differing routes depending on the co-ligand and the carbyne substituent (Scheme 2.11).[229,230] When the bulky Tp* ligand was utilised, formation of an η^2-B(R')CH_2R complex occurred, whereas with Cp* or η^5-C_5Me_4Et an α-boryl-η^3-benzyl complex or an η^2-CH_2=CH_2 complex was obtained. The reaction of **2** with borane might therefore take competitive courses, affording an opportunity to probe the reactivity at the phosphine compared to the W≡C bond.

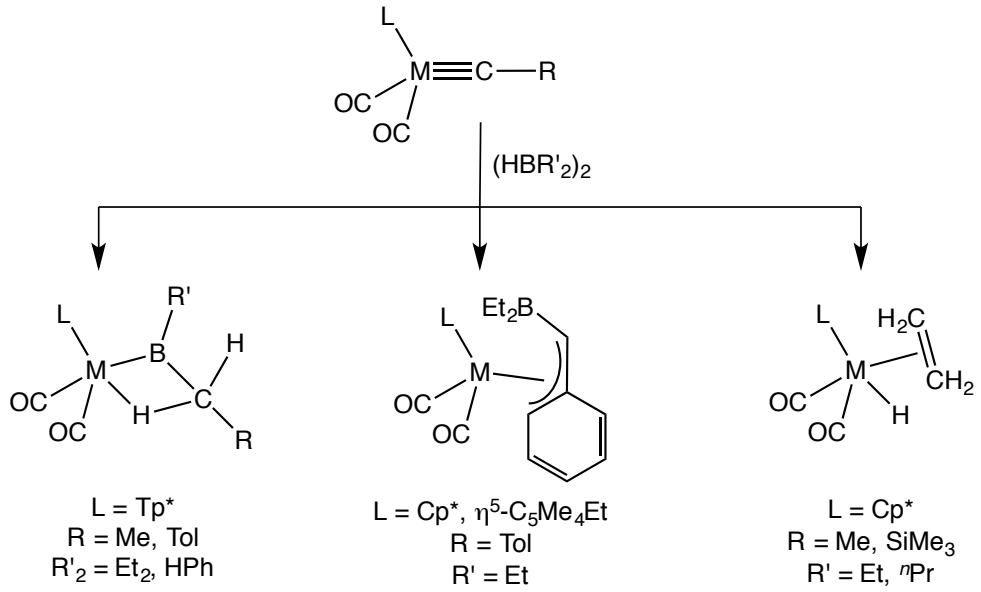

Scheme 2.11. Wadepohl's hydroboration of carbyne complexes (M = Mo, W).

An orange toluene solution of **2** was treated with 1.2 equivalents of $BH_3{\cdot}SMe_2$, resulting in overnight formation of a brown suspension. Infrared monitoring of the reaction mixture showed replacement of the starting material (ν_{CO} 1981, 1893 cm^{-1}) by new ν_{CO} absorptions at 2004 and 1917 cm^{-1} with shoulders at 1995 and 1906 cm^{-1}. Filtration and trituration of the resulting filtrate in Et_2O afforded the phosphine-borane adduct [W(≡C$PPh_2{\cdot}BH_3$)$(CO)_2$(Tp*)] (**4**) as a brown powder in 58% yield (Scheme 2.12).

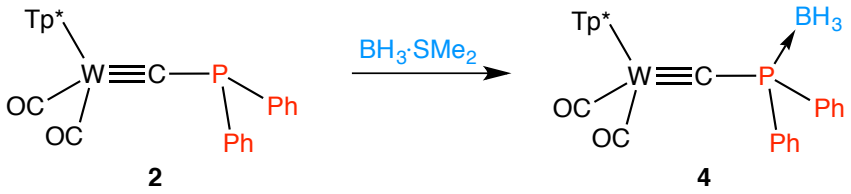

Scheme 2.12. Synthesis of [W(≡CPPh$_2$·BH$_3$)(CO)$_2$(Tp*)] (**4**).

Appending of the borane to phosphorus was confirmed by the $^{31}P\{^1H\}$ NMR spectrum of complex **4** which showed a broad peak at δ_P 32.0 due to coupling to the quadrupolar ^{11}B nucleus. The $^{11}B\{^1H\}$ NMR spectrum showed two singlets, one at δ_B −10.1 corresponding to the Tp* boron and one at δ_B −37.8 due to the BH$_3$ group, both within the typical region of four-coordinate boron. A proton-coupled ^{11}B NMR spectrum was acquired, but no coupling to the attached protons was resolved as is typical in non-symmetrical boron environments.

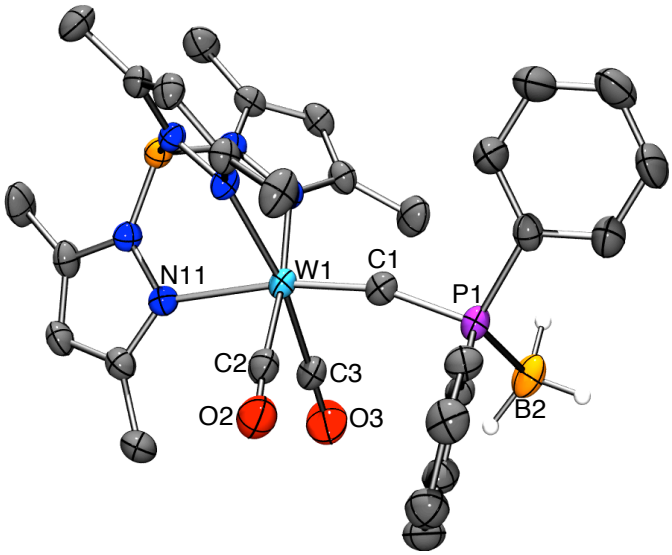

Figure 2.7. Molecular structure of **4** in a crystal of **4**·CHCl$_3$ (50% displacement ellipsoids, selected hydrogen atoms omitted). Selected bond lengths (Å) and angles (°): W1−C1 1.824(4), C1−P1 1.782(4), P1−B2 1.935(5), W1−C1−P1 164.1(2), C1−P1−B2 115.5(2).

Crystals of **4** obtained from CHCl$_3$/hexane were the subject of an X-ray crystallographic study, the results of which are summarised in Figure 2.7. The structural features of the [W(≡CP)(CO)$_2$(Tp*)] fragment are largely unremarkable. The geometry about P1 is pseudo-tetrahedral, with the most obtuse angle being that of C1−P1−B2 (115.5(2)°). The P1−B2 bond length of 1.935(5) Å is similar to that in the related compounds (*S*,*S*)-

{P(C≡CPh)(^{t}Bu)(BH_3)}$_2C_2H_4$ (average P−B distance 1.918 Å)[231] and Ph_3PBH_3 (average P−B distance 1.917 Å).[232]

Under the conditions used, no evidence of a reaction between BH_3 and the W≡C bond was observed, in contrast to Stone and Wadepohl's work. Heating a solution of **4** to 80°C in toluene-d_8 resulted in no change other than partial decomposition of **4** to regenerate **2** via loss of BH_3, as indicated by the ^1H and $^{31}P\{^1H\}$ NMR spectra. No peaks that might correspond to BH_3 migration to W≡C were observed.

2.6 Protonation of [W(≡CPPh$_2$)(CO)$_2$(Tp*)]

2.6.1 Protonation of carbyne complexes

The reactivity of **2** towards electrophiles displayed thus far raises the question of the simplest electrophile, H^+. In contrast to amines, phosphines are comparatively weak bases (e.g. pK_a (MeCN) PMe_3 = 15.5,[233] NMe_3 = 17.6[234]). Protonation of carbyne complexes is known to take a variety of routes: protonation at the metal centre, the M≡C bond or the carbyne carbon atom,[235-238] with a number of factors involved in determining the site of protonation. Molecular orbital calculations suggest frontier orbital controlled protonation occurs at the metal centre, whereas charge-controlled protonation is directed at the carbyne carbon atom.[239,240] McElwee-White and co-workers found that electronic effects determine the ultimate site of protonation in the series [Mo(≡CBu)(L)$_2$(L')] (L = CO, $P(OMe)_3$, $P(OPh)_3$; L' = Cp, Tp).[236] Increasing the basicity at the metal shifts the site of protonation from the carbon to the metal centre, as outlined in Scheme 2.13.

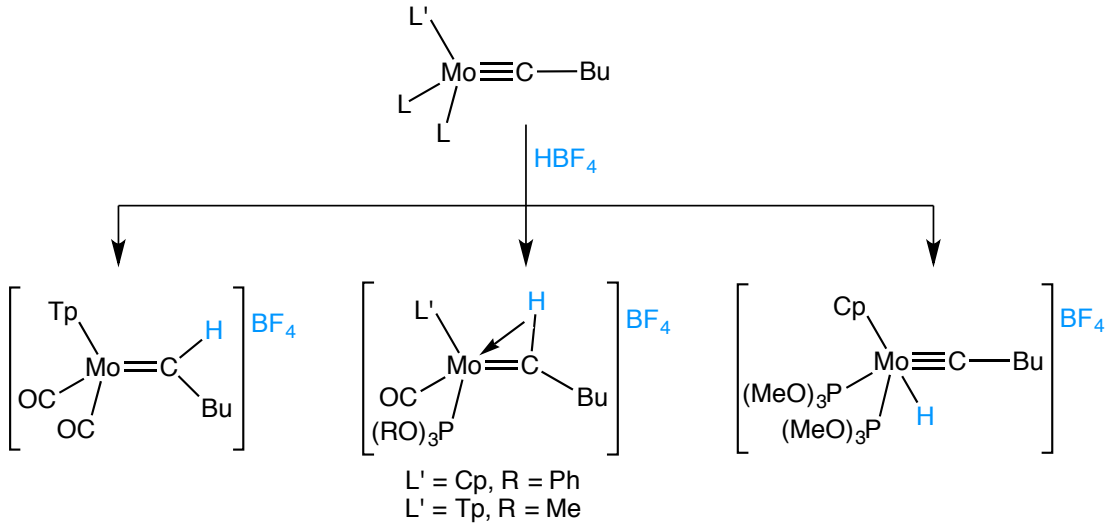

Scheme 2.13. Effect of ligand variation on the site of protonation (L' = Cp, Tp; L = CO, $P(OMe)_3$, $P(OPh)_3$).

In the case of $[W(\equiv CH)Cl(L)_4]$ (L_4 = $(PMe_3)_4$, $(dmpe)_2$), the outcome of protonation with HOTf differs based on the sterics of the phosphine co-ligands.[237,238] With dmpe co-ligands, protonation occurs at the metal centre to give $[WH(\equiv CH)Cl(dmpe)_2]^+$, whereas with PMe_3 co-ligands protonation gives an α-agostic complex $[W(=CH_2)Cl(PMe_3)_4]^+$. This was rationalised sterically by the fact that a pentagonal $H(PMe_3)_4$ coordination plane is inaccessible, whereas the smaller dmpe ligands can accommodate the requisite trigonal bipyramidal structure.

Predicting the outcome of protonation is further complicated by the distinction between kinetic and thermodynamic sites of protonation that arises in some cases.[235] For example, protonation of $[Mo(\equiv CCH_2{}^tBu)\{P(OMe)_3\}_2(Cp)]$ with HBF_4 occurs initially at the carbyne carbon atom to form $[Mo(=CHCH_2{}^tBu)\{P(OMe)_3\}_2(Cp)]^+$. A subsequent α-hydride elimination reaction transpires, resulting in the cationic hydride complex $[MoH(\equiv CCH_2{}^tBu)\{P(OMe)_3\}_2(Cp)]^+$.[241]

2.6.2 Synthesis of $[W(\equiv CPHPh_2)(CO)_2(Tp^*)]BF_4$ and $[W\{\eta^2\text{-}C(H)PPh_2\}(CO)_2(Tp^*)]BF_4$

This array of possible outcomes prompted an investigation into the reactivity of **2** with Brønsted acids. A suspension of **2** in Et_2O at –78°C was treated with $HBF_4{\cdot}Et_2O$. Upon warming to room temperature a pink precipitate formed ([**5**]BF_4) which was isolated by filtration. This precipitate was dissolved in $CDCl_3$ or CD_3CN for NMR analysis,

resulting in a dark purple solution. The ^{1}H, $^{13}C\{^{1}H\}$ and $^{31}P\{^{1}H\}$ NMR spectra are consistent with the formulation of an η^2-carbene complex $[W\{\eta^2\text{-}C(H)PPh_2\}(CO)_2(Tp^*)]BF_4$ ([**6**]BF_4), resulting from protonation at the carbyne carbon atom (Scheme 2.14). The $^{31}P\{^{1}H\}$ NMR spectrum contains a singlet at δ_P −101.3 ($CDCl_3$) with ^{183}W satellites ($^{1}J_{WP}$ 138.5 Hz). This resonance is shifted 130 ppm upfield compared to the starting material (δ_P 32.0), diagnostic of a phosphorus-containing three-membered ring,[242,243] and within the range for other $M\{\eta^2\text{-}C(R)PR'_2\}$ complexes (−94 to −155 ppm).[69,109,114-118]

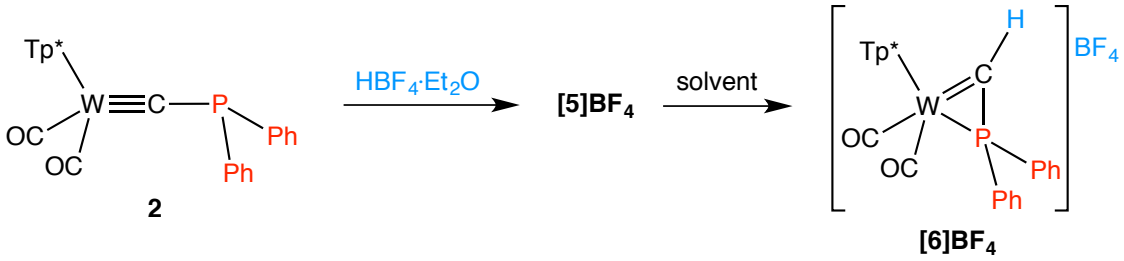

Scheme 2.14. Protonation of **2** with $HBF_4{\cdot}Et_2O$ (solvent = CH_2Cl_2, $CHCl_3$, MeCN).

The ^{1}H NMR spectrum includes a doublet resonance at δ_H 14.78, straddled by ^{183}W satellites, with couplings of $^{2}J_{PH}$ 4.8 Hz and $^{2}J_{WH}$ 13.8 Hz. The significantly downfield chemical shift is characteristic of a secondary carbene M=CH peak, comparable to those observed in $[W\{\eta^2\text{-}C(H)PC(NEt_2)_2\}(CO)_2(Tp^*)]OTf$ (δ_H 14.24, $^{2}J_{PH}$ 16.9 Hz),[69] $[W\{\eta^2\text{-}C(H)PMe_2\}(H)(PMe_3)_4]I$ (δ_H 11.86, $^{2}J_{PH}$ 11),[118] $[W\{\eta^2\text{-}C(H)SMe\}(CO)_2(Tp)]OTf$ (δ_H 12.93)[244] and $[W\{\eta^2\text{-}C(H)SMe\}(CO)_2\{CH(pz)_3\}][BF_4]_2$ (δ_H 13.15).[245] Although the magnitude of the P−H coupling is smaller in [**6**]BF_4 than in these previously reported carbenes (4.8 *cf.* 11 and 16.9 Hz), Weber's complex is a phosphaalkenylcarbene (rather than a phosphinocarbene) so a higher degree of *s*-character exists in the phosphorus-carbon bond. The Tp* resonances appear in a 2:1 ratio, consistent with either a mirror plane through the WCHP moiety or a fluxional process allowing rotation of the $HCPPh_2$ unit.

The $^{13}C\{^{1}H\}$ NMR spectrum showed, in addition to the Tp*, Ph and CO resonances, a peak at 237.1 ppm corresponding to the carbene carbon atom. The $^{1}J_{PC}$ coupling of 46.3 Hz is within the expected range for salts of the type $[W\{\eta^2\text{-}C(R)PR'R''\}(CO)_2(L)]^+$ of 17.5 - 62.5 Hz.[115,116] Coupling to ^{183}W is observed ($^{1}J_{WC}$ 21.5 Hz). Most previous

relevant work has not reported the W−C coupling constant, presumably due to low signal-to-noise ratios (^{183}W 14% natural abundance). Kreissl has, however, reported W−C coupling values of 53.3 Hz (R = Me) and 34.9 Hz (R = Ph) for [W{η^2-C(R)PPh$_2$}(CO)(PMe$_3$)(Cp)]PF$_6$,[114,117] these being somewhat larger than that seen for [**6**]BF$_4$. The ^{1}H-coupled ^{13}C NMR spectrum reveals the one-bond C−H coupling of the carbene carbon to be 199.0 Hz, comparable to what is seen in [W{η^2-C(H)SMe}(CO)$_2$(Tp)]$^+$ (211 Hz) but much larger than those seen in η^1-carbene complexes such as [Fe(=CHPh)(CO)$_2$(Cp)]$^+$ (δ_C 324.4, $^1J_{CH}$ 146 Hz),[246] [W(=CHNEt$_2$)(CN^{t}Bu)(CO)$_2$(Cp*)]PF$_6$ (δ_C 233.5, $^1J_{CH}$ 137 Hz)[184] and *syn*-[Mo(=CHPPh$_2$)(=NDipp)(OC$_6$HPh$_4$-2,3,5,6){N(C(Me)CH)$_2$}] (δ_C 276, $^1J_{CH}$ 130 Hz).[128]

In the IR spectrum in CH$_2$Cl$_2$ carbonyl absorptions are observed at 2054 and 1982 cm^{-1}. These bands appear at significantly higher frequencies than those of the starting material **2** (1982, 1891 cm^{-1}) due to the decreased electron density available at the metal centre in the cationic species [**6**]BF$_4$. Again, these absorptions are similar to those in the related thiocarbene [W{η^2-C(H)SMe}(CO)$_2$(Tp)]OTf (2067, 1996 cm^{-1})[244] and phosphinocarbene complexes [W{η^2-C(Ph)PPh$_2$}(CO)$_2$(Tp)]PF$_6$ (2036, 1969 cm^{-1}).[116]

For carbynes bearing heteroatom substituents, precedent exists for the formation of η^2-carbenes upon protonation.[69,244,245] The thiocarbyne complex [W(≡CSMe)(CO)$_2$(Tp)] reacts with strong acids to provide the η^2-carbene complex [W{η^2-C(H)SMe}(CO)$_2$(Tp)]$^+$ containing a W−C−S metallacyclopropene ring (Scheme 2.15).[244] Similarly, Weber has found that protonation of the phosphaalkenylcarbyne complex [W{≡CPC(NEt$_2$)$_2$}(CO)$_2$(Tp*)] leads to [W{η^2-C(H)PC(NEt$_2$)$_2$}(CO)$_2$(Tp*)]$^+$, albeit via [W{≡CPHC(NEt$_2$)$_2$}(CO)$_2$(Tp*)]$^+$.[69]

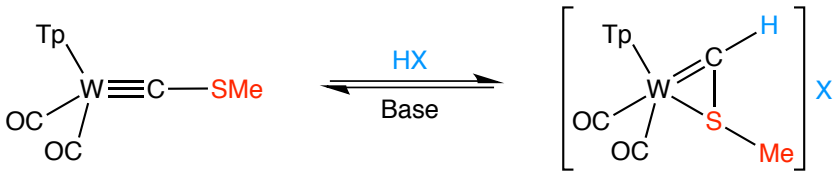

Scheme 2.15. Angelici's protonation of a thiocarbyne to produce an η^2-carbene (X = BF$_4$, CF$_3$SO$_3$, CF$_3$CO$_2$).

A variety of strategies exist for the preparation of η^2-phosphinocarbenes.[109] Kreissl and co-workers have effected addition of $[PR'R'']^+$ across the M≡C bond of aryl- and alkylcarbyne complexes to produce $[M\{\eta^2\text{-}C(R)PR'R''\}(CO)_2(L)]X$ (M = Mo, W; L = Cp, $\eta^5\text{-}C_5H_4Me$, Tp; R = Me, Ph, Tol; R' = R'' = Me, Ph; R' = Me, R'' = Cl) using PClR'R'' in the presence of a halide abstracting agent ($NaBPh_4$, $TlPF_6$) (Scheme 2.16). Decarbonylation of the tungstaphosphabicyclo[1.1.0]butanone salt $[W\{\kappa^3\text{-}C(O)C(R)PPh_2\}(CO)(PMe_3)(Cp)]PF_6$ under mild conditions (30 – 38°C, 1 – 2 hours) furnishes the η^2-phosphinocarbene salt $[W\{\eta^2\text{-}C(R)PPh_2\}(CO)(PMe_3)(Cp)]PF_6$ (Scheme 2.16).[114,117] Other examples of η^2-phosphinocarbene complexes include: the thermal rearrangement of $[W\{=C(NEt_2)PMePh\}(CO)_4(PHMePh)]$ to $[W\{\eta^2\text{-}C(NEt_2)PMePh\}(CO)_4]$;[119] the reduction of the tantalum complexes $[TaCl_5]$ and $[TaCl_4(Cp^*)]$ with sodium in PMe_3 to give $[Ta\{\eta^2\text{-}C(H)PMe_2\}\{\eta^2\text{-}CH_2PMe_2\}(PMe_3)_3]$[120,121,123] and $[Ta\{\eta^2\text{-}C(H)PMe_2\}(H)_2(PMe_3)(Cp^*)]$,[122] respectively, via double C−H activation; and hydride abstraction from $[W\{\eta^2\text{-}CH_2PMe_2\}(H)(PMe_3)_4]$ with ArX to give $[W\{\eta^2\text{-}C(H)PMe_2\}(H)(PMe_3)_4]X$ (X = Br, I; Ar = Ph, Tol).[118] This is another point wherein the reactivities of phosphorus and nitrogen contrast in such systems; η^2-aminocarbenes are extremely rare (known only for $[M\{\eta^2\text{-}C(N^iPr_2)N^iPr_2\}(CO)_4]$ (M = Cr, Mo, W)),[247,248] and protonation of aminocarbynes yields η^1-aminocarbene complexes.[182-184,249]

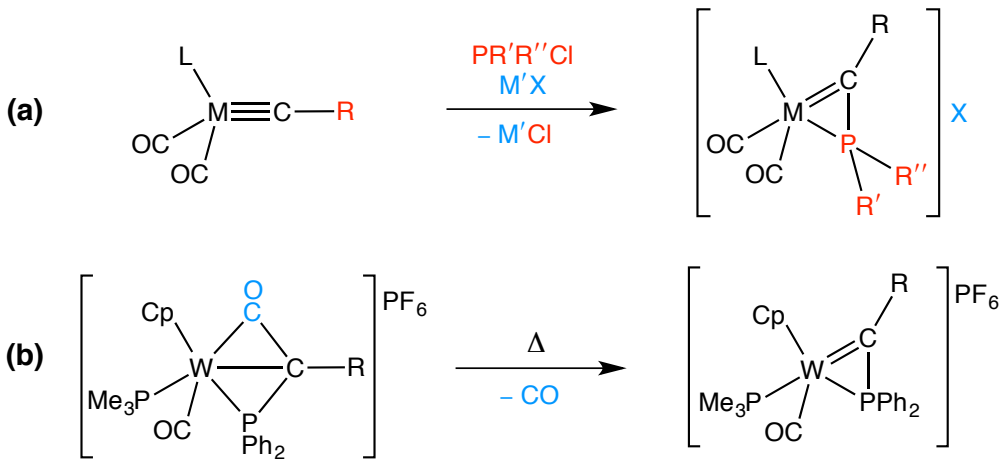

Scheme 2.16. Kreissl's synthesis of η^2-phosphinocarbene salts via (a) electrophilic addition (M = Mo, W; L = Cp, $\eta^5\text{-}C_5H_4Me$, Tp; R = Me, Ph, Tol; R' = R'' = Me, Ph; R' = Me, R'' = Cl; M'X = $NaBPh_4$, $TlPF_6$) or (b) decarbonylation (R = Me, Ph).

Intriguingly, the solid state IR spectrum (Nujol) of the isolated pink precipitate [**5**]BF_4 showed CO stretching frequencies at 2022 and 1937 cm^{-1}, to significantly lower frequency than what was observed in the CH_2Cl_2 solution infrared spectrum of 2054 and 1982 cm^{-1}. Such a significant shift (ca. 45 cm^{-1}) seemed unlikely to be due to solid state effects, and instead suggested that these spectra were actually of different compounds. Having acquired all the solution NMR data, we were confident that the η^2-phosphinocarbene [**6**]BF_4 was indeed the thermodynamic product of the reaction. This suggested that the isolated pink precipitate [**5**]BF_4 was in fact the kinetic product, which subsequently underwent a transformation when dissolved in solution (CH_2Cl_2, $CHCl_3$, CH_3CN) to provide [**6**]BF_4.

The possible sites of initial protonation are the phosphine, the metal centre, the carbon atom (without pendant PPh_2 stabilisation of tungsten) or the W≡C bond, depicted in Scheme 2.17. Following Marcus theory, Norton has identified that significant structural and electronic changes leads to slow rates of protonation.[250] Protonation of lone pairs of electrons on heteroatoms is fast because little structural and electronic modification is required. A low energy barrier for protonation is consistently observed, resulting in the heteroatom as the kinetic site of protonation. Protonation at carbon and transition metal atoms is, in contrast, slow because it requires considerable electronic and structural rearrangement, leading to high kinetic barriers. Based on Norton's theories, we would expect that the phosphine would be the kinetic site of protonation in [**5**]BF_4.

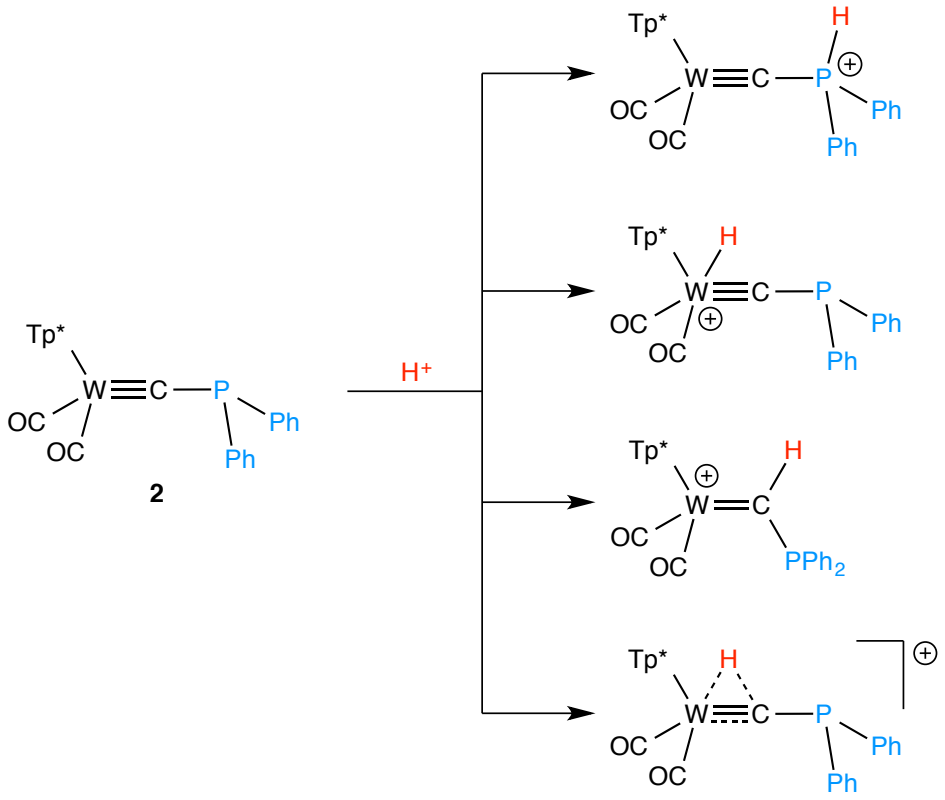

Scheme 2.17. Possible sites of kinetic protonation of **2**.

The rearrangement of the kinetic product [**5**]BF_4 to [**6**]BF_4 was very rapid in solution which precluded acquisition of NMR data for this intermediate. Conversion of [**5**]BF_4 to [**6**]BF_4 in CH_2Cl_2 was monitored by IR spectroscopy. After two minutes in solution the IR spectrum indicated [**6**]BF_4 to be the major component (2054, 1982 cm^{-1}), although peaks attributable to [**5**]BF_4 remained evident at 2022 and 1937 cm^{-1}. However, these do not persist beyond six minutes. As we were unable to obtain spectroscopic data for [**5**]BF_4 in solution, we were limited to interrogating the IR data to infer its structure. On the basis of this, in conjunction with Norton-Marcus considerations, [**5**]BF_4 is postulated to be the phosphonium salt [W(≡CPHPh$_2$)(CO)$_2$(Tp*)]BF_4 (Scheme 2.18). The ν_{CO} frequencies (Nujol: 2022, 1937 cm^{-1}) are in a similar region to those seen for other phosphonium carbyne salts [W(≡CPR$_3$)(CO)$_2$(Tp*)]PF_6 of 2026 – 2015 and 1940 – 1933 cm^{-1} (R$_3$ = Me$_3$, Et$_3$, Cy$_3$, Ph$_3$, Me$_2$Ph; CH_2Cl_2 solution),[62,66] and 2015 and 1925 cm^{-1} for [W(≡CPMePh$_2$)(CO)$_2$(Tp*)]I ([**3**]I, Nujol). The ν_{CO} absorptions of [W(≡CPMePh$_2$)(CO)$_2$(Tp*)]$^+$ are shifted to slightly lower frequency than those for [**5**]BF_4, consistent with $PMePh_2$ being a stronger electron donor than $PHPh_2$, thus rendering the metal more electron rich.

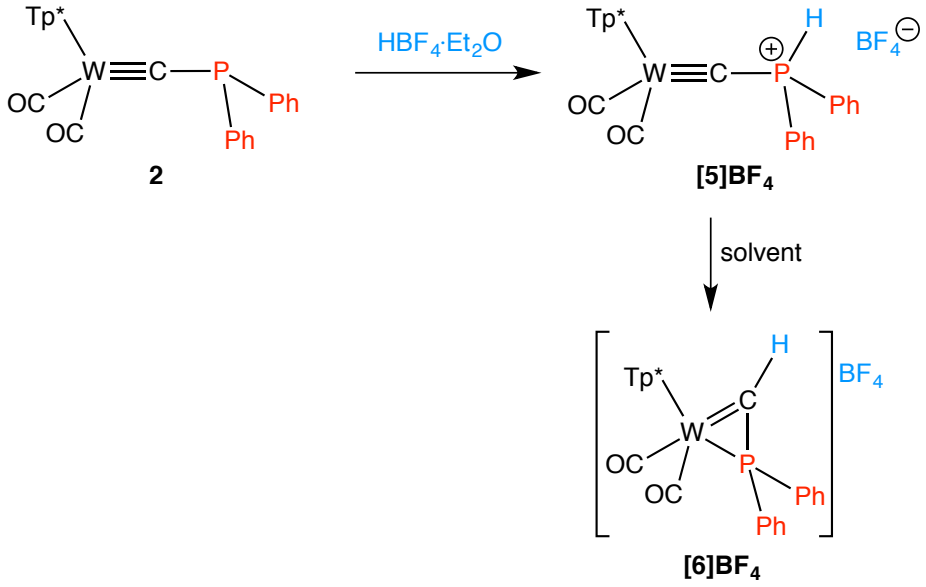

Scheme 2.18. Kinetic ([**5**]BF_4) and thermodynamic ([**6**]BF_4) products of protonation of **2** with $HBF_4{\cdot}Et_2O$ (solvent = CH_2Cl_2, $CHCl_3$, MeCN).

Unfortunately, the W≡C bond is not readily identifiable in IR spectra of these species. No ν_{WH} absorption could be identified in the IR spectrum, but this is not conclusive evidence that protonation did not occur on the metal because ν_{MH} modes are not unambiguously identifiable in IR spectra, may be weak, and typically couple with ν_{CO} modes. There is a very weak absorption in the infrared spectrum at 2457 cm^{-1}, which is proposed to be the ν_{PH} mode of [**5**]BF_4 and which is absent from the infrared spectrum of [**6**]BF_4. This absorption is in the expected region for a P–H phosphonium salt (e.g. $[HPPh_3][WCl_4(O)(OPPh_3)]$ ν_{PH} 2415 cm^{-1} and $[dppeH_2]_3[MoCl_6]_2{\cdot}12H_2O$ ν_{PH} 2400 cm^{-1}).[251,252] However, as the absorption is very weak, the assignment is not conclusive but is nevertheless consistent with the formulation of [**5**]BF_4. Further support for kinetic protonation at a heteroatom, i.e. phosphorus, is provided by the observation that [**5**]BF_4 is very easily deprotonated. Solutions of [**5**]BF_4 in the weakly basic solvents THF or Et_2O are orange, not purple, and contain the phosphinocarbyne **2**, as confirmed by NMR and IR spectroscopies.

With trifluoromethanesulfonic acid (HOTf) the reaction proceeds in an analogous manner to $HBF_4{\cdot}Et_2O$, but less cleanly, and the product formed is less stable than the BF_4^- salt. After stirring overnight in Et_2O $[W\{\eta^2\text{-}C(H)PPh_2\}(CO)_2(Tp^*)]OTf$ is present in the reaction mixture, as indicated by ^1H NMR spectroscopy (CD_3CN), but is accompanied by a significant number of other species.

By analogy with Templeton's synthesis,[62,66] it was envisaged that the reaction of **1** with the secondary phosphine $PHPh_2$ might furnish the phosphoniocarbyne $[\mathbf{5}]^+$ or the rearranged product $[\mathbf{6}]^+$. An acetonitrile solution of $[W(\equiv CBr)(CO)_2(Tp^*)]$ and $NaBF_4$ was treated with $PHPh_2$ and the reaction was monitored by IR spectroscopy (Scheme 2.19). After two days at 82°C the infrared spectrum indicated that **1** was still present, in addition to a number of other absorptions in the carbonyl region (2022 (w), 2002 (w), 1937 (m), 1917 (m), 1819 (m) cm^{-1}), none of which correspond to $[\mathbf{6}]BF_4$ (2054, 1892 cm^{-1} in CH_2Cl_2). However, the bands at 2022 and 1937 cm^{-1} were suggestive of $[\mathbf{5}]BF_4$ for which the carbonyl absorptions appear at 2022 and 1937 cm^{-1} in the CH_2Cl_2 spectrum. However, neither product was identifiable in the ^1H and $^{31}P\{^1H\}$ spectra in $CDCl_3$. The $^{31}P\{^1H\}$ NMR spectrum of the reaction mixture indicated a large number of products in the range −40 to 80 ppm, while a peak due to the desired product (δ_P −101.3) was conspicuously absent.

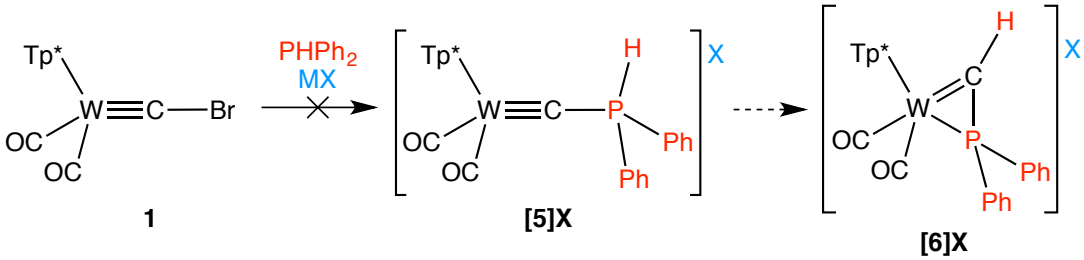

Scheme 2.19. Attempted synthesis of [**5**]X or [**6**]X using Templeton's route (MX = $NaBF_4$, $TlPF_6$).

When the reaction was carried out using $TlPF_6$, a more effective halide abstracting agent, no evidence for $[\mathbf{6}]^+$ was seen in the ^1H or $^{31}P\{^1H\}$ NMR spectra, even after five days. The ^1H NMR spectrum showed mainly unreacted **1**, while the largest peak in the $^{31}P\{^1H\}$ NMR spectrum was, interestingly, that of **2**. Although based on the ^1H NMR spectrum this represents a minor component of the overall mixture, its formation is consistent with the rapid deprotonation of transient $[\mathbf{5}]^+$ prior to rearrangement under these conditions.

The lack of success in this reaction is an interesting contrast to Templeton's work. Although the reaction was only reported using tertiary phosphines, the reaction time and temperature required were found to increase with the steric bulk of the phosphine

(PMe_2Ph eight hours room temperature, PPh_3 two days 82°C, PCy_3 four days 82°C). Therefore on steric grounds the reaction with $PHPh_2$ would be expected to be facile, though on electronic grounds primary and secondary phosphines are less basic or nucleophilic than tertiary phosphines.[253]

Following the work of Kreissl[114,116] an alternative route to [**6**]BF_4 was explored. A suspension of the methylidyne complex [W(≡CH)$(CO)_2$(Tp*)] and $NaBF_4$ in Et_2O was treated with $PClPh_2$ and allowed to stir for 24 hours. Instead of producing the expected purple colour of [**6**]BF_4, a brown suspension was obtained, NMR analysis (CD_3CN) of which unfortunately indicated that none of the desired η^2-phosphinocarbene had been formed in the reaction (Scheme 2.20).

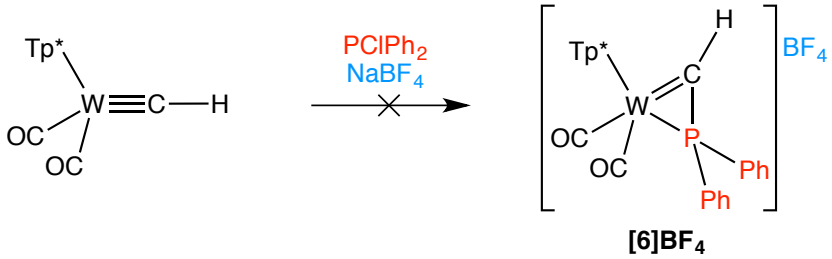

Scheme 2.20. Attempted synthesis of [**6**]BF_4 using Kreissl's methodology.

2.6.3 Computational studies

Calculations performed by Dr Manab Sharma on $[\mathbf{5}]^+$ and $[\mathbf{6}]^+$ reconciled the irreversible isomerisation observed experimentally with the relative energies of the two isomers ($\Delta G_{\mathbf{5}\rightarrow\mathbf{6}}$ −22.4 kJ/mol (gas phase)). Interrogation of an intramolecular proton-transfer process found that this pathway was not accessible as it required traversing a transition state 171.5 kJ/mol higher in energy than $[\mathbf{5}]^+$ (Figure 2.8). It was thus concluded that the $[\mathbf{5}]^+ \rightarrow [\mathbf{6}]^+$ isomerisation must involve *intermolecular* proton transfer via the solvent, rather than a concerted phosphorus to carbon proton transfer. The combined experimental and computational evidence suggests that protonation at phosphorus is rapid but reversible, whereas the subsequent direct protonation at carbon is slow but irreversible.

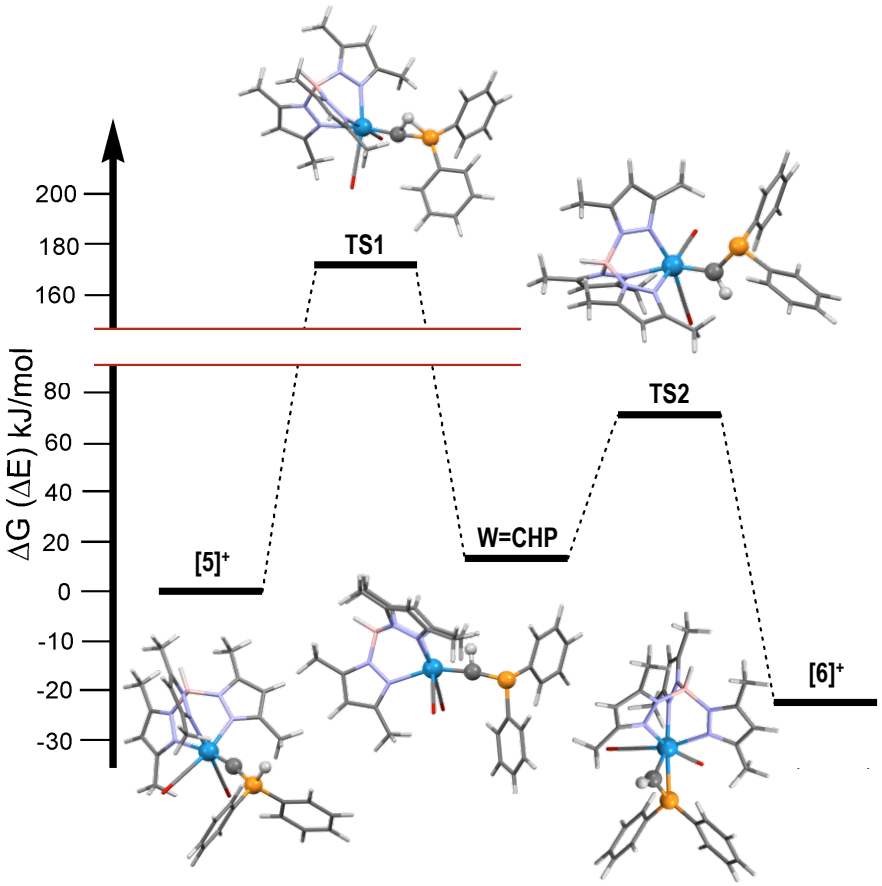

Figure 2.8. Calculated prototropic trajectory for the intramolecular isomerisation of $[\mathbf{5}]^+$ to $[\mathbf{6}]^+$ via the intermediate $[W(=CHPPh_2)(CO)_2(Tp^*)]$.

2.6.4 Reactivity of $[W\{\eta^2\text{-}C(H)PPh_2\}(CO)_2(Tp^*)]BF_4$

Attempted deprotonation of $[W\{\eta^2\text{-}C(H)PPh_2\}(CO)_2(Tp^*)]BF_4$

In Angelici's η^2-thiocarbene salts a degree of reversibility in the protonation reaction was observed. Upon treatment with a diverse range of bases, partial reversion to $[W(\equiv CSMe)(CO)_2(Tp)]$ was observed (Scheme 2.15).[244,254] These reactions also produced another isolable product $[W\{\eta^2\text{-}CH(SMe)SMe\}(CO)_2(Tp)]$ (Scheme 2.21) in yields of 5 – 40%. Similar bis(thiolato)alkyl complexes were obtained from the reactions of the thiolatocarbenes $[Mo\{\eta^2\text{-}C(SMe)Ar\}(CO)_2(Tp)]BF_4$ (Ar = C_6H_4OMe-4) with thiols.[255] Reducing agents ($Na[C_{10}H_8]$, $Na[Fe(CO)_2(Cp)]$, $[N(Ph_3P)_2][Co(CO)_4]$) also give rise to these two products, suggesting that the bases used may in fact be acting as reducing agents. The mechanism of this rearrangement is unclear, but transfer of SMe^- must be involved, which was attributed to the propensity of the SMe^- group to act as a good leaving group.

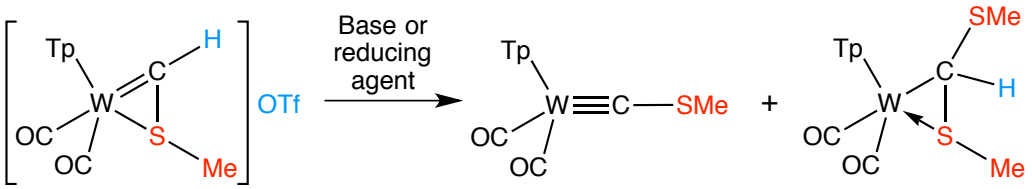

Scheme 2.21. Angelici's reactions of [W{η^2-C(H)SMe}(CO)$_2$(Tp)]OTf with bases and reducing agents.

Attempts to deprotonate [**6**]BF_4 were less successful. Addition of NEt_3 to a sample of [**6**]BF_4 in $CDCl_3$ resulted in no reaction over the course of four days, other than the gradual partial decomposition of [**6**]BF_4 to give a number of species in the range δ_P 40 to −20. No peak corresponding to **2** was seen in the $^{31}P\{^1H\}$ NMR spectrum (δ_P 32.0) (Scheme 2.22). In Angelici's case, although the yields were often low, deprotonation was seen with a large range of bases including amines, and the reaction times were only three hours. The complete absence of **2** in the spectra of this reaction indicates that [**6**]BF_4 is less acidic than its thiocarbene counterpart.

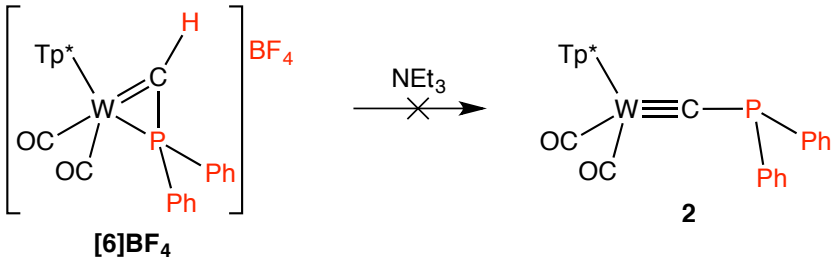

Scheme 2.22. Attempted deprotonation of [**6**]BF_4.

Reaction with $NaBH_4$

In light of Angelici's work,[245,254] the reactivity of [**6**]BF_4 towards $NaBH_4$ was explored with three possible products being envisaged (Scheme 2.23). The $NaBH_4$ might act as a base, to produce **2** (or its BH_3 adduct **4**), which would seem unlikely as no evidence of **2** was seen when NEt_3 was used as the base. The $NaBH_4$ may act as a hydride source, which would be expected to result in nucleophilic attack at the carbene to produce [W(η^2-CH_2PPh_2)(CO)$_2$(Tp*)], similar to nucleophilic addition reactions seen by Kreissl.[256] The third option is addition of a PPh_2 moiety to the carbene carbon to afford [W{η^2-$CH(PPh_2)PPh_2$}(CO)$_2$(Tp*)] as was seen for the thiocarbene.

A solution of [**6**]BF_4 and $NaBH_4$ in CD_2Cl_2 was monitored by ^1H and $^{31}P\{^1H\}$ NMR spectroscopy, but no reaction was observed over the course of eight days (Scheme 2.23). This again exemplifies the differing reactivities of the phosphino- and thiocarbene complexes. It is, however, not surprising that [W{η^2-$CH(PPh_2)PPh_2$}$(CO)_2$(Tp*)] was not observed as the thiocarbene example implicates the SMe^- leaving group, whereas PPh_2^- is a much poorer leaving group.

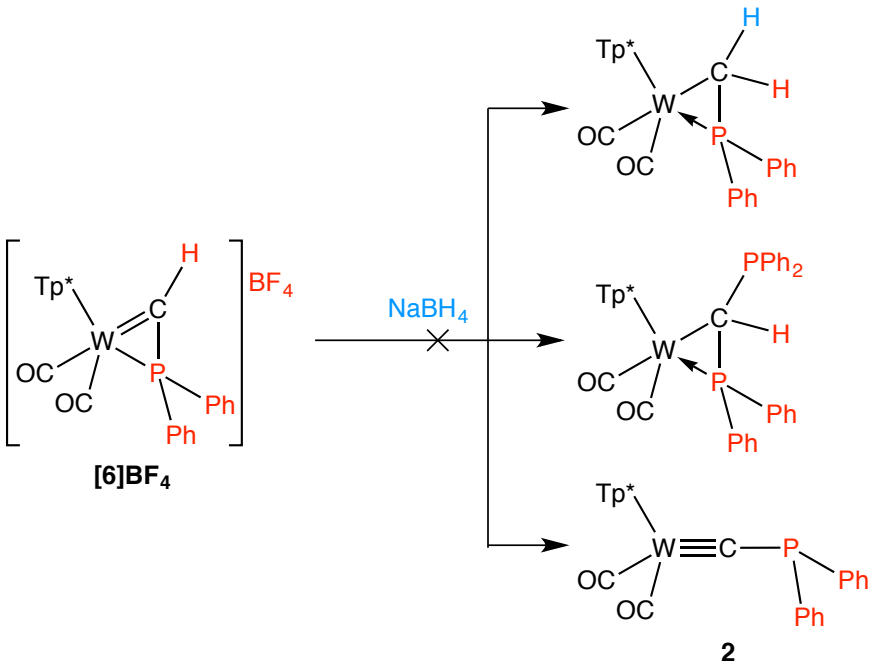

Scheme 2.23. Attempted reaction of $NaBH_4$ with [**6**]BF_4.

Reaction with [N^nBu_4]I

Difficulties in the purification and crystallisation of [**6**]BF_4 led us to investigate the reaction of [**6**]BF_4 with iodide, in anticipation of iodide/carbonyl substitution resulting in the neutral complex [W{η^2-C(H)PPh_2}I(CO)(Tp*)], which could then afford the possibility of purification via chromatography. A solution of [**6**]BF_4 and [N^nBu_4]I in CD_2Cl_2 was monitored by ^1H and $^{31}P\{^1H\}$ NMR spectroscopy over the course of four days (Scheme 2.24). No reaction was observed except for the gradual partial decomposition of [**6**]BF_4 to a number of species (δ_P 40 to −32), akin to what was seen for decomposition of [**6**]BF_4 in the presence of $NaBH_4$. This demonstrates that, despite the decreased retrodonation to the carbonyl ligands in the positively charged [**6**]BF_4, the carbonyl ligands remain strongly bound to the metal centre.

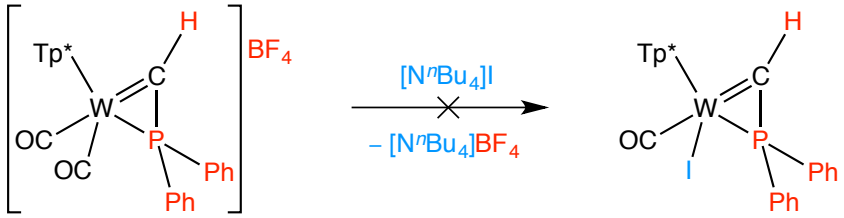

Scheme 2.24. Attempted reaction of [**6**]BF_4 with [N^nBu_4]I.

2.7 Metallation reactions

Phosphines are ubiquitous in coordination chemistry as ligands for transition metals. Stone and co-workers have extensively researched the coordination of carbyne complexes to transition metals and shown that complexation of the metal-carbon bond to one or two metals occurs readily.[257-270] Complex **2** offers the opportunity to probe the donor properties of the phosphine versus the tungsten-carbon bond through reactions with metal complexes.

2.7.1 Synthesis of [W{≡CPPh$_2$RhCl$_2$(Cp*)}(CO)$_2$(Tp*)]

Alkynylphosphines have been shown to react with the rhodium, iridium and ruthenium dimers [MCl_2(Cp*)]$_2$ to form P-coordinated species, an example of which is shown in Scheme 2.25.[271] These species can undergo subsequent reactions with *cis*-[Pt(C_6F_5)$_2$(THF)$_2$], via displacement of the labile THF ligands, to give bimetallic species with bridging chloride ligands or via coordination of the alkyne. The analogous reaction with [$RhCl_2$(Cp*)]$_2$ and **2** was investigated to see if this would yield the equivalent P-coordinated species.

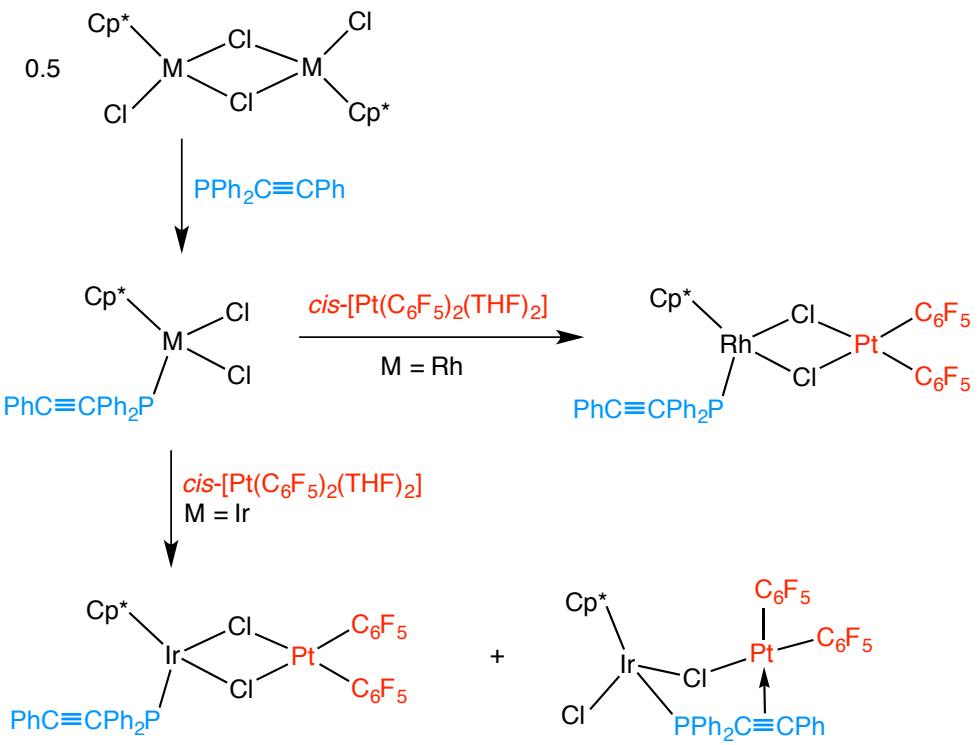

Scheme 2.25. Forniés and Lalinde's coordination chemistry of alkynylphosphines.

Reaction of **2** with half an equivalent of $[RhCl_2(Cp^*)]_2$ in CH_2Cl_2 resulted in a dark red solution that showed two bands in the IR spectrum at 2008 and 1916 cm^{-1} (*cf.* 1982, 1891 cm^{-1} in **2**). After chromatographic purification the bimetallic species $[W\{\equiv CPPh_2RhCl_2(Cp^*)\}(CO)_2(Tp^*)]$ (**7**) was isolated as a red solid (Scheme 2.26). Electron donation to the Lewis-acidic rhodium is manifest in the shift of ν_{CO} to higher frequency with respect to the precursor **2**. The $^{31}P\{^1H\}$ NMR spectrum shows only a very slight downfield shift upon coordination of the phosphine to δ_P 37.0 with coupling to rhodium ($^1J_{RhP}$ 139.2 Hz) within the typical range.[272] The carbyne resonance is shifted upfield compared to **2** and appears in the $^{13}C\{^1H\}$ NMR spectrum as a doublet straddled by ^{183}W satellites at δ_C 273.0 ($^1J_{PC}$ 28.7 Hz, $^1J_{WC}$ 208.2 Hz).

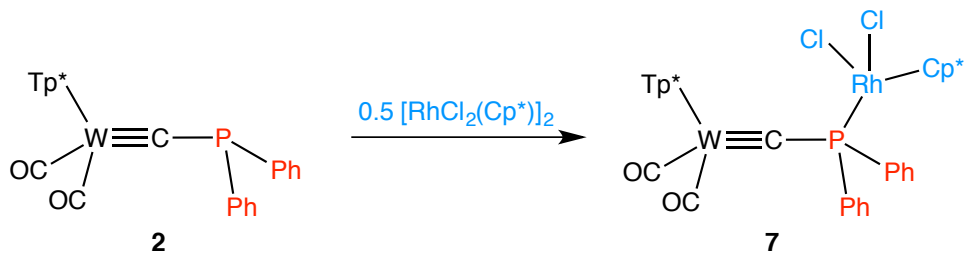

Scheme 2.26. Synthesis of $[W\{\equiv CPPh_2RhCl_2(Cp^*)\}(CO)_2(Tp^*)]$ (**7**).

The characterisation of **7** included an X-ray crystallographic study, the results of which are summarised in Figure 2.9. The geometry about rhodium is pseudo-octahedral and is comparable to that found in similar Rh(III) complexes.[271,273] The sterically demanding Cp* ligand is oriented away from the tungsten centre so as to minimise interactions. The W1−C1 (1.824(4) Å) and C1−P1 (1.798(4) Å) distances are unchanged from those of **2** (1.827(2), 1.783(3) Å), but the W1−C1−P1 angle in **7** approaches linearity (175.8(2)°), in contrast to that of **2** (166.62(15)°).

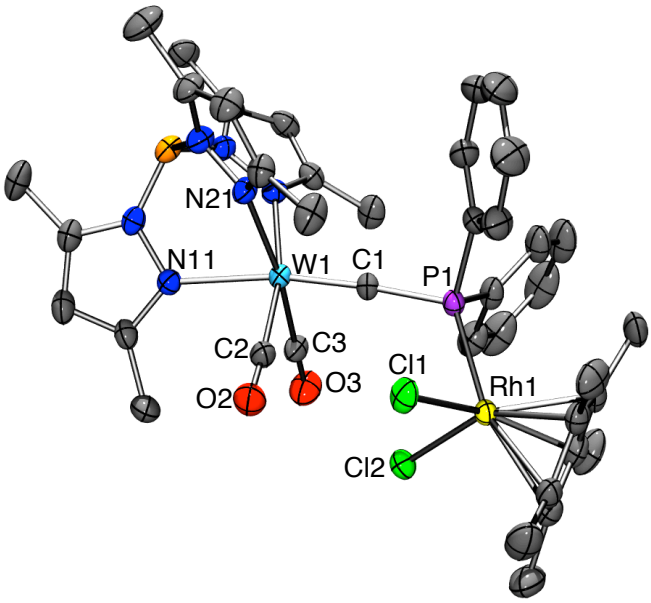

Figure 2.9. Molecular structure of **7** in a crystal of **7**·$(CH_2Cl_2)_2$ (50% displacement ellipsoids, hydrogen atoms omitted). Selected bond lengths (Å) and angles (°): W1−C1 1.824(4), C1−P1 1.798(4), P1−Rh1 2.3198(10), W1−C1−P1 175.8(2), C1−P1−Rh1 119.23(13).

The possibility of coordination of a third metal to the W≡C bond was explored in the reaction of **2** with one equivalent of $[RhCl_2(Cp^*)]_2$. Although the reactions of carbyne complexes with the rhodium(I) species $[Rh_2(\mu\text{-}CO)_2(Cp^*)_2]$ have been described,[258,262,269,274] the reactions of carbynes with trivalent rhodium reagents have not. Stirring a solution of **2** with one equivalent of $[RhCl_2(Cp^*)]_2$ at room temperature for three days yielded only the bimetallic species **7**. Subsequent heating at 110°C resulted in a number of IR bands in the carbonyl region. The $^{31}P\{^1H\}$ NMR spectrum showed that a number of phosphorus-containing species were present in the reaction mixture, but none of these peaks displayed ^{103}Rh coupling. It was thus concluded that

the trimetallic species [W{η²-C(RhCl₂Cp*)PPh₂RhCl₂(Cp*)}(CO)₂(Tp*)] does not form, which is not surprising given the demanding steric requirements of these species.

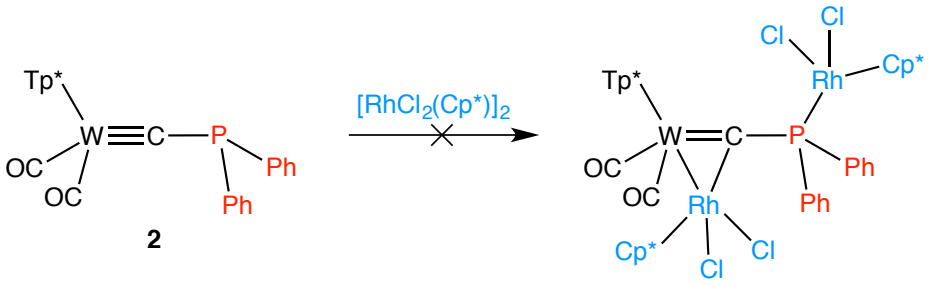

Scheme 2.27. Attempted synthesis of the trimetallic complex [W{η²-C(RhCl₂Cp*)PPh₂RhCl₂(Cp*)}(CO)₂(Tp*)].

2.7.2 Reactions with [AuCl(SMe₂)]

The literature hosts numerous reports documenting addition of gold(I) reagents to tungsten carbyne complexes of the form [W(≡CR)(L)$_n$] in which the metal-carbon triple bond is the reactive site.[261,263,275-281] In these cases a W−C−Au metallacycle is formed, such as that seen in the reaction of [AuCl(PPh₃)] with a tungsten tolylcarbyne, shown in Scheme 2.28.[263] In this case, mono-addition of the [Au(PPh₃)]$^+$ moiety occurred, but solution NMR studies showed that the complex dissociates into [Au{W(≡CTol)(CO)₂(Cp)}₂]PF₆ and [Au(PPh₃)₂]PF₆. A particularly fascinating example of such chemistry is that of the tetrameric complex [W(CAu)(CO)₂(Tp*)]₄, which forms a remarkable C₄Au₄ ring in which each carbyne carbon is bound to two adjacent gold atoms and one {W(CO)₂Tp*} moiety.[211]

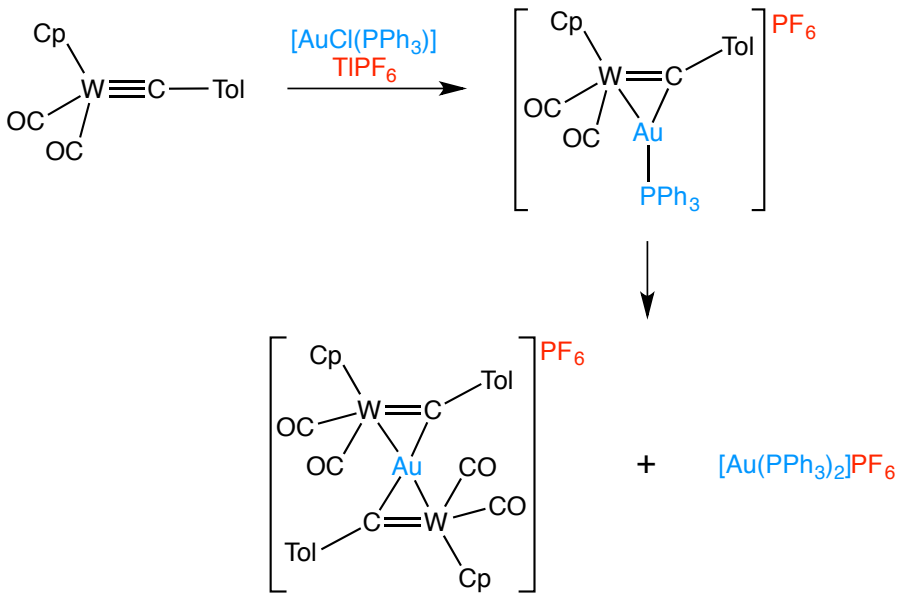

Scheme 2.28. Addition of $[Au(PPh_3)]^+$ to the W≡C bond and subsequent dissociation of PPh_3.

In contrast to this, Weber and co-workers have reported the addition of [AuCl(CO)] to the phosphaalkenylcarbyne series $[M\{\equiv CP{=}C(NMe_2)_2\}(CO)_2(Tp^*)]$ (M = Mo, W), in which two AuCl moieties add to the phosphorus atom to give $[M\{\equiv CP(AuCl)_2C(NMe_2)_2\}(CO)_2(Tp^*)]$ (Scheme 2.29).[72] Intriguingly, in the case of the arsenic analogues, [AuCl(CO)] instead effects carbene abstraction, and subsequent trimerisation of the resultant '$M(CAs)(CO)_2(Tp^*)$' fragment gives the fascinating cyclic triarsine structure $[M(\equiv CAs)(CO)_2(Tp^*)]_3$.

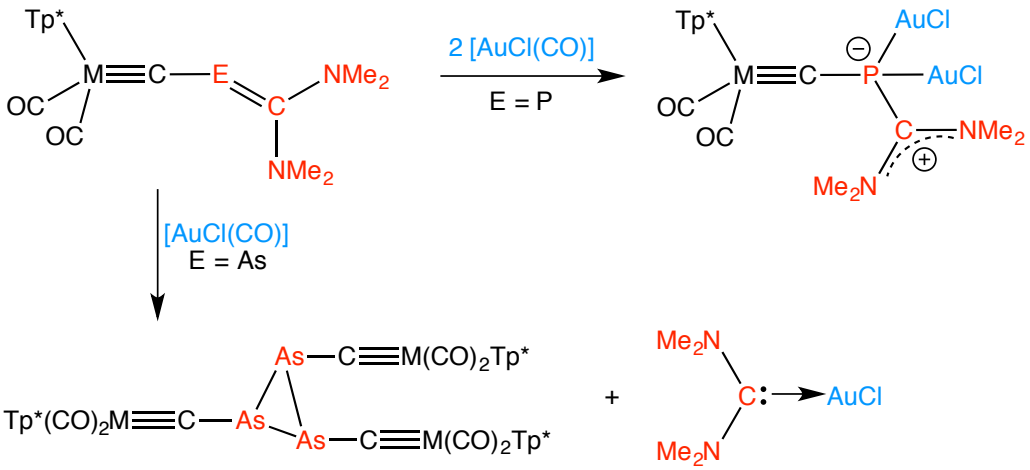

Scheme 2.29. Weber's reactions of phosphaalkene- and arsaalkene-substituted carbynes with [AuCl(CO)] (M = Mo, W).

In light of these contrasting reactivities, the reaction of the phosphinocarbyne **2** with gold(I) reagents was of interest. Upon treatment of **2** with one equivalent of [AuCl(SMe$_2$)], infrared monitoring of the red THF solution showed replacement of the starting material (ν_{CO} 1981, 1893 cm^{-1}) by new bands to higher frequency (2002, 1917 cm^{-1}). Both the shift in frequency and the intensity profile of the two absorptions were similar to those observed for the formation of **7**.[‡‡] Filtration through diatomaceous earth provided [W(≡CPPh$_2$AuCl)(CO)$_2$(Tp*)] (**8**) as a red solid in 81% yield (Scheme 2.30). The ^{31}P{^{1}H} NMR spectrum of **8** comprises a singlet with ^{183}W satellites at δ_P 37.5, with $^2J_{WP}$ (139.3 Hz) being slightly smaller than the $^2J_{WP}$ values observed for tungsten phosphoniocarbynes (150 – 200 Hz).[58,61,62,73] The carbyne resonance is observed as a doublet accompanied by ^{183}W satellites at δ_C 263.3 ($^1J_{PC}$ 22.1 Hz, $^1J_{WC}$ 199.9 Hz). The phosphorus-carbon coupling is significantly smaller than that of the starting material (74.5 Hz), reflecting the increased coordination about the phosphorus atom.

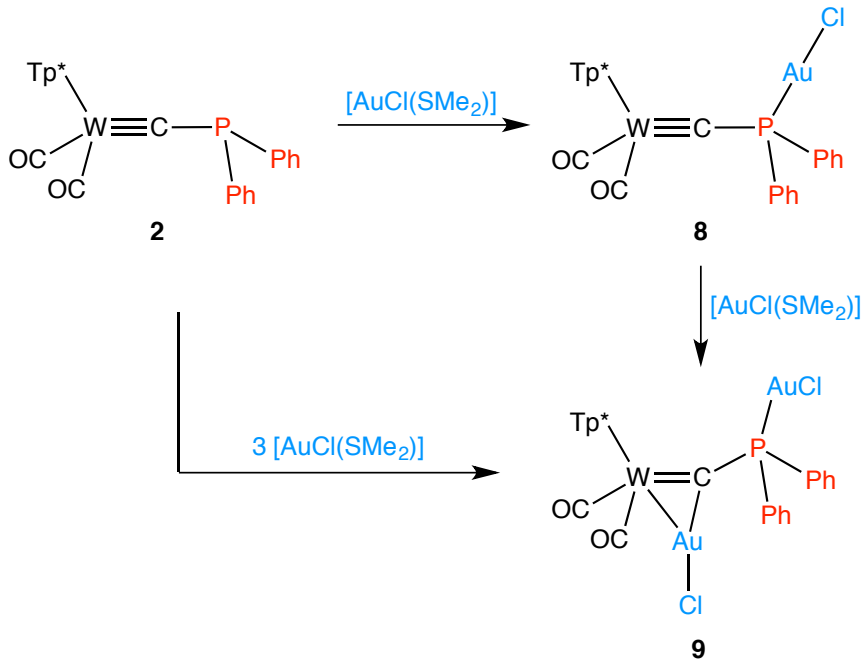

Scheme 2.30. Reaction of **2** with [AuCl(SMe$_2$)] to provide [W(≡CPPh$_2$AuCl)(CO)$_2$(Tp*)] (**8**) and [W{η^2-C(AuCl)PPh$_2$AuCl}(CO)$_2$(Tp*)] (**9**).

An X-ray crystallographic study of **8** corroborated ligation of AuCl to the phosphine (Figure 2.10). The W1−C1 bond length of 1.821(4) Å is consistent with a W≡C triple

[‡‡] Addition to the W≡C bond would result in an increased coordination number at tungsten, causing a variation in the intercarbonyl angle and thus also in the intensities of ν_s and ν_{as}.

bond,[21] while the C1−P1 bond length of 1.773(4) Å is crystallographically identical to that of the precursor **2** (1.783(3) Å) and that observed in Weber's diauro compound [W{≡CP(AuCl)$_2$C(NMe$_2$)$_2$}(CO)$_2$(Tp*)] (1.782(11) Å).[72] The Au1−P1 distance of 2.2234(10) Å is consistent with a Au−P single bond[282,283] and is slightly shorter than those observed in Weber's compound of 2.250(3) Å. The P1−Au1−Cl1 angle approaches linearity (177.17(5)°), which is in contrast to the P−Au−Cl angles observed in Weber's more sterically congested complexes of 168.06(11) and 169.61(11)°.

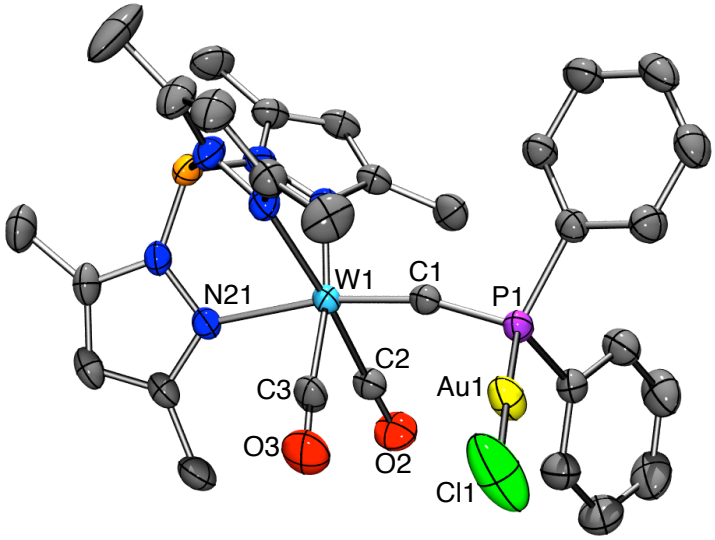

Figure 2.10. Molecular structure of **8** in a crystal (50% displacement ellipsoids, hydrogen atoms omitted). Selected bond lengths (Å) and angles (°): W1−C1 1.821(4), C1−P1 1.773(4), P1−Au1 2.2234(10), Au1−Cl1 2.2724(13), W1−C1−P1 165.5(2), C1−P1−Au1 113.02(12), P1−Au1−Cl1 177.17(5).

Treatment of complex **2** with two equivalents of [AuCl(SMe$_2$)] led to two sets of carbonyl absorptions; one attributable to **8** at 2002 and 1917 cm^{-1}, accompanied by new bands at 2022 and 1944 cm^{-1}. Addition of a further equivalent of [AuCl(SMe$_2$)] led to a weakening of the ν_{CO} bands due to **8** and strengthening of the new ν_{CO} absorptions. Concentrating the reaction mixture caused precipitation of a pink powder which was isolated and found to be the trimetallic complex [W{η^2-C(AuCl)PPh$_2$AuCl}(CO)$_2$(Tp*)] (**9**), the result of AuCl addition across the W≡C triple bond, as shown in Scheme 2.30. Complex **9** also forms from addition of [AuCl(SMe$_2$)] to the mono-aurated species **8**. Notably, no evidence was obtained for the formation of

the complex [W{η^2-C(AuCl)PPh_2}$(CO)_2$(Tp*)], suggesting that the phosphine, rather than the W≡C bond, is the stronger donor.

The ESI(+) mass spectrum (MeCN) clearly demonstrated the presence of two AuCl moieties. A shift of the carbonyl absorptions to higher frequency is observed for **9** compared to that of **8**, reflecting the expected decrease in electron density at tungsten that accompanies complexation of AuCl to the carbyne. The intensity profile of the ν_{CO} absorption bands suggests an opening of the intercarbonyl angle relative to **8**, consistent with what is observed in the solid state structure. Complex **9** appears in the $^{31}P\{^1H\}$ NMR spectrum as a singlet that displays ^{183}W satellites at δ_P 53.6, with $^2J_{WP}$ 84.3 Hz significantly smaller than that observed for **8** ($^2J_{WP}$ 139.3 Hz), in accordance with the decreased *s*-character along the W−C−P spine. In the $^{13}C\{^1H\}$ NMR spectrum the carbyne resonance is shifted downfield to δ_C 253.6. The modification of the carbyne moiety is evident in the significant decrease of both the phosphorus-carbon and tungsten-carbon coupling constants ($^1J_{PC}$ 1.5 Hz, $^1J_{WC}$ 99.6 Hz), reflecting the higher degree of substitution along the WCP spine. The magnitude of the tungsten-carbon coupling is half that typically seen in carbyne complexes (e.g **8** $^1J_{WC}$ 199.9 Hz).

The characterisation of complex **9** included an X-ray crystallographic study, the results of which are shown in Figure 2.11. The geometry about the W1−Au2−C1 metallacycle is similar to that observed in related compounds.[260,275-277,284] The W1−C1 bond length of 1.897(4) Å is significantly elongated compared to that in **8** (1.821(4) Å) and falls within the range of both WC double and triple bonds, consistent with a dimetallacyclopropene description.[285] Stone has observed semi-bridging carbynes, such as [Au{W(μ-CTol)$(CO)_2$(η^5-$C_2B_9H_9Me_2$)}(PPh_3)], in which the CTol moiety asymmetrically bridges the tungsten-gold bond (W−C 1.88(3), Au−C 2.19(3) Å).[267] Although the disparity in **9** is not as great as in Stone's example, the carbyne ligand is asymmetrically disposed along the W−Au bond (W1−C1 1.897(4), Au2−C1 2.031(4) Å). Coordination of AuCl to the W≡C bond would appear to reduce the usually strong *trans* influence of the carbyne ligand such that the three W−N bonds are of comparable lengths (2.208(4), 2.189(4), 2.207(4) Å).

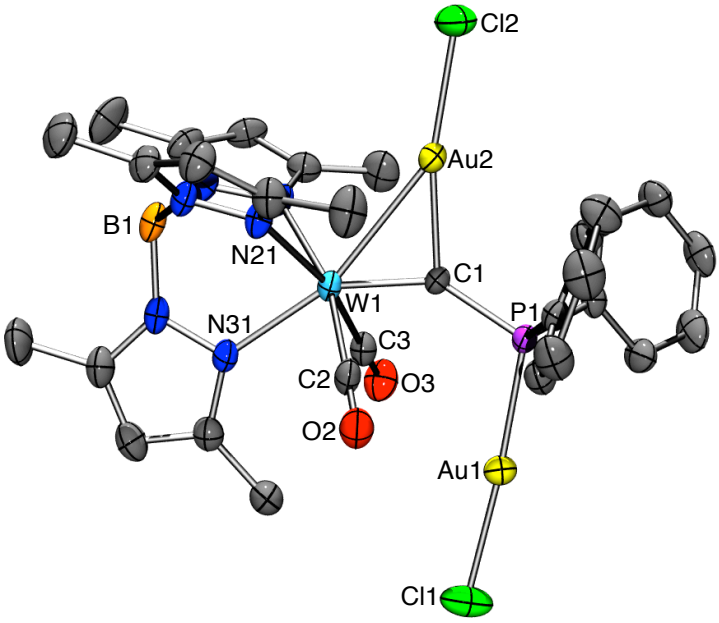

Figure 2.11. Molecular structure of **9** in a crystal (50% displacement ellipsoids, hydrogen atoms omitted). Selected bond lengths (Å) and angles (°): W1−C1 1.897(4), W1−Au2 2.8011(3), C1−P1 1.802(4), C1−Au2 2.031(4), P1−Au1 2.2278(12), W1−N11 2.208(4), W1−N21 2.189(4), W1−N31 2.207(4), W1−C1−P1 145.1(3), C1−P1−Au1 110.50(15), C1−Au2−Cl2 167.42(14), W1−C1−Au2 90.90(18), C1−W1−Au2 46.47(13), P1−Au1−Cl1 175.66(6).

2.8 Reactions with chalcogens

There are two pathways in the literature for addition of chalcogens to carbyne complexes. One equivalent of chalcogen may add to the M≡C bond, generating an η^2-chalcoacyl complex. To this effect, Roper has obtained chalcoaroyl complexes by the reaction of elemental chalcogens with the carbyne complex $[Os(\equiv CTol)Cl(CO)(PPh_3)_2]$, or by addition of HE^- to the chlorocarbene complex $[Os(=CClTol)Cl_2(CO)(PPh_3)_2]$ (Scheme 2.31).[35,286] When the nucleophile is HO^- the η^2-OCR complex is not seen; instead the complex rearranges to give the dicarbonyl species $[Os(Tol)Cl(CO)_2(PPh_3)_2]$.

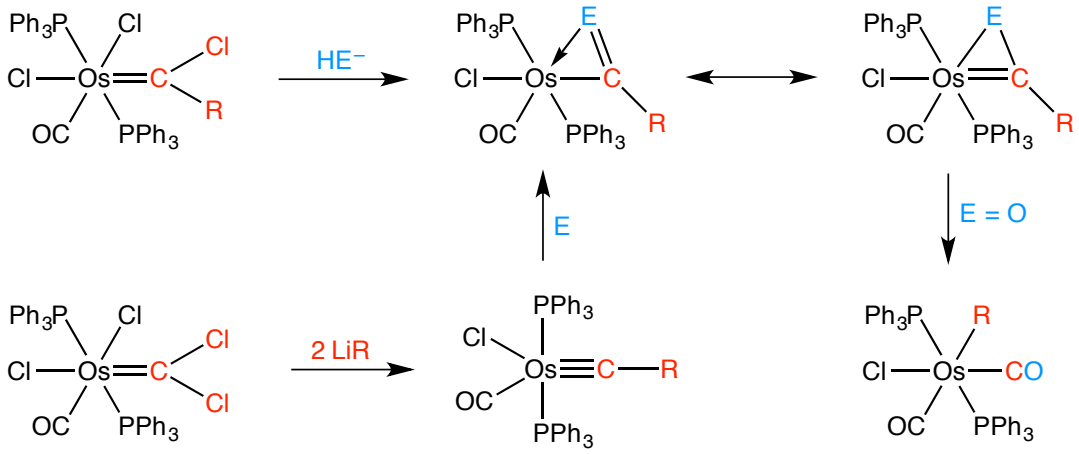

Scheme 2.31. Roper's preparation of chalcoaroyl complexes (R = Tol, E = O, S, Se, Te).

Alternatively, addition of two equivalents of chalcogen may provide the corresponding dichalcocarboxylate complex. Stone has shown that addition of elemental sulfur or selenium to [M(≡CR)(L)$_2$(Cp)] gave the corresponding dichalcocarboxylate species [M(κ^2-E$_2$CR)(L)$_2$(Cp)] (Scheme 2.32).[287]

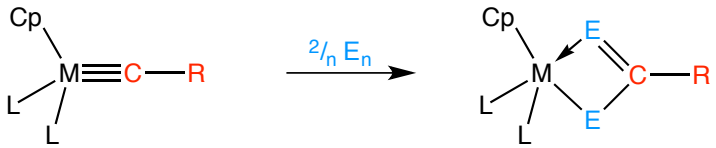

Scheme 2.32. Stone's synthesis of dichalcocarboxylate complexes (E = S, M = Mo, R = CH$_2$^{t}Bu, L = P(OMe)$_3$ or CO; M = W, R = Tol, L = CO; E = Se, M = Mo, R = CH$_2$^{t}Bu, L = CO; M = W, R = Tol, L = CO).

With phosphinocarbyne complexes chalcogen addition to the phosphine offers an alternative course, as phosphine chalcogenides are ubiquitous in synthetic chemistry (Scheme 2.33). The reactions of **2** with sulfur and selenium were undertaken to probe these possible reactivities.

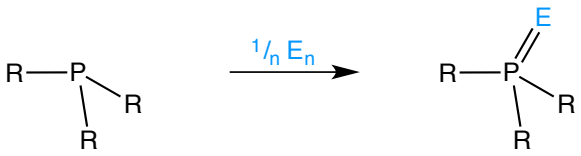

Scheme 2.33. Addition of chalcogens to phosphines typically affords phosphine chalcogenides (E = O, S, Se).

2.8.1 Reactions with sulfur

A solution of **2** in THF was stirred with one equivalent of elemental sulfur ($^1/_8$ S_8). After 16 hours the IR spectrum revealed two pairs of CO absorptions at 2003, 1917 and 1996, 1908 cm^{-1}. Cryostatic chromatography (−30°C) provided a purple band (minor product) and an orange band as the major product.

The orange fraction gave rise to two CO absorption bands in the infrared spectrum at 2004 and 1916 cm^{-1} in CH_2Cl_2. The mass spectra and microanalytical data supported addition of one sulfur atom. The $^{31}P\{^1H\}$ NMR spectrum showed a singlet with ^{183}W satellites at δ_P 41.1, with coupling of $^2J_{WP}$ 150.9 Hz suggestive of a four-coordinate phosphorus, supporting formulation of the major product as the phosphine sulfide complex [W{≡CP(=S)Ph_2}$(CO)_2$(Tp*)] (**10**) (Scheme 2.34). The carbyne resonance appears in the $^{13}C\{^1H\}$ NMR spectrum at δ_C 270.1 with a very small $^1J_{PC}$ value (4.9 Hz) in accordance with a carbyne complex containing a four-coordinate phosphorus, while the large $^1J_{WC}$ coupling seen for the carbyne resonance (198.4 Hz) is consistent with retention of a W≡C triple bond.

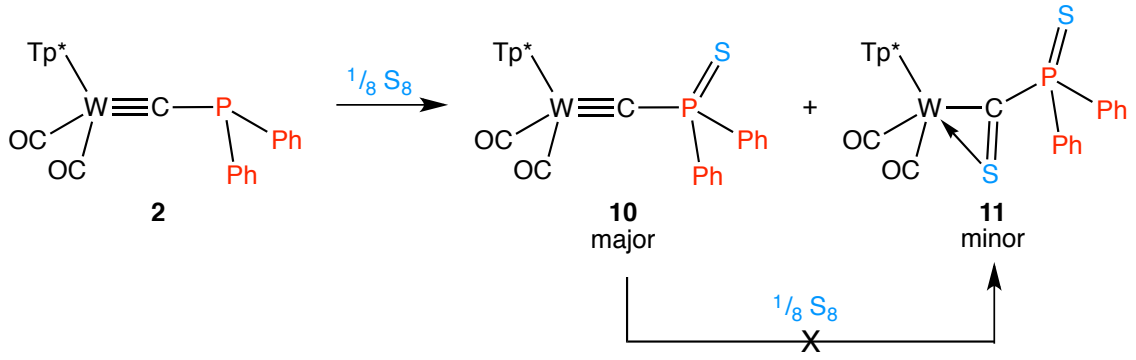

Scheme 2.34. Reaction of **2** with sulfur to provide [W{≡CP(=S)Ph_2}$(CO)_2$(Tp*)] (**10**) and [W{η^2-SCP(=S)Ph_2}$(CO)_2$(Tp*)] (**11**).

An X-ray crystal structure determination of **10** served to corroborate the formulation proposed on the basis of spectroscopic data (Figure 2.12). The conversion of **2** to **10** does not significantly affect the W≡C bond length (1.829(4) *cf.* 1.827(2) Å), though the W1−C1−P1 spine is further distorted from linearity (160.5(3) *cf.* 166.62(15)°). The angles about P1 are close to tetrahedral (104.35(19) – 113.97(15)°), the largest of these

being between the sulfur and carbyne carbon atoms. In spite of the increased coordination number at phosphorus, the C1−P1 bond (1.785(4) Å) does not differ significantly from that found for **2**.

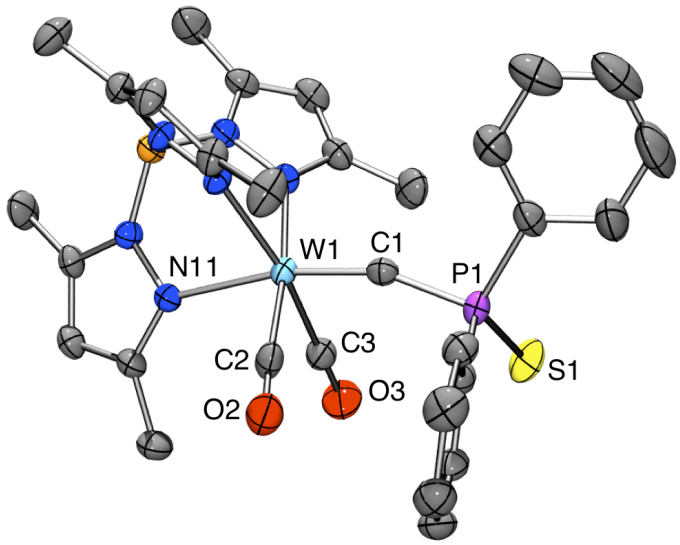

Figure 2.12. Molecular structure of **10** in a crystal (50% displacement ellipsoids, hydrogen atoms omitted). Selected bond lengths (Å) and angles (°): W1−C1 1.829(4), C1−P1 1.785(4), P1−S1 1.9568(16), W1−C1−P1 160.5(3), C1−P1−S1 113.97(15).

IR spectroscopy of the purple fraction revealed two carbonyl bands at 1995 and 1907 cm^{-1} in CH_2Cl_2. The ESI(+) mass spectrum was consistent with the addition of two sulfur atoms. The ^1H NMR spectrum showed the typical 2:1 ratio of Tp* peaks and the presence of the PPh_2 group, while the $^{31}P\{^1H\}$ NMR spectrum consisted of a single peak at δ_P 52.9 without any discernable ^{183}W satellites. The absence of tungsten-phosphorus coupling led us to initially suspect the compound might be the dithiocarboxylate complex $[W(\kappa^2\text{-}S_2CPPh_2)(CO)_2(Tp^*)]$, although phosphinodithiocarboxylate complexes remain rare.[288-290] The $^{13}C\{^1H\}$ NMR spectrum contained a doublet straddled by ^{183}W satellites at δ_C 250.1 ($^1J_{PC}$ 42.0 Hz, J_{WC} 42.8 Hz), which was assigned to the *C*−PPh_2 carbon because of the diagnostic phosphorus-carbon coupling. The chemical shift, while slightly downfield from what is typically seen for dithiocarboxylates, could be consistent with either a dithiocarboxylate or a thioacyl group.[287,291-293] Mayr and co-workers have reported the complex $[W(\kappa^2\text{-}S_2CNEt_2)(\eta^2\text{-}SCNEt_2)(\eta^2\text{-}SCHPh)(CO)]$ which contains both a dithiocarbamate and a thiocarbamoyl

group.[292] In the $^{13}C\{^1H\}$ NMR spectrum ($CDCl_3$) of this compound the η^2-S*C*NEt$_2$ carbon appears at δ_C 256.9 with ^{183}W satellites ($^1J_{WC}$ 111 Hz) while the κ^2-S$_2$*C*NEt$_2$ carbon appears at δ_C 214.6 with no visible ^{183}W coupling. Since the value of J_{WC} observed for **11** falls between those for the two ligand environments in Mayr's compound, this data cannot be used to unequivocally define the nature of the product.

Fortunately, crystals of **11** were acquired, an X-ray crystallographic study of which revealed the structure of the minor product to be the thioacyl complex [W{η^2-SCP(=S)Ph$_2$}(CO)$_2$(Tp*)] (**11**), as shown in Figure 2.13. The W1−C1 bond (2.003(13) Å) is significantly elongated compared to that in **2** (1.827(2) Å), reflecting the decrease in bond order, while the C1−P1 bond length is slightly shorter (1.770(14) *cf.* 1.783(3) Å). The geometry about the W1−C1−S1 metallacycle is similar to that seen for [W(κ^2-S$_2$CNEt$_2$)(η^2-SCNEt$_2$)(η^2-SCHPh)(CO)].[292] The W1−C1−P1 angle is considerably opened (145.4(7)°) from the ideal 120° expected for an sp^2 carbon as a result of the constraints of the metallacycle. As seen for **9**, the three W−N bond lengths are equivalent (2.206(9), 2.203(9), 2.218(10) Å), indicating the thioacyl ligand has a comparable *trans* influence to that of a CO ligand.

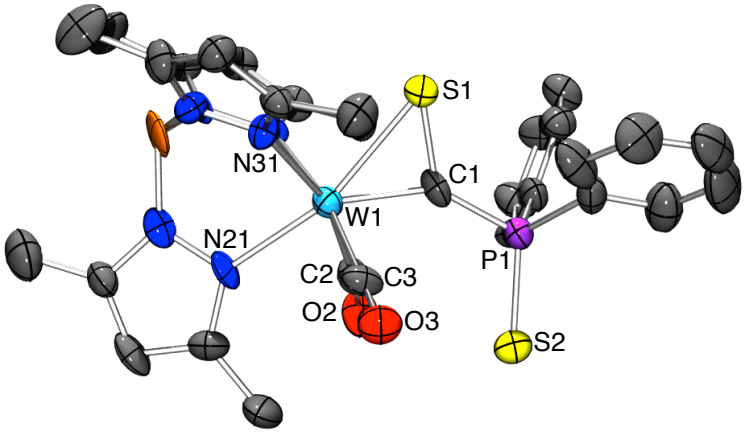

Figure 2.13. Molecular structure of **11** in a crystal (50% displacement ellipsoids, hydrogen atoms omitted). Selected bond lengths (Å) and angles (°): W1−C1 2.003(13), W1−S1 2.561(3), C1−S1 1.707(14), C1−P1 1.770(14), P1−S2 1.970(5), W1−N11 2.206(9), W1−N21 2.203(9), W1−N31 2.218(10), W1−C1−P1 145.4(7), W1−C1−S1 86.9(6), C1−W1−S1 41.7(4), W1−S1−C1 51.4(4), C1−P1−S2 113.2(4).

Two limiting valence bond descriptions may be invoked to explain the bonding within the WCS ring and the associated geometrical parameters; an η^2-*C,S*-thioacyl ligand or a metallathiirene, each providing three valence electrons to the metal centre (neutral formalism). The former is supported by the comparatively short C1−S1 bond length (1.707(14) Å) consistent with some degree of multiple bond character (*cf*. 1.708(2) Å in $Ph_3PCHC(=S)^tBu$[294] and 1.654, 1.687 Å in ^{t}BuC(=S)C(=S)NMe_2).[295] Conversely, as noted above, the W−C bond clearly also retains a degree of multiple bonding in support of the tungstathiirene description. Structural data for mononuclear transition metal thioacyls are somewhat rare, being limited to those for the complexes $[Os(SCR)(O_2CCF_3)(CO)(PPh_3)_2]$ (R = Tol,[296,297] CH=CHMe,[298] C_6H_4X-2, X = Cl, Br[299]), $[Ru\{SCC(CCPh)=CHPh\}Cl(CO)(PPh_3)_2]$,[300] $[Ru(SCPh)Cl(CS)(PPh_3)_2]$,[301] $[Co(SCCH^tBu_2)(PMe_3)(Cp)]BF_4$,[302] and $[Zr(SCCHC_5H_7Me_4)Cl(Cp)_2]$[303] in addition to a small number of metallacyclic examples.[304,305] Thus there are no directly comparable data for group 6 metals, though the C–S bond of **11** falls within the range observed for the more numerous group 8 examples (1.636 – 1.76 Å).

As seen for **2**, rotational isomers were observed in the infrared spectra of **10**. In the solid state (Nujol) spectrum, bands were observed at 1996 (s), 1924 (s) and 1909 (s) cm^{-1}, while the spectrum in THF contained two pairs of absorptions (2004 (s), 1997 (sh), 1918 (s), 1908 (sh) cm^{-1}) (Figure 2.14). In the case of **11**, three absorptions were seen in the solid state spectrum (1992 (s), 1902 (s), 1892 (s) cm^{-1}), but as only two bands were present in solution (THF, CH_2Cl_2) the presence of the extra band might be attributed to solid state effects.

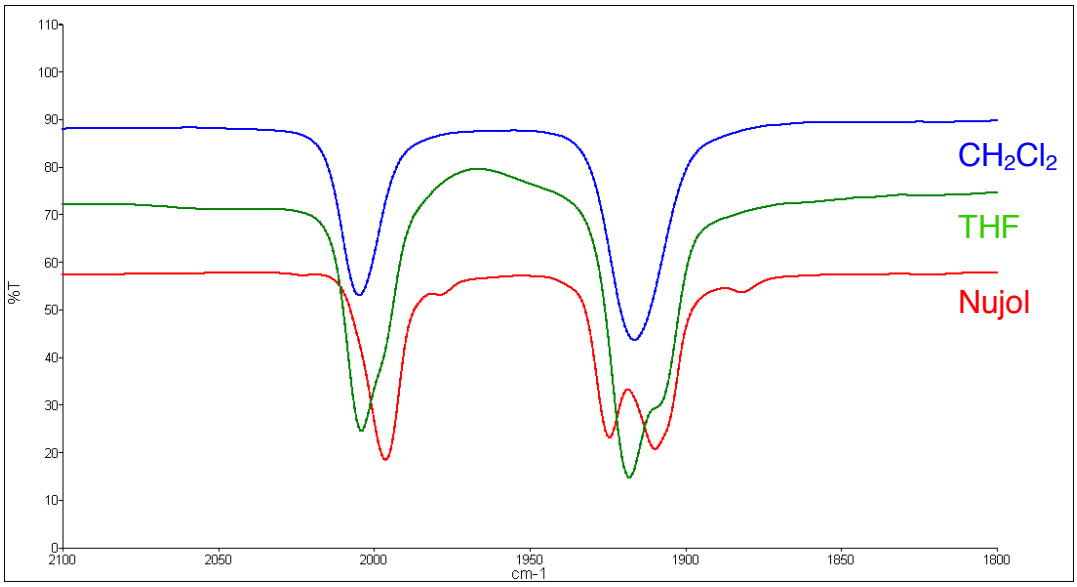

Figure 2.14. Carbonyl absorption region of the infrared spectra for **10** in different media.

Calculations confirmed that three rotational isomers of **10** exist with free energies within 4.1 kJ/mol of each other, and three for **11** within 2.2 kJ/mol. The coexistence of rotamers in solution would therefore seem entirely plausible. Rotational isomers were not observed in the NMR spectra, consistent with the low calculated barriers to rotation. The calculated geometry that corresponds most closely to the solid state structure is that in which the SPWC(O) dihedral angle is 34° (*cf.* 17.6° in the crystal structure). This rotamer lies 2.3 kJ/mol higher in energy than the ground state structure in which the P=S bond bisects the intercarbonyl angle, an energy difference which would be easily overcome by crystal packing forces.

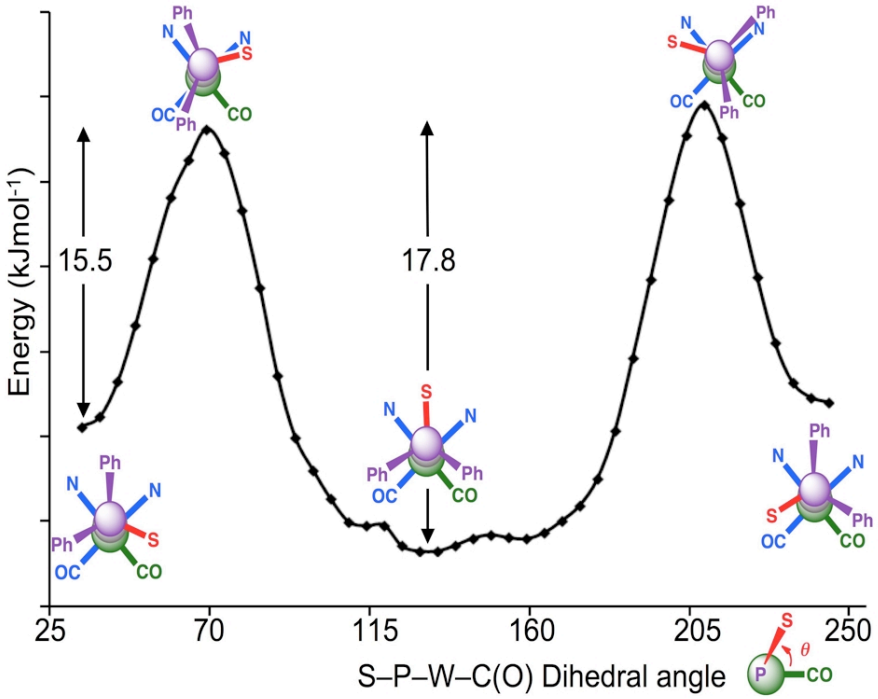

Figure 2.15. Rotational conformers and relative energies of **10** (θ = 250 – 25° generated by symmetry).

Interestingly, this reaction provides a mixture of products, the amounts of which are dependent on the solvent and stoichiometry of the reactants, as outlined in Table 2.1. The highest yields of **11** were obtained when toluene was used as the solvent. Surprisingly, addition of an excess of sulfur actually favoured the mono-addition product **10** rather than **11**.

Table 2.1. Addition of sulfur to **2**.

Solvent	Equivalents of S_8	Conditions[a]	Yield 10 (%)	Yield 11 (%)
THF	~ $^1/_8$	-	81[b]	9[b]
Toluene	~ $^1/_8$	-	80	16
THF	~ $^1/_8$	Slow dropwise addition of S in THF	86	7
THF	~ $^1/_8$	Fast addition of S in THF at −78°C	98	0.6
THF	$^5/_8$	-	90	6
CH_2Cl_2	$^{10}/_8$	-	98	0.5

Yields quoted represent the % yield as estimated by $^{31}P\{^1H\}$ NMR spectroscopy. [a] Unless stated otherwise, **2** and sulfur were combined as solids then dissolved in the specified solvent. [b] Yields quoted represent the isolated % yield.

Addition of a second equivalent of sulfur to **10** did not generate **11**, and even after six days at 110°C no evidence of **11** was seen in the NMR or IR spectra. This reveals that formation of **11** must proceed via initial competitive sulfur addition to the W≡C bond, followed by addition to the phosphine (Scheme 2.35). Once phosphine sulfide formation has occurred the W≡C bond is deactivated towards electrophilic attack, hence **11** cannot be formed from **10**. Conversely, addition of sulfur to the W≡C linkage does not deactivate the phosphorus lone pair. The complete mechanism for formation of **11** is anticipated to be much more complex that than depicted below, as reaction mechanisms involving elemental sulfur are complicated by the cyclic S_n allotropes,[306,307] yet it does provide an understanding of the order of addition in the reaction. The possibility of employing a single sulfur atom delivery agent (propylene sulfide) is discussed below.

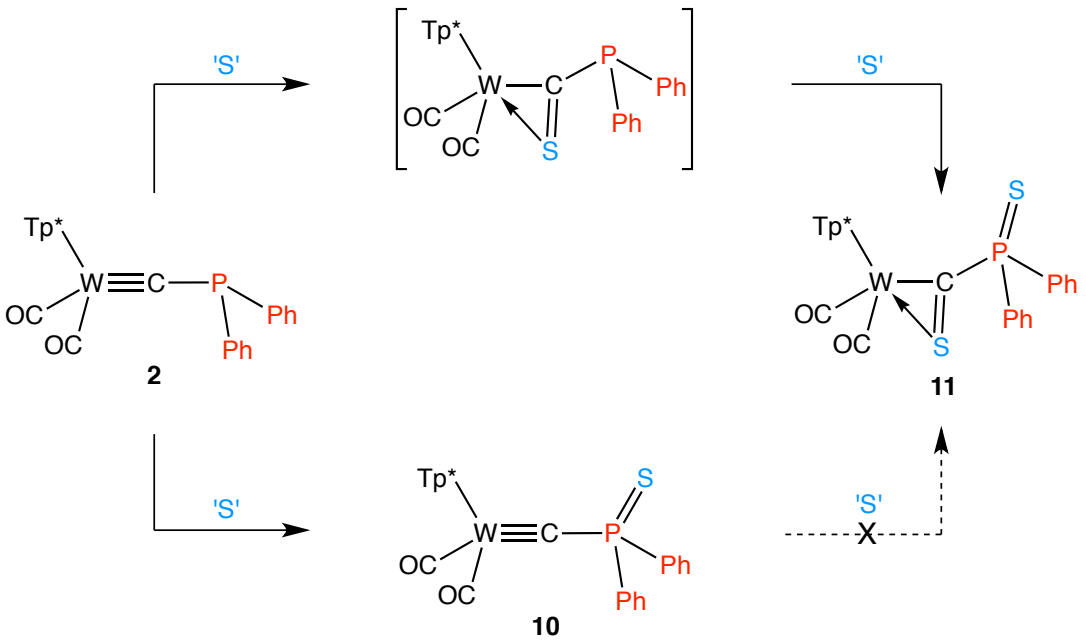

Scheme 2.35. Order of addition of sulfur to **2** to form **10** and **11**.

In order to probe the hypothesis that oxidation of the phosphorus deactivates the W≡C bond, reactions of [W(≡CPRPh$_2$)(CO)$_2$(Tp*)] (R = AuCl, BH$_3$, [Me]I) with sulfur were explored. In all cases no reaction occurred, even after extended reaction times (six days) (Scheme 2.36). This implies that, as in the case of the phosphine sulfide, these four-coordinate phosphorus moieties deactivate the W≡C moiety to electrophilic addition. In contrast, in the reactions of **2** with [AuCl(SMe$_2$)] the bis-addition product **9** could be formed from either **2** or **8** (Scheme 2.30).

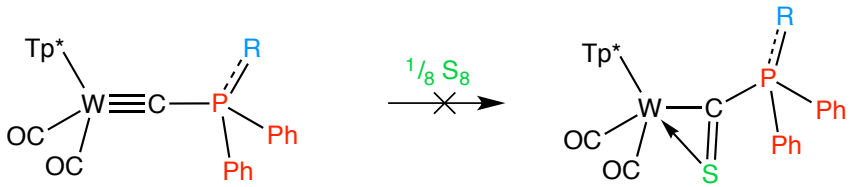

Scheme 2.36. Attempted reactions of [W(≡CPRPh$_2$)(CO)$_2$(Tp*)] with sulfur (R = AuCl, BH$_3$, [Me]I, S).

In all of the reactions of **2** with elemental sulfur, no evidence of a dithiocarboxylate complex [W(κ^2-S$_2$CPPh$_2$)(CO)$_2$(Tp*)] or [W{κ^2-S$_2$CP(=S)Ph$_2$}(CO)$_2$(Tp*)] was seen. Reactions of carbyne complexes with the single sulfur atom sources propylene sulfide and cyclohexene sulfide have been shown to provide thioacyl[255,308] and dithiocarboxylate[255,308,309] complexes. The reaction of **2** with propylene sulfide was

carried out and some formation of **10** was observed, but no evidence of **11**, thioacyl or dithiocarboxylate or complexes was seen in the IR or NMR spectra and the reaction was, on the whole, not very successful, in contrast to those with elemental sulfur.

2.8.2 Reaction with selenium

In light of the interesting results obtained from the reaction of **2** with sulfur, the analogous reaction with selenium was investigated. A solution of **2** in CH_2Cl_2 was stirred with elemental selenium overnight. After chromatography, the phosphine selenide [W{≡CP(=Se)Ph_2}$(CO)_2$(Tp*)] (**12**) was obtained in 92% yield as an orange powder (Scheme 2.37). Although selenoacyl complexes have been reported to arise from the reactions of group 6 carbyne complexes with isoselenocyanates,[310] formation of **12** was very clean and no evidence of a selenoacyl or a diselenocarboxylate was seen in the NMR or IR spectra. Even when the reaction was carried out with excess selenium at 110°C only **12** was produced.

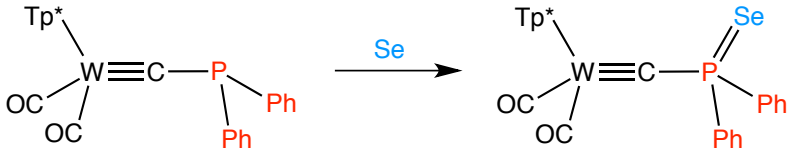

2 **12**

Scheme 2.37. Synthesis of [W{≡CP(=Se)Ph_2}$(CO)_2$(Tp*)] (**12**).

The ^{1}H and ^{13}C{^{1}H} NMR spectra of **12** are largely unremarkable. The carbyne resonance occurs within the typical range at δ_C 265.2 ($^1J_{PC}$ 13.6 Hz, $^1J_{WC}$ 201.4 Hz). The small phosphorus-carbon coupling constant is indicative of the four-coordinate nature of the phosphorus and the large tungsten-carbon coupling constant is characteristic of a tungsten-carbon triple bond. The ^{31}P{^{1}H} NMR chemical shift is unchanged (δ_P 31.9 *cf.* 32.0 for **2**) but the presence of ^{77}Se satellites (I = 1/2, 7.6% natural abundance, $^1J_{SeP}$ 711.8 Hz) is evidence of the formation of **12**. The observed selenium-phosphorus coupling is comparable to that in the alkynylphosphine selenide P(=Se)(C≡CPh)^{t}BuPh of $^1J_{SeP}$ 742.7 Hz (δ_P 34.3).[311]

Values of $^1J_{SeP}$ have been correlated to the basicity of phosphines in the literature,[312] and applying the same formula here gives a calculated pK_B value of 8.7 for the phosphine **2**. This is similar to what is seen for PMe_2Ph (pK_B 8.4 calculated *cf.* 7.50

experimental) and $P(C_6H_4OMe\text{-}4)_3$ (pK_B 8.6 calc. *cf.* 9.43 exp.), but lower than that of PPh_3 (pK_B 11.3 calc. *cf.* 11.27 exp.).[312] This suggests electron donation from the carbyne moiety results in increased electron density at phosphorus compared to PPh_3, unsurprising given the marked π-acidity of carbyne ligands, which translates to the calculated increase in basicity. The high basicity at phosphorus is consistent with the observed (initial) formation of the phosphonium salt **[5]**$^+$ upon protonation of **2**, although in this case proton migration occurs due to the enhanced stability of the η^2-phosphinocarbene **[6]**$^+$.

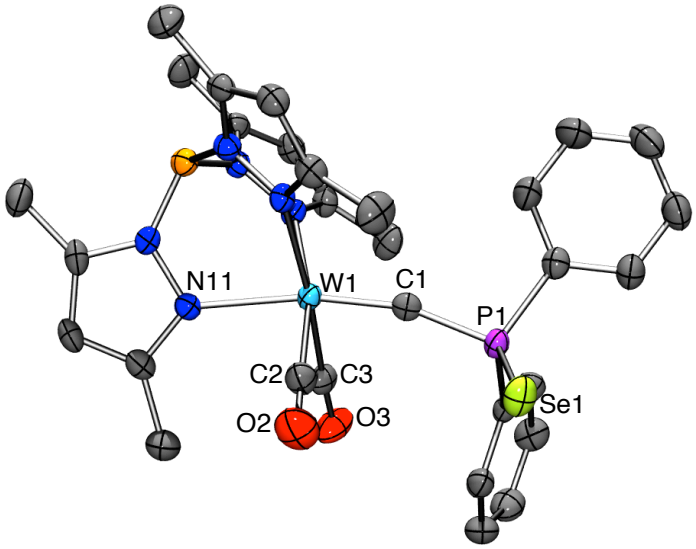

Figure 2.16. Molecular structure of **12** in a crystal of **12**·$CHCl_3$ (50% displacement ellipsoids, hydrogen atoms omitted). Selected bond lengths (Å) and angles (°): W1−C1 1.823(4), C1−P1 1.784(4), P1−Se1 2.1120(11), W1−C1−P1 164.6(2), C1−P1−Se1 114.25(12).

The crystal structure of **12** (Figure 2.16) reveals that the geometry about P1 is pseudo-tetrahedral, with angles about P1 ranging from 103.69(17)° to 114.25(12)°. The W1−C1 bond length of 1.823(4) Å is consistent with a triple bond, and the remaining structural parameters show little deviation from those observed for **2**.

2.8.3 Synthesis of [W{≡CP(=O)Ph$_2$}(CO)$_2$(Tp*)]

In contrast to the rapid reactivity of the phosphinocarbyne $[W(\equiv CPPh_2)(CO)_2(Tp^*)]$ towards sulfur and selenium, complex **2** is comparatively air-stable. Stirring a CH_2Cl_2 solution of **2** in air for 14 days resulted in only 43% conversion to the phosphine oxide $[W\{\equiv CP(=O)Ph_2\}(CO)_2(Tp^*)]$ (**13**) (Scheme 2.38). However, heating an aerobic

solution of **2** at 110°C resulted in complete consumption of **2** within eight hours, and NMR spectroscopy indicated **13** to be the major product of this reaction (ca. 70% by $^{31}P\{^{1}H\}$ NMR spectroscopy).

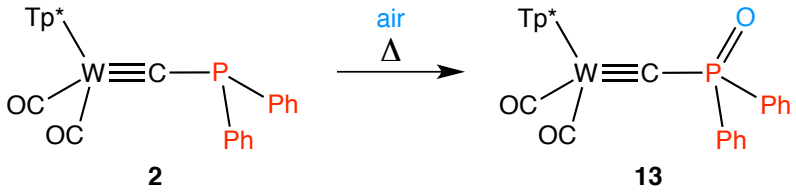

Scheme 2.38. Synthesis of [W{≡CP(=O)Ph$_2$}(CO)$_2$(Tp*)] (**13**).

Complex **13** appears in the $^{31}P\{^{1}H\}$ NMR spectrum as a singlet accompanied by ^{183}W satellites at δ_P 19.9 ($^{2}J_{WP}$ 145.2 Hz). The shift of this peak to higher field when compared to the phosphine **2** is somewhat puzzling, as oxidation of tertiary phosphines typically leads to downfield shifts in the ^{31}P NMR spectra.[313] However, all other spectroscopic data support the formulation of **13** as the oxide through comparison with the precursor (**2**), sulfide (**10**) and selenide (**12**) complexes (Table 2.2). As can be seen, the carbyne resonance shifts upfield in the progression from the oxide to sulfide to selenide species.

Table 2.2. Selected spectroscopic data for phosphinocarbyne-chalcogenide complexes.

Complex	δ_P ($^{2}J_{WP}$ (Hz)	δ_C WC ($^{1}J_{PC}$, $^{2}J_{WC}$ (Hz))	ν_{CO} THF (cm^{-1})	ν_{CO} Nujol (cm^{-1})
[W(≡CPPh$_2$)(CO)$_2$(Tp*)] (**2**)	32.0 (69.0)	292.6 (74.5, 187.9)	1981, 1893	2001, 1974, 1912, 1883
[W{≡CP(=O)Ph$_2$}(CO)$_2$(Tp*)] (**13**)	19.9 (145.2)	281.2 (16.1, 190.6)	2001, 1975, 1911	2002, 1987, 1913
[W{≡CP(=S)Ph$_2$}(CO)$_2$(Tp*)] (**10**)	41.0 (152.5)	270.1 (4.9, 198.4)	2004, 1997, 1918, 1908	1996, 1924, 1909
[W{≡CP(=Se)Ph$_2$}(CO)$_2$(Tp*)] (**12**)	31.9 (152.6)	265.2 (13.6, 201.4)	2004, 1997, 1918, 1907	2002, 1912
[W{η^2-CSP(=S)Ph$_2$}(CO)$_2$(Tp*)] (**11**)	52.9 (-)	250.1 (42.0, 42.8)	1993, 1908	1992, 1902, 1892

The infrared spectrum of **13** in THF is very similar to that of the sulfide and selenide complexes **10** and **12** (Table 2.2). Very strong ν_{CO} bands 2001 and 1911 cm^{-1} are accompanied by a medium absorption at 1975 cm^{-1}. The P=O stretching frequency was not unambiguously identifiable in the infrared spectra. Unfortunately, satisfactory microanalytical data were not obtained for **13**, but the low and high resolution ESI(+) mass spectra confirmed the formulation of **13** as [**2** + O] through the observation of $[M + H]^+$, $[M + Na]^+$ and $[M + K]^+$ peaks.

Given the counter-intuitive upfield shift in the $^{31}P\{^1H\}$ NMR spectrum upon oxidation of **2**, proof of the identity of **13** by unequivocal synthesis was explored. Platinum group metal complexes have been used to catalyse the oxidation of phosphines;[314] however, treating **2** with $[Ni(COD)_2]$ and exposure of the solution to air did not yield **13**, perhaps due to the use of air rather than purified oxygen gas for the reaction. A more common method in the literature is the stoichiometric oxidation of phosphines with hydrogen peroxide.[315,316] Treating **2** with aqueous H_2O_2 led to the formation of **13** in approximately 80% yield, based on the $^{31}P\{^1H\}$ NMR spectrum (Scheme 2.39). Only a marginal improvement in purity was obtained by column chromatography, and efforts to crystallise **13** were fruitless.

These two successful protocols involve reactions in air in which moisture is present, raising the possibility that hydration of the P=O bond might account for the anomalous ^{31}P NMR shift. An anaerobic and anhydrous synthesis of **13** was performed in one step from **1** via the reaction of the lithiocarbyne with $P(=O)ClPh_2$. NMR spectroscopy indicated formation of **13** as the major product (Scheme 2.39), and no change in the NMR spectrum was observed under these anhydrous conditions.

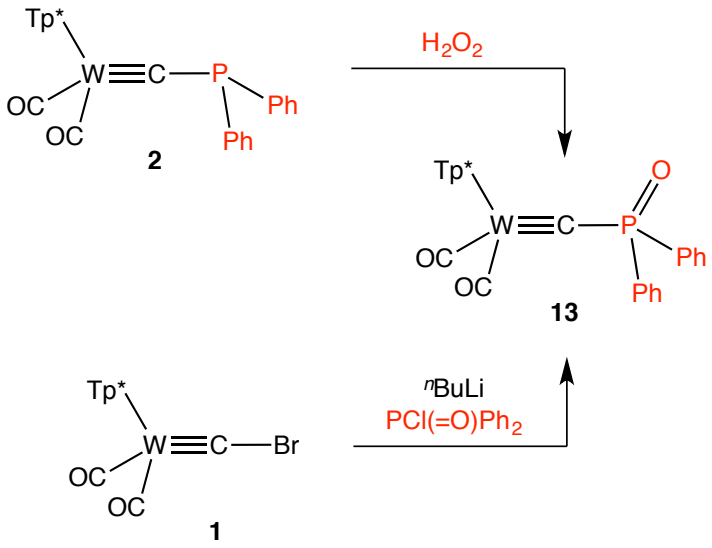

Scheme 2.39. Alternative synthetic routes to **13**.

Throughout this work a number of methods were developed to synthesise **13**, and spectroscopic data combined with unequivocal synthesis confirm that the isolated product is the phosphine oxide, despite the anomalous ^{31}P chemical shift. The alkynyl phosphine P(C≡CPh)Ph$_2$ appears in the ^{31}P NMR at δ_P –33.5,[317] whereas the resonance for the oxide P(=O)(C≡CPh)Ph$_2$ occurs downfield of this at δ_P 8.3.[318] The carbyne moiety in **13** resembles an alkyne electronically, so the upfield shift must result from the presence of the tungsten, although the origin of this phenomenon is not fully understood. However, in the case of the phosphine sulfide and selenide carbynes the chemical shifts are unremarkable.

2.8.4 Synthesis of [W{η^2-C(AuCl)P(=S)Ph$_2$}(CO)$_2$(Tp*)]

Although the gold complex **8** did not react with sulfur to give [W(η^2-CSPPh$_2$AuCl)(CO)$_2$(Tp*)], **8** did react with a second equivalent of [AuCl(SMe$_2$)] to afford the di-aurated complex **9**. This suggests that, despite the observed deactivation of the W≡C bond upon quaternisation of the phosphine, in some cases addition to the W≡C bond can take place. Curiosity led us to investigate this reaction but with reversal of the order of reagent addition.

A solution of **10** and one equivalent of [AuCl(L)] (L = SMe$_2$, THT) in CH$_2$Cl$_2$ was stirred for two hours, resulting in a red solution and a golden precipitate. The infrared spectrum indicated a mixture of starting material (ν_{CO} 2004, 1916 cm^{-1}) and a new compound (ν_{CO} 2031, 1952 cm^{-1}). Extending the reaction time did not lead to any

change in the infrared spectrum, so a further half equivalent of [AuCl(L)] was added, leading to almost complete conversion, as indicated by infrared spectroscopy. After chromatography, [W{η²-C(AuCl)P(=S)Ph₂}(CO)₂(Tp*)] (**14**) was obtained as an orange powder in 57% yield (Scheme 2.40).

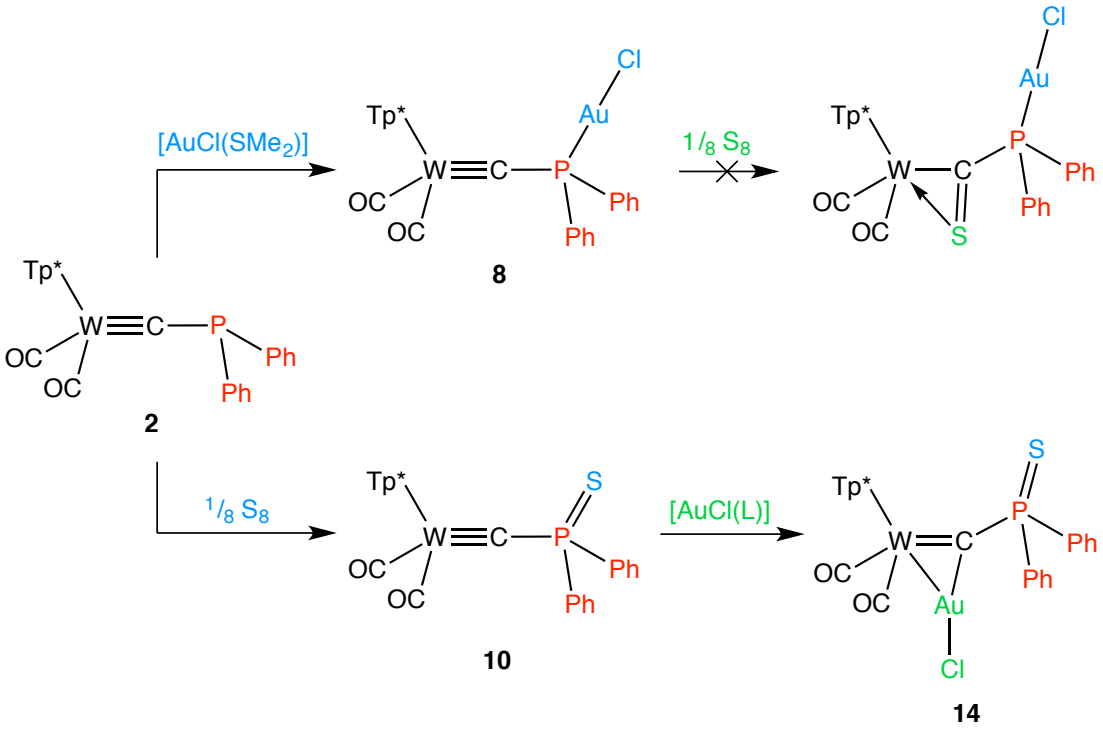

Scheme 2.40. Synthesis of [W{η²-C(AuCl)P(=S)Ph₂}(CO)₂(Tp*)] (**14**) (L = SMe_2, THT).

Complex **14** appears in the $^{31}P\{^{1}H\}$ NMR spectrum as a broad singlet at δ_P 52.3 with no discernable ^{183}W satellites. Broad peaks are also seen in the $^{13}C\{^{1}H\}$ NMR spectrum for the carbyne, carbonyl and $C^{1,4}$-phenyl peaks. This broadening in the NMR spectra is not due to dissociation of the AuCl moiety, since in a $^{31}P\{^{1}H\}$ NMR spectrum containing both **10** and **14**, the resonance for **10** is a sharp singlet with visible tungsten coupling, whereas the resonance for **14** is a broad singlet. If the AuCl group were dissociating on the NMR timescale we would expect to see broadening of both peaks. Hence this is most likely due to restricted rotation about the P–C bond, although this was not apparent in the NMR spectra for **9**.

The carbyne resonance is observed at δ_C 262.4, intermediate between **10** (δ_C 270.1) and **9** (δ_C 253.6). No coupling to either tungsten or phosphorus was resolvable due to the

broad nature of the peak, although the analogous $^{1}J_{PC}$ coupling in **9** is only 1.5 Hz so the absence of discernable coupling here may simply reflect its small magnitude. The ^{1}H and $^{13}C\{^{1}H\}$ NMR spectra display the typical 2:1 ratio of Tp* peaks, consistent with a time-averaged mirror plane through the W{η^2-C(AuCl)P(=S)} functionality.

Crystallographic grade crystals of **14** were obtained from chloroform/^{n}hexane and the results of a crystallographic study are summarised in Figure 2.17. The geometry about the metallacyclopropene ring is similar to that seen in **9**. As expected, the W1−C1 bond length (1.907(10) Å) is significantly elongated compared to that of **10** (1.829(4) Å). A slight lengthening of the P1−S1 bond is observed compared to **10** (1.992(5) *cf.* 1.9568(16) Å), attributable to the higher degree of substitution along the W−C−P spine. As is inferred from the NMR spectra, a (non-crystallographic) mirror plane is present through the W{η^2-C(AuCl)P(=S)}, bisecting the $W(CO)_2$, PPh_2 and Tp* moieties. A slight bending out of this mirror plane is seen for the phosphine sulfide, with a W1−C1−P1−S1 torsion angle of 8.43°.

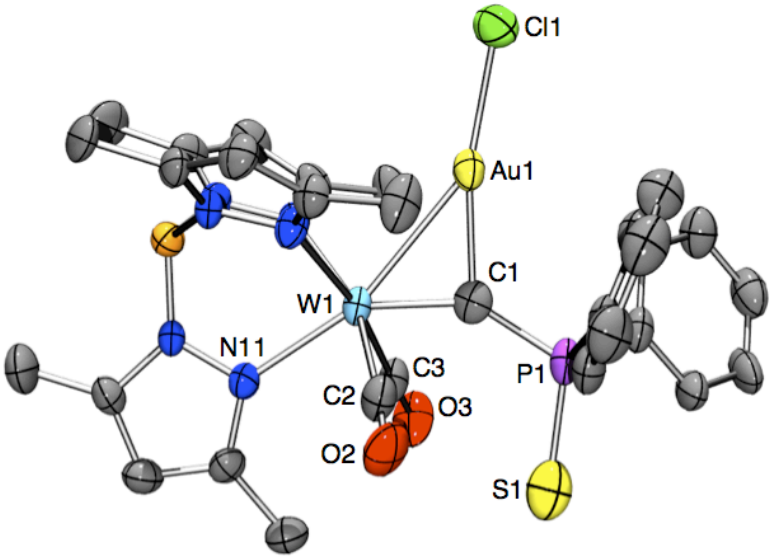

Figure 2.17. Molecular structure of **14** in a crystal (50% displacement ellipsoids, hydrogen atoms omitted). Selected bond lengths (Å) and angles (°): W1−C1 1.907(10), W1−Au1 2.7940(5), C1−P1 1.788(10), C1−Au1 2.043(10), P1−S1 1.992(5), W1−C1−P1 146.6(6), C1−P1−S1 113.3(3), C1−Au1−Cl1 166.8(3), W1−C1−Au1 90.0(4), C1−W1−Au1 47.0(3), W1−Au1−C1 43.0(3).

The formation of **14** demonstrates that, although the nucleophilicity of the W≡C bond decreases upon quaternisation of the phosphorus centre, with an appropriate choice of reagent reaction at this site can still occur. This offers the possibility of targeted reactivity at the W≡C bond through the use of a protecting group to inhibit reactivity at the phosphine, such as the borane adduct **4**, which might then be removed after addition of the desired electrophile to the W≡C bond.

2.9 Frontier orbitals of [W(≡CPPh$_2$)(CO)$_2$(Tp*)]

In order to better understand the reactivity features of **2**, molecular orbital calculations were performed by Dr Manab Sharma.[§§] The HOMO is located on the W(CO)$_2$ fragment, although no experimental evidence of reactivity at the W(CO)$_2$ moiety has been observed. The salient orbitals for electrophilic addition are the HOMO–1 and HOMO–2 orbitals, depicted in Figure 2.18. As can be seen the HOMO–1 orbital resides on the phosphine lone pair and the W≡C and W−C(O) bonds. The HOMO–2 orbital is that perpendicular to HOMO–1 with respect to the W≡C and W−C(O) bonds. Evidently the HOMO−1 comprises a significant phosphorus component, thus reconciling the experimentally observed electrophilic attack at phosphorus in **2**. This is in contrast to aminocarbynes, which typically undergo addition of electrophiles at the carbyne carbon atom.

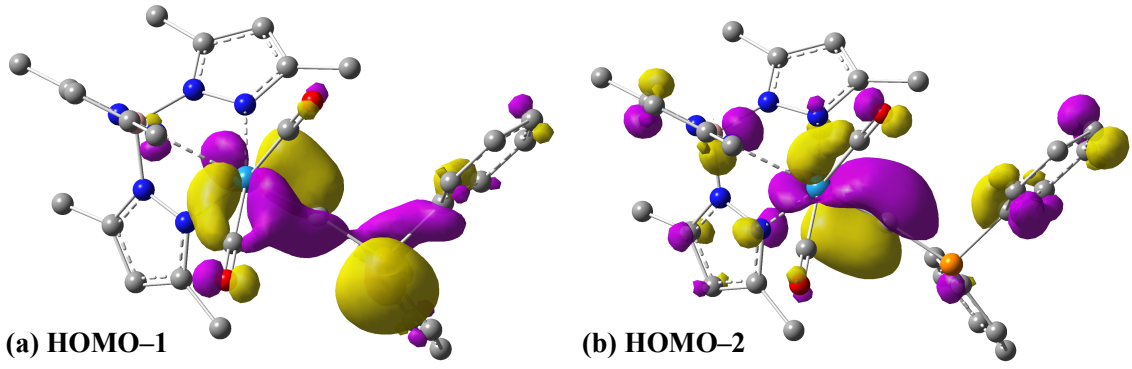

(a) HOMO–1 **(b) HOMO–2**

Figure 2.18. (a) HOMO–1 and (b) HOMO–2 calculated orbitals.

The energy difference between these two orbitals is 0.5576 eV (HOMO–1 = −4.8343 eV, HOMO–2 = −5.3919 eV); therefore it is conceivable that either may be involved in reactions with electrophiles. Experimentally, the phosphine appears to be the primary

[§§] Specific details of computational studies performed by Dr Sharma, whose expertise is gratefully acknowledged, may be found in the Appendix.

site for electrophilic addition, i.e. the HOMO–1 orbital. As this orbital is based on both the phosphine and the W≡C bond, we would expect little electronic preference for one site over the other in a frontier orbital-controlled reaction. Furthermore, the Mulliken charges suggest that charge-controlled electrophilic addition would in fact occur at carbon (C −0.27, P +0.31, W +0.36). In contrast to these findings, a strong preference for the phosphine is observed experimentally, suggesting that the reactivity is most likely dictated by steric factors. The bulky Tp* ligand, in conjunction with the phenyl groups of the PPh_2 moiety, shield the W≡C bond from electrophiles, whilst the lone pair of electrons on phosphorus is exposed.

The LUMO (−2.0895 eV) and LUMO+1 (−1.7291 eV) orbitals depicted in Figure 2.19 show that nucleophilic attack would be expected to occur at the carbonyl ligands or at the carbyne carbon atom. This has not been investigated experimentally, but it is worth noting that Templeton has observed the kinetic product of nucleophilic attack by $Li[BHEt_3]$ on $[W(\equiv CPPh_3)(CO)_2(Tp^*)]PF_6$ to indeed be the result of attack at a carbonyl co-ligand, rather than the carbyne carbon, although the carbyne is where the nucleophile ultimately transfers.[64]

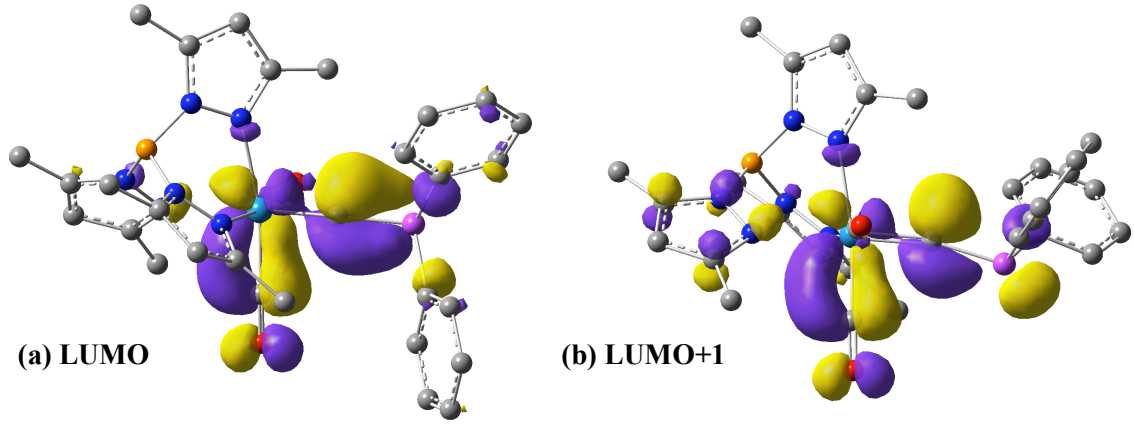

Figure 2.19. (a) LUMO and (b) LUMO+1 calculated orbitals.

2.10 Summary

The synthesis of the first tungsten phosphinocarbyne complex [W(≡CPPh$_2$)(CO)$_2$(Tp*)] (**2**) has been accomplished in a one pot protocol commencing with the bromocarbyne complex [W(≡CBr)(CO)$_2$(Tp*)]. This conversion can be achieved by lithium-halogen exchange and subsequent nucleophilic substitution of a chlorophosphine, or by palladium-catalysed phosphination (Scheme 2.41). Both methods represent viable, potentially generalisable synthetic strategies towards a variety of phosphorus-functionalised carbyne complexes, to be discussed in subsequent Chapters.

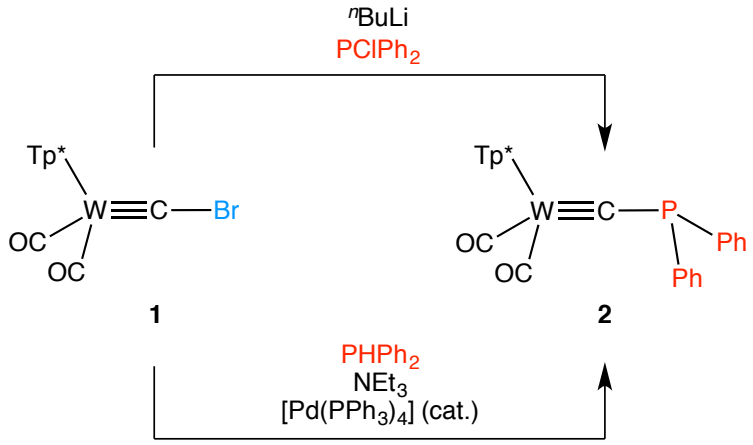

Scheme 2.41. Synthesis of a phosphinocarbyne complex via lithium-halogen exchange and via palladium-mediated P–C bond formation.

Reactions of **2** with electrophiles have shown that, despite calculations showing that the HOMO–1 comprises both the W≡C bond and the phosphine lone pair, the phosphine is almost invariably the preferred site for electrophilic attack (Scheme 2.42). With selected electrophiles a second addition to the tungsten-carbon bond can occur, allowing for targeted functionalisation of phosphinocarbyne complexes. In the reaction with sulfur, the thioacyl phosphine sulfide [W{η^2-SCP(=S)Ph$_2$}(CO)$_2$(Tp*)] has been isolated as a minor product. Kinetic protonation of **2** occurs on the phosphine, which rearranges in polar solvents to afford the η^2-carbene complex [W{η^2-C(H)PPh$_2$}(CO)$_2$(Tp*)]BF$_4$.

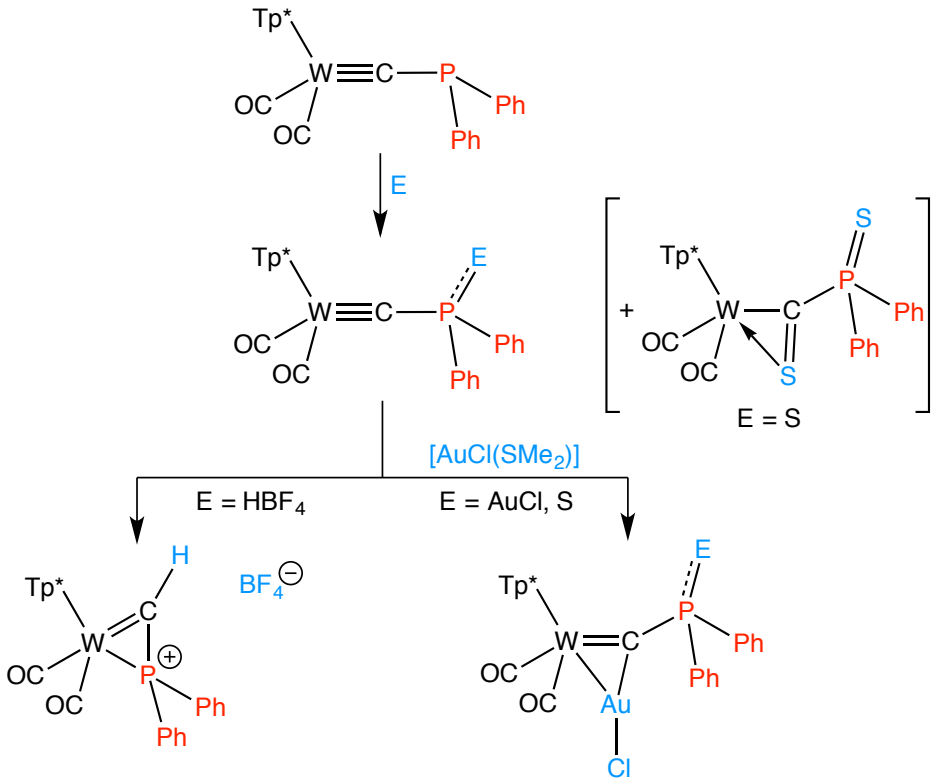

Scheme 2.42. Electrophilic addition reactions of $[W(\equiv CPPh_2)(CO)_2(Tp^*)]$ (E = O, S, Se, BH_3, Me^+, H^+, AuCl, $RhCl_2Cp^*$).

CHAPTER 3.

Chlorophosphinocarbyne complexes

CHAPTER 3: Chlorophosphinocarbyne complexes

3.1 Introduction

Halophosphines (PX_3, PX_2R, PXR_2) are among the most important compounds in synthetic organophosphorus chemistry. Halophosphines are highly reactive, particularly towards nucleophiles, which gives rise to their extensive use as synthetic precursors to countless phosphines. A search of the SciFinder database reveals more than 90,000 reactions in which PCl_3, one of the simplest halophosphines, is employed as a reactant or reagent. In many cases, halophosphines are the reagent of choice as starting materials to produce all varieties of phosphorus containing compounds.

The use of halophosphines as precursors to substituted phosphines dates back to as early as 1879 when Michaelis reported his synthesis of dichlorophenylphosphine and dichlorotolylphosphine via a Friedel-Crafts type reaction of PCl_3 with benzene or toluene in the presence of $AlCl_3$.[319] Nowadays, functionalisation of halophosphines is most commonly achieved via nucleophilic substitution of chloride by an organometallic reagent. Typically, organolithium (RLi) or Grignard reagents (RMgX) are used, but there are examples of the effective use of many other organometallics such as zinc, tin, copper and cadmium, particularly when mono-halide substitution is desired.[313]

The first reported examples of phosphinocarbyne complexes by Cummins included two chlorophosphinocarbyne complexes $[Mo(\equiv CPClR)(X)_3]$ (R = Cl, Ph; X = $N^tBu(3,5\text{-}C_6H_3Me_2)$).[40,41] This P−Cl motif is of interest because in principle it allows for installation of further functionality into the carbyne complex via nucleophilic substitution of the chloride group. In Cummins' case, their motivation was the synthesis of a coordinated phosphaisocyanide analogue. Reduction of the chlorophosphinocarbyne complex $[Mo(\equiv CPClPh)(X)_3]$ with sodium amalgam gave the ion paired complex $[Mo(\equiv CPPhNa)(X)_3(L)_2]_2$ (L = Et_2O, THF) containing a $CPPh^-$ ligand, as depicted in Scheme 3.1. The utility of $[Mo(\equiv CPClPh)(X)_3]$ as a synthetic precursor was further demonstrated by the reaction with $[Mo(\equiv CPPhNa)(X)_3(L)_2]$ to provide the dimeric complex $[Mo_2(\mu\text{-}CPPh)_2(X)_6]$.

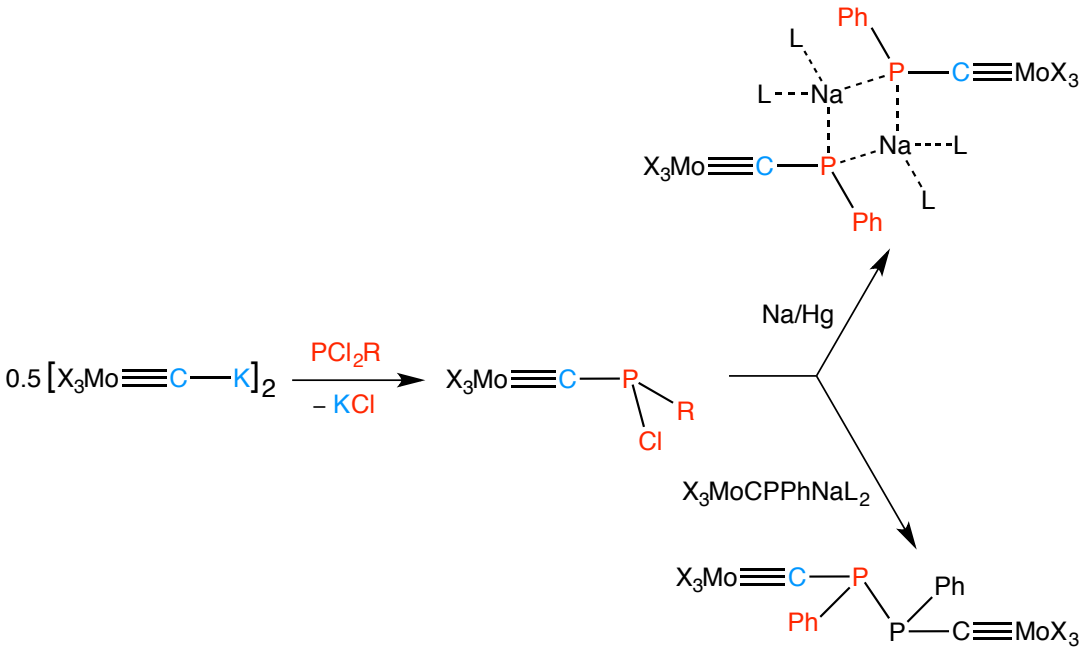

Scheme 3.1. Cummins' synthesis and subsequent reactions of chlorophosphinocarbyne complexes (X = N^{t}Bu(3,5-$C_6H_3Me_2$); R = Cl, Ph; L = Et_2O, THF).

Similarly, the potential to harness reactivity at the P−Cl site served as the motivation by which chlorophosphinocarbyne complexes were chosen as targets in this work. It was envisaged that such complexes would constitute late stage synthetic intermediates, derivatisation of which might provide a variety of species of interest. Following studies into the reactivity of the tertiary phosphine **2** towards electrophiles, discussed in Chapter 2, the possibility of extending the reactivity of phosphinocarbyne complexes to allow the introduction of nucleophiles at the phosphine was considered. Accordingly, the reactions of the lithiocarbyne [W(≡CLi)$(CO)_2$(Tp*)] towards a range of di- and tri-halophosphines were of interest.

Preliminary studies by Shang on the reactivity of the molybdenum lithiocarbyne [Mo(≡CLi)$(CO)_2$(Tp*)] towards dichlorophenylphosphine, whilst not completed, nevertheless appeared promising.[220] The reaction of [Mo(≡CBr)$(CO)_2$(Tp*)] with ^{n}BuLi and PCl_2Ph at −78°C led to isolation of the phosphinocarbyne complex [Mo(≡CPClPh)$(CO)_2$(Tp*)] (Scheme 3.2). The $^{31}P\{^1H\}$ NMR spectrum contained a singlet at δ_P 85.3 (C_6D_6), and the carbyne resonance was identified in the $^{13}C\{^1H\}$ NMR spectrum as a doublet at δ_P 299.6 ($^1J_{PC}$ 106 Hz). However, attempts to synthesise the bis-substituted product [Mo_2(μ-C_2PPh)$(CO)_4$(Tp*)$_2$] using a 2:1 stoichiometry gave a

mixture of products, with the desired product accounting for only 3% of the crude mixture on the basis of $^{31}P\{^{1}H\}$ NMR spectroscopy (Scheme 3.2). This was in contrast to a similar reaction involving dichlorodimethylstannane in which the chlorostannylcarbyne intermediate could not be isolated or observed en route to the binuclear complex $[Mo_2(\mu\text{-}C_2SnMe_2)(CO)_4(Tp^*)_2]$.

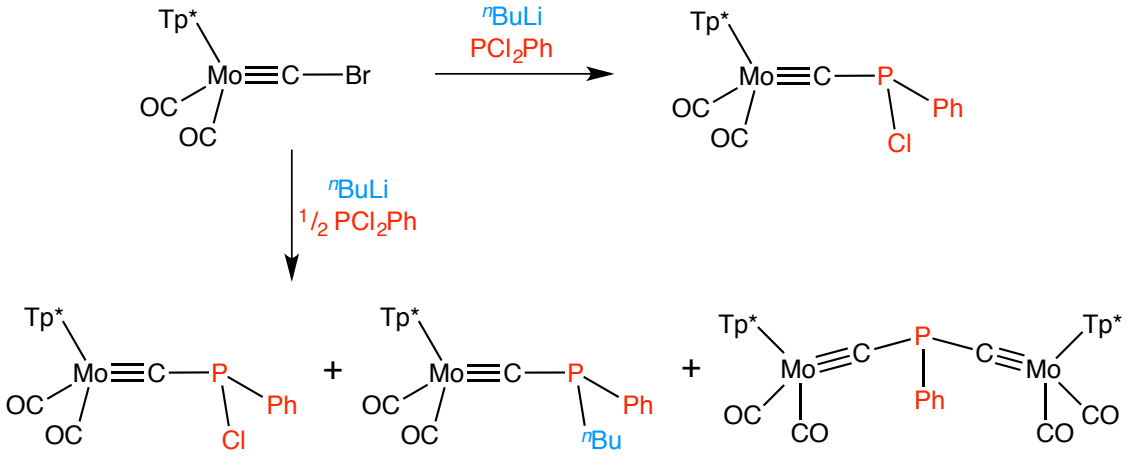

Scheme 3.2. Previous work on chlorophosphinocarbyne complexes.

Amongst the product mixture, the butyl-substituted phosphinocarbyne $[Mo(\equiv CP^{n}BuPh)(CO)_2(Tp^*)]$ was identified and attributed to a side reaction of the mono-substituted complex $[Mo(\equiv CPClPh)(CO)_2(Tp^*)]$ with extraneous ^{n}BuLi present in the reaction mixture. Incorporation of ^{n}butyl groups into products was a recurrent problem in this preliminary study. To avoid these problems, tungsten was utilised in the present work, rather than molybdenum, as it was anticipated that the slower kinetics might hamper these types of side reactions.

3.2 Synthesis of chlorophosphinocarbyne complexes via the lithiocarbyne approach

3.2.1 Synthesis of $[W(\equiv CPClPh)(CO)_2(Tp^*)]$

Using the same electrophilic addition methodology described in the previous chapter, the synthesis of the chlorophosphinocarbyne complex $[W(\equiv CPClPh)(CO)_2(Tp^*)]$ (**15**) was investigated (Scheme 3.3). A solution of the bromocarbyne in THF at −78°C was treated with one equivalent of ^{n}BuLi, followed by one equivalent of dichlorophenylphosphine. Extraction with ^{n}pentane, concentration and cooling provided the desired product as a peach coloured precipitate in 71% yield.

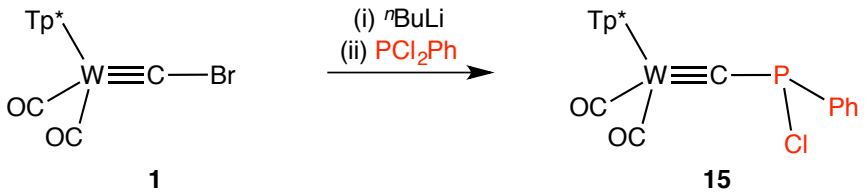

1 **15**

Scheme 3.3. Synthesis of [W(≡CPClPh)(CO)$_2$(Tp*)] (**15**).

The infrared spectrum of **15** includes ν_{CO} absorption bands at 1992 and 1905 cm^{-1} (THF), at higher frequency compared to those of **2** (1981, 1893 cm^{-1}), indicating the increased π-acceptor capacity of the carbyne ligand resulting from negative hyperconjugation involving the P−Cl σ* orbitals. As expected, the $^{31}P\{^1H\}$ NMR spectrum of **15** displays a significantly downfield shift compared to the tertiary phosphine **2** (91.2 ppm *cf.* 32.0 ppm for **2**), but only slightly downfield with respect to that of the molybdenum analogue [Mo(≡CPClPh)(CO)$_2$(Tp*)] (δ_P 85.3),[220] and very similar to what was observed for [Mo(≡CPClPh)(X)$_3$] (δ_P 94.0; X = N^{t}Bu(3,5-C$_6$H$_3$Me$_2$)).[40] Coupling to ^{183}W was observed, with a $^2J_{WP}$ value of 77.9 Hz, slightly larger than that of **2** (69.0 Hz).

In the ^{1}H NMR spectrum a 1:1:1 ratio of the three Tp* pyrazolyl rings is observed, rather than the 2:1 ratio observed for **2** and its derivatives, reflecting the reduced symmetry (C_1) as a consequence of the chiral phosphorus centre. This lower symmetry is also indicated by three pyrazolyl environments being observed in the $^{13}C\{^1H\}$ NMR spectrum, in addition to two resonances due to the diastereotopic carbonyl ligands. The carbyne carbon appears at δ_C 285.2 as a doublet with a large $^1J_{PC}$ coupling constant of 96.0 Hz (*cf.* **2** 74.5 Hz) and with $^1J_{WC}$ 189.0 Hz. The susceptibility of the P−Cl bond to hydrolysis precluded the acquisition of analysable mass spectrometric data using conventional ESI conditions.

The existence of rotational isomers due to restricted rotation about the carbyne C−P bond was inferred from the appearance of a shoulder to lower ppm of the main resonance in the $^{31}P\{^1H\}$ NMR spectrum. Variable temperature NMR studies in toluene-d_8 over the temperature range –90 to +90°C failed to resolve signals attributable to the presumed rotamers (Figure 3.1). Between –60°C and +60°C the shoulder was still visible, whilst at –90°C and +90°C the resolution was too poor to resolve the broad

singlet into the constituent peaks. Complex **15** is the only species in this work for which rotational isomerism about the phosphorus-carbon bond was evident on the ^{31}P NMR timescale (121 MHz) although in a number of cases the co-existence of such isomers was apparent on the infrared timescale.

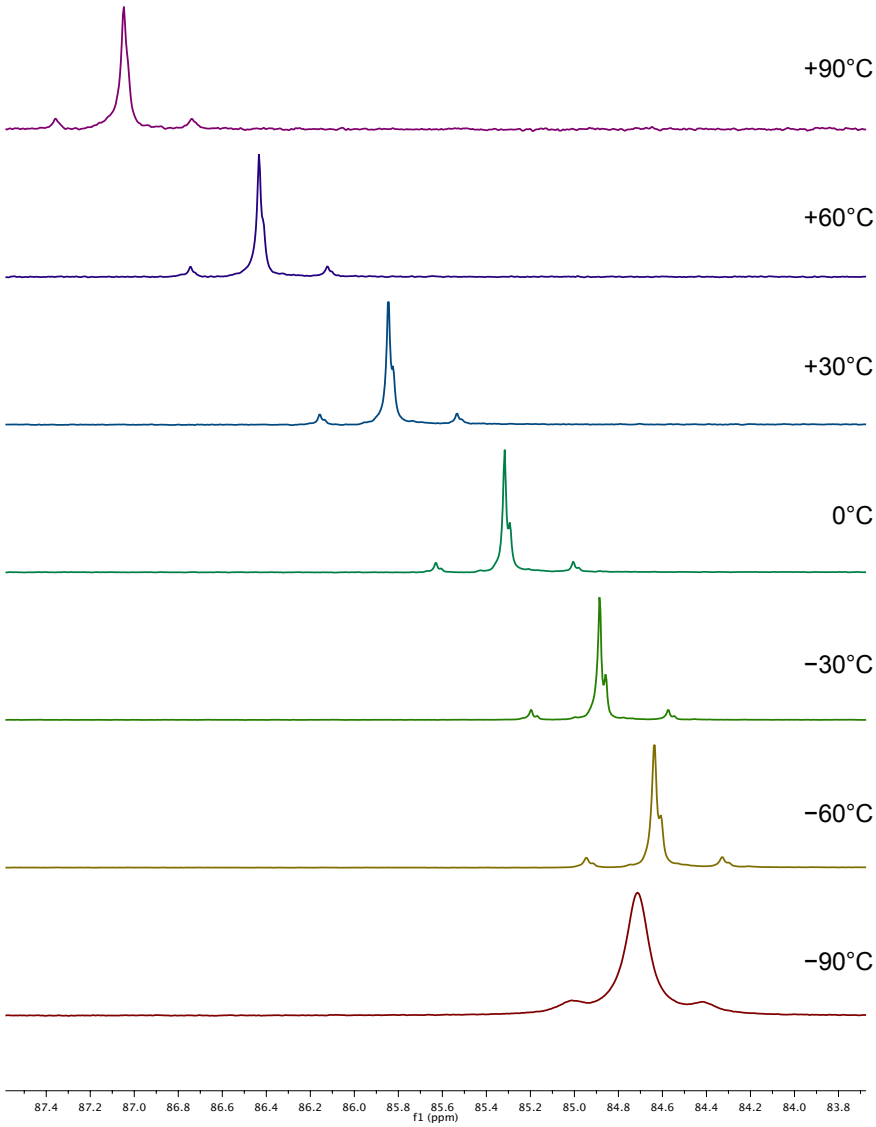

Figure 3.1. Variable temperature $^{31}P\{^{1}H\}$ NMR spectra of **15** (−90 to +90°C, toluene-d_8, 121 MHz).

One difficulty encountered in the preparation of chlorophosphinocarbyne complexes was that the products were generally obtained as a mixture of the mono-substitution [W(≡CPClR)(CO)$_2$(Tp*)] and the bis-substitution products [W$_2$(μ-C$_2$PR)(CO)$_4$(Tp*)$_2$]. This issue is not unique to the present study, but rather a recurrent feature of the reactions of organolithium species with trihalophosphines.[313] The product distribution

varied depending on the R group used, and when R = NEt_2, N^iPr_2 none of the bimetallic species was formed. For R = Cy, Ph, the bulk sample often contained ca. 5% of the bimetallic complex. The intentional synthesis of the bimetallic complexes [W_2(μ-C_2PR)$(CO)_4$(Tp*)$_2$] is discussed in Chapter 5. As the P–Cl bond is very sensitive to hydrolysis, chromatographic purification was not feasible for the separation of the mono- and bimetallic complexes. The products obtained were solids, so distillation was also not viable, unlike traditional organophosphines. In general, purification of the reaction mixture was effected by extraction and fractional crystallisation with varying degrees of success. Unfortunately, in some cases this led to less than ideal standards of purity (e.g. [W{≡CPCl(NEt_2)}$(CO)_2$(Tp*)], Section 3.2.4).

3.2.2 Synthesis of [W(≡CPClCy)$(CO)_2$(Tp*)]

Dichlorocyclohexylphosphine was used to extend this methodology to an alkyl derivative in the expectation that the steric bulk imposed by the cyclohexyl group might allow more control over the degree of substitution at phosphorus. Treating [W(≡CLi)$(CO)_2$(Tp*)] with one equivalent of PCl_2Cy resulted in the immediate formation of a dark red coloured solution. After removal of the volatiles, extraction of the solid residue with pentane and subsequent concentration and cooling resulted in precipitation of the desired phosphinocarbyne [W(≡CPClCy)$(CO)_2$(Tp*)] (**16**) (Scheme 3.4).

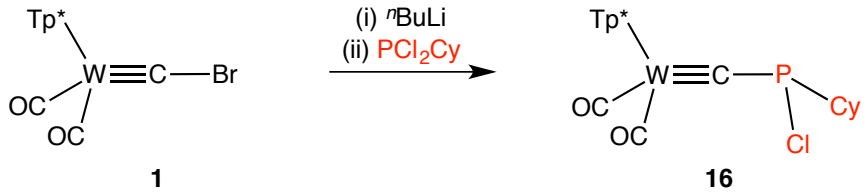

1 **16**

Scheme 3.4. Synthesis of [W(≡CPClCy)$(CO)_2$(Tp*)] (**16**).

The key spectroscopic features of **16** are similar to those seen for **15**. The THF infrared spectrum contains three carbonyl absorption bands at 1989 (s), 1969 (m) and 1901 (s) cm^{-1}, implicating the co-existence of rotamers. The observed frequencies appear close to those of **15** (ν_{CO} 1992, 1905 cm^{-1}), demonstrating the similar π-acceptor capacities of the two ligands. The solid state infrared spectrum contains five ν_{CO} bands. As the solution spectrum also contains more than two ν_{CO} absorptions, this suggests that rotational isomers are present, although solid state effects may also contribute to the

complexity of the spectrum. The $^{31}P\{^{1}H\}$ NMR spectrum contains a singlet at δ_P 120.2 ($^{2}J_{WP}$ 67.9 Hz), significantly downfield from the aryl phosphine **15** (δ_P 91.2). The ^{1}H and $^{13}C\{^{1}H\}$ NMR spectra reveal the expected 1:1:1 ratio of the pyrazolyl ring environments due to the chiral phosphorus atom. As with **15**, the two diastereotopic carbonyl ligands give rise to discrete resonances (δ_C 227.2, 225.8) whilst the appearance of a single carbyne resonance (δ_C 292.2) indicates that interconversion of the rotational isomers suggested by IR data is rapid on both the ^{13}C and ^{31}P NMR timescales. It may also be concluded that inversion of the phosphorus centre does not occur on these timescales as this would render the CO ligands chemically equivalent for both **15** and **16**.

3.2.3 Synthesis of [W(≡CPCl$_2$)(CO)$_2$(Tp*)]

When the reaction of the lithiocarbyne [W(≡CLi)(CO)$_2$(Tp*)] with one equivalent of PCl_3 was examined, a mixture of products was obtained (Scheme 3.5). The $^{31}P\{^{1}H\}$ NMR spectrum indicated that the desired product [W(≡CPCl$_2$)(CO)$_2$(Tp*)] (**17**) (δ_P 136.2, $^{2}J_{WP}$ 80.5 Hz) constituted ca. 90% of the isolated product, but it was contaminated with ca. 10% of the bimetallic complex [W$_2$(μ-C$_2$PCl)(CO)$_4$(Tp*)$_2$] (**35**) (δ_P 124.7, $^{2}J_{WP}$ 70.3 Hz). While purification options beyond this level were somewhat restricted due to the hydrolytically sensitive P−Cl linkage precluding chromatography, the IR and NMR data obtained substantiate the formation of **17**. The phosphorus resonance for **17** appears at δ_P 136.2, close to that of [Mo(≡CPCl$_2$)(X)$_3$] (X = N^{t}Bu(3,5-C$_6$H$_3$Me$_2$)) (δ_P 120.1),[41] while the $^{2}J_{WP}$ coupling constant (80.5 Hz) is indicative of the three-coordinate environment at phosphorus.

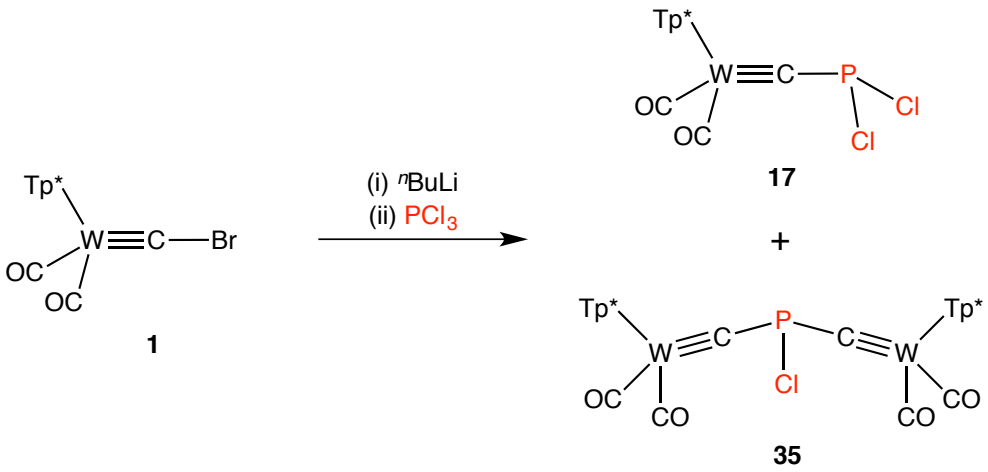

Scheme 3.5. Synthesis of [W(≡CPCl$_2$)(CO)$_2$(Tp*)] (**17**).

Table 3.1 summarises some of the key spectroscopic data for the phosphinocarbyne complexes [W(≡CPRR')(CO)$_2$(Tp*)] (R, R' = Cl, Ph). From this it can be seen that substitution of phenyl substituents for chloro groups leads to a downfield shift in the ^{31}P NMR spectrum, while a modest increase in the tungsten-phosphorus coupling constant is observed. The infrared frequencies of the carbonyl absorption bands shift to higher frequency upon replacement of phenyl substituents by chloro groups. This might be understood in terms of negative hyperconjugation between the W≡C π system and the empty P−Cl σ* orbitals.

Table 3.1. Selected spectroscopic data for [W(≡CPRR')(CO)$_2$(Tp*)] (R, R' = Cl, Ph).

Complex	δ_P	$^2J_{WP}$ (Hz)	ν_{CO} (cm^{-1})
[W(≡CPPh$_2$)(CO)$_2$(Tp*)] (**2**)	32.2	66.2	1981, 1893
[W(≡CPClPh)(CO)$_2$(Tp*)] (**15**)	91.2	74.9	1992, 1905
[W(≡CPCl$_2$)(CO)$_2$(Tp*)] (**17**)	136.2	80.5	2005, 1920

NMR spectra were recorded in C_6D_6. IR spectra were recorded in THF.

Variation in the stoichiometry in the reactions of [W(≡CLi)(CO)$_2$(Tp*)] with PCl_3 or dichlorophosphines can be used to deliberately target bi- and trimetallic phosphinocarbyne complexes. Chapter 5 details findings in this area.

3.2.4 Synthesis of [W{≡CPCl(NEt$_2$)}(CO)$_2$(Tp*)]

The preparation of nitrogen-functionalised phosphinocarbyne complexes was explored because it was anticipated that the presence of the positively mesomeric amino group might alter the reactivity compared to the alkyl and aryl analogues. In particular it should assist in stabilising species such as the phosphenium cation [W(≡CPNR$_2$)(CO)$_2$(Tp*)]$^+$. P−N cleavage of aminophosphines is also a useful synthetic protocol for the further functionalisation of aminophosphines.[320-325]

Some preliminary research carried out by Shang yielded the first examples of carbyne complexes bearing nitrogen-functionalised phosphorus substituents.[220] Unfortunately, many of these attempts were hampered by decomposition of the products or competing

side reactions, particularly with ^{n}butyl incorporation into products. The reaction of [Mo(≡CLi)(CO)$_2$(Tp*)] with (ClPN^{t}Bu)$_2$ gave the desired dimeric complex [Mo$_2$(μ-CPN^{t}Bu)$_2$(CO)$_4$(Tp*)$_2$] (Scheme 3.6). However, when the reaction of [M(≡CLi)(CO)$_2$(Tp*)] (M = Mo, W) and the iminophosphinyl chloride ClP=NMes* was performed, butyl-substituted products were isolated from the reaction mixtures, albeit in low yields (Scheme 3.6). In contrast to these studies, the current work focuses on species containing saturated amino groups and reactive substituents at phosphorus to allow for further derivatisation at this site.

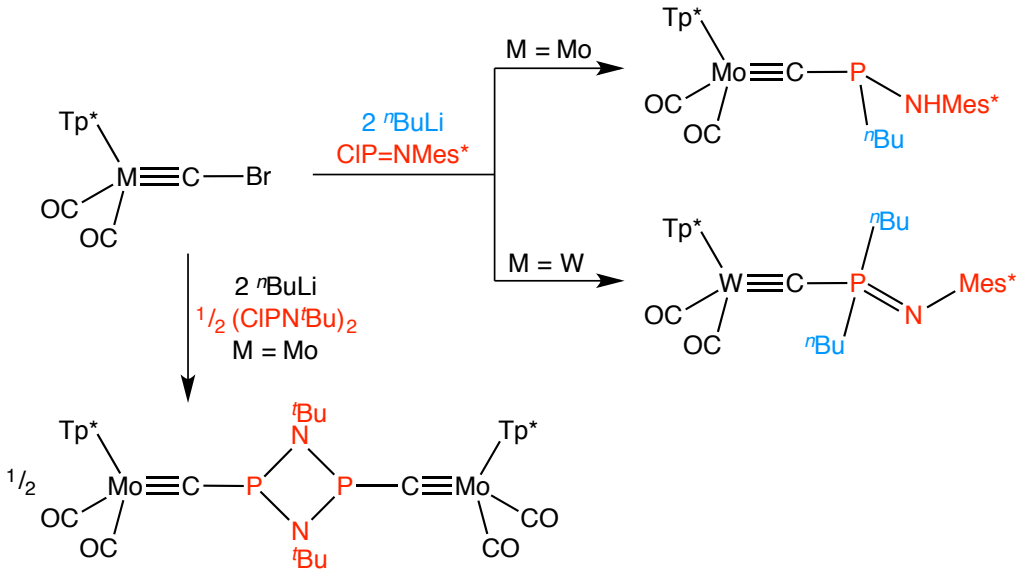

Scheme 3.6. Shang's syntheses of nitrogen-substituted phosphorus carbyne complexes.

It was anticipated that, based on previous successes in simple electrophilic substitution reactions with chlorophosphines, the same outcome would be attained by using σ^3,λ^3-chloroaminophosphines. The reaction of [W(≡CLi)(CO)$_2$(Tp*)] with dichloro(diethylamino)phosphine resulted in formation of one major product with ν_{CO} bands at 1993 and 1904 cm^{-1}, which was identified as the desired phosphinocarbyne [W{≡CPCl(NEt$_2$)}(CO)$_2$(Tp*)] (**18**) (Scheme 3.7). The ^{31}P{^{1}H} NMR spectrum supported this formulation by the presence of a singlet with ^{183}W satellites at δ_P 136.7 with coupling to tungsten ($^{2}J_{WP}$ 76.4 Hz) within the expected range for a three-coordinate phosphorus.

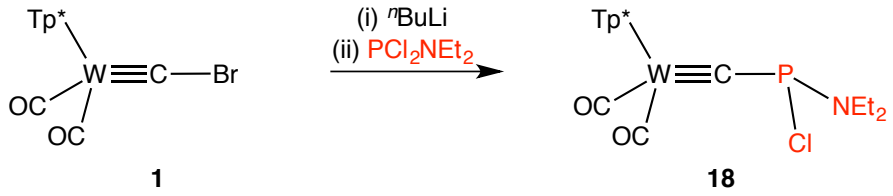

1 18

Scheme 3.7. Synthesis of [W{≡CPCl(NEt_2)}$(CO)_2$(Tp*)] (**18**).

Unfortunately, although $^{31}P\{^1H\}$ NMR spectroscopy indicated that the desired product had formed in ca. 80% yield, purification beyond this level was unsuccessful. Extraction with pentane or toluene (to remove the liberated lithium chloride) followed by concentration and cooling did not yield any precipitate, even at −78°C. Chromatography is not feasible due to the presence of the hydrolytically sensitive P−Cl bond, which was confirmed by TLC. The impure nature of the product meant that unambiguous identification of resonances attributed to **18** in the ^1H NMR spectrum was not possible, particularly in the alkyl region. Because of these difficulties efforts were redirected towards the diisopropylamino analogue as it was hoped that this might have a greater propensity to crystallise whilst still providing informative spectroscopic characteristics in the ^1H NMR spectrum.

3.2.5 Synthesis of [W{≡CPCl(N^iPr_2)}$(CO)_2$(Tp*)]

The synthesis of the diisopropyl analogue was carried out in an analogous manner to **18**. Fortunately, in this case concentration of the filtered hexane extract from the crude reaction mixture residue afforded [W{≡CPCl(N^iPr_2)}$(CO)_2$(Tp*)] (**19**) as a spectroscopically and analytically pure brown solid in excellent yield (96%) (Scheme 3.8).

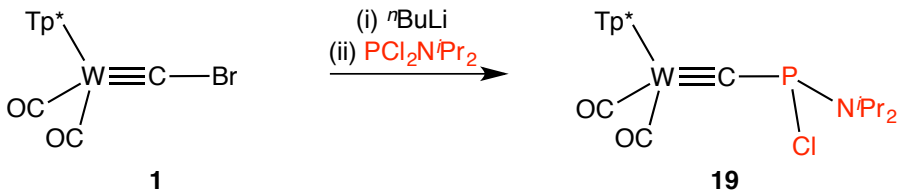

1 19

Scheme 3.8. Synthesis of [W{≡CPCl(N^iPr_2)}$(CO)_2$(Tp*)] (**19**).

The spectroscopic data for **19** are as expected. The THF infrared spectrum contains two carbonyl absorption bands at 1992 and 1904 cm^{-1}, very close to those observed for the phenyl analogue **15** (1992, 1905 cm^{-1}), indicating that the incorporation of the

positively mesomeric amine group does not result in a marked increase of electron density at the metal centre. The $^{31}P\{^{1}H\}$ NMR spectrum shows a peak at δ_P 130.3, with $^{2}J_{WP}$ 81.2 Hz, similar to the coupling constants observed for other three-coordinate chlorophosphinocarbyne complexes encountered in this work.

The carbyne carbon appears in the $^{13}C\{^{1}H\}$ NMR spectrum in the typical downfield region at δ_C 291.3, accompanied by phosphorus-carbon (93.5 Hz) and tungsten-carbon (187.2 Hz) coupling constants similar to those of other chlorophosphinocarbynes. In the ^{1}H and $^{13}C\{^{1}H\}$ NMR spectra of **19** the peaks due to the isopropyl groups are broad. The rest of the molecule displays sharp peaks, indicating that there must be fluxional rotation about the phosphorus-nitrogen bond on both the ^{1}H and ^{13}C NMR timescales. Four distinct $^{i}Pr(CH_3)$ environments and two distinct $^{i}Pr(CH)$ environments are observed as a result of this restricted rotation.

Variable temperature NMR demonstrated changes in the ^{1}H NMR spectrum over the temperature range −60°C to +100°C (Figure 3.2). At −60°C four $^{i}Pr(CH_3)$ environments were observed, although two of these resonances overlap, indicating restricted rotation. At 40°C this collapses into two broad resonances, and at 100°C two doublets are observed. These two doublets correspond to the two diastereotopic methyl groups of the isopropyl substituents (Me and Me', Figure 3.2), indicating that this temperature is sufficient to overcome the energy barrier and thus allow free rotation about the P−N bond. At high temperatures broad unresolved $^{i}Pr(CH)$ resonances are observed at 3.5 – 5 ppm. Following measurements at 100°C, the spectrum remeasured under ambient conditions showed no sign of decomposition of the complex, indicative of a high degree of thermal stability.

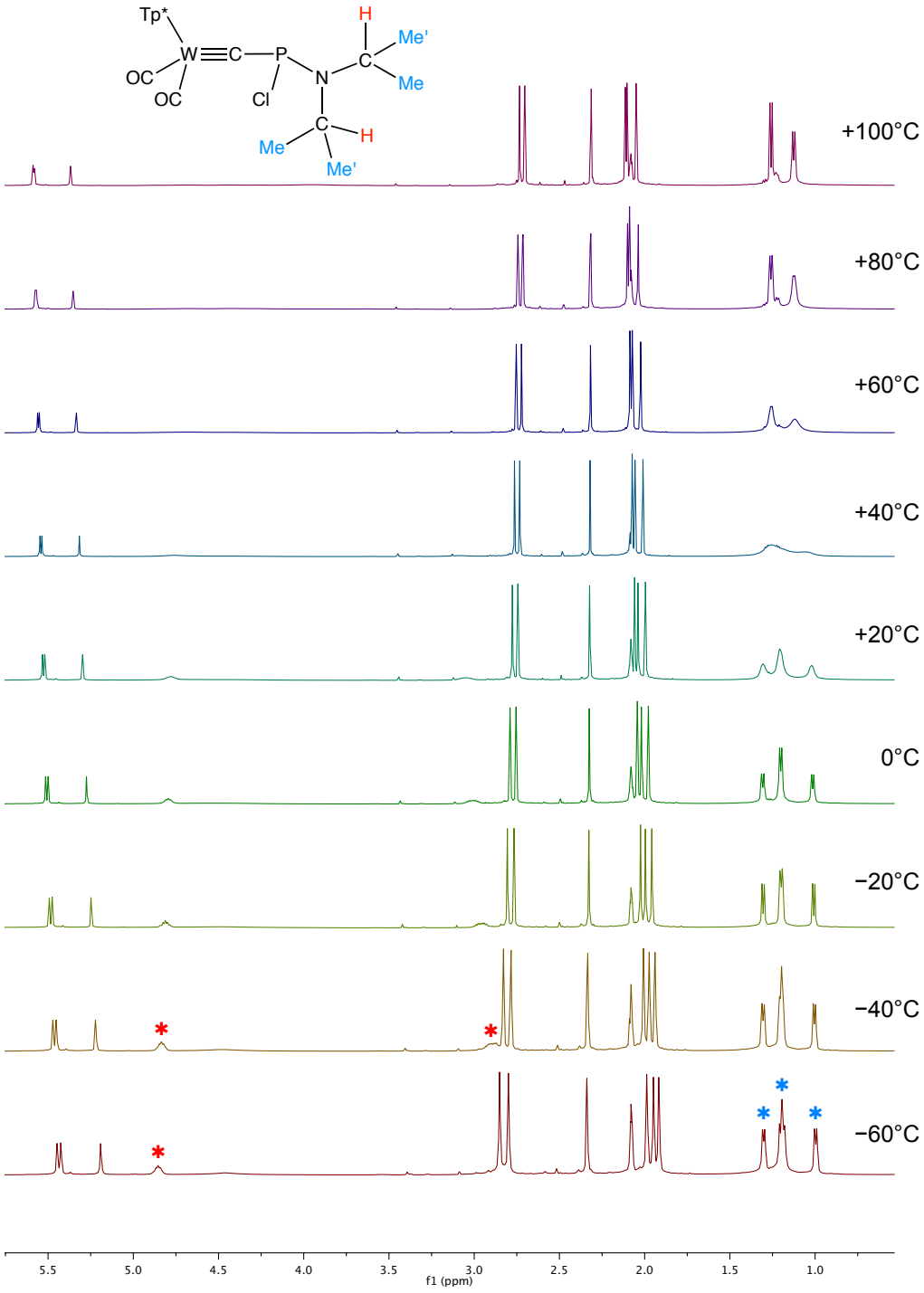

Figure 3.2. Variable temperature ^{1}H NMR spectra of **19** (−60°C to +100°C, toluene-d_8, 500 MHz).

Unfortunately, X-ray quality crystals of **19** were not forthcoming. However, the crystallographically characterised compounds $[PCl(N^iPr_2)\{C(PPh_3)_2\}]AlCl_4$,[326] $PCl(N^iPr_2)(CMeCCl_2)$[327] and $\{PCl(N^iPr_2)\}_2(C_2B_{10}H_{10})$[328] all contain trigonal pyramidal (sp^3) phosphorus atoms and trigonal planar (sp^2) nitrogen atoms (Figure 3.3), and it is

assumed that the amine moiety in complex **19** would similarly adopt a trigonal planar geometry, consistent with the observation that all four ^{i}Pr(CH$_3$) groups are inequivalent.

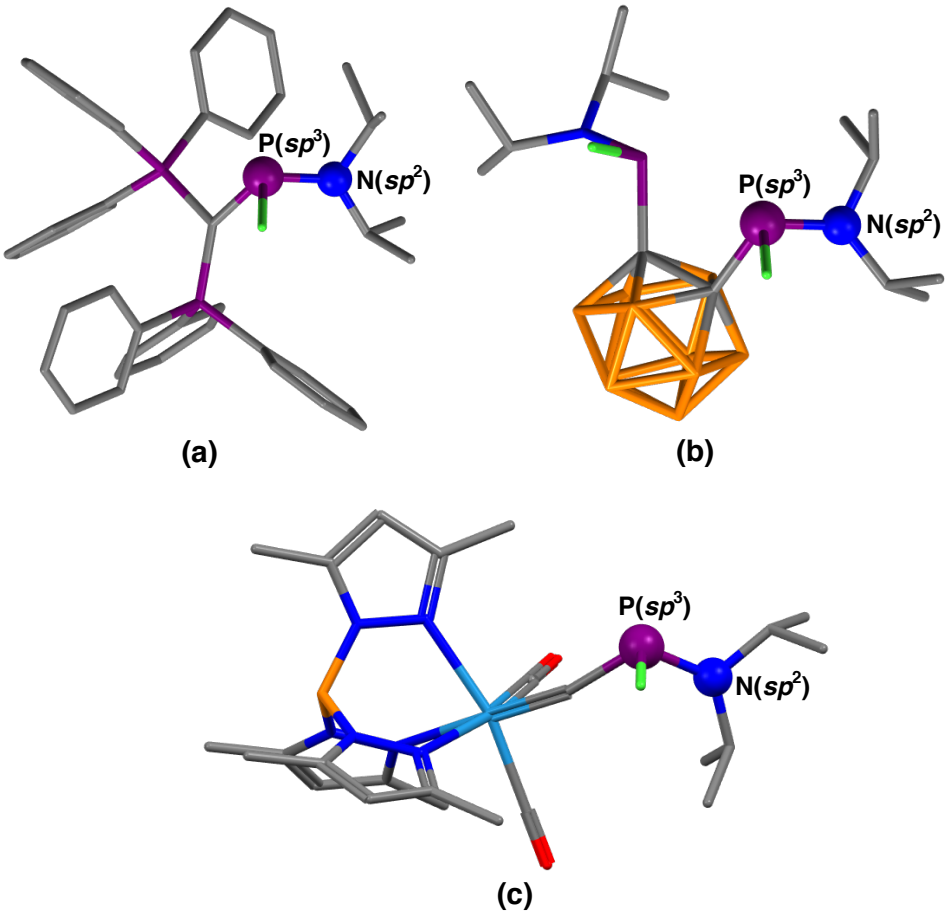

Figure 3.3. Depiction of the geometries at phosphorus and nitrogen in the molecular structures of (a) [PCl(N^{i}Pr$_2$){C(PPh$_3$)$_2$}]AlCl$_4$, (b) {PCl(N^{i}Pr$_2$)}$_2$(C$_2$B$_{10}$H$_{10}$) and (c) in the calculated* structure of **19**.

3.3 Reactions of [W(≡CPClPh)(CO)$_2$(Tp*)]

The reactivity of chlorophosphinocarbyne [W(≡CPClPh)(CO)$_2$(Tp*)] **15** is potentially interesting because of the added dimension it presents over its tertiary analogue [W(≡CPPh$_2$)(CO)$_2$(Tp*)] **2** – the reactive P–Cl bond. The following sections of this chapter detail investigations into exploitation of this facet of chlorophosphinocarbyne complexes.

* Calculated using Spartan 14 at the semi-empirical PM3 level of theory to qualitatively illustrate the molecular topology of **19**.

Complex **15** exhibits reasonable thermal stability; no significant decomposition was observed over eight days at 80°C in a toluene solution. However, **15** is much more aerobically sensitive than its tertiary analogue **2** due to the hydrolytically sensitive P−Cl bond. Whilst **2** is moderately stable to air and moisture both as a solid and in solution, **15** decomposes within minutes in solution when exposed to either air or moisture.

Addition of degassed H_2O to a $CDCl_3$ solution of **15** resulted in complete consumption of **15** within ten minutes, coupled with the appearance of new peaks in the $^{31}P\{^1H\}$ NMR spectrum at δ_P 25.3 (4.0%), 23.0 (14.0%), 22.3 (broad, 49.2%), 13.9 ($^2J_{WP}$ 156.1 Hz, 27.1%) and 12.0 (broad, 5.7%). The hydrolysis pathway is postulated to follow that outlined in Scheme 3.9. Hydrolysis of monohalophosphines produces the corresponding hydroxyphosphines (i.e. [W{≡CP(OH)Ph}(CO)$_2$(Tp*)]), but these compounds actually exist as the phosphine oxide tautomer (i.e. [W{≡CP(=O)HPh}(CO)$_2$(Tp*)]).[253,313] This secondary phosphine oxide [W{≡CP(=O)HPh}(CO)$_2$(Tp*)] corresponds to the resonance observed at δ_P 13.9 ($^2J_{WP}$ 156.1 Hz), which was confirmed by the oxidation of [W(≡CPHPh)(CO)$_2$(Tp*)] (see Section 4.2) with hydrogen peroxide.

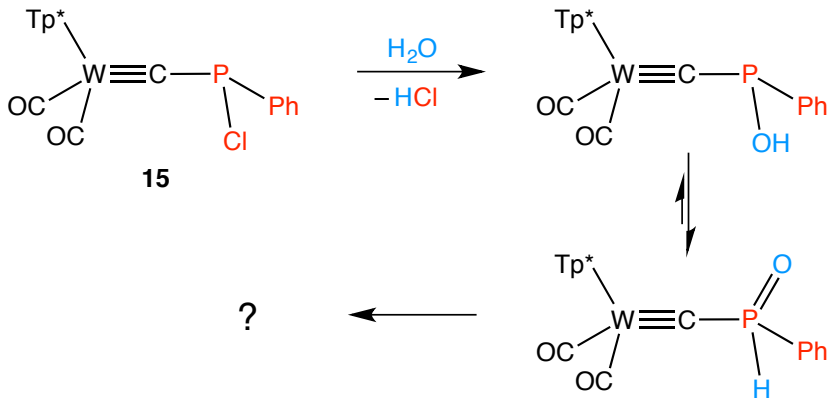

Scheme 3.9. Hydrolysis of [W(≡CPClPh)(CO)$_2$(Tp*)].

However, the hydrolysis of **15** was found to be more complicated than simply formation of [W{≡CP(=O)HPh}(CO)$_2$(Tp*)], as evidenced by the numerous other resonances present in the NMR spectra. After 16 hours, the $^{31}P\{^1H\}$ NMR spectrum indicated that δ_P 23.7 represented the major P-containing species (ca. 89%), and no peak due to [W{≡CP(=O)HPh}(CO)$_2$(Tp*)] was observed. The ^1H NMR spectrum indicated one major Tp*-containing complex was present which displayed a 1:1:1 ratio of the pyrazolyl peaks, possibly corresponding to Templeton's nonclassical vinylidene-bridged

complex $[W_2(\mu\text{-}CCH_2)(CO)_4(Tp^*)]$. This bimetallic complex results from dimerisation of the methylidyne $[W(\equiv CH)(CO)_2(Tp^*)]$,[65] which in this case might arise from hydrolysis of the P−C(carbyne) bond.

The absence of ^{183}W satellites from all observed $^{31}P\{^1H\}$ NMR resonances except one (i.e. $[W\{\equiv CP(=O)HPh\}(CO)_2(Tp^*)]$) led to the supposition that these hydrolysis products involved cleavage of the P−C(carbyne) bond, consistent with the suspected formation of $[W_2(\mu\text{-}CCH_2)(CO)_4(Tp^*)]$. Secondary alkynylphosphine oxides HP(=O)(R)(C≡CR') are not stable and have been found to be susceptible to P−C(alkyne) bond cleavage to provide the corresponding phosphinic acid HP(=O)(R)(OH).[329] The equivalent decomposition reaction could account for one of the observed $^{31}P\{^1H\}$ NMR peaks (e.g. δ_P 22.3, 23.0, 23.7), as these are found near the reported value for HP(=O)(Ph)(OH) (δ_P 21.5).[330] Decomposition is likely to be complicated by the presence of the tautomer $[W\{\equiv CP(OH)Ph\}(CO)_2(Tp^*)]$ as these species are known to be reactive intermediates in reactions of secondary phosphine oxides,[253] as well as by the presence of liberated HCl.

3.3.1 Reactions with organolithium reagents

In the literature, conventional syntheses of phosphines are commonly carried out by reaction of the corresponding halophosphine with an organometallic reagent, typically organolithium (RLi) or Grignard reagents (RMgX).[253,313] One of the key reasons for targeting chlorophosphinocarbyne complexes was that they should allow for this facet of functionalisation through reaction with organometallic reagents, providing access to ideally any phosphine, limited only by imagination.

Synthesis of $[W(\equiv CPPh_2)(CO)_2(Tp^*)]$

To begin these investigations, the reaction of **15** with phenyllithium was examined so as to provide proof of concept through formation of the previously prepared complex **2**. Treatment of a THF solution of **15** at –78°C with a slight excess of PhLi resulted in the exclusive formation of **2**, as indicated by ^1H and $^{31}P\{^1H\}$ NMR analysis of the crude reaction mixture (Scheme 3.10).

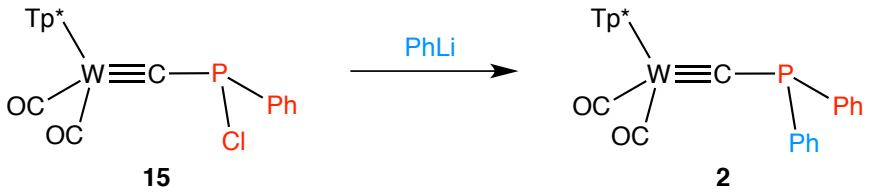

15 2

Scheme 3.10. Synthesis of **2** by reaction of **15** with phenyllithium.

Synthesis of [W(≡CPMePh)(CO)$_2$(Tp)]*

Having established the viability of this approach, the generality of the protocol was explored. A diethyl ether suspension of **15** was cooled to −78°C and treated with methyllithium, resulting in a brown suspension. Following chromatography on silica gel, [W(≡CPMePh)(CO)$_2$(Tp*)] (**20**) was obtained as a yellow powder in 49% yield (Scheme 3.11).

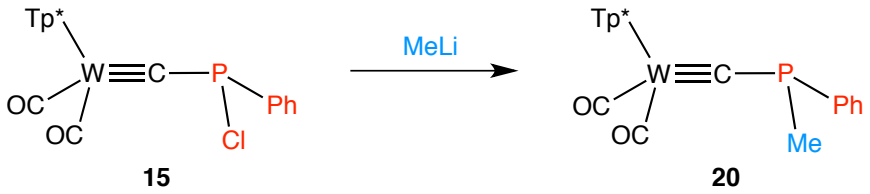

15 20

Scheme 3.11. Synthesis of [W(≡CPMePh)(CO)$_2$(Tp*)] (**20**).

The spectroscopic data for **20** are largely unremarkable. The presence of the methyl group is evident in the ^{1}H and ^{13}C{^{1}H} NMR spectra as doublets at δ_H 1.67 ($^2J_{PH}$ 3.6 Hz) and δ_C 11.6 ($^1J_{PC}$ 15.1 Hz) due to coupling to the phosphorus nucleus. The ^{1}H and ^{13}C{^{1}H} NMR spectra display the anticipated 1:1:1 ratio pyrazolyl environments invoked by the presence of the chiral phosphorus centre. The infrared spectrum in THF shows a shift to lower frequency (ν_{CO} 1977, 1888 cm^{-1}) upon substitution of the electron-withdrawing chloride for the methyl group (**15**: ν_{CO} 1992, 1905 cm^{-1}).

The electron-releasing methyl substituent renders complex **20** considerably more air-sensitive than the diphenylphosphinocarbyne **2**. While a solution of **2** in air showed only 43% conversion to the oxide over 14 days, a solution of **20** in air was completely oxidised in three days, yielding [W{≡CP(=O)MePh}(CO)$_2$(Tp*)] (**21**). This was identified on the basis of ^{1}H and ^{31}P{^{1}H} NMR data (δ_P 26.4, $^2J_{WP}$ 144.9 Hz) comparable to what was seen for [W{≡CP(=O)Ph$_2$}(CO)$_2$(Tp*)] (δ_P 19.9, $^2J_{WP}$ 145.2 Hz), as well as ESI(+) mass spectrometry.

Synthesis of [W{≡CP(C≡CPh)Ph}(CO)$_2$(Tp)]*

The synthesis of an alkynylphosphinocarbyne was considered attractive as this would allow for comparison of a carbyne M≡C and an alkyne C≡C group bound to phosphorus within the one molecule. A THF solution of **15** at −78°C was treated with a THF solution of lithium phenylacetylide. The solution turned orange, and after chromatographic work up the alkynylphosphine [W{≡CP(C≡CPh)Ph}(CO)$_2$(Tp*)] (**22**) was obtained as a spectroscopically and analytically pure yellow powder in excellent yield (90%) (Scheme 3.12).

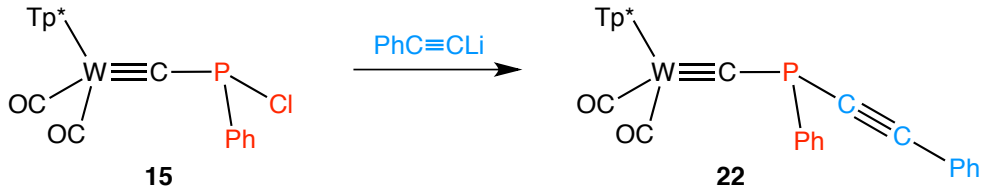

Scheme 3.12. Synthesis of [W{≡CP(C≡CPh)Ph}(CO)$_2$(Tp*)] (**22**).

A significant upfield shift (95 ppm) in the $^{31}P\{^1H\}$ NMR spectrum of **22** (δ_P –4.0, $^2J_{WP}$ 82.5 Hz) demonstrates the replacement of chloride from the precursor **15**. The resonance appears downfield from that of the organoalkynylphosphine P(C≡CPh)Ph$_2$ (δ_P −33.5).[317] The infrared spectrum (Nujol) contains carbonyl absorption bands at 1981 and 1890 cm^{-1}, similar to what is seen for **2** (1981, 1893 cm^{-1}). Additionally, a weak absorption band at 2162 cm^{-1} is observed, attributed to the C≡C stretch of the alkynyl unit, close to that of P(C≡CPh)Ph$_2$ ($\nu_{C\equiv C}$ 2161 cm^{-1}).[317]

The inclusion of the alkynyl moiety leads to a slight upfield shift of the carbyne resonance (δ_C 281.5) compared to that of **2** (δ_C 292.6). The observed coupling constants ($^1J_{PC}$ 75.9 Hz, $^1J_{WC}$ 192.1 Hz) are comparable to those seen for [W(≡CPRPh)(CO)$_2$(Tp*)] (R = H, Me, Ph). The presence of the alkynyl unit is evident in the $^{13}C\{^1H\}$ NMR spectrum from peaks at δ_C 107.4 (PC≡*C*Ph, $^2J_{PC}$ 3.5 Hz) and δ_C 82.6 (P*C*≡CPh, $^1J_{PC}$ 7.5 Hz). Curiously, the magnitude of this $^1J_{PC}$ coupling seems remarkably small compared to the $^1J_{PC}$(carbyne) value of 75.9 Hz. This is, however, not unprecedented, as demonstrated in the literature by Tilley and co-workers, as the corresponding resonance of the alkynylphosphine P(C≡CMes)Ph$_2$ appears as a doublet at δ_C 94.2 with $^1J_{PC}$ 6 Hz.[317]

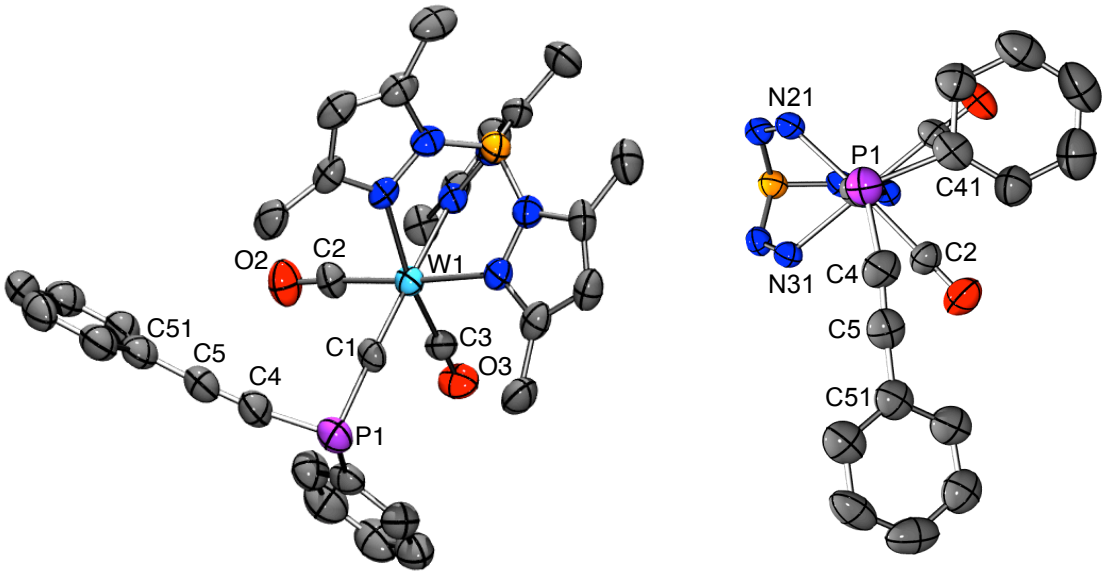

Figure 3.4. Full view (left) and simplified view (right) of the molecular structure of **22** in a crystal (50% displacement ellipsoids, hydrogen atoms omitted). Selected bond lengths (Å) and angles (°): W1−C1 1.823(6), C1−P1 1.790(6), P1−C4 1.747(8), C4−C5 1.224(10), C5−C51 1.451(11), W1−C1−P1 169.4(4), C1−P1−C4 97.9(3), P1−C4−C5 172.3(7), C4−C5−C51 176.0(8).

Gratifyingly, crystals were obtained from a solution of **22** in benzene/hexane at −20°C, thus allowing for a comparison of the geometric features of the alkyne versus carbyne moieties (Figure 3.4). The W1−C1 (1.823(6) Å) and P1−C1 (1.790(6) Å) distances do not differ significantly from those of **2** (W1−C1 1.827(2), P1−C1 1.783(3) Å), despite incorporation of the alkynyl unit. The alkynylphosphino moiety resembles that of $Ph_2PC{\equiv}CMe$, with a formal phosphorus-carbon single bond (P1−C4 1.747(8) Å, *cf.* 1.759(2) Å) and carbon-carbon triple bond (C4−C5 1.224(10) Å, *cf.* 1.206(2) Å).[213] It is interesting to note that, although P1−C1 and P1−C4 can both be considered as phosphorus-carbon single bonds, the P1−C1(carbyne) linkage is marginally (5 – 6 e.s.d.) elongated compared to the P1−C4(alkyne) bond (1.790(6) Å *cf.* 1.747(8) Å), perhaps reflecting the comparative steric bulk of the CPh and $[W(CO)_2(Tp^*)]$ termini. The P(C≡CPh)Ph moiety is oriented such that the phenyl group eclipses one carbonyl ligand, while the C≡CPh group bisects the N31−W1−C2(O) angle. This differs from the PPh_2 conformation in **2** in which the two phenyl groups eclipse one carbonyl ligand and one pyrazolyl ring. However, the opposing orientational preferences of **2** and **22** are not

surprising since calculations have shown that conversion between conformers of **2** is facile due to the low energy differences involved (Section 2.2).

3.3.2 Reactions with alcohols and amines

Synthesis of [W{≡CP(OPh)Ph}(CO)$_2$(Tp)]*

Driven by the ease of substitution with carbon-based nucleophiles, attempts to extend this chemistry to alkoxy and amino reagents were undertaken. Chlorophosphines generally react with alcohols to provide the corresponding alkoxy- or aryloxyphosphine[253,313] in the presence of a base (Scheme 3.13).[331-338]

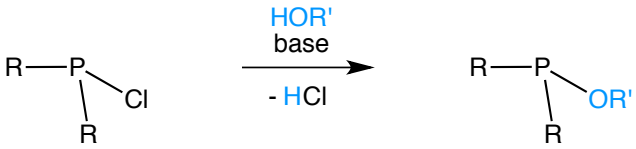

Scheme 3.13. Preparation of alkoxy- and aryloxyphosphines.

It was anticipated that applying similar conditions to the chlorophosphinocarbyne **15** would provide an aryloxy-substituted phosphinocarbyne. This was initially attempted following the method of Le Lagadec and co-workers.[331] A solution of phenol in THF was treated with one equivalent of dried and degassed triethylamine, and after ten minutes this was added to **15** (Scheme 3.14). The infrared spectrum of the reaction mixture indicated two pairs of CO stretching frequencies at 1999, 1911 cm^{-1} and 1983, 1896 cm^{-1}. No bands corresponding to the starting material could be seen (1992 and 1905 cm^{-1}). While this was promising, the ^{31}P{^{1}H} NMR spectrum of the reaction mixture unfortunately contained more than 15 peaks (mostly within the region δ_P 13.6 – 47.2), none of which predominated. Identifiable amongst the mixture were peaks attributed to the desired product **23**, (δ_P 126.4, $^{2}J_{WP}$ 76.1 Hz, 9.8%), the secondary phosphine [W(≡CPHPh)(CO)$_2$(Tp*)] (δ_P −12.0, 1.6%, see Section 4.2) and the corresponding oxide [W{≡CP(=O)HPh}(CO)$_2$(Tp*)] (δ_P 13.6, $^{2}J_{WP}$ 155.4 Hz, 3.4%) which is known to form upon reaction of **15** with H_2O.

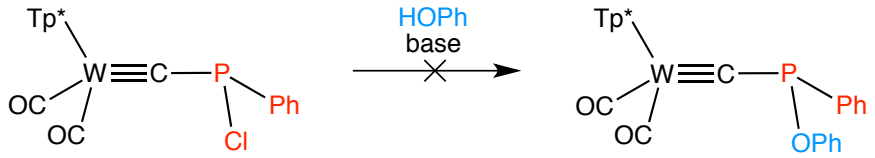

15 **23**

Scheme 3.14. Attempted synthesis of [W{≡CP(OPh)Ph}(CO)$_2$(Tp*)] (base = NEt$_3$, KH).

Stephan and co-workers have prepared the phenoxyphosphine P(OPh)^{t}Bu$_2$ from the reaction of phenol with PCl^{t}Bu$_2$ using potassium hydride as the base.[338] The use of potassium hydride is attractive because this should limit the side products in the reaction mixture as, in theory, the deprotonation produces only potassium phenoxide and dihydrogen gas. A solution of phenol in THF was treated with one equivalent of potassium hydride and stirred for 30 minutes, then added to a solution of **15** in THF (Scheme 3.14). After stirring overnight the IR spectrum contained a number of peaks in the carbonyl region, including those observed in the previous triethylamine-mediated reaction. Unfortunately, as was seen in that case, NMR spectroscopy revealed that the reaction had produced a large number of compounds, the majority of which were common to both protocols, and the desired product represented only 7.6% of the mixture.

This result was surprising, and it was postulated that formation of the phenoxide anion in solution was leading to the multitude of products in the reaction. To circumvent this, potassium phenoxide was synthesised and purified by filtration through diatomaceous earth, and the resulting product was isolated.[336] A THF solution of this isolated KOPh was added slowly to a THF solution of **15** at 0°C (Scheme 3.15). After warming to room temperature, infrared spectroscopy indicated that all of the starting material had been consumed and new ν_{CO} bands were present at 1987 and 1899 cm^{-1}, accompanied by shoulders at 1999, 1971 and 1914 cm^{-1}. The ^{31}P{^{1}H} NMR spectrum of the crude reaction mixture showed one major product at δ_P 127.1 with $^2J_{WP}$ 74.0 Hz, which had been observed as a minor component (< 10%) in the reactions involving KH or NEt$_3$. Both the chemical shift (*cf.* P(OPh)Ph$_2$ δ_P 111.0)[339] and the magnitude of the coupling constant are consistent with the desired product [W{≡CP(OPh)Ph}(CO)$_2$(Tp*)] (**23**).

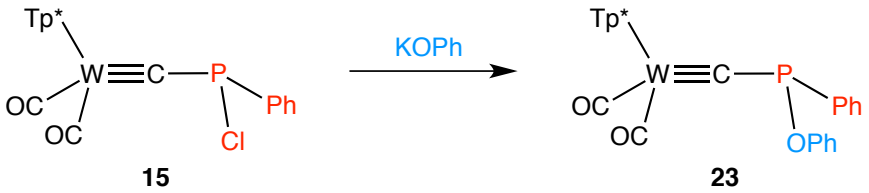

15 23

Scheme 3.15. Synthesis of [W{≡CP(OPh)Ph}(CO)$_2$(Tp*)] (**23**).

Although the spectroscopic yield for the reaction was respectable (ca. 65% by $^{31}P\{^1H\}$ NMR spectroscopy), attempts to chromatograph the crude reaction mixture led to significant decomposition, with **23** being isolated in only 17% yield, presumably due to partial hydrolysis of the phosphorus-oxygen bond on the acidic silica gel. Pleasingly, spectroscopically and analytically pure **23** was obtained in 44% yield by filtration through diatomaceous earth and precipitation of the impurities from benzene/hexane.

Attempted synthesis of [W{≡CP(N^{i}Pr$_2$)Ph}(CO)$_2$(Tp)]*

Since amines react with chlorophosphines in a similar way to alcohols, but serve the dual role of nucleophile and base, it was thought that an amino-substituted phosphinocarbyne might be obtained via the reaction of **15** with a secondary amine. A toluene solution of **15** at 0°C was treated with two equivalents of diisopropylamine, resulting in a brown solution (Scheme 3.16). Unfortunately, the $^{31}P\{^1H\}$ NMR spectrum of the reaction mixture contained 30 peaks in the region −15 to 50 ppm, and as such the reaction was deemed not viable.

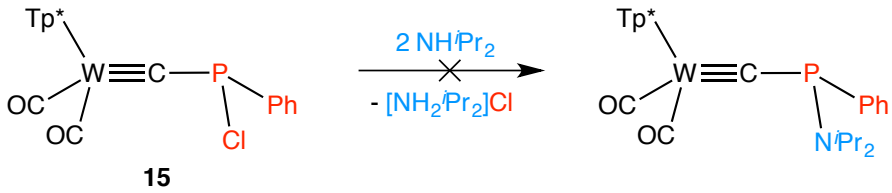

15

Scheme 3.16. Attempted synthesis of [W{≡CPPh(N^{i}Pr$_2$)}(CO)$_2$(Tp*)].

3.3.3 Attempted reactions with metal carbonyl anions

The success of halide metathesis reactions of **15** with organometallic and aryloxide nucleophiles prompted the elaboration of this chemistry to metal-based nucleophiles, with the aim of preparing bimetallic complexes. As noted in Section 1.4.2, bridging phosphaisocyanide complexes have been previously reported, and replacing the chloro substituent of **15** with a second metal would provide an alternative approach to the

synthesis of bimetallic μ-CPR complexes. Metal carbonyl anions react with a range of electrophiles E−X to form new E−M bonds. This strategy has been used to synthesise phosphido complexes $[M(PR_2)(CO)_m(L)_n]$ by reacting metal carbonyl anions $[M(CO)_m(L)_n]^-$ with the corresponding halophosphine PXR_2.[340-346] Gröer and Scheer found that the reaction of $[W(CO)_3(Cp)]^-$ with PCl_3 gives both monometallic $[W(PCl_2)(CO)_3(Cp)]$ and bimetallic products $[W_2(\mu\text{-}PCl_2)Cl(CO)_5(Cp)_2]$ (Scheme 3.17).[346] Interestingly, when $[W(PCl_2)(CO)_3(Cp)]$ was treated with $[M(CO)_3(\eta^5\text{-}C_5H_4{}^tBu)]^-$ (M = Mo, W), cyclo-P_3 complexes $[M(\eta^3\text{-}P_3)(CO)_3(\eta^5\text{-}C_5H_4{}^tBu)]$ were formed.

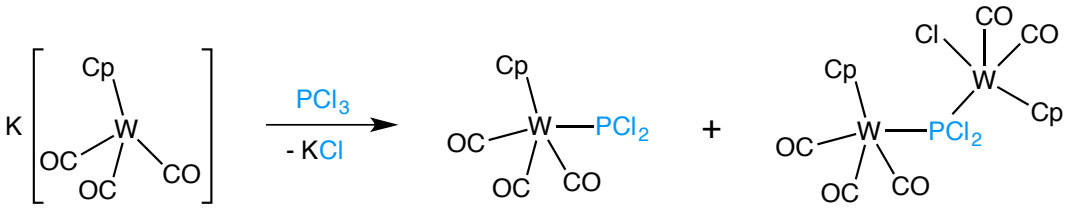

Scheme 3.17. Reaction of PCl_3 with $K[W(CO)_3(Cp)]$.

Based on the success of $[Mo(CO)_3(L)]^-$ (L = Tp, Tp*) in reactions with tin and copper electrophiles,[347] attempts were made to extend this methodology to our systems. A THF solution of KTp and $[Mo(CO)_3(C_7H_8)]$ (ν_{CO} 1981, 1910, 1881 cm^{-1}) was monitored by infrared spectroscopy to confirm the formation of $K[Mo(CO)_3(Tp)]$ (ν_{CO} 1984, 1768, 1729 cm^{-1}), then this solution was added to one equivalent of $[W(\equiv CPClPh)(CO)_2(Tp^*)]$ (Scheme 3.18). Infrared spectroscopy of the reaction showed broad infrared absorptions at 1999, 1928, 1910, 1894 and 1851 cm^{-1}, in addition to $K[Mo(CO)_3(Tp)]$ bands. The ^1H and $^{31}P\{^1H\}$ NMR spectra of the reaction mixture were very complex. In case some of the peaks in these spectra were due to intermediates, the NMR sample was heated to 55°C and monitored for three days, but unfortunately no conversion to a major product was observed.

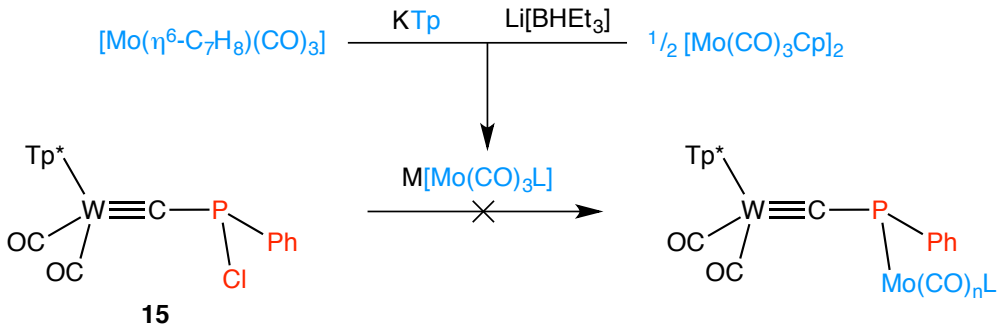

Scheme 3.18. Attempted synthesis of [W{≡CPPhMo(CO)$_n$(L)}(CO)$_2$(Tp*)] (L = Cp, Tp; n = 2, 3).

Steric constraints associated with the bulky Tp* and Tp ligands might be the reason for the lack of success in this reaction. Consequently, the smaller Cp complex Li[Mo(CO)$_3$(Cp)] was trialled. Unfortunately, this reaction was similarly unsuccessful and no major product could be isolated from the reaction (Scheme 3.18). This suggests that either the Cp complex is similarly too large for the substitution to be favourable, or the origin of the failure of this reaction may in fact be electronic, in which case increasing the nucleophilicity of the anion might alleviate such problems.

King has studied the nucleophilicities of various metal carbonyl anions and found that the nucleophilicity of [Fe(CO)$_2$(Cp)]$^-$ is one million times greater than that of the molybdenum anion [Mo(CO)$_3$(Cp)]$^-$.[348] It was thus hoped that using the iron anion [Fe(CO)$_2$(Cp)]$^-$ would result in the desired nucleophilic substitution of chloride in a relatively clean fashion. In situ formation of K[Fe(CO)$_2$(Cp)] was achieved by reduction of [Fe(CO)$_2$(Cp)]$_2$ with K[BH^{s}Bu$_3$], as confirmed by infrared spectroscopy,[349,350] and this was added to a THF solution of **15** (Scheme 3.19). The infrared spectrum of the reaction mixture contained a number of broad bands in the carbonyl region. The ^{31}P{^{1}H} NMR spectrum contained a major product at δ_P 19.4 with a small J_{WP} coupling constant of 51.7 Hz. This coupling might be consistent with the desired product [W{≡CPPhFe(CO)$_2$(Cp)}(CO)$_2$(Tp*)] because, although the magnitude is smaller than that seen for other [W(≡CPPhR)(CO)$_2$(Tp*)] complexes in this work (68.0 – 77.9 Hz), the presence of the metal substituent would be expected to alter the coupling when compared to organo or halo substituents. Unfortunately, attempts to isolate this product via extraction and precipitation were unsuccessful, and led instead to the decomposition of the sample.

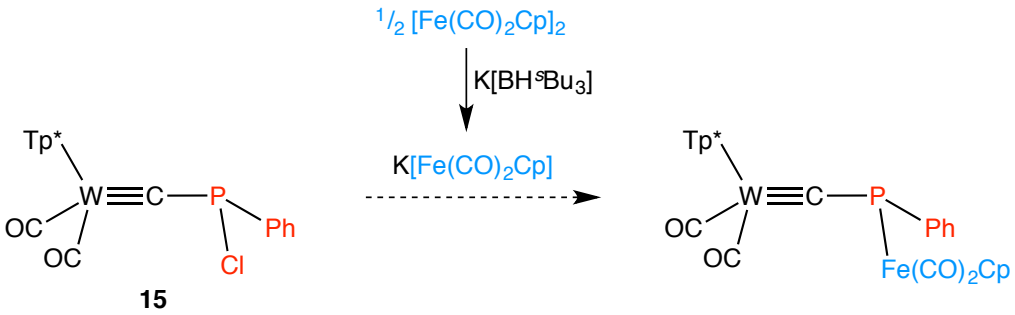

15

Scheme 3.19. Attempted synthesis of [W{≡CPPhFe(CO)$_2$(Cp)}(CO)$_2$(Tp*)].

King has reported that the cobalt anion $[Co(CO)_4]^-$ is much less nucleophilic than $[Fe(CO)_2(Cp)]^-$ (relative nucleophilicities 1:70,000,000).[348] Despite the low nucleophilicity, it was thought that $[Co(CO)_4]^-$ could be an ideal nucleophile for this reaction because of its small size, therefore limiting the steric restrictions that were thought to have hampered the molybdenum reactions discussed previously. Reduction of $[Co_2(CO)_8]$ with Li[BHEt$_3$] was carried out to generate Li[Co(CO)$_4$],[349] which was then added to a solution of **15** (Scheme 3.20). The $^{31}P\{^1H\}$ NMR spectrum indicated that the reaction was relatively clean, containing a broad singlet at δ_P 219.8 as the major component. No ^{183}W satellites were visible, though the broadness of the peak could be consistent with complexation of phosphorus to quadrupolar ^{59}Co (100% natural abundance, I = 7/2). The considerably downfield chemical shift is suggestive of the desired product [W{≡CPPhCo(CO)$_4$}(CO)$_2$(Tp*)] as the resonance for the phosphido complex [Co{PCl(N^{i}Pr$_2$)}(CO)$_3$(PPh$_3$)] occurs at δ_P 282.8.[351] However, this compound was quite unstable and could not be successfully isolated. TLC indicated that chromatographic separation was not viable, and crystallisation attempts were fruitless.

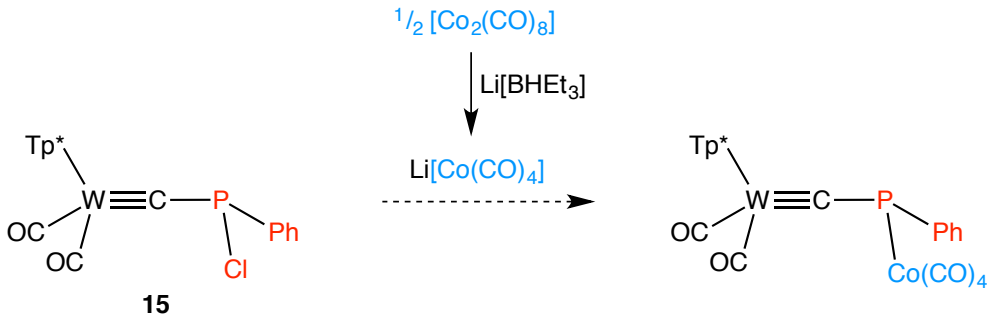

15

Scheme 3.20. Attempted synthesis of [W{≡CPPhCo(CO)$_4$}(CO)$_2$(Tp*)].

Based on the lack of success in these reactions, further attempts to synthesise bimetallic phosphinocarbyne complexes via nucleophilic substitution were abandoned. However, preliminary spectroscopic data did support the formation of [W{≡CPPhFe(CO)$_2$(Cp)}(CO)$_2$(Tp*)] and [W{≡CPPhCo(CO)$_4$}(CO)$_2$(Tp*)], suggesting that such species are viable, but in these cases were unable to be isolated due to their instability.

3.4 Reactions of [W{≡CPCl(N^{i}Pr$_2$)}(CO)$_2$(Tp*)]

3.4.1 Reaction with HCl

Problems were encountered in the synthesis of **17** due to contamination with the bis-substitution product **35** (Scheme 3.5). Aminophosphines can be cleaved with HCl to provide the corresponding chlorophosphines,[313] and it was thought this could provide an alternative route to **17** thus circumventing the problem of **35** formation. A benzene-d_6 solution of **19** was treated with two equivalents of HCl (1.0 M in Et$_2$O) and the reaction progress was monitored by NMR spectroscopy. After 15 minutes, the major product was indeed **17** (δ_P 136.1, $^2J_{WP}$ 78.6 Hz), although the ^{31}P{^{1}H} NMR spectrum contained six other peaks and **17** constituted only ca. 40% of the mixture. After 20 hours, the peak due to **17** had virtually disappeared and the largest peak in the ^{31}P{^{1}H} NMR spectrum was PCl$_2$N^{i}Pr$_2$ (δ_P 172.3). The ^{1}H NMR spectrum comprised one major Tp*-containing compound which was identified as [W(≡CH)(CO)$_2$(Tp*)]. These products are thought to have resulted from the reaction of the liberated [H$_2$N^{i}Pr$_2$]Cl with **17** (Scheme 3.21). It was therefore concluded that, although **17** was produced in this reaction, this does not represent an expedient synthetic route to access **17**.

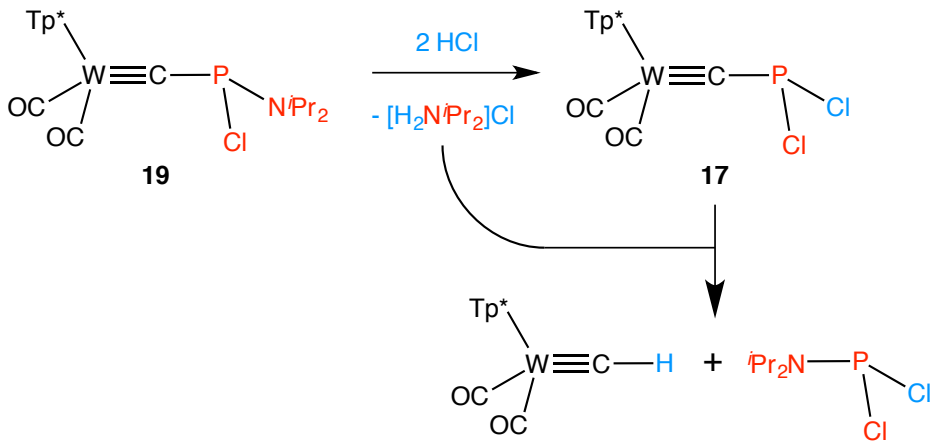

Scheme 3.21. Reaction of **19** with HCl.

3.4.2 Reaction with methyllithium

As seen in Section 3.3.1, nucleophilic substitution of chloride with methyllithium produced the methyl substituted carbyne [W(≡CPMePh)(CO)$_2$(Tp*)]. Following the same protocol, treatment of the aminophosphine **19** with methyllithium at –78°C resulted in a brown solution. After chromatography on alumina, the methyl derivative [W{≡CPMe(N^{i}Pr$_2$)}(CO)$_2$(Tp*)] (**24**) was obtained in 57% yield (Scheme 3.22).

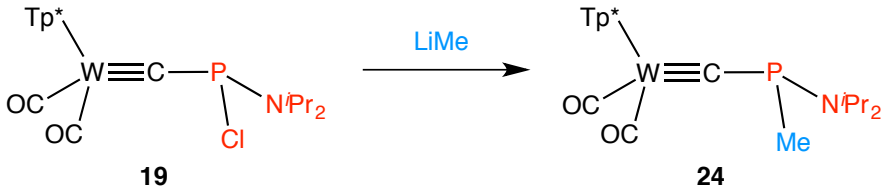

Scheme 3.22. Synthesis of [W{≡CPMe(N^{i}Pr$_2$)}(CO)$_2$(Tp*)] (**24**).

The ^{31}P{^{1}H} NMR spectrum of **24** showed a significant upfield shift compared to that of **19** (δ_P 54.0 *cf.* 130.3). The ^{1}H and ^{13}C{^{1}H} NMR spectra of **24** contain only one ^{i}Pr(CH) resonance and two ^{i}Pr(CH$_3$) resonances, whereas for the precursor **19** there were two ^{i}Pr(CH) resonances and four ^{i}Pr(CH$_3$) resonances. The presence of only one isopropyl environment in the NMR spectra of **24** is indicative of free rotation about the P–N linkage. This is in contrast to what was seen for **19**, which displays restricted rotation about the phosphorus-nitrogen bond at ambient temperatures. Low temperature ^{1}H NMR studies of **24** in toluene-d_8 did not completely resolve the two diastereotopic methyl group resonances into four constituent peaks (Figure 3.5). At −80°C three broad resonances are observed, indicating some degree of fluxionality in the rotation about the P–N bond. Notably, the resonance due to the PCH$_3$ group was essentially invariant throughout this temperature range and accordingly the possibility may be discarded that phosphine inversion accounts for higher time-averaged symmetry. The solid state infrared spectrum (Nujol) contains six bands in the carbonyl region, but as only two bands are observed in the solution state spectrum (THF: 1974, 1884 cm^{-1}) this might be attributable to solid state effects rather than rotational isomerism.

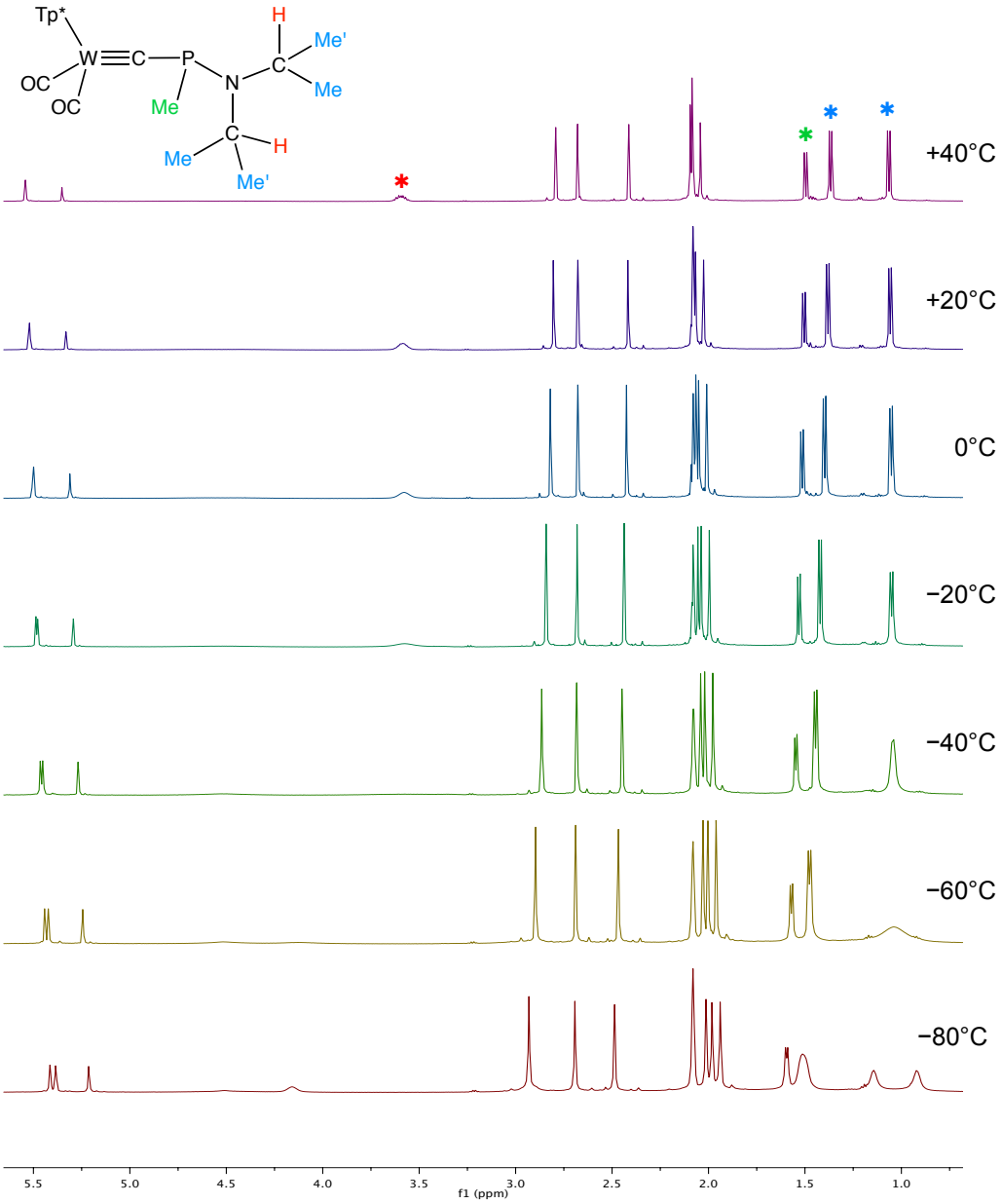

Figure 3.5. Variable temperature ^{1}H NMR spectra of **24** (−80°C to +40°C, toluene-d_8, 500 MHz).

The greater ease of rotation about the P−N bond in the methyl derivative **24** as compared to the chlorophosphine **19** presumably results from the electron-withdrawing ability of the chloro substituent. Negative hyperconjugation from the (trigonal) nitrogen to the P−Cl σ* orbital has an angular dependence, being maximised when the Cl−P−N−C dihedral angles are 90°, such that the loss of this interaction contributes to the rotation barrier (Figure 3.6). The energies of P−CH_3 σ* orbitals in contrast are so high as to make negative hyperconjugation of negligible impact.

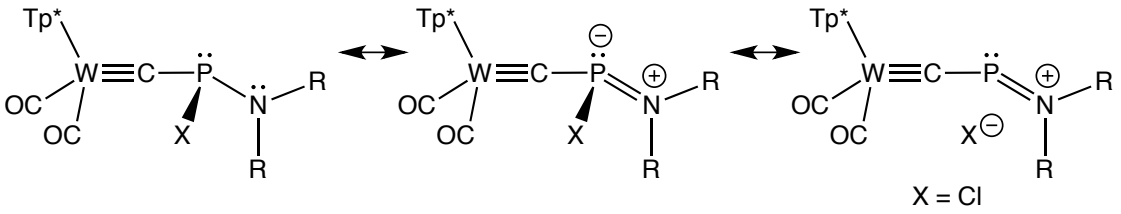

Figure 3.6. Resonance contributing forms of [W{≡CPX(NR_2)}($CO)_2$(Tp*)] (R = ^{i}Pr; X = Cl (**19**), Me (**24**)).

3.4.3 Abstraction of chloride

Numerous two-coordinate phosphine species are known, most of which involve a multiple bond to phosphorus, for example, phosphaalkenes RP=CR_2 and unsaturated phosphorus heterocycles such as phosphabenzene. Those that contain only formal single bonds to phosphorus are phosphenium cations PR_2^+ and phosphide anions PR_2^- (Figure 3.7). Phosphenium ions are two-coordinate phosphorus cations in which a large degree of the positive charge density is localised upon the phosphorus, as distinct from phosphamethine cyanins in which the positive charge is delocalised.[352] Phosphenium cations are much less stable than phosphide anions and typically require at least one substituent to be a positively mesomeric amino group, thus stabilising the cation by charge dispersion through resonance. There are many examples of coordinated phosphenium ions and the bonding of these species may be considered in some ways analogous to that of Fischer carbenes.[353-355]

Figure 3.7. Phosphenium ($6e^-$) PR_2^+ and phosphide ($8e^-$) PR_2^- ions.

Abstraction of chloride from chlorophosphines is the most common route to phosphenium ions.[356] There are a range of chloride abstracting agents used in the literature, by far the most common of which is aluminium trichloride, providing the phosphenium as the $AlCl_4^-$ salt (Scheme 3.23).[351,356-367] Examples of other chloride abstracting agents are known, such as $GaCl_3$,[366,368-370] $SnCl_4$,[366] $NaBPh_4$,[371] $SiMe_3OTf$,[370,372,373] and TlOTf.[374] In many cases, isolation of the phosphenium salt is not possible due to the instability of such species. However, undertaking the reaction in

the presence of a Lewis base such as an alkene,[371] alkyne,[351,371,372,375,376] phosphine[360,370,377] or arsine[373] affords the corresponding Lewis base-stabilised cations.

Scheme 3.23. Chloride abstraction from chlorophosphines to give phosphenium ions.

Chloride abstraction from **19** was targeted as a potential route to a carbyne-functionalised phosphenium salt with possible phosphaisocyanide character. The aminophosphine **19** was chosen because the electron donating amino substituent should render the chloride more labile. A number of chloride abstracting agents were trialled, but reactions of **19** with Me_3SiOTf, $AgPF_6$ and $Na[B\{C_6H_3(CF_3)_2\text{-}3,5\}_4]$ led to a number of peaks in the $^{31}P\{^1H\}$ NMR spectra, none of which fell in the expected range for the phosphenium salt $[W\{\equiv CP(N^iPr_2)\}(CO)_2(Tp^*)]^+$ ($[\mathbf{25}]^+$), as the literature indicates that the chemical shifts for more conventional phosphenium cations occur approximately 100 ppm downfield of those of the chlorophosphine precursors (**19** δ_P 130.3).[356]

When a CD_2Cl_2 solution of **19** was treated with an excess of $AlCl_3$, the $^{31}P\{^1H\}$ NMR spectrum comprised a broad singlet at δ_P 401.2 ($LW_{1/2}$ 24 Hz) without resolvable ^{183}W satellites. This low-field chemical shift is strongly suggestive of reduced coordination at phosphorus and formation of the phosphenium ion $[W\{\equiv CP(N^iPr_2)\}(CO)_2(Tp^*)]AlCl_4$ ($[\mathbf{25}]AlCl_4$) (Scheme 3.24). Organophosphenium ions have been reported in the wide range of δ_P 513.2 – 111.0,[356] but when one of the phosphenium substituents is a transition metal the phosphorus resonances can occur above δ_P 800,[351,361,377] and even as high as δ_P 1007.5 for $[Mo\{P(N^iPr_2)\}(CO)_3(Cp^*)]AlCl_4$.[378] The chemical shift of $[\mathbf{25}]AlCl_4$ displays a downfield shift of 270.9 ppm with respect to the precursor **19**, more than the typical 100 ppm shift noted in the literature.[356] However, this is dependent upon the conjugative strength of the substituents, as well as steric effects and the degree, if any, of ion pairing. The C–P–N comparator $[P(Mes)(N^iPr_2)]AlCl_4$ (δ_P 500) is shifted 368 ppm downfield compared to $PCl(Mes)(N^iPr_2)$ (δ_P 132).[365] In any event, the large shift observed on treating **19** with $AlCl_3$ is sufficient to discount simple

P−Al Lewis adduct formation, given the ample precedent and associated NMR data. Unfortunately, resonances attributable to [**25**]$AlCl_4$ could not be unambiguously identified in the ^1H NMR spectrum. Due to the perceived sensitivity of such a species, [**25**]$AlCl_4$ was not isolated. Instead, attempts to prepare a Lewis base-stabilised adduct were undertaken, as outlined below.

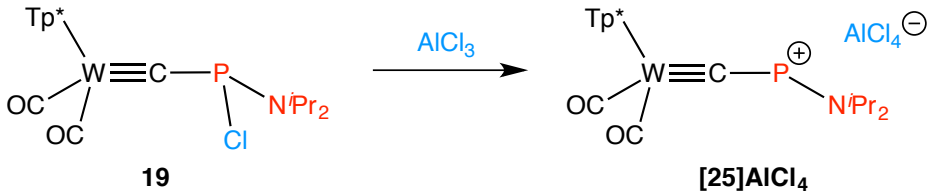

Scheme 3.24. Synthesis of [W{≡CP(N^{i}Pr$_2$)}(CO)$_2$(Tp*)]$AlCl_4$ ([**25**]$AlCl_4$).

Synthesis of [W{≡CP(N^{i}Pr$_2$)(CPhCPh)}(CO)$_2$(Tp)]$AlCl_4$*

Phosphenium salts can undergo [2 + 2] cycloaddition reactions with alkynes, yielding phosphirenium salts $[PR_2(CRCR)]^+$.[375,376] Sterenberg and Carty have extended this to terminal phosphinidene complexes $[M(PR)(L)_n]^+$ to afford phosphirenium complexes $[M\{PR(CRCR)\}(L)_n]^+$.[351,360,371] In the absence of a positively mesomeric amino substituent on the phosphorus, the phosphinidene complex $[Mo(P^iPr)(CO)_3(Cp^*)]^+$ is unstable and could not be observed by NMR. However, addition of diphenylacetylene trapped the transient phosphinidene as the phosphirene cation $[Mo\{P^iPr(CPhCPh)\}(CO)_3(Cp^*)]^+$ (Scheme 3.25).[360]

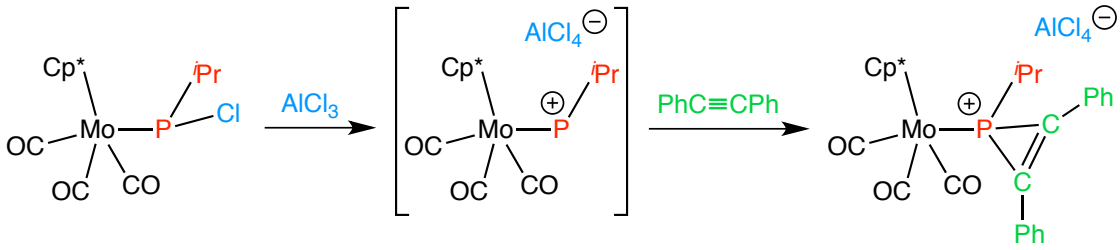

Scheme 3.25. Sterenberg's synthesis of [Mo{P^{i}Pr(CPhCPh)}(CO)$_3$(Cp*)]$AlCl_4$.

It was anticipated that this methodology might allow for the synthesis of phosphirenium-functionalised carbyne complexes. Abstraction of chloride from **19** with $AlCl_3$ in the presence of diphenylacetylene provided a new compound, the $^{31}P\{^1H\}$ NMR spectrum of which contained a singlet at δ_P −77.3 straddled by tungsten satellites

($^2J_{WP}$ 219.9 Hz). This upfield chemical shift is consistent with what would be expected for a phosphirenium cation (e.g. δ_P −57.3 to −69.2 for [PClR(CR'CR")]$AlCl_4$ (R, R', R" = H, Me, Ph)),[375] supporting formation of the phosphirenium carbyne [W{≡CP(N^{i}Pr$_2$)(CPhCPh)}(CO)$_2$(Tp*)]$AlCl_4$ ([**26**]$AlCl_4$) (Scheme 3.26). Examination of the ^{1}H NMR spectrum of [**26**]$AlCl_4$ revealed a 2:1 ratio of the Tp* pyrazolyl peaks, and two doublets at δ_H 1.50 ($^3J_{HH}$ 6.4 Hz) and δ_H 1.27 ($^3J_{HH}$ 6.8 Hz) for the ^{i}Pr-Me peaks, indicating free rotation about the P−N bond.

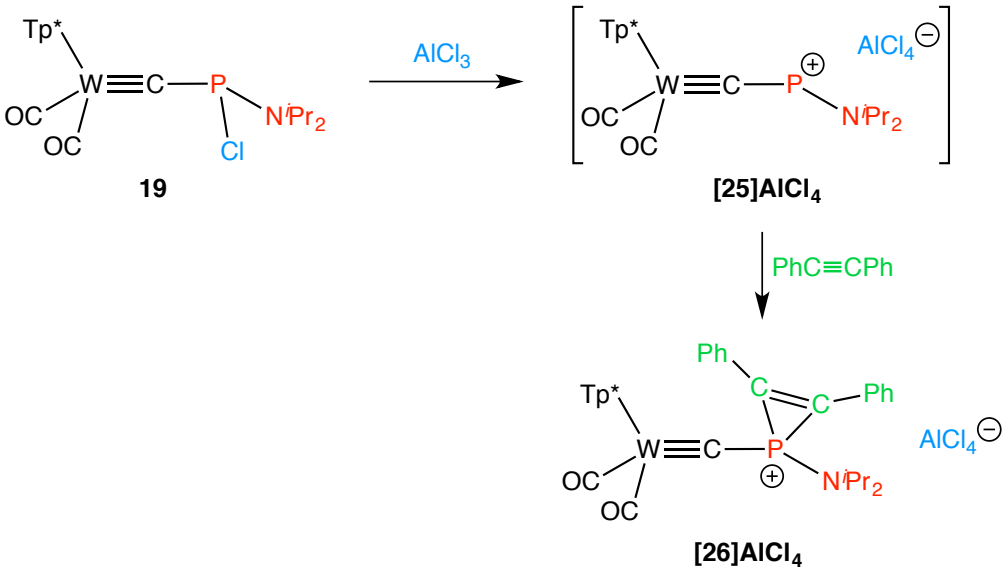

Scheme 3.26. Synthesis of [W{≡CP(N^{i}Pr$_2$)(CPhCPh)}(CO)$_2$(Tp*)]$AlCl_4$ ([**26**]$AlCl_4$).

In the present context, the description as a phosphirenium carbyne is illustrative. By analogy with [W(≡CPMe$_2$Ph)(CO)$_2$(Tp*)]I (Section 2.5.1), the complex could also be described as a phosphoniocarbyne based on the phosphine P(N^{i}Pr$_2$)(C$_2$Ph$_2$). Whilst this phosphine might appear somewhat exotic, it has recently been isolated.[371]

Unfortunately, various attempts to synthesise [**25**]$AlCl_4$ and [**26**]$AlCl_4$ were hampered by protolytic cleavage of the amine group to yield [W(≡CPCl$_2$)(CO)$_2$(Tp*)], presumably due to the presence of HCl as a consequence of the hygroscopic nature of $AlCl_3$. Although isolation of [**25**]$AlCl_4$ and [**26**]$AlCl_4$ has so far not eventuated, it should be possible with a more thorough screening of experimental conditions. These test reactions nevertheless serve to demonstrate the viability of such species and represent an area to be targeted in future work.

3.5 Summary

The synthesis of a range of tungsten carbyne complexes bearing chlorophosphine substituents has been accomplished, further demonstrating the utility of the lithiocarbyne route for the generation of diversely functionalised phosphinocarbyne complexes (Scheme 3.27). The reactive nature of the phosphorus-chlorine bond in these complexes can be exploited, enabling late-stage functionalisation of such species. Halide metathesis with organometallic alkyl, aryl, alkynyl and aryloxy nucleophiles has provided mixed phosphinocarbynes [W(≡CPRR')(CO)$_2$(Tp*)]. However, attempts to replicate this success using metal carbonyl anions were ineffective. Chloride abstraction proceeds with aluminium trichloride, generating a phosphenium-functionalised carbyne, or a phosphirenium-functionalised carbyne if performed in the presence of an alkyne.

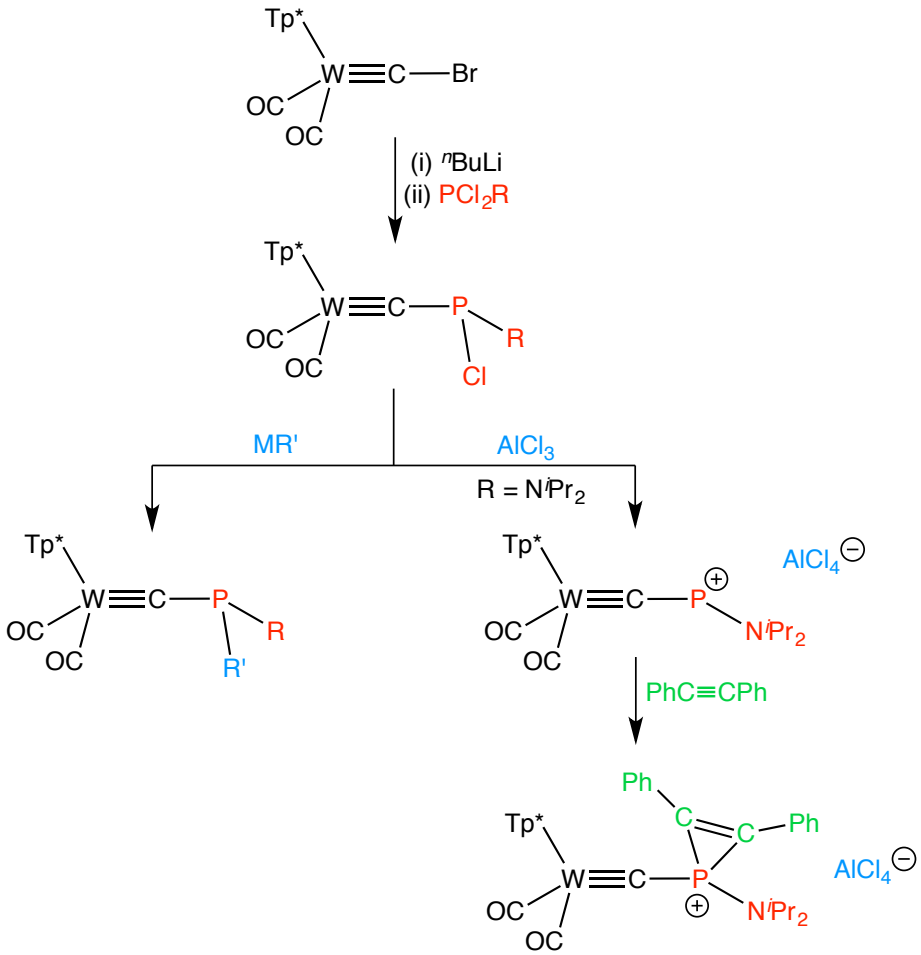

Scheme 3.27. Synthesis and reactions of chlorophosphinocarbyne complexes.

CHAPTER 4.
Secondary phosphinocarbyne complexes

CHAPTER 4: Secondary phosphinocarbyne complexes

4.1 Introduction

While the selection of a P–Cl motif provides an attractive means for further functionalisation of phosphinocarbynes via nucleophilic substitution, inclusion of a P–H group, in principle, allows for functionalisation via electrophilic substitution, either directly or via deprotonation of the phosphine. Terminal phosphinocarbyne complexes bearing P–H groups have not been previously reported, and thus it remains to be established whether this simply reflects the limited extent to which these complexes have been studied, or if there is an inherent instability associated with such complexes. A bridging secondary phosphinocarbyne complex $[Fe_2\{\mu\text{-}CPH(^tBu)\}(\mu\text{-}SMe)(CO)_2(Cp)_2]$ has, however, been prepared by addition of $PH(^tBu)(SiMe_3)$ to $[Fe_2(\mu\text{-}CSMe)(\mu\text{-}CO)(CO)_2(Cp)_2]OTf$ (Scheme 1.17).

Angelici and co-workers have prepared primary and secondary aminocarbyne complexes $[W(\equiv CNHR)(CO)_2(Tp)]$ (R = H, Me, Et, $(CH_2)_2OH$, ^{i}Pr, ^{t}Bu, Tol) from the reaction of the η^2-thiocarbene salt $[W\{\eta^2\text{-}C(H)SMe\}(CO)_2(Tp)]^+$ with primary amines and ammonia.[254] These reactions result in a mixture of products, as outlined in Scheme 4.1, with the aminocarbyne complex obtained in 25 – 35% yield. In contrast to conventional tertiary aminocarbynes $[M(\equiv CNR_2)(CO)_2(Tp')]$ (M = Mo, W; R = Me, Et; Tp' = Tp, Tp*),[147,168,194,379] these aminocarbynes were found to be too air-sensitive to isolate and were instead identified on the basis of their IR and NMR spectra through comparison with the tertiary analogues.

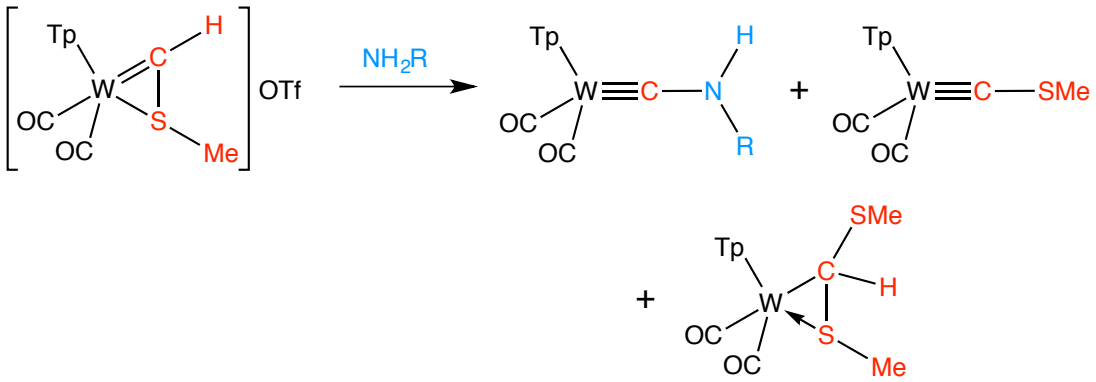

Scheme 4.1. Angelici's synthesis of primary and secondary aminocarbyne complexes (R = H, Me, Et, $(CH_2)_2OH$, ^{i}Pr, ^{t}Bu, Tol).

Interestingly, the alkyl substituted species [W(≡CNHR)(CO)$_2$(Tp)] (R = Me, Et, (CH$_2$)$_2$OH, ^{i}Pr, ^{t}Bu) were found to contain a weak band in the infrared spectrum in the region 2125 – 2090 cm^{-1}, characteristic of the C≡N stretch of coordinated isocyanides, suggesting the presence of an isocyanide C≡NR ligand. Additionally, resonances were observed in the hydride region of the ^{1}H NMR spectra (ca. δ_H –2.3), along with a second set of R group peaks. This signified the presence of an isomer containing a hydride and an isocyanide ligand, namely [WH(C≡NR)(CO)$_2$(Tp)], which exists in equilibrium with the aminocarbyne complex (Scheme 4.2).

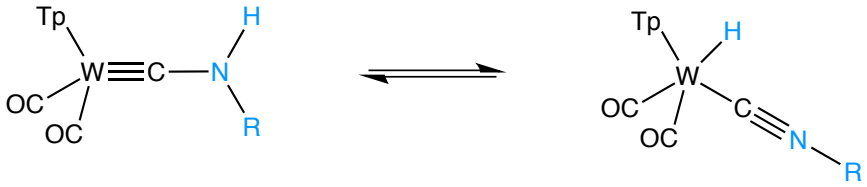

Scheme 4.2. Aminocarbyne and isocyanide-hydride tautomerisation (R = Me, Et, (CH$_2$)$_2$OH, ^{i}Pr, ^{t}Bu).

The ratio of the carbyne to isocyanide-hydride tautomers varied with the solvent used and was independent of the steric bulk of the R group. Isomeric carbyne:isocyanide ratios were observed as 4:1 in CD_2Cl_2, 5:1 in $CDCl_3$ and 9:1 in CD_3NO_2. The primary aminocarbyne [W(≡CNH$_2$)(CO)$_2$(Tp)] and the aryl aminocarbyne [W{≡CNH(Tol)}(CO)$_2$(Tp)] showed no evidence of a ν_{CN} stretch or a hydride resonance. The fact that these species exist solely as the aminocarbyne tautomers was attributed to the lower electron-donating ability of these R substituents compared to their alkyl counterparts. No indication of the corresponding iminoformyl tautomers was observed.

Richards and co-workers have shown that protonation of electron-rich isocyanide complexes [M(CNR)$_2$(dppe)$_2$] (M = Mo, W; R = Me, ^{t}Bu, Tol) occurs at nitrogen to form aminocarbynes [M(CNHR)(CNR)(dppe)$_2$]$^+$ and [M(CNHR)$_2$(dppe)$_2$]$^{2+}$.[145,152] Similarly, protonation[379] or alkylation[147] of Na[M(CNR)(CO)$_2$(Tp*)] (M = Mo, W; R = Et, ^{t}Bu) provides aminocarbynes. In the case of [Mo(≡CNH^{t}Bu)(CO)$_2$(Tp*)] no evidence of the hydride-isocyanide tautomer [MoH(CN^{t}Bu)(CO)$_2$(Tp*)] was seen, in contrast to the tungsten analogue.[254] Similar methodology encompassing protonation or alkylation of coordinated isocyanide ligands has been subsequently expanded to provide

aminocarbyne complexes of rhenium,[12,154,380,381] as well as further molybdenum[165] and tungsten[382] examples. Pickett and co-workers have shown that cyanide complexes $[M(C{\equiv}N)Cl(dppe)_2]$ (M = Mo, W) can also act as precursors to aminocarbynes $[M(\equiv CNH_2)Cl(dppe)_2]^{n+}$ (n = 0, 1), in this case via electrochemical reduction in the presence of the weak acid phenol.[383,384]

As no examples of terminal secondary phosphinocarbyne complexes are known, the possibility of phosphaisocyanide-hydride or phosphaiminoformyl tautomers existing remains unexplored. Our investigations into the first terminal secondary phosphinocarbyne complexes are detailed here.

4.2 Synthesis of secondary phosphinocarbyne complexes

4.2.1 Reduction of chlorophosphinocarbyne complexes with borohydride reagents

The use of hydride reagents to convert halophosphines PXR_2 to the corresponding secondary phosphines PHR_2 is well documented.[385-389] In the hopes of achieving the first terminal carbyne complex bearing a secondary phosphine substituent, the reaction of [W(≡CPClPh)(CO)$_2$(Tp*)] with borohydride reagents (Li[BHEt$_3$] or K[BH^{s}Bu$_3$]) was investigated. A THF solution of the chlorophosphinocarbyne **15** at room temperature was treated with M[BHR$_3$] (M = Li, R = Et; M = K, R = ^{s}Bu; Scheme 4.3). After 30 minutes the infrared spectrum of the reaction mixture showed the starting material (ν_{CO} 1992, 1905 cm^{-1}) had been replaced by new bands at 1980 and 1892 cm^{-1}. The $^{31}P\{^1H\}$ NMR spectrum comprised one major product as a singlet with ^{183}W satellites at δ_P −12.8, shifted 100 ppm upfield from that of **15**, with a tungsten-phosphorus coupling of 67.3 Hz typical of a phosphinocarbyne, thus substantiating formation of the desired secondary phosphine [W(≡CPHPh)(CO)$_2$(Tp*)] (**27**). The only known example of a secondary phosphinocarbyne complex is the bridging diiron complex [(Cp)(CO)Fe{μ-CPH(^{t}Bu)}(μ-SMe)Fe(CO)(Cp)] (Scheme 1.17), which appears in a similar region of the ^{31}P NMR spectrum at δ_P −6.0 ($^1J_{PH}$ 265 Hz).[108]

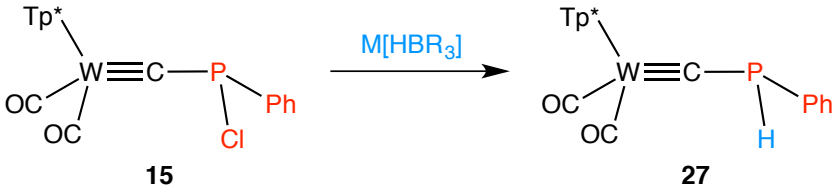

15 **27**

Scheme 4.3. Synthesis of [W(≡CPHPh)(CO)$_2$(Tp*)] (**27**) (M = Li, R = Et; M = K, R = ^{s}Bu).

The ^{1}H NMR spectrum showed, in addition to phenyl and Tp* resonances, a doublet straddled by tungsten satellites due to the PH proton at δ_H 5.81 ($^1J_{PH}$ 222.7 Hz, $^3J_{WH}$ 7.8 Hz). This magnitude of $^1J_{PH}$ (222.7 Hz) closely resembles that of diphenylphosphine (219 Hz), although the chemical shift is downfield relative to diphenylphosphine (δ_P –41.0).[390] The only structurally authenticated[391] secondary alkynylphosphine PH(C≡CMes*)(Mes*) has δ_H 6.13, δ_P −98.6 and $^1J_{PH}$ 244.2 Hz.[97] In the ^{13}C{^{1}H} NMR spectrum the carbyne appears as a doublet at δ_C 289.5, shifted only marginally downfield from that of **15** (δ_C 286.6). Couplings are observed to phosphorus ($^1J_{PC}$ 74.2 Hz) and tungsten ($^1J_{WC}$ 187.8 Hz). The phosphorus-carbon coupling is 21 Hz less than that of **15**, closely resembling that of the methyl derivative [W(≡CPMePh)(CO)$_2$(Tp*)] (75.4 Hz), as would be expected. The carbyne resonance of the bimetallic phosphinocarbyne [Fe$_2${μ-CPH(^{t}Bu)}(μ-SMe)(CO)$_2$(Cp)$_2$] (δ_C 420.0) lies considerably downfield from that of **27** as a result of the bridging nature of the carbyne. However, the $^1J_{PC}$ values of the two complexes are remarkably similar despite differing coordination numbers at the carbyne carbon ($^1J_{PC}$ 83 Hz *cf.* 74.2 Hz for **27**).[108]

In the solution infrared spectrum (THF), the PH stretch is present as a very weak absorption at 2257 cm^{-1}, close to that of [Fe$_2${μ-CPH(^{t}Bu)}(μ-SMe)(CO)$_2$(Cp)$_2$] (KBr: ν_{PH} 2279 cm^{-1}),[108] along with carbonyl absorption bands at 1980 and 1892 cm^{-1}. The ν_{CO} absorption bands of **27** are shifted to higher frequency compared to the aminocarbyne [W{CNH(Tol)}(CO)$_2$(Tp*)] (CH_2Cl_2: 1956, 1860 cm^{-1})[254] as anticipated based on the increased π-acceptor capacity of phosphinocarbyne ligands over aminocarbynes. The solid state Nujol spectrum is much more complicated. The ν_{CO} region displays bands at 2000 (m), 1977 (vs), 1911 (m), 1895 (vs), 1879 (vs) and 1865 (sh) cm^{-1}, while in the ν_{PH} region very weak bands are observed at 2269, 2244 and 2222 cm^{-1}. The observation of so many bands could be due to solid state effects, such as a number of crystalline polymorphs in the bulk solid sample, or more than one molecule

in the crystallographic asymmetric unit, either of which may result in different local environments for CO ligands in contrast to the essentially isotropic environment in solution. The presence of rotational isomers as an alternative explanation, as has been observed in other complexes of this type, is disfavoured by the appearance of only one set of CO and PH bands in solution, though again, packing forces in the rigid crystalline state may well perturb the conformer distribution that prevails in solution.

X-ray quality crystals and satisfactory elemental analysis data have not been forthcoming for **27**. However, in addition to the IR and NMR spectroscopic data, mass spectrometry and unequivocal synthesis (see Section 4.2.3), confirm the formulation of **27** as the complex [W(≡CPHPh)(CO)$_2$(Tp*)]. The positive ion ESI mass spectrum contains peaks attributable to $[M + H]^+$ and $[M + K]^+$, and high resolution data confirm the formulation through the accurate mass match of $[M + K]^+$.

Conveniently, the synthesis of **27** can also be achieved in a one-pot reaction from **1** (Scheme 4.4), which allows the preparation of bulk samples of **27** with relative ease, obviating the purification of the intermediate halophosphine. While this procedure proceeds smoothly and the NMR spectra of the reaction mixture show the desired product as the major compound (ca. 90% by $^{31}P\{^1H\}$ NMR spectroscopy), sufficiently pure for many further purposes, a number of minor impurities are present as well. Frustratingly, purification beyond this level has proven difficult. Chromatography on silica or alumina results in decomposition. Removal of the liberated salts can be achieved via extraction with pentane or filtration through diatomaceous earth, but unlike the chlorophosphinocarbyne complexes, the product does not precipitate from the solution upon concentration and cooling so removal of non-polar impurities is not effected. Numerous attempts to crystallise the product were unsuccessful.

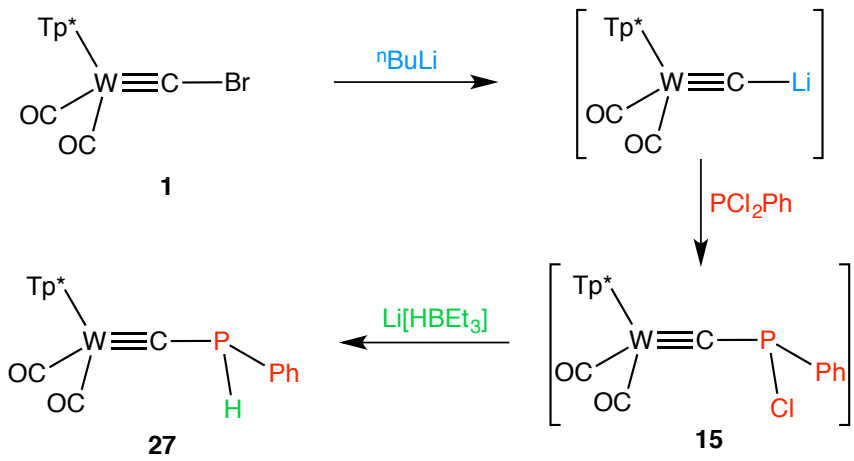

Scheme 4.4. One-pot synthesis of **27** from **1**.

Cryostatic chromatography on silica gel using a gradient of toluene/hexane at –40°C to minimise decomposition during the chromatographic process afforded spectroscopically pure **27**, although unfortunately significant losses accompany this process, presumably due to hydrolysis on the silica gel support. From a sample containing crude **27** (61% by $^{31}P\{^{1}H\}$ NMR spectroscopy), pure **27** was isolated in only 20% yield.

Protection as the borane adduct, chromatographic purification and subsequent deprotection is a popular method in the synthesis and purification of phosphines.[225,392] Treatment of a toluene solution of **27** with $BH_3{\cdot}SMe_2$ resulted in new IR bands in the carbonyl region at 1998 and 1892 cm^{-1}, shifted to higher frequency than those of **27**. A similar shift accompanied the addition of borane to the complex $[W(\equiv CPPh_2)(CO)_2(Tp^*)]$, discussed in Chapter 2. The $^{31}P\{^{1}H\}$ NMR spectrum showed a broad singlet at δ_P 10.8, indicative of formation of the borane adduct $[W(\equiv CPHPh{\cdot}BH_3)(CO)_2(Tp^*)]$. The reaction mixture was chromatographed on silica at –30°C to minimise decomposition using 2:1 CH_2Cl_2:hexane. Disappointingly, chromatography resulted in partial cleavage of the borane and fractions were collected containing **27** and **27·BH₃** but neither of these species was obtained purely.

Using this borohydride reduction route, synthesis of the cyclohexyl analogue $[W(\equiv CPHCy)(CO)_2(Tp^*)]$ (**28**) was also achieved (Scheme 4.5). Treatment of a solution of **16** with $Li[BHEt_3]$ resulted in a brown solution, the $^{31}P\{^{1}H\}$ NMR spectrum of which contained a singlet at δ_P –4.6 with ^{183}W satellites ($^{2}J_{WP}$ 64.7 Hz). Removal of the ^{1}H-decoupling gave a doublet of multiplets with a $^{1}J_{PH}$ coupling of 209.8 Hz,

consistent with the expected one-bond phosphorus-hydrogen coupling of **28**. This coupling is replicated in the ^{1}H NMR spectrum in the observation of a doublet of doublets due to the PH proton at δ_H 4.71 with couplings of $^{1}J_{PH}$ 210.0 Hz and $^{3}J_{HH}$ 6.0 Hz. In the infrared spectrum (THF), in addition to the typical ν_{CO} (1976, 1887 cm^{-1}) and ν_{BH} (2550 cm^{-1}) bands, an absorption band is seen at 2243 cm^{-1} for the PH stretch.

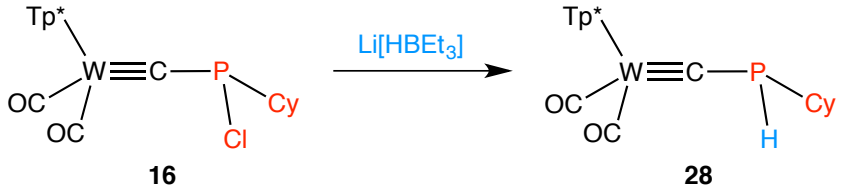

16 **28**

Scheme 4.5. Synthesis of [W(≡CPHCy)(CO)$_2$(Tp*)] (**28**) via reduction of the chlorophosphine.

Satisfactory elemental analysis could not be obtained for **28**. However, excitingly, crystals suitable for X-ray diffraction were obtained from an Et_2O/pentane solution of **28** at −24°C. The results of the X-ray study are shown in Figure 4.1. The crystal structure is racemic ($P2_1/n$), with each unit cell containing two molecules of *R*-**28** and two molecules of *S*-**28**. The W1−C1−P1 angle shows a moderate distortion from linearity (168.7(7)°). The geometry about phosphorus is tetrahedral. The location of H1 could not be determined from the difference electron density map. However, inclusion of two hydrogen atoms with 50% occupancy at calculated positions on P1 led to a short intermolecular H−H distance of 1.87 Å from one P1−H hydrogen atom to a Tp*−CH_3 hydrogen atom of a neighbouring molecule. Thus this hydrogen atom was removed and the remaining hydrogen atom (H1) was assigned full occupancy.

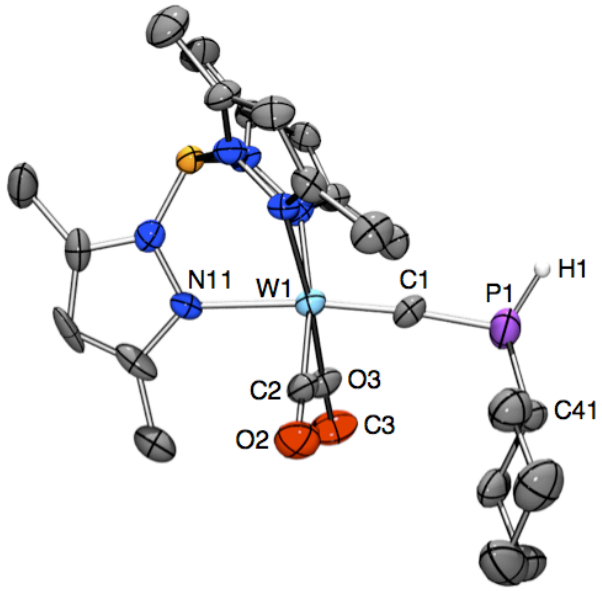

Figure 4.1. Molecular structure of *S*-**28** in a crystal of *rac*-**28** (50% displacement ellipsoids, hydrogen atoms except H1 omitted, *R*-enantiomer generated by $P2_1/n$ symmetry). Selected bond lengths (Å) and angles (°): W1−C1 1.835(11), C1−P1 1.785(11), P1−C41 1.872(11), W1−C1−P1 168.7(7), C1−P1−C41 106.4(5).

In both the phenyl and cyclohexyl species no evidence of a phosphaisocyanide-hydride tautomer was seen in the NMR or IR spectra (Scheme 4.6). The existence of a C≡P bond would not be as diagnostic as the $\nu_{C\equiv N}$ stretch that was seen in Angelici's case as the $\nu_{C\equiv P}$ mode would be expected to appear in a region of the infrared spectrum already cluttered by pyrazolyl modes. The accompanying W−H moiety would be obvious in the ^{1}H NMR spectrum, however, no hydride resonance was observed and neither was a second ^{31}P NMR resonance.

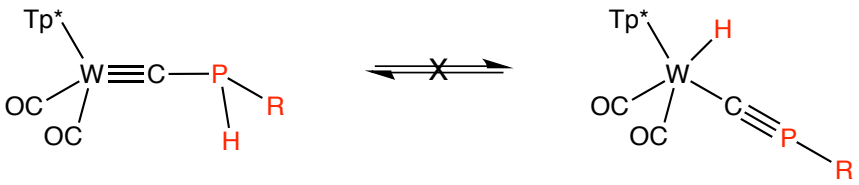

Scheme 4.6. No evidence for a phosphaisocyanide-hydride tautomer of **27** or **28** was observed (R = Ph, Cy).

The absence of a phosphaisocyanide-hydride isomer is not unexpected. Unlike the commonly encountered isocyanide ligands, true phosphaisocyanide ligands and

complexes thereof remain unknown. Previous attempts to synthesise such species tended to result in isomerisation to the phosphaalkyne isomers P≡CR and M−P≡CR which was attributed to the reticence of phosphorus to undergo *s-p* mixing of valence orbitals.[95]

4.2.2 Other attempted syntheses of secondary phosphinocarbyne complexes

The difficulties encountered in obtaining large quantities of pure compound led us to explore a number of alternative routes for the synthesis of [W(≡CPHCy)(CO)$_2$(Tp*)]. A simpler one step reaction would be that of the bromocarbyne complex **1** with cyclohexylphosphine, which was anticipated to produce the desired carbyne **28** with concomitant loss of HBr (Scheme 4.7). However, after two days the ^{1}H NMR spectrum revealed that the major component was unreacted **1**. The ^{31}P{^{1}H} NMR spectrum indicated a mixture of **28**, unreacted PH_2Cy, the bis-substituted complex [W(μ-C_2PCy)(CO)$_2$(Tp*)] (**34**) and an unknown species (δ_P 43.0). Although this reaction does produce some of the desired product, it proceeds too slowly to be synthetically viable.

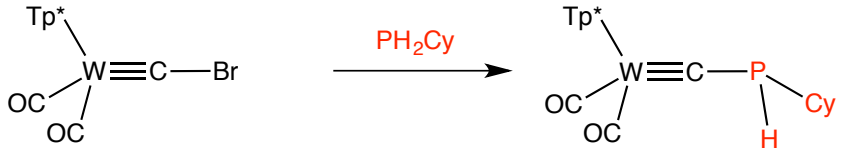

1 **28**

Scheme 4.7. One step synthesis of [W(≡CPHCy)(CO)$_2$(Tp*)] (**28**).

Reaction of lithium phosphide salts with transition metal halides has been used to synthesise phosphide complexes with extrusion of the lithium halide.[393] Elaboration of this methodology to the reaction of **1** with lithium cyclohexylphosphide resulted in over 20 peaks in the ^{31}P{^{1}H} NMR spectrum (Scheme 4.8). The desired product was present (δ_P –4.6), but unfortunately not in a sufficient quantity to deem this route viable (ca. 6% by ^{31}P{^{1}H} NMR spectroscopy).

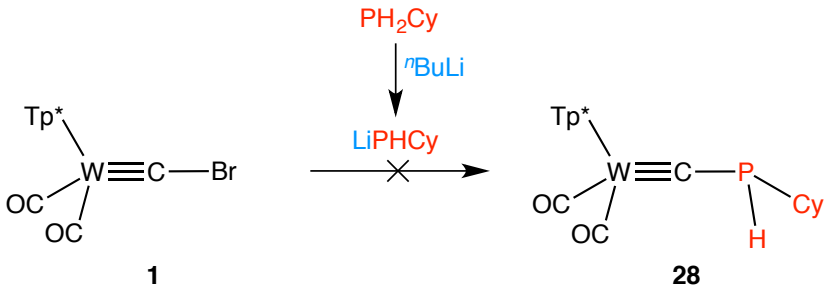

Scheme 4.8. Attempted synthesis of **28** using LiPHCy.

It was hoped that use of the phosphine-borane adduct would decrease the reactivity of the intermediates formed in this reaction and hopefully result in a cleaner reaction. Repeating this reaction with the borane adduct led to only six products in the $^{31}P\{^{1}H\}$ NMR spectrum, unfortunately none of which corresponded to the desired product [W(≡CPHCy·BH_3)$(CO)_2$(Tp*)] (δ_P 20.0, Scheme 4.9). It is perhaps not surprising that these lithium phosphide syntheses were unsuccessful as the attempted synthesis of [Mo(≡CPPh_2)$(CO)_2$(Tp*)] via the reaction of [Mo(≡CBr)$(CO)_2$(Tp*)] with LiPPh_2 did not furnish the desired phosphinocarbyne complex (Scheme 1.5).[54]

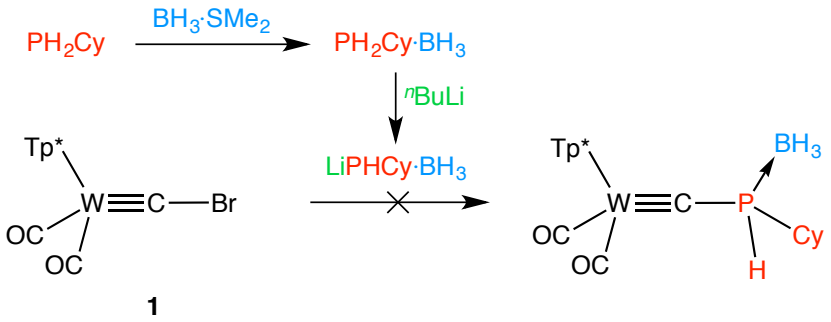

Scheme 4.9. Attempted synthesis of [W(≡CPHCy·BH_3)$(CO)_2$(Tp*)].

4.2.3 Palladium-catalysed phosphination

As introduced in Section 2.3, a palladium-mediated P–C bond forming reaction between **1** and diphenylphosphine provided access to **2**. Palladium-catalysed reactions of this type are well established for secondary phosphines and C(sp^2)–X functionalities, but are uncommon for primary phosphines.[83,215,216,394] The P–H substitutions of primary phosphines proceed in a stepwise fashion, and in some cases isolation of the secondary phosphines is possible when the appropriate stoichiometry is employed,[83,215] although this may also require quenching of the reaction mixtures at the maximal PHRR' concentration.[394]

To this end, the reaction of **1** with cyclohexylphosphine, NEt_3 and $[Pd(PPh_3)_4]$ (5 mol%) was carried out (Scheme 4.10). Initial monitoring of the reaction at room temperature saw the gradual disappearance of the starting material (ν_{CO} 1987, 1896 cm^{-1}) and appearance of the product (ν_{CO} 1976, 1888 cm^{-1}). After one day the IR spectrum showed approximately equal intensity bands for both species, and after two days a significant amount of starting material still remained. Gratifyingly, when the reaction was heated to 80°C, complete consumption of **1** occurred within one hour.

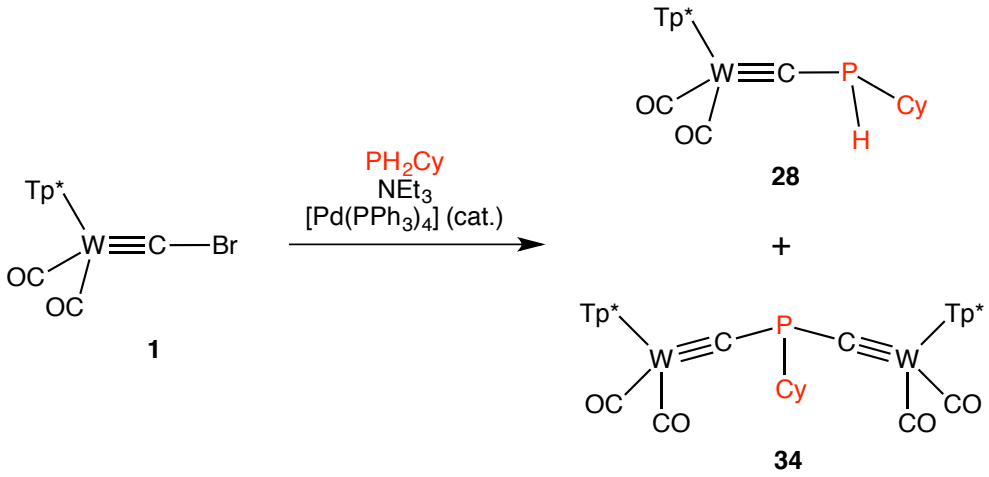

Scheme 4.10. Synthesis of $[W(\equiv CPHCy)(CO)_2(Tp^*)]$ (**28**) via palladium-catalysed P–C bond formation.

$^{31}P\{^1H\}$ NMR spectroscopy of the reaction mixture indicated that the desired product $[W(\equiv CPHCy)(CO)_2(Tp^*)]$ (**28**) represented the major component (δ_P −4.6, $^2J_{WP}$ 64.7 Hz), but this was accompanied by two significant impurities: $[W_2(\mu\text{-}C_2PCy)(CO)_4(Tp^*)_2]$ (**34**, δ_P 89.9, $^2J_{WP}$ 67.5 Hz) as a result of a second P–H substitution, and PPh_3 (δ_P −4.6). The $^{31}P\{^1H\}$ NMR spectrum indicated a considerable quantity of PPh_3 was present, liberated from the $[Pd(PPh_3)_4]$ catalyst used (5 mol% $[Pd(PPh_3)_4]$ equates to 20 mol% PPh_3 and thus represents a significant impurity).

Chromatography at –40°C on silica gel using 3:2 hexane:CH_2Cl_2 as the eluent afforded spectroscopically pure **28** as a yellow powder in 43% yield. Although this secondary phosphinocarbyne is somewhat stable, it does still appear to undergo partial hydrolysis during chromatography, resulting in the low isolated yield. Attempts to scale up the

reaction to gram scales disappointingly resulted in decreased isolated yields as a consequence of an increased proportion of the product hydrolysing on the silica column.

These conditions provide yields of ca. 90% of the desired product based on $^{31}P\{^{1}H\}$ NMR spectra of reaction mixtures, but unfortunately the long times and low yields obtained by cryostatic chromatography are not amenable to providing large quantities of high purity **28** for use as a synthetic precursor to functionalised carbynes. Repeated efforts to purify bulk samples of **28** by precipitation or crystallisation were ineffectual.

A number of variations in the experimental conditions were trialled to address two issues that arising from this reaction: formation of the bis-substituted complex and removal of the PPh_3 impurity. Attempts to limit formation of the bis-substituted complex $[W_2(\mu\text{-}C_2PCy)(CO)_4(Tp^*)_2]$ (**34**) by conducting the reaction at a lower temperature (THF at reflux) did not supress the second substitution. A variety of palladium catalysts were screened for this reaction (Table 4.1). A survey of the literature showed that although $[Pd(PPh_3)_4]$ appears to be the most common catalyst, a number of other catalysts have been demonstrated to effect P−C bond forming reactions.[395,396]

Table 4.1. Coupling reactions of **1** with PH_2Cy.

Catalyst	Loading (mol% Pd)	Base	Temp. (°C)	Time (hours)	Yield 28 (%)	Yield 34 (%)
None	-	-	25	48	35	11
None	-	NEt_3	80	24	39	32
$[Pd(PPh_3)_4]$	5	NEt_3	80	1	88[a]	12[a]
$[Pd(OAc)_2]$	3	NEt_3	80	24	11	59
$[PdCl_2(dppe)]$	10	NEt_3	80	48	14	28
$[Pd_2(dba)_3]$	5	NEt_3	80	24	9	22

Yields quoted represent the % yield as estimated by $^{31}P\{^{1}H\}$ NMR spectroscopy. [a] Yields are approximate due to the overlapping chemical shifts of **28** and PPh_3.

The palladium catalysts $[Pd(OAc)_2]$, $[PdCl_2(dppe)]$ and $[Pd_2(dba)_3]$ were anticipated to alleviate the purification difficulties encountered. Removal of ligand-derived impurities from the phosphine-free catalysts $[Pd(OAc)_2]$ and $[Pd_2(dba)_3]$ was envisaged to be more

straightforward (e.g. by filtration or chromatography), whereas the bidentate phosphine dppe was selected as chelation should render it more tightly bound to the palladium centre and hence lead to less liberated phosphine ligand in the reaction mixture. However, all three catalysts were relatively ineffectual for the synthesis of **28**, as outlined in Table 4.1, requiring longer reaction times whilst providing lower yields and favouring formation of the bis-substitution product **34** over the desired mono-substituted species.

When the reaction was attempted in the absence of palladium, IR spectroscopy indicated that only **1** was present after one hour at 80°C. After 24 hours at this temperature, consumption of **1** was complete. However, the $^{31}P\{^{1}H\}$ NMR spectrum showed **28** constituted only 39% of the reaction mixture, accompanied by a considerable amount of **34** (32%) as well as more than ten other phosphorus-containing species.

Of the systems screened, $[Pd(PPh_3)_4]$ catalysis gave by far the best results. When these conditions were applied to the reaction of **1** with phenylphosphine, the mono-substituted $[W(\equiv CPHPh)(CO)_2(Tp^*)]$ (**27**) and bis-substituted $[W_2(\mu\text{-}C_2PPh)(CO)_4(Tp^*)_2]$ (**33**) complexes were obtained in a ratio of approximately 2:1 (Scheme 4.11). Conducting the reaction with a large excess of phosphine to try to favour formation of **27** did not affect the production distribution. Slow addition of **1** to the reaction did not provide appreciable quantities of **27**.

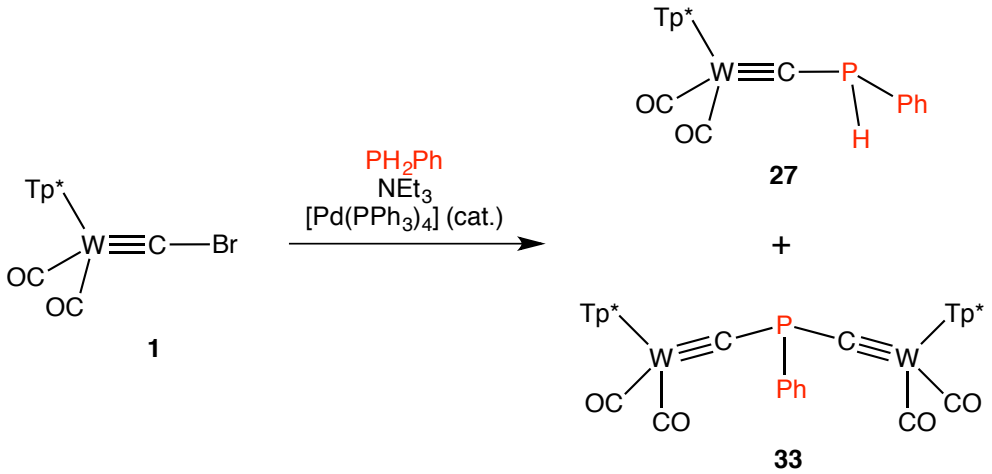

Scheme 4.11. Synthesis of $[W(\equiv CPHPh)(CO)_2(Tp^*)]$ (**27**) via palladium-catalysed P−C bond formation.

The increased production of the bimetallic carbyne **33** means that the second substitution (i.e. that of **27**) is more favourable than in the cyclohexyl complex. This is thought to be predominantly a steric effect; the large bulk of the cyclohexyl substituent means that the second substitution is less favoured. This is consistent with the sterically demanding [$Pd(PPh_3)_4$] catalyst favouring formation of the monometallic carbynes, although the formulation of the active catalyst and the precise mechanism for the catalysis are not known. The extended reaction times required might also contribute to the larger quantities of **34** formed in these cases.

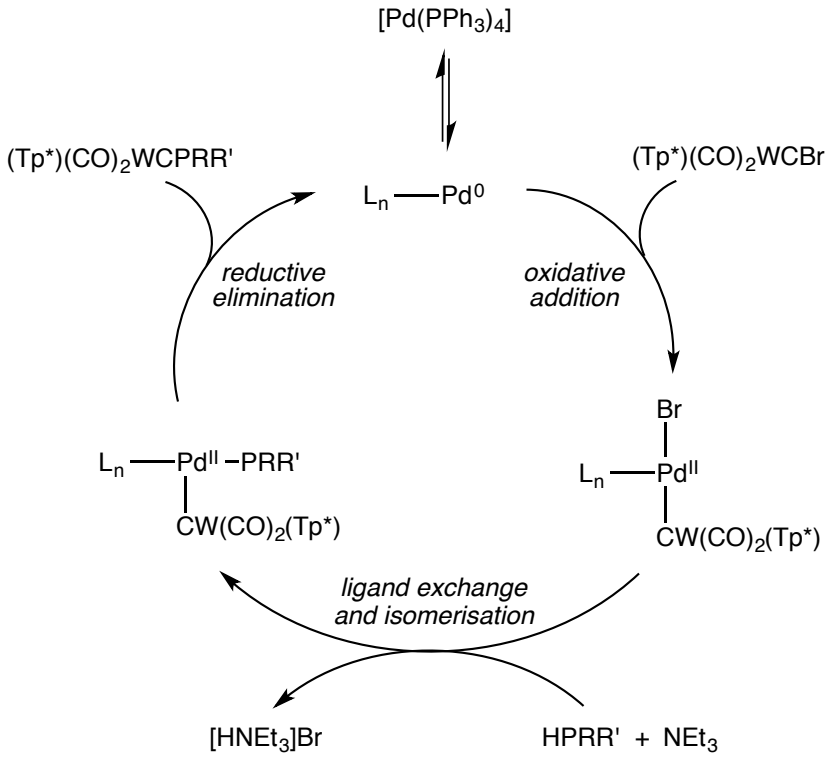

Figure 4.2. Proposed catalytic cycle for the palladium-catalysed phosphination of **1**.

The catalytic cycle is thought to follow the typical route for palladium-catalysed C–P cross-coupling reactions,[396] and is outlined in Figure 4.2. The palladium(0) pre-catalyst [$Pd(PPh_3)_4$] dissociates in solution to form the active catalyst, presumably a 14-electron [Pd^0L_2] species, wherein L could be PPh_3, PHRR' or indeed even [$W(\equiv CPRR')(CO)_2(Tp^*)$] during the catalytic cycle. Oxidative addition of halocarbynes to zero-valent palladium complexes gives *trans*-[$PdX(L)_2\{C\equiv M(CO)_2(Tp^*)\}$] complexes, implicit in previous palladium-mediated coupling processess.[54,397,398] A ligand exchange reaction and *trans-cis* isomerisation occurs, although the order of these

steps is indeterminate, then subsequent reductive elimination of the phosphinocarbyne product ensues.

4.2.4 Thermal stability of [W(≡CPHPh)(CO)$_2$(Tp*)]

As will be shown in Chapter 5, the bimetallic complexes [W_2(μ-C_2PR)(CO)$_4$(Tp*)$_2$] undergo a fascinating thermal rearrangement to the bridging metallaphosphirene species [W_2{μ:η^1-*C*;η^2-*C,P*-CC(PR)}(CO)$_4$(Tp*)$_2$]. It was hoped that a similar rearrangement would occur with the monometallic complex **27** to form a metallaphosphirene [W{η^2-C(H)PPh}(CO)$_2$(Tp*)], reminiscent of the rearrangement of [W(≡CPHPh$_2$)(CO)$_2$(Tp*)]$^+$ discussed in Section 2.6. Heating a solution of **27** in toluene at 110°C yielded numerous products, as evident in the ^{1}H NMR, ^{31}P{^{1}H} NMR and IR spectra (Scheme 4.12). The major species in the ^{31}P{^{1}H} NMR spectrum was a singlet at δ_P 32.3 without discernable ^{183}W satellites. Disappointingly, no resonances were observed below −25 ppm in the expected region for a phosphorus-containing three-membered ring, demonstrating that the thermal decomposition of **27** does not follow the same pathway as that of [W_2(μ-C_2PR)(CO)$_4$(Tp*)$_2$].

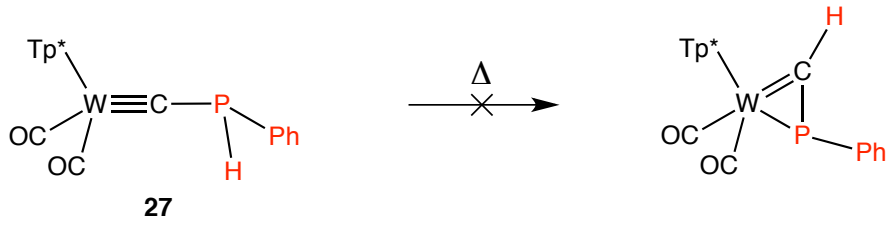

27

Scheme 4.12. Attempted thermal rearrangement of **27**.

4.3 Synthesis of an amino-substituted secondary phosphinocarbyne complex

Aminophosphines bearing a P−H bond are relatively rare. In most cases they are thermally unstable with respect to amine elimination and formation of cyclopolyphosphines, and require steric protection or incorporation into a cyclic framework in order to be prepared. In these cases, reduction of the corresponding chlorophosphine using lithium aluminium hydride is commonly employed as a preparative route (Scheme 4.13),[399-401] although isolated examples of alternative routes have been reported.[402-404]

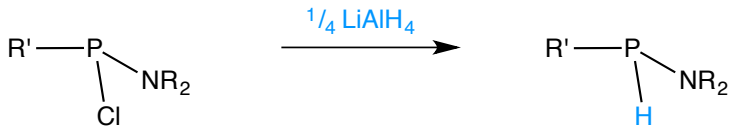

Scheme 4.13. Synthesis of secondary aminophosphines via reduction with lithium aluminium hydride.

As the [W{≡CP(N^{i}Pr$_2$)}(CO)$_2$(Tp*)] moiety is sterically demanding, we envisaged that it might impart sufficient kinetic stability to allow isolation of the secondary phosphine. Treatment of a THF solution of **19** with Li[BHEt$_3$] resulted in a mixture of compounds as determined by IR and NMR spectroscopies. The ^{31}P{^{1}H} NMR spectrum contained a peak corresponding to the desired secondary phosphine [W{≡CPH(N^{i}Pr$_2$)}(CO)$_2$(Tp*)] (**29**) at δ_P 22.6 with coupling to tungsten of 77.6 Hz, consistent with a three-coordinate phosphine (Scheme 4.14). Removal of the ^{1}H-decoupling gave a doublet of triplets resonance with $^1J_{PH}$ 229.5 Hz due to the P−H proton and $^3J_{PH}$ 20.8 Hz due to the ^{i}Pr(CH) protons.

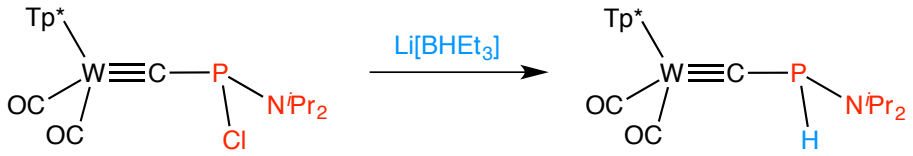

19 **29**

Scheme 4.14. Synthesis of [W{≡CPH(N^{i}Pr$_2$)}(CO)$_2$(Tp*)] (**29**) by reduction of **19** with Li[BHEt$_3$].

Attempts to replicate this reaction led to varying proportions of **29** and a second species at δ_P 69.0, denoted **30**. This compound also displays tungsten-phosphorus coupling indicative of a three-coordinate phosphine (71.7 Hz), for which a number of possible products were envisaged, outlined in Figure 4.3.

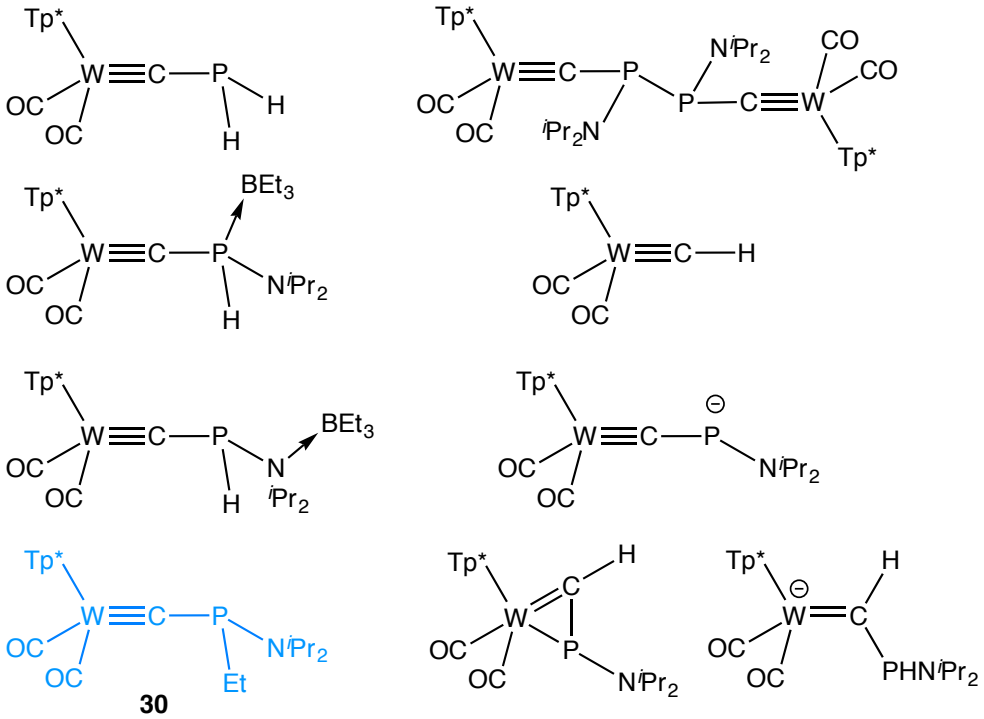

Figure 4.3. Possible side products from the reaction of **19** with Li[BHEt$_3$].

The ^{1}H-coupled ^{31}P NMR spectrum of **30** appears as a broad multiplet (LW$_{1/2}$ 50 Hz), indicating that **30** does not contain any P−H protons, as this would lead to a diagnostic coupling of ca. 200 Hz. Additionally, the phosphorus atom must be within two or three bonds of other protons to give rise to the multiplet observed. If the only protons with which the phosphine was coupling were those on the ^{i}Pr group we would expect to see a triplet resonance, as the ^{31}P NMR spectrum of **29** showed a resolved doublet of triplets resonance. If the product obtained was the triethylborane adduct of **29** then the ^{31}P{^{1}H} NMR spectrum should show a broad singlet resonance due to coupling to the quadrupolar ^{11}B nucleus. Of those products envisaged, the only one that matches the ^{31}P and ^{31}P{^{1}H} NMR data is [W{≡CPEt(N^{i}Pr$_2$)}(CO)$_2$(Tp*)] (**30**, shown in blue in Figure 4.3). This compound would result from transfer of an Et$^-$ group from the Li[BHEt$_3$] reductant rather than the desired H$^-$ transfer.

Unfortunately, separation of **29** and **30** was not effected by chromatography on alumina. Rather, both species seemed to decompose, and neither eluted from the column. Hence confirmation of the formulation of **30** as the ethyl-substituted phosphine through analysis of ^{1}H and ^{13}C{^{1}H} NMR spectra was not possible as the NMR spectra of the crude mixture were too complicated in the alkyl region to be reliably assigned. The high

resolution mass spectrum of the crude mixture did contain a peak corresponding to [**30** + H]$^+$, supporting the identity of **30** as the ethyl-substituted phosphine. It is interesting to note, however, that no evidence of replacement of the diisopropylamino group was observed, even when Li[BHEt$_3$] was added in excess (two equivalents).

In an attempt to circumvent these problems, the reaction of **19** with K[BH^{s}Bu$_3$] was carried out, but this resulted in a number of broad peaks in the ^{31}P{^{1}H} NMR spectrum (δ_P 155.3, 130.2, 86.8, 24.6, 20.9, 13.4 and 3.2). Phosphorus coordination of liberated B^{s}Bu$_3$ might account for the broad nature of the peaks. A peak at δ_P 69.0 was conspicuously absent, supporting the assignment of this as the ethylphosphine **30**. In the ^{1}H NMR spectrum a very weak doublet at δ_H 6.43 with $^1J_{PH}$ 232.1 Hz suggested that a small quantity of **29** did form, but the Tp* and alkyl regions of the spectrum indicated a multitude of species were present in the reaction mixture.

The use of lithium aluminium hydride as the reductant was trialled, but this was met with limited success. Addition of 0.25 equivalents of LiAlH$_4$ to **19** produced only 9% of **29**, with unreacted **19** accounting for the bulk of the reaction mixture. Addition of further LiAlH$_4$ did not produce appreciable quantities of **29**, and as a consequence of the lack of success attempts to synthesise **29** were abandoned.

4.4 Deprotonation of secondary phosphinocarbyne complexes

Secondary phosphines are weakly acidic (e.g. PHPh$_2$: pK_a 22)[313] and deprotonation with a strong base yields phosphide anions PR$_2^-$. Phosphide anions are considerably more stable than carbanions and can often be isolated, accounting for their common use as nucleophiles in syntheses. Based on these common observations of the stability and reactivity of phosphide anions, the synthesis of carbyne-substituted phosphide anions appeared attractive, especially due to the interest they incite from their analogy with phosphaisocyanide ligands.

As mentioned in Section 4.1, protonation of electron-rich isocyanide complexes at nitrogen leads to the formation of aminocarbyne complexes. Although this methodology has not been tested in reverse, it is conceivable that deprotonation of a secondary aminocarbyne complex could generate the corresponding isocyanide species. Indeed this may be implicit in Angelici's observed aminocarbyne/hydride-isocyanide

tautomerism if inter- rather than intramolecular proton transfer was to operate. Extending this to phosphorus, it was envisaged that deprotonation of secondary phosphinocarbynes might produce phosphaisocyanide complexes similar to that prepared by Cummins [Mo(≡CPPhNa)(S')$_2$(X)$_3$]$_2$ (S' = Et$_2$O, THF; X = N^{t}Bu(3,5-C$_6$H$_3$Me$_2$)), in that case via reduction of the chlorophosphinocarbyne [Mo(≡CPClPh)(X)$_3$].[40] As outlined in Section 1.4.2, a true terminally-ligated phosphaisocyanide complex remains unknown, the closest example being that of [Mo(≡CPPhNa)(S')$_2$(X)$_3$]$_2$, which crystallographic data indicated was most aptly described as a phosphidocarbyne rather than an anionic complex of a phosphaisocyanide.

4.4.1 Deprotonation with butyllithium

A solution of **28** was treated with an excess of ^{n}BuLi and stirred at –78°C for 30 minutes followed by 90 minutes at room temperature, then quenched with D$_2$O (Scheme 4.15). ^{31}P{^{1}H} NMR spectroscopy indicated that the product consisted of **28** and the deuterated species [W(≡CPDCy)(CO)$_2$(Tp*)] (**28a**) in a 2:1 ratio. Incorporation of deuterium leads to a diagnostic 1:1:1 triplet (^{2}H, I = 1) at δ_P –6.2 (C$_6$D$_6$) with a phosphorus-deuterium coupling constant of $^1J_{PD}$ 32.3 Hz, indicative of **28a**.

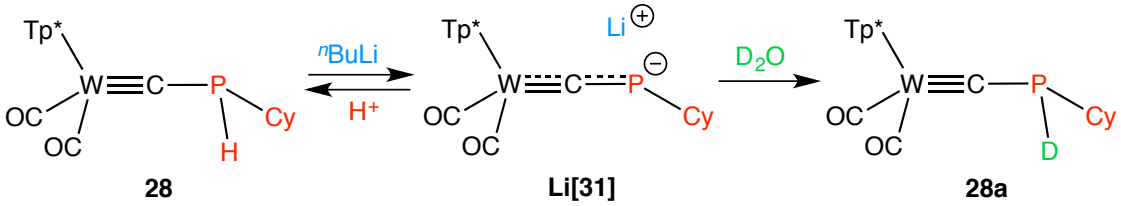

Scheme 4.15. Deprotonation of **28** with ^{n}BuLi.

Attempts to increase this conversion by using extended reaction times, higher temperatures and more reactive bases (^{t}BuLi, ^{n}BuLi + tmeda) were unsuccessful. Further investigations led to the assertion that the anion [W(CPCy)(CO)$_2$(Tp*)]$^-$ ([**31**]$^-$), which can be described as a phosphidocarbyne or an anionic phosphaisocyanide complex, is extremely basic and any trace quantities of proton sources results in reprotonation to reform **28**. Although standard precautions were taken in these reactions for the removal of air and moisture, the sensitivity of [**31**]$^-$ is such that rigorous drying of all glassware and fresh distillation of solvents is necessary. Due to the continual

presence of **28** in attempted reactions with BuLi, efforts were redirected towards a different base.

4.4.2 Deprotonation with potassium hydride

Morris and co-workers have successfully synthesised phosphide anions by deprotonating the corresponding secondary phosphine using potassium hydride.[405,406] Although the low solubility of potassium hydride is sometimes a limitation, the attraction of this base is that the only by-product of the reaction is hydrogen gas, thus obviating the need for purification, which given the highly reactive nature of the product would most likely be problematic.

The reaction of **28** with excess potassium hydride in THF was carried out, in which visible effervescence was observed in the resulting brown solution. In the $^{31}P\{^{1}H\}$ NMR spectrum a broad singlet was present at δ_P 115.3, which disappeared upon addition of D_2O, coupled with the appearance of a 1:1:1 triplet at δ_P –6.2 ($^{2}J_{PD}$ 32.8 Hz) assigned to the deuterated phosphine **28a** (Scheme 4.16). In the absence of moisture or acidic protons, K[**31**] is reasonably stable; in the presence of excess KH the NMR sample of K[**31**] showed little change over 24 hours.

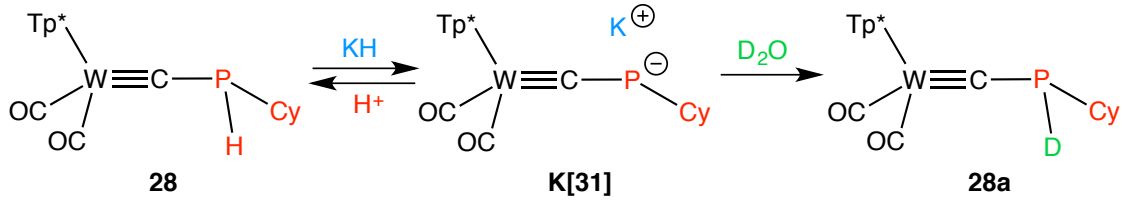

Scheme 4.16. Deprotonation of **28** with potassium hydride.

The NMR value for K[**31**] is comparable to that observed by Cummins for his salt $[Mo(\equiv CPPhNa)(X)_3(Et_2O)(THF)]_2$ (X = N^{t}Bu(3,5-$C_6H_3Me_2$)) in THF-d_8 of δ_P 103.5.[40] Interestingly, this signal showed significant dependence upon solvation of the sodium counter ion; in the presence of 12-crown-4 the value occurs at δ_P 126.1 (THF-d_8), while in benzene-d_6 the resonance shifts upfield to δ_P 68.8 (broad). The chemical shift of the salt K[**31**] is relatively independent of the solvation of the potassium cation in the $^{31}P\{^{1}H\}$ NMR spectra. In benzene-d_6, K[**31**] appears at δ_P 113.9 whereas in THF in the presence of dibenzo-18-crown-6 it is observed at δ_P 114.5. This demonstrates that the degree of ion pairing is less dependent upon solvation for K[**31**] than for

$[Mo(\equiv CPPhNa)(X)_3(Et_2O)(THF)]_2$ as the anion $[\mathbf{31}]^-$ and the K^+ cation effectively act as free ions in solution. The phosphorus resonances for the bridging phosphaisocyanide complexes $[Pt_2(\mu\text{-}C{=}PR)XX'(PEt_3)_3]$ (R = Mes, X = X' = Cl, Br; R = Me, X = Cl, X' = I) appear slightly downfield (δ_P 142.3 - 155.4)[88,90,103] compared to that of K[**31**], yet the only other examples of bridging phosphaisocyanide complexes $[Fe_2(\mu\text{-}C{=}PAr)(\mu\text{-}CO)(CO)_2(Cp)_2]$ (Ar = 2,4,6-$C_6H_2R_3$; R = Me, ^{i}Pr, ^{t}Bu) occur 100 ppm downfield of this (δ_P 249.3 - 258.0),[106] illustrating the extreme variation that is possible for phosphorus in phosphaisocyanide environments.

Acquisition of infrared data for K[**31**] was hampered by the continual presence of **28**. IR spectra were recorded in THF solution in a KBr cell made up under an argon atmosphere in a glove box, but the small quantities required for the measurement of IR spectra (< 0.1 mL) meant that inclusion of **28** in the spectra was unavoidable due to proton scavenging by K[**31**]. Nevertheless, the ν_{CO} bands of K[**31**] were identifiable in spectra containing a mixture of K[**31**] and **28** at 1862 and 1753 cm^{-1} (THF). This is a considerable shift compared to **28** (1976, 1887 cm^{-1}), and may be rationalised in valence bond terms by the relative contribution of the phosphaisocyanide resonance form (Figure 4.4(b)) to the bonding description. This involves some localisation of electron density at the tungsten centre, which results in increased retro-donation to the carbonyl ligands, as evidenced by the shift to lower frequency. Further discussions of the infrared spectroscopic data follow below.

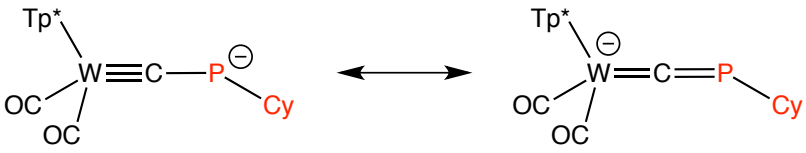

Figure 4.4. (a) Phosphidocarbyne and (b) phosphaisocyanide resonance contributing forms of **31**.

Application of these conditions to **27** provided the phenyl-substituted phosphaisocyanide salt K[W(CPPh)$(CO)_2$(Tp*)] (K[**32**]) (Scheme 4.17). Treatment of a THF solution of **27** with excess potassium hydride afforded a red suspension, the $^{31}P\{^1H\}$ NMR spectrum of which contained a singlet at δ_P 81.9 with resolvable tungsten satellites ($^2J_{WP}$ 47.0 Hz). The tungsten-phosphorus coupling is less than that of the

precursor **27** ($^2J_{WP}$ 67.3 Hz), and follows the previously observed trend wherein higher coordination numbers at phosphorus lead to larger $^2J_{WP}$ values. The ^{1}H NMR spectrum displays a 2:1 ratio of the Tp* environments, consistent with what is expected for K[**32**] as chirality is lost upon deprotonation.

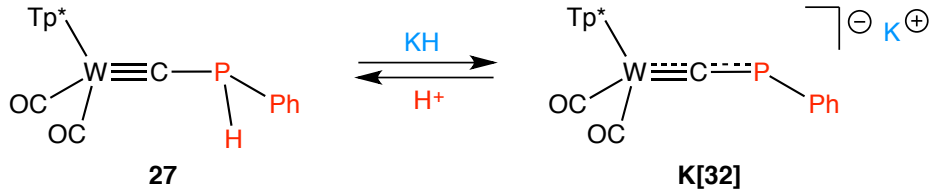

27 **K[32]**

Scheme 4.17. Deprotonation of **27** with potassium hydride.

The $^{13}C\{^1H\}$ NMR spectrum of K[**32**] in THF-d_8 showed a significant downfield shift of almost 70 ppm for the "carbyne" resonance (δ_C 358.9, *cf.* δ_C 289.5 (C_6D_6) for **27**). The magnitude of $^1J_{PC}$ (100.6 Hz) is the largest that has been observed in this work, and might result from increased multiple bonding (and hence increased *s*-character) along the W−C−P linkage. Unfortunately, the carbyne resonance for [Mo(≡CPPhNa)(X)$_3$(Et_2O)(THF)]$_2$ (X = N^{t}Bu(3,5-$C_6H_3Me_2$)) has not been reported, and the isocyanide [M(CNR)(CO)$_2$(L)]$^-$ and thiocarbonyl [M(CS)(CO)$_2$(L)]$^-$ analogues of [**32**]$^-$ have not been characterised by ^{13}C NMR spectroscopy. In the absence of other directly related complexes little data is available for comparison. $^{13}C\{^1H\}$ NMR data have been reported for the bridging phosphaisocyanide complexes [Fe_2(μ-C=PAr)(μ-CO)(CO)$_2$($Cp)_2$] (Ar = 2,4,6-$C_6H_2R_3$; R = Me, ^{i}Pr, ^{t}Bu) and in these cases the CFe_2 resonances occur in a similar region to K[**32**] (δ_C 338.8 - 345.8), with comparable $^1J_{PC}$ values (92 - 97 Hz), although the bimetallic nature of these species means that only tentative parallels can be drawn.[106]

The salt K[**32**] is not as basic as K[**31**], and clean infrared data were obtained for a sample of K[**32**] made in a glove box. In the infrared spectrum bands are observed in the carbonyl region at 1889, 1877 and 1771 cm^{-1} (THF). These absorptions lie to higher frequency than was seen for K[**31**], suggesting that the CPPh ligand is a better π-acceptor than the cyclohexyl analogue, consistent with the electron-releasing nature of the cyclohexyl moiety.

Table 4.2 details the carbonyl absorption data for a series of complexes $[M(CER)(CO)_2(Tp^*)]$ and $[M(CE)(CO)_2(Tp^*)]^-$ (M = Mo, W; E = PCy, PPh, NEt, S, O, CH_2; R = H, Me, Et), along with $[W(\equiv CH)(CO)_2(Tp^*)]$ and $[W(\equiv CLi)(CO)_2(Tp^*)]$ for comparison. As can be seen, the expected general trend prevails of a shift in the ν_{CO} frequency to lower frequency upon formation of the anionic $[M(CE)(CO)_2(Tp^*)]^-$ salts. Typically, shifts in the order of 100 cm^{-1} are observed, although in the most extreme example ($[W(\equiv CNEt_2)(CO)_2(Tp^*)]$ *cf.* $Na[W(CNEt)(CO)_2(Tp^*)]$) a difference of ca. 200 cm^{-1} is seen.[147] Carbonyl absorption bands to lower frequency signify increased electron density at the metal centre, i.e. greater contributions from the $^-M=C=E$ resonance descriptor, and consequently increased retrodonation to the carbonyl co-ligands. In the case of the phosphorus-functionalised salts K[**31**] and K[**32**], the ν_{CO} bands appear at more than 100 cm^{-1} higher in frequency than the isocyanide analogue $Na[W(CNEt)(CO)_2(Tp^*)]$.[147] On the basis of this, bonding in the CPR ligands of K[**31**] and K[**32**] should not be viewed as entirely phosphaisocyanide in character. However, the dramatic alteration of the ν_{CO} frequencies upon deprotonation indicates a substantial amount of charge density has been transferred to the tungsten centre, and as such the phosphidocarbyne canonical form is also insufficient to explain the WCPR bonding. These data together indicate that the complexes $[\mathbf{31}]^-$ and $[\mathbf{32}]^-$ lie between these two extreme descriptions, but give considerable weight to these species being the first examples of terminal phosphaisocyanide complexes.

Table 4.2. Selected infrared spectroscopic data for [M(CER)(CO)$_2$(Tp*)] and [M(CE)(CO)$_2$(Tp*)]$^-$.

Complex	ν_{CO} (cm^{-1})	k_{CO} (N m^{-1})	Δk_{CO}
[W(≡CPHCy)(CO)$_2$(Tp*)] (**28**)	1976, 1887	15.07	
K[W(CPCy)(CO)$_2$(Tp*)] (K[**31**])	1862, 1753	13.21	1.86
[W(≡CPHPh)(CO)$_2$(Tp*)] (**27**)	1980, 1892	15.14	
K[W(CPPh)(CO)$_2$(Tp*)] (K[**32**])	1889, 1877, 1771	13.49[d]	1.65
[W(≡CNEt$_2$)(CO)$_2$(Tp*)][147]	1936, 1833[a]	14.35	
Na[W(CNEt)(CO)$_2$(Tp*)][147]	1731, 1685, 1649	-	-
[Mo(≡CSMe)(CO)$_2$(Tp*)][201]	1987, 1904[b]	15.29	
[NEt$_4$][Mo(CS)(CO)$_2$(Tp*)][201]	1886, 1794[c]	13.68	1.61
[W(≡COMe)(CO)$_2$(Tp*)][407]	1958, 1862	14.74	
[NEt$_4$][W(CO)$_3$(Tp*)][407]	1876, 1737[a]	13.20	1.54
[W(≡CCH$_3$)(CO)$_2$(Tp*)][64]	1968, 1876	14.53	
Li[W(CCH$_2$)(CO)$_2$(Tp*)][64]	1858, 1686	12.71	1.82
[W(≡CH)(CO)$_2$(Tp*)][64]	1986, 1893	15.20	
Li[W(C)(CO)$_2$(Tp*)][64]	1916, 1819	14.09	1.11

IR spectra were recorded in THF, unless otherwise indicated. [a] CH_2Cl_2. [b] Unspecified medium. [c] KBr. [d] Based on average value for ν_{sym}.

Attempts to crystallise K[**31**] and K[**32**] were unsuccessful. However, excitingly, crystals were obtained from a THF/Et$_2$O solution of K[**32**] in the presence of 2.2.2-cryptand at −25°C. The results of an X-ray crystallographic study of [K(2.2.2-cryptand)][W(CPPh)(CO)$_2$(Tp*)] are shown in Figure 4.5. The solid state structure clearly demonstrates the two-coordinate environment at phosphorus, which exhibits a bent geometry with a C1−P1−C41 angle of 104.4(3)°, close to what was seen in [W(≡CPHCy)(CO)$_2$(Tp*)] (**28**, 106.4(5)°), [W(≡CPPh$_2$)(CO)$_2$(Tp*)] (**2**, 101.52(12)°, 106.02(12)°) and [Mo(≡CPPhNa)(X)$_3$(Et$_2$O)(THF)]$_2$ (X = N^{t}Bu(3,5-C$_6$H$_3$Me$_2$), 106.0(2)°), as well as in the calculated geometry for the model system [Mo(CPPh)(NH$_3$)$_3$]$^-$ (104.7°).[40] Isocyanide ligands bound to electron-rich metal centres can, in the absence of steric effects, exhibit pronounced bending of the C−N−R spine (e.g. 139.4(10)° in [Re(CNMe)Cl(dppe)$_2$]),[408] ascribed to extensive π retrodonation to

the isocyanide C≡N π* orbital, formalised by significant contributions from the M=C=N−R canonical form.[13] The W1−C1−P1 angle is distorted from linearity (167.0(4)°), as is commonly observed for carbyne complexes.

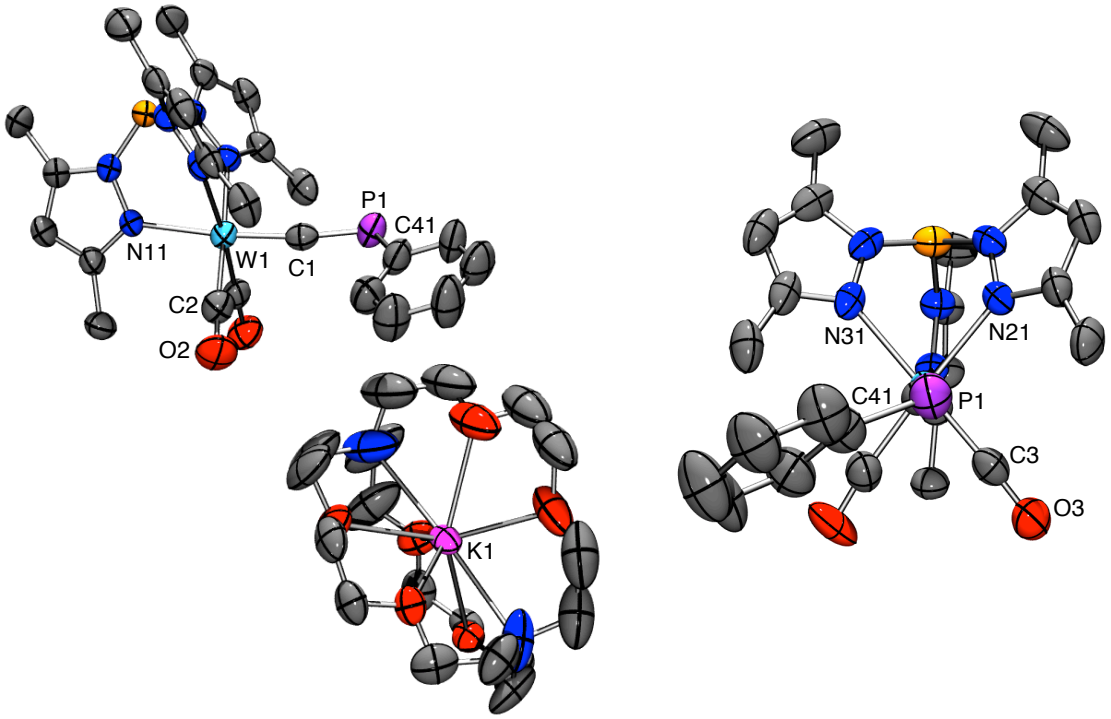

Figure 4.5. Full view (left) and simplified view (right – depicted looking down the P1−C1−W1 axis) of the molecular structure of [K(2.2.2-cryptand)][**32**] in a crystal (50% displacement ellipsoids, hydrogen atoms omitted). Selected bond lengths (Å) and angles (°): W1−C1 1.915(7), C1−P1 1.692(7), P1−C41 1.830(8), W1−C1−P1 167.0(4), C1−P1−C41 104.4(3).

Importantly, the W1−C1 bond length (1.915(7) Å) is significantly elongated compared to conventional tungsten carbyne complexes and compared to phosphinocarbynes (e.g. **28** 1.835(11) Å, **2** 1.827(2) Å). In Cummins' molybdenum phosphidocarbyne species $[Mo(\equiv CPPhNa)(X)_3(Et_2O)(THF)]_2$ the Mo−C bond length is even shorter at 1.762(5) Å. The elongated W1−C1 bond in [K(2.2.2-cryptand)][**32**] demonstrates that the phosphaisocyanide resonance description is a significant contributor to the ground state structure. The W1−C1 bond length approaches that of isocyanide complexes (e.g. W−CNR 2.079(12) and 2.047(12) Å in $[W(C\equiv N^tBu)(STol)(CO)_2(Cp)]$),[409] and is comparable to that of thiocarbonyl complexes (e.g. W−CS 1.944(19) Å in $[W(CS)(CO)_2(CNCy)]$).[410] Additionally, the C1−P1 bond (1.692(7) Å) is contracted

compared to the phosphinocarbyne complexes **28** (1.785(11) Å) and **2** (1.783(3) Å), and the phosphidocarbyne $[Mo(\equiv CPPhNa)(X)_3(Et_2O)(THF)]_2$ (1.771(5) Å), yet DFT studies of the model system $[Mo(CPPh)(NH_2)_3]^-$ revealed a degree of Mo−C−P π bonding.[40] The C1−P1 bond length is comparable to the C=P bond lengths in phosphaalkenes (e.g. $(Mes)P{=}CPh_2$ 1.692(3) Å).[411] Taken together these data establish that, although contributions from both the phosphidocarbyne and phosphaisocyanide canonical forms are evident, those from the phosphaisocyanide form are indisputable. As such, [**32**]$^-$ can confidently be regarded as the first known example of a terminal phosphaisocyanide complex.

4.4.3 Reaction with methyl iodide

In order to demonstrate the synthetic utility of these anions, alkylation was probed through the reaction of K[**32**] with the methylating agent methyl iodide. A THF solution of **27** was treated with potassium hydride to generate K[**32**], as confirmed by $^{31}P\{^1H\}$ NMR spectroscopy, followed by addition of methyl iodide. $^{31}P\{^1H\}$ NMR spectroscopy indicated that $[W(\equiv CPMePh)(CO)_2(Tp^*)]$ (**20**) was the major component of the reaction mixture (Scheme 4.18). Electrophilic addition of Me^+ to K[**32**] complements the previous strategy in which nucleophilic addition of Me^- (as MeLi) to $[W(\equiv CPClPh)(CO)_2(Tp^*)]$ generated **20** (Section 3.3.1).

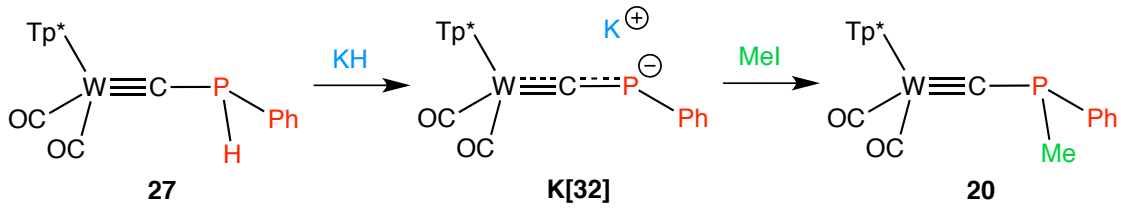

Scheme 4.18. Synthesis of **20** via deprotonation and alkylation.

This preliminary result suggests that the phosphorus is the preferred site for electrophilic addition to [**32**]$^-$, rather than the metal. But as was seen in Chaper 2, electrophilic addition reactions to phosphorus-functionalised carbynes can take a number of pathways. It is possible that in the future more extensive studies might demonstrate similarly diverse reactivity for [**32**]$^-$.

4.5 Summary

The synthesis of the first examples of terminal secondary phosphinocarbyne complexes has been achieved. Transformation of the bromocarbyne complex **1** into secondary phosphinocarbyne complexes can be accomplished in a one-pot reaction involving metal-halogen exchange, electrophilic addition and reduction, or alternatively, via palladium-catalysed phosphination (Scheme 4.19). Synthesis of a rare example of a secondary aminophosphine [W{≡CPH(N^{i}Pr$_2$)}(CO)$_2$(Tp*)] has been accomplished by reduction of the chlorophosphine species, although isolation of this complex has so far not eventuated.

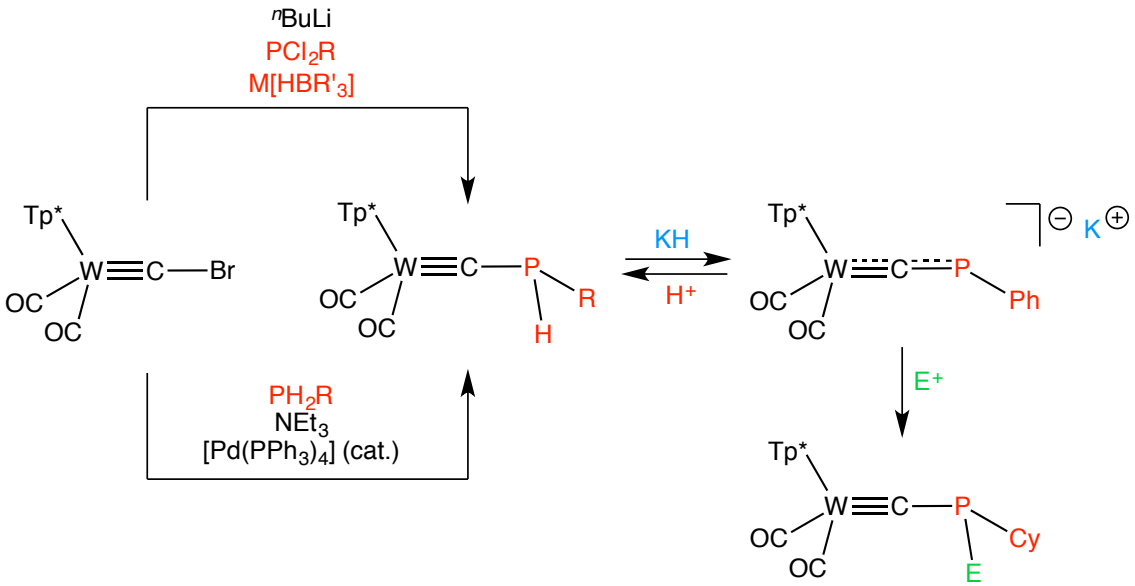

Scheme 4.19. Synthesis and reactivity of secondary phosphinocarbyne complexes (R = Cy, Ph; E = D, Me).

Deprotonation of these complexes with potassium hydride provides access to the salts K[W(CPR)(CO)$_2$(Tp*)]. Spectroscopic and structural data reveal considerable contributions from the phosphaisocyanide canonical description, and support formulation of these anions as the first examples of terminally ligated phosphaisocyanide complexes. These anions were found to be extremely basic and undergo reactions with electrophiles (D$^+$, Me$^+$) at phosphorus.

CHAPTER 5.
Bi- and polymetallic phosphinocarbyne complexes

CHAPTER 5: Bi- and polymetallic phosphinocarbyne complexes

5.1 Synthesis of bimetallic phosphinocarbyne complexes

The use of secondary (PH_2R) and dichloro- (PCl_2R) phosphines in the syntheses of phosphinocarbyne complexes affords the possibility of multiple substitutions. Indeed, in the syntheses of [W(≡CPXR)(CO)$_2$(Tp*)] (X = H, Cl; R = Cl, Cy, Ph) the bimetallic complexes [W_2(μ-C_2PR)(CO)$_4$(Tp*)$_2$] were observed as minor impurities as a result of substitution of the second H or Cl group on the phosphine. For studies directed towards mononuclear complexes, this proved to be somewhat problematic as the bimetallic complexes were found to have very similar solubilities to their monomeric counterparts, complicating purification procedures. These binuclear complexes are, however, interesting and novel species in their own right, worthy of further investigation.

5.1.1 Synthesis of [W_2(μ-C_2PPh)(CO)$_4$(Tp*)$_2$]

Deliberate attempts to synthesise the dimeric compound [W_2(μ-C_2PPh)(CO)$_4$(Tp*)$_2$] (**33**) by reaction of [W(≡CBr)(CO)$_2$(Tp*)] with ^{n}butyllithium and half an equivalent of dichlorophenylphosphine resulted in the desired product (Scheme 5.1). Alternatively, the reaction of **1** with half an equivalent of phenylphosphine in the presence of triethylamine and a catalytic amount (5 mol%) of [Pd(PPh_3)$_4$] also provided **33**. Chromatographic purification yielded **33** contaminated with triphenylphosphine (liberated from the [Pd(PPh_3)$_4$] catalyst), which was removed by precipitation from CH_2Cl_2 and EtOH to give **33** as an orange powder in 67% yield.

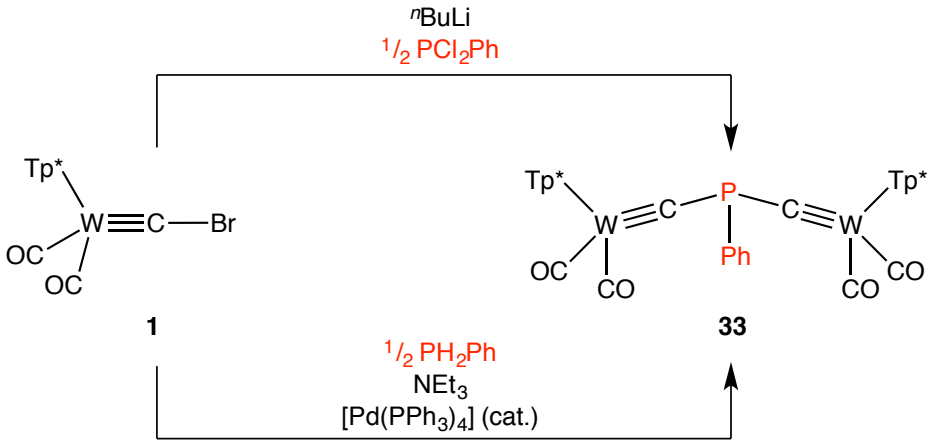

Scheme 5.1. Synthesis of [W_2(μ-C_2PPh)(CO)$_4$(Tp*)$_2$] (**33**).

The presence of two metallocarbyne moieties at phosphorus results in a $^{31}P\{^{1}H\}$ NMR chemical shift (δ_P 80.4) to lower field than what is seen for conventional tertiary phosphines, but very close to that of the molybdenum analogue [$Mo_2(\mu$-$C_2PPh)(CO)_4(Tp^*)_2$] (δ_P 80.2, see Section 3.1).[220] The observed coupling ($^2J_{WP}$ 76.2 Hz) is slightly larger than that seen for **2** ($^2J_{WP}$ 66.2 Hz), and confirms the σ^3, λ^3 environment at phosphorus. The carbyne resonance occurs within the typical region (δ_C 285.0, $^1J_{PC}$ 78.6 Hz, $^1J_{WC}$ 192.4 Hz), slightly upfield compared to the corresponding resonance for the molybdenum analogue (δ_C 297.6, $^1J_{PC}$ 92 Hz),[220] and the remaining $^{13}C\{^{1}H\}$ and ^{1}H NMR data are as expected and call for little comment. In the infrared spectrum of **33** carbonyl absorption bands are observed at 1984, 1974 and 1892 cm^{-1} in THF, indicating coupling of the carbonyl oscillations. This number expands to six bands in the solid state spectrum, implicating solid state effects, consistent with the observation of two crystallographically independent molecules in the asymmetric cell of the crystallographically determined structure of **33**. In contrast, only two carbonyl absorption bands were seen in the IR spectrum of the molybdenum analogue [$Mo_2(\mu$-$C_2PPh)(CO)_4(Tp^*)_2$] (hexane: ν_{CO} 1992, 1922 cm^{-1}), to higher frequency than those of **33**.[220]

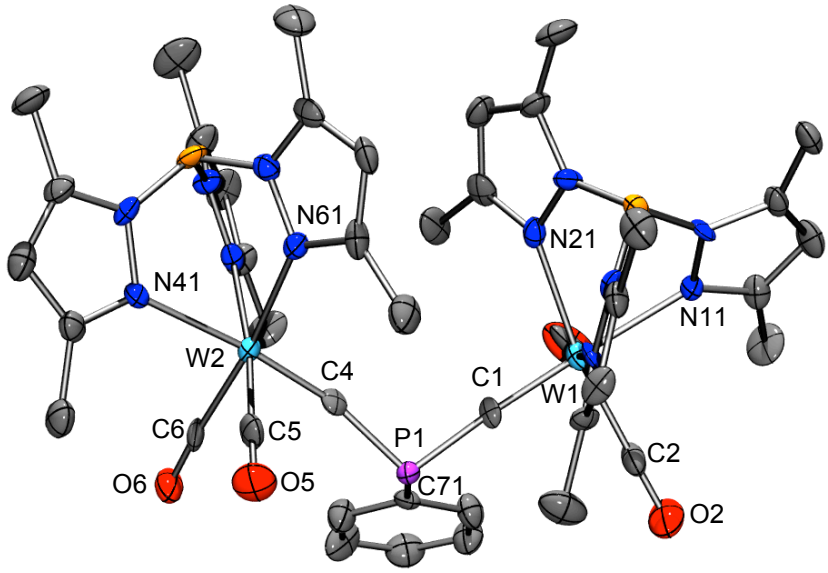

Figure 5.1. Molecular structure of **33** in a crystal of **33**·$(C_5H_{12})_{0.25}$ (50% displacement ellipsoids, hydrogen atoms omitted). Selected bond lengths (Å) and angles (°): W1−C1 1.834(12), W2−C4 1.826(12), P1−C1 1.777(12), P1−C4 1.792(13), P1−C71 1.831(13), W1−C1−P1 175.1(8), W2−C4−P1 163.7(8), C1−P1−C4 102.6(2).

The characterisation of **33** included an X-ray crystallographic study (Figure 5.1). The geometry of the phosphinocarbyne ligand does not differ significantly from that of the mononuclear complex **2**. Although the W−C and P−C bond lengths do not differ between the two arms of the complex, the two W−C−P angles differ significantly for each arm of the complex – a feature that persists for both molecules of **33** in the asymmetric cell (P1−C1−W1 175.1(8)° *cf.* P1−C4−W2 163.7(8)°, P2−C101−W3 172.4(8)° *cf.* P2−C104−W4 164.0(8)°). This might occur so as to allow the pyrazolyl rings to interlock, as illustrated in Figure 5.2. The bis-substituted carbyne complexes $[W_2(\mu\text{-}C_2EPh_2)(O^tBu)_6]$ (E = Si, Ge, Sn) contain either identical W−C−E angles (E = Si, Ge) or similar angles (E = Sn, 173.8(2)° and 170.6(2)°).[412] Disparity is seen in the Mo−C−Sn angles of the Tp*-ligated complex $[Mo_2(\mu\text{-}C_2SnMe_2)(CO)_4(Tp^*)_2]$ (162.0(2)° *cf.* 169.2(2)°), which also displays some stacking of the pyrazolyl rings.

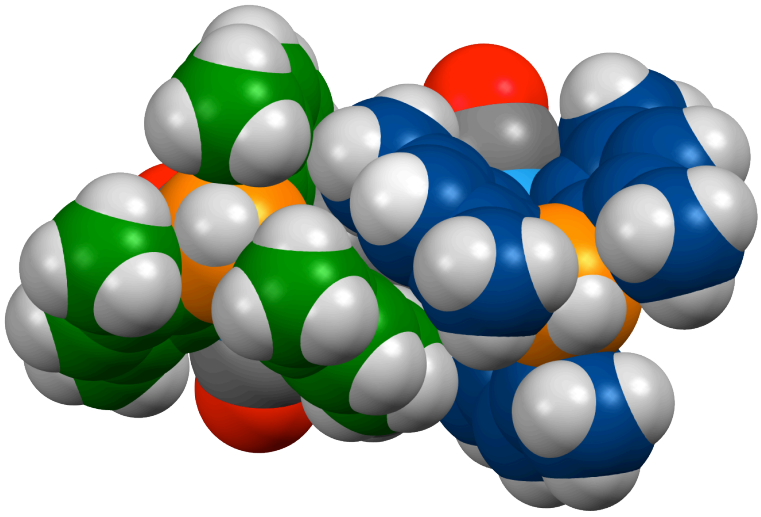

Figure 5.2. Space-filling representation of the molecular structure of **33** showing the alignment of the pyrazolyl rings in the solid state. Colours are as in **Figure 5.1** except the pyrazolyl C and N atoms are colour coded in green (W(1)-Tp*) and dark blue (W(2)-Tp*) to differentiate the two arms of the complex.

Unlike the monometallic complex **2**, **33** is quite prone to oxidation to give $[W_2\{\mu\text{-}C_2P(=O)Ph\}(CO)_4(Tp^*)_2]$, identifiable by the high-field chemical shift (δ_P 16.2) and large tungsten-phosphorus coupling constant ($^2J_{WP}$ 144.9 Hz). The shift to high-field upon oxidation is atypical for tertiary phosphines. But as was seen for the monometallic

phosphinocarbyne **2** and its oxide **13**, the presence of the {W(≡C)(CO)$_2$(Tp*)} fragment leads to this unconventional behaviour (albeit to a much smaller extent for **13**, perhaps due to the presence of only one carbyne moiety), although the reasons as to why are not understood.

5.1.2 Synthesis of [W$_2$(μ-C$_2$PCy)(CO)$_4$(Tp*)$_2$]

Preparation of the bimetallic cyclohexyl analogue was achieved by the reaction of **1** with ^{n}butyllithium and half an equivalent of dichlorocyclohexylphosphine. After chromatography [W$_2$(μ-C$_2$PCy)(CO)$_4$(Tp*)$_2$] (**34**) was obtained as a red-orange powder in 57% yield (Scheme 5.2). Synthesis of **34** via palladium-catalysed phosphination was also successful. However, co-elution of **34** with triphenylphosphine made this a less expedient route to **34**.

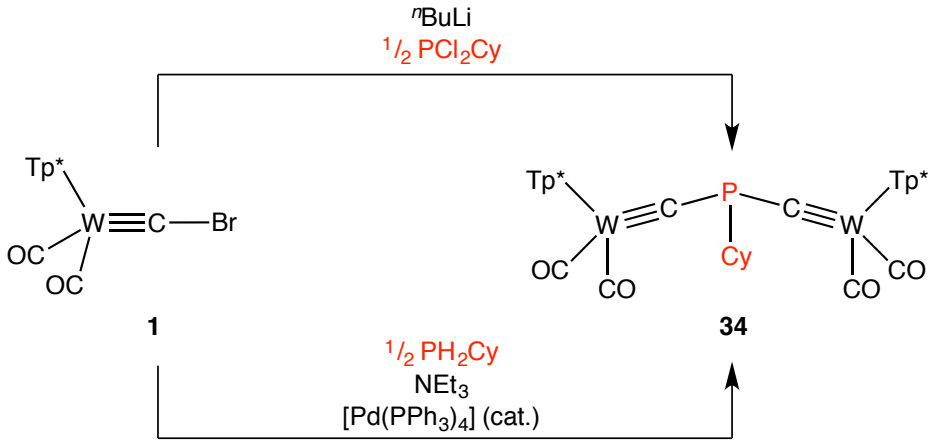

Scheme 5.2. Synthesis of [W$_2$(μ-C$_2$PCy)(CO)$_4$(Tp*)$_2$] (**34**).

The spectroscopic data for **34** largely conform to what was seen for **33**. The phosphorus resonance appears similarly downfield at δ_P 89.9. In the $^{13}C\{^1H\}$ NMR spectra broad singlets are observed for the carbonyl ligands in both **34** (δ_C 227.1) and **33** (δ_C 226.4). The broadness of these peaks is unexpected but suggests that some degree of fluxional rotation is occurring on this timescale.

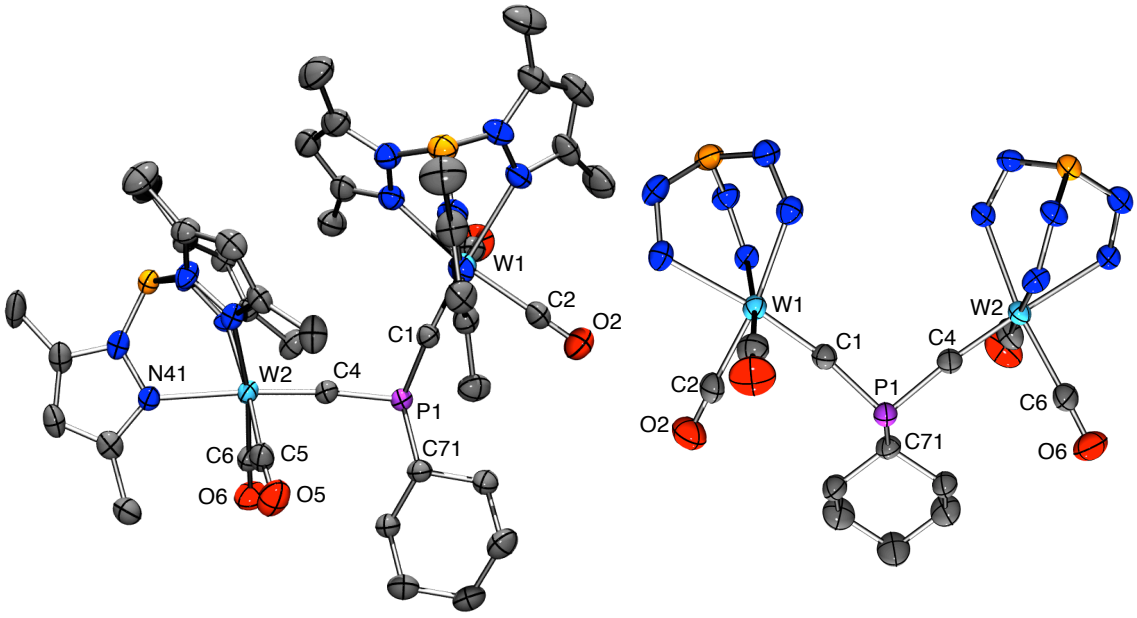

Figure 5.3. Full view (left) and simplified view (right) of the molecular structure of **34** in a crystal of **34**·C_6H_6 (50% displacement ellipsoids, hydrogen atoms omitted). Selected bond lengths (Å) and angles (°): W1−C1 1.837(5), W2−C4 1.832(5), P1−C1 1.788(5), P1−C4 1.784(5), P1−C71 1.852(5), W1−C1−P1 167.0(3), W2−C4−P1 174.5(3), C1−P1−C4 100.4(2).

Crystals grown from a solution of **34** in benzene/hexane at −12°C were the subject of an X-ray crystallographic study, the results of which are summarised in Figure 5.3. The phosphorus atom adopts a distorted trigonal pyramidal geometry (angle sum at P1 309.9°), with the C1−P1−C4 angle being the most contracted (100.4(2)°). As was seen in **33**, the W−C and P−C bond lengths are comparable between the two arms of the complex, yet the two W−C−P angles differ significantly (W1−C1−P1 167.0(3)° *cf.* W2−C4−P1 174.5(3)°). This is thought to occur so as to allow stacking of the pyrazolyl rings, as was seen for **33**.

The solid state structure of **34** does not possess any elements of symmetry (C_1), whereas the solution state NMR data show two pyrazolyl environments in a 2:1 ratio, consistent with local C_s symmetry in which two of the pyrazolyl rings lie in the W−C−P−C−W mirror plane. From this it can be inferred that in solution there must be sufficiently free rotation about the P−C bonds such that the molecule is able to traverse this geometry on the NMR timescale.

5.1.3 Synthesis of $[W_2(\mu\text{-}C_2PCl)(CO)_4(Tp^*)_2]$

Synthesis of the chloro-substituted analogue $[W_2(\mu\text{-}C_2PCl)(CO)_4(Tp^*)_2]$ (**35**) was achieved in a similar fashion, as depicted in Scheme 5.3. In this case, isolation of a pure sample of **35** was not achieved because the hydrolytic susceptibility of the P−Cl linkage precludes chromatographic purification. Intriguingly, complex **35** was found to isomerise at room temperature to give the bridging carbyne-tungstaphosphirene complex $[W_2\{\mu{:}\eta^1\text{-}C;\eta^2\text{-}C,P\text{-}CC(PCl)\}(CO)_4(Tp^*)_2]$ (**36** – see Section 5.1.5), which further thwarted efforts to obtain pure samples of **35** through precipitation and recrystallisation attempts. Benzene extraction of the reaction mixture residue provided a dark red solid, the $^{31}P\{^1H\}$ NMR spectrum of which revealed that the crude sample comprised 72% **35**, contaminated with 12% **36**, 3.6% $[W_3(\mu\text{-}C_3P)(CO)_6(Tp^*)_3]$ and ten other minor impurities (≤2% each).

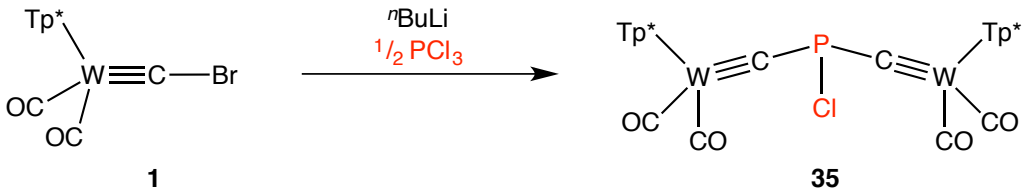

Scheme 5.3. Synthesis of $[W_2(\mu\text{-}C_2PCl)(CO)_4(Tp^*)_2]$ **(35)**.

Complex **35** is evident in the $^{31}P\{^1H\}$ NMR spectrum by a singlet accompanied by ^{183}W satellites at δ_P 124.9 ($^2J_{WP}$ 66.4 Hz), only marginally upfield shifted with respect to the monometallic complex $[W(\equiv CPCl_2)(CO)_2(Tp^*)]$ (δ_P 136.2). The carbyne resonance falls within the expected region (δ_C 280.0, $^1J_{PC}$ 97.9, $^1J_{WC}$ 194.0 Hz), whilst the remaining ^1H and $^{13}C\{^1H\}$ NMR data demonstrate the presence of two carbonyl environments and three pyrazolyl environments in a 1:1:1 ratio. This is in contrast to what was observed for **33** and **34** wherein the pyrazolyl rings exist in a 2:1 ratio and only one CO resonance is observed. The data obtained are consistent with the two tungsten centres being equivalent, but not with a mirror plane through the N−W≡C axis, unlike what was seen previously for **33**, **34** and the complexes prepared in Chapter 2 (see Figure 2.3). Evidently **35** is not able to traverse such a geometry on the NMR timescale, leading to the observed inequivalence of these ligands.

5.1.4 Attempted synthesis of $[W_2\{\mu\text{-}C_2P(NR_2)\}(CO)_4(Tp^*)_2]$

When $[W(\equiv CLi)(CO)_2(Tp^*)]$ was treated with half an equivalent of the amino-substituted phosphines $PCl_2(NR_2)$ (R = Et, ^{i}Pr) no evidence of the bimetallic species $[W_2\{\mu\text{-}C_2P(NR_2)\}(CO)_4(Tp^*)_2]$ was observed in the IR or NMR spectra (Scheme 5.4). Instead, the mono-substitution products $[W\{\equiv CPCl(NR_2)\}(CO)_2(Tp^*)]$ were formed and the remaining lithiocarbyne complex decomposed to give a mixture of species including the methylidyne complex $[W(\equiv CH)(CO)_2(Tp^*)]$.

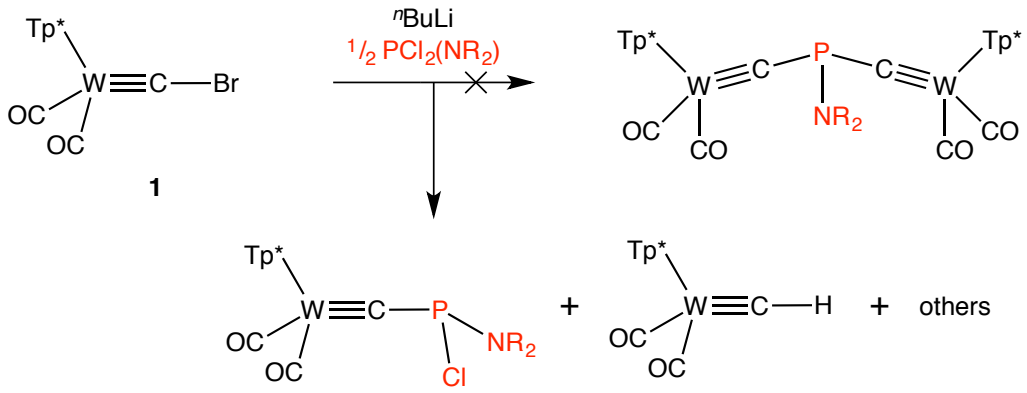

Scheme 5.4. Attempted synthesis of $[W_2\{\mu\text{-}C_2P(NR_2)\}(CO)_4(Tp^*)_2]$ (R = Et, ^{i}Pr).

Whilst in these cases steric hindrance might prevent the second substitution from taking place, the size of the chloro(dimethylamino)phosphino group $PCl(NMe_2)$ should not be prohibitive considering that the reaction proceeds with cyclohexyldichlorophosphine. Based on this rationale the reaction was repeated using $PCl_2(NMe_2)$, and the outcome of this reaction did differ from that of the ethyl and isopropyl complexes, although not as anticipated. The $^{31}P\{^1H\}$ NMR spectrum showed 12 peaks of comparable intensities in the region of 15 – 145 ppm. Resonances at δ_P 140.4, 131.4, 84.7, 83.1, 80.9 and 79.2 all displayed ^{183}W satellites consistent with three-coordinate phosphinocarbynes ($^2J_{WP}$ 64.7 – 78.7 Hz), of which $[W\{\equiv CPCl(NMe_2)\}(CO)_2(Tp^*)]$ and $[W_2\{\mu\text{-}C_2P(NMe_2)\}(CO)_4(Tp^*)_2]$ might account for two signals. The ^1H NMR spectrum showed a multitude of Tp* environments, from which the methylidyne $[W(\equiv CH)(CO)_2(Tp^*)]$ was identifiable by a singlet at δ_H 8.23 for WCH with $^2J_{WH}$ 83.7 Hz, in agreement with the values reported by Templeton.[65]

As the difference in electronics between the three aminophosphines used is minimal, it indicates that the steric factors do influence the reactivity to some extent. However, in the absence of significant steric hindrance a multitude of products are formed, from which it can be inferred that either formation of the bis-substituted phosphine $[W_2\{\mu\text{-}C_2P(NMe_2)\}(CO)_4(Tp^*)_2]$ is unfavourable, or that formation occurs but this complex is unstable under the reaction conditions employed.

5.1.5 Thermal rearrangement of $[W_2(\mu\text{-}C_2PR)(CO)_4(Tp^*)_2]$

Interestingly, the bimetallic carbyne complex $[W_2(\mu\text{-}C_2PCl)(CO)_4(Tp^*)_2]$ (**35**) was found to rearrange spontaneously in solution. NMR samples of **35** contained, in addition to the product peak at δ_P 124.9, a broad resonance at δ_P 92.7 without resolvable ^{183}W satellites. Crystals obtained from a solution of **35** in CH_2Cl_2/pentane at −15°C were found to be not the expected symmetric complex $[W_2(\mu\text{-}C_2PCl)(CO)_4(Tp^*)_2]$ but rather the complex $[W_2\{\mu\text{:}\eta^1\text{-}C;\eta^2\text{-}C,P\text{-}CC(PCl)\}(CO)_4(Tp^*)_2]$ (**36**) in which the PCl moiety has migrated to one of the W≡C bonds, forming an extremely unusual tungstaphosphirene ring (Scheme 5.5).

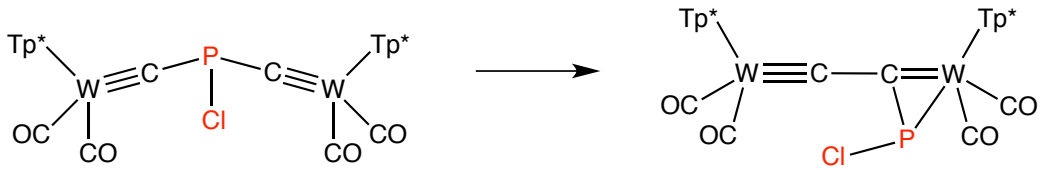

35 **36**

Scheme 5.5. Synthesis of $[W_2\{\mu\text{:}\eta^1\text{-}C;\eta^2\text{-}C,P\text{-}CC(PCl)\}(CO)_4(Tp^*)_2]$ (**36**).

This isomerisation occurs slowly in solution. After 70 hours a benzene solution of **35** contained **35** and **36** in a 5:3 ratio, and after seven days the two isomers existed in almost equal proportions. The rearrangement can be accelerated by heating and proceeds within 13 hours at 50°C. Unfortunately, isolation of a pure bulk sample of **36** was not accomplished, and as such spectroscopic data for **36** are limited to the $^{31}P\{^1H\}$ NMR spectrum as the ^1H NMR spectrum was too complex for analysis. However, crystals of **36** were acquired, and the single crystal X-ray structure was determined, as depicted in Figure 5.4. Unfortunately, the result obtained is of low precision (R = 0.096) due to systematic twinning of the crystals, which limited the quality of the data available to refine the structural model. Nevertheless, the molecular structure confirmed the unusual formulation of **36**.

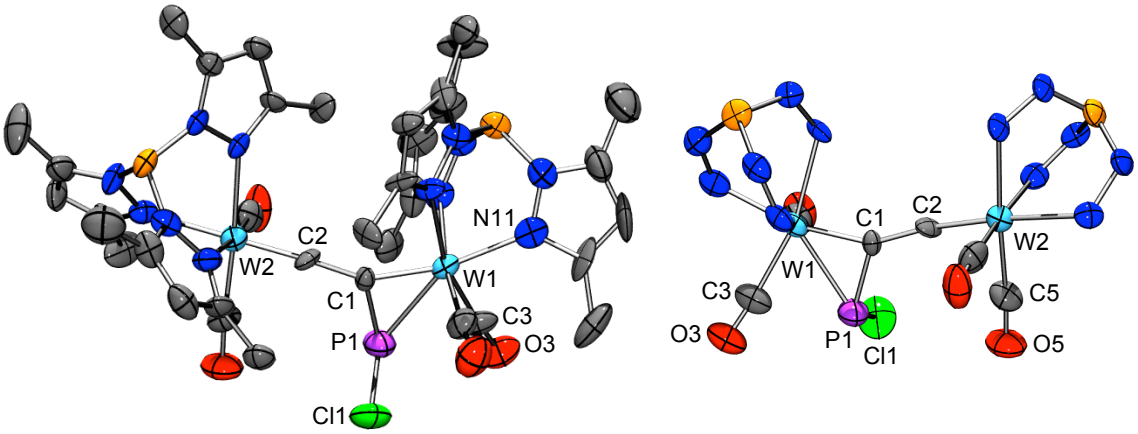

Figure 5.4. Full view (left) and simplified view (right) of the molecular structure of *R*-**36** in a crystal of *rac*-**36**·$(CH_2Cl_2)_2$ (50% displacement ellipsoids, hydrogen atoms omitted, *S*-enantiomer generated by $P2_1/c$ symmetry). Selected bond lengths (Å) and angles (°): W1−C1 1.958(19), W2−C2 1.82(2), C1−C2 1.47(3), C1−P1 1.75(2), W1−P1 2.517(7), P1−Cl1 2.155(12), W1−C1−C2 152.1(16), W2−C2−C1 171.3(17), W1−P1−C1 50.8(7), W1−C1−P1 85.3(9), P1−C1−C2 122.4(15), P1−W1−C1 43.8(6), W1−P1−Cl1 110.2(4), C1−P1−Cl1 105.2(8).

While there are a number of reports of complexes containing three-membered [M{η^2-C(R)PR_2}$(L)_n$] rings in which the phosphorus is four-coordinate, metallaphosphirene complexes [M{η^2-C(R)PR}$(L)_n$] are exceedingly rare. Metallaphosphirene complexes are limited to the iridium species [Ir{η^2-C(^{t}Bu)PCy}(CO)(PPh_3)(L)] (L = CO, PPh_3),[413] although related compounds are known, such as Weber's σ^3, λ^4 phosphaalkenyl complex [W{η^2-C(H)P{$C(NEt_2)_2$}}$(CO)_2$(Tp*)]X (X = OTf, BF_4)[69] and Mathey's $W(CO)_5$-coordinated tungstaphosphirene [W{η^2-C(Ph)PPh($W(CO)_5$)}$(CO)_2$(Cp)].[126]

The iridaphosphirene complex [Ir{η^2-C(^{t}Bu)PCy}(CO)(PPh_3)$_2$] was prepared by reaction of the phosphavinyl Grignard reagent *Z*-[CyP=C(^{t}Bu)MgCl(OEt_2)] with Vaska's complex [IrCl(CO)(PPh_3)$_2$] (Scheme 5.6).[413] The observed P−C (1.753(13) Å) and Ir−C (1.918(14) Å) bond lengths and the attendant distorted trigonal pyramidal geometry at phosphorus support the formulation of the complex as an iridaphosphirene species rather than the alternative η^2-phosphavinyl description. Reactions with a range of electrophiles (H^+, Me^+, S, Se, AgCl, AuCl, $AuPPh_3^+$, HgPh) proceeded via electrophilic addition to the phosphine.[414,415] However, in the case of protonation a

rearrangement to the η^1-phosphaalkene salt $[Ir\{\eta^1\text{-}P(Cy)=CH^tBu\}(CO)(PPh_3)_2]^+$ is observed.

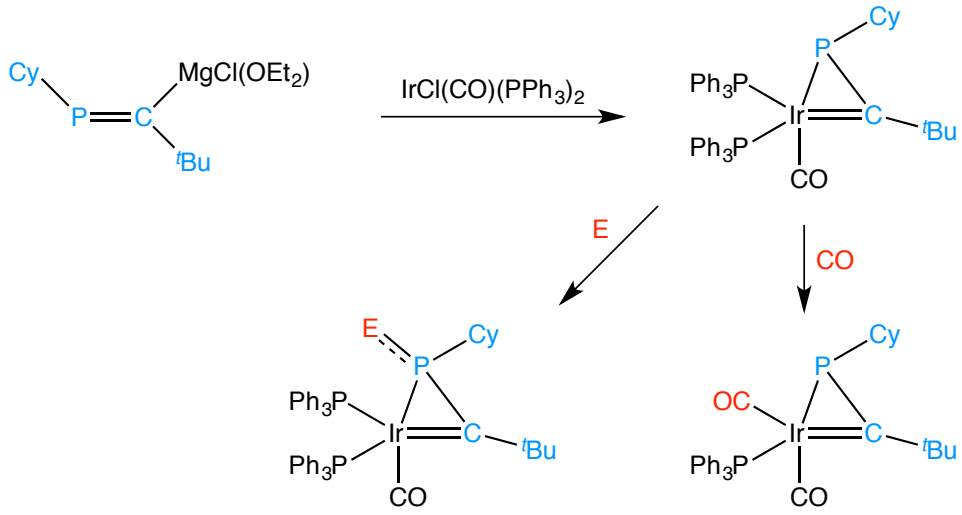

Scheme 5.6. Jones' synthesis and electrophilic addition reactions of iridaphosphirene complexes (E = H^+, Me^+, S, Se, AgCl, AuCl, $AuPPh_3^+$, HgPh).

While transfer reactions of complexed phosphinidine moieties ($RPML_n$) have been increasingly utilised,[416,417] free phosphinidenes (P−R) are exceptionally reactive and remain to be isolated, so it is unlikely that the rearrangement proceeds via extrusion of the phosphinidene moiety. More likely is that the process involves a concerted migration of the PR moiety, in conjunction with P−C bond cleavage and C−C bond formation processes. There are a number of methods which can be used for the preparation of phosphirenes,[418,419] and while the intermolecular addition of transient phosphirenes to alkynes has been reported,[420] the cyclisation of a C≡C−PR unit remains unprecedented. Although this intramolecular migration of a PR moiety to a carbyne appears unique, Fischer has noted the thermal rearrangement of the terminal phosphinocarbene complex $[W\{=C(NEt_2)(PMePh)\}(CO)_4(PHMePh)]$ to form a cyclic η^2-carbene structure $[W\{\eta^2\text{-}C(NEt_2)PMePh\}(CO)_4]$, although this process does not invoke cleavage of any P−C bonds.[119] In contrast, Eisch and co-workers have demonstrated the formation of borirenes via migration of a BMes fragment to the C≡C bond of an alkynyl substituent.[421,422]

Based on this curious rearrangement of the chlorophosphine complex **35** we wished to explore the scope of such reactivity. In solutions of the phenyl derivative **33** no rearrangement is observed at room temperature, and the thermal stability of **33** is implicit in the conditions used for its synthesis (palladium catalysis, 80°C, 18 hours). Accordingly, a toluene solution of **33** was heated to 110°C and the reaction progress was monitored by infrared spectroscopy. After 16.5 hours carbonyl absorption bands due to **33** (1985, 1974, 1893 cm^{-1}) were accompanied by new bands at 1940 and 1876 cm^{-1}. After 41 hours, the major bands were those at 1940 and 1876 cm^{-1}, assigned to the rearranged tungstaphosphirene complex $[W_2\{\mu{:}\eta^1\text{-}C;\eta^2\text{-}C,P\text{-}CC(PPh)\}(CO)_4(Tp^*)_2]$ **(37)** (Scheme 5.7), although weak bands at 1970, 1892 and 1858 cm^{-1} were evident. These might be attributed to **37**, residual **33**, or other side products formed in the reaction.

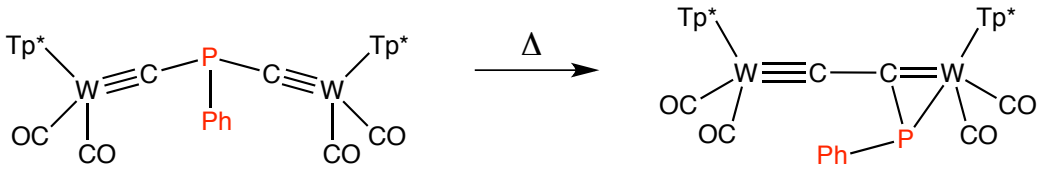

33 **37**

Scheme 5.7. Synthesis of $[W_2\{\mu{:}\eta^1\text{-}C;\eta^2\text{-}C,P\text{-}CC(PPh)\}(CO)_4(Tp^*)_2]$ (**37**).

The $^{31}P\{^1H\}$ NMR spectrum indicated a mixture of phosphorus-containing products formed in the reaction (> 15 peaks), although the major component was a broad peak at δ_P −74.5 without visible ^{183}W satellites. Attempts to purify the mixture by chromatography or fractional crystallisation were unsuccessful. Filtration through diatomaceous earth and removal of the solvent yielded a dark purple solid containing ca. 61% **37**, as estimated by $^{31}P\{^1H\}$ NMR spectroscopy. Unfortunately the ^1H NMR spectrum contained too many resonances for those due to **37** to be unambiguously identified. Given that the molecule has C_1 symmetry (chiral at phosphorus), up to twelve methyl peaks would be expected. Although the inability to obtain a pure sample of **37** precluded the acquisition of useful spectroscopic data, high resolution mass spectrometric data confirmed the formulation of the complex by the observation of an $[M + H]^+$ peak.

Interestingly, the chemical shift of **37** (δ_P −74.5) is dramatically shifted with respect to that of **36** (δ_P 92.7). The appearance of the phosphorus resonance to high-field is

expected based on the iridaphosphirene complexes [Ir{η^2-C(^{t}Bu)PCy}(CO)(PPh_3)(L)] (L = CO, δ_P −188.7; PPh_3, δ_P −152.3)[413] and [W{η^2-C(Ph)PPh($W(CO)_5$)}$(CO)_2$(Cp)] (δ_P −157.2),[126] and the generally observed high-field shifts for phosphorus in small rings (e.g. δ_P −77.3 for [W{≡CP(N^{i}Pr$_2$)(CPhCPh)}$(CO)_2$(Tp*)]$AlCl_4$ (Section 3.4.3)). Replacement of aryl substituents with chloro groups does cause downfield shifts in the NMR spectra of phosphorus compounds, but the magnitude of the shift in this case is much larger than expected (e.g. PhP(CPhCPh){$W(CO)_5$} δ_P −159.4[423] *cf.* ClP(CPhCPh){$W(CO)_5$} δ_P −109.2).[424] In the case of the precursors, a comparatively small downfield shift of 45 ppm is observed for the chloro complex **35** (δ_P 124.9) compared to the phenyl analogue **33** (δ_P 80.4).

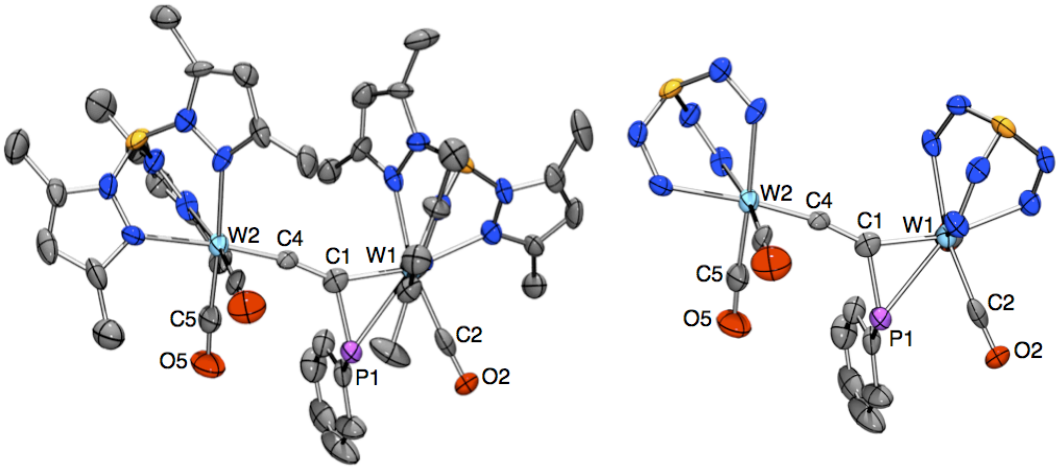

Figure 5.5. Full view (left) and simplified view (right) of the molecular structure of *R*-**37** in a crystal of *rac*-**37**·C_6H_6 (50% displacement ellipsoids, hydrogen atoms omitted, *S*-enantiomer generated by *Pca*2_1 symmetry). Selected bond lengths (Å) and angles (°): W1−C1 2.014(12), W2−C4 1.865(10), C1−C4 1.380(14), C1−P1 1.790(12), W1−P1 2.585(3), P1−C71 1.821(15), W1−C1−C4 148.1(9), W2−C4−C1 169.2(10), W1−P1−C1 51.0(4), W1−C1−P1 85.4(5), P1−C1−C4 124.5(9), P1−W1−C1 43.7(3), W1−P1−C71 109.6(5), C1−P1−C71 107.8(7).

Fortunately, crystals of **37** were obtained which provided confirmation of the formulation of **37**. The results of an X-ray crystallographic study are summarised in Figure 5.5. The geometry of the WCCPW unit in **37** mirrors that of **36**, with the exception of the W−P bond which is slightly elongated in **37** (2.585(3) *cf.* 2.517(7) Å). The phosphorus atoms of both **36** and **37** display significantly distorted trigonal

pyramidal geometries (angle sum at P 266.2° (**36**), 268.4° (**37**)) as a consequence of incorporation in a constrained three-membered ring. The W2−C4 bond (1.865(10) Å) can be formalised as a W−C triple bond, the length of which does not differ significantly from what was observed for the W≡C bonds of the precursor **33** (1.834(12) and 1.826(12) Å). The W1−C1 linkage (2.014(12) Å) points towards the retention of considerable multiple bond character, being shorter than that typically observed for tungsten bound to η^1-C(sp^2) vinyl, acyl or N-heterocyclic carbene ligands (2.15 – 2.30 Å), and falling between the ranges typical of Fischer-type (> 2.0 Å) and Schrock-type carbene (< 2.0 Å) ligands.[425] The W1−C1 linkage closely resembles the W−C bond length in the thioacyl complex [W{η^2-SCP(=S)Ph_2}$(CO)_2$(Tp*)] (2.003(13) Å). The P1−C1 bond length (1.790(12) Å) is consistent with a P−C single bond, as seen in the cyclic phosphirene complexes [W{η^2-C(Ph)PPh(W$(CO)_5$)}$(CO)_2$(Cp)] (1.775(8) Å),[126] [Pt{η^1-P(Ph)C(Ph)C(Ph)}$Cl_2(PEt_3)$] (average 1.78 Å)[426] and [Ir{η^2-C(^{t}Bu)PCy}(CO)$(PPh_3)_2$] (1.753(13) Å).[413] These data support the valence bond description of **37** as a tungstaphosphirene complex, rather than alternative descriptors such as an η^2-phosphaalkene complex.

Given that the transformation is intramolecular with comparatively little rearrangement, attempts to effect the isomerisation via a solid state reaction were unsuccessful; heating solid **33** under argon at 100°C resulted in no reaction, while at 180°C decomposition was observed to yield a brown-black solid that did not display any $^{31}P\{^1H\}$ NMR resonances. Attempts to synthesise **37** from **1** in a one-pot procedure were similarly unsuccessful. Heating a toluene solution of **1**, PH_2Ph, NEt_3 and a catalytic amount of [Pd$(PPh_3)_4$] at 100°C did produce **33**, but continued heating did not afford appreciable quantities of **37**, even after four days. The presence of base in this reaction may inhibit the isomerisation from occurring, although the mechanism by which the rearrangement occurs is unknown.

5.2 Reactions with [AuCl(SMe_2)]

It was of interest to investigate reactions of **33** with electrophiles in order to compare the reactivity of this complex to that of the monometallic analogue [W(≡CPPh_2)$(CO)_2$(Tp*)] (**2**), discussed in Chapter 2, in which the phosphorus was found to be the most nucleophilic site. [AuCl(SMe_2)] was chosen as the electrophile of interest because it displayed the most controllable reactivity towards **2**, wherein mono-

or bis-addition of AuCl could be effected through stoichiometric control. Preliminary studies by Shang involving the reaction of $[Mo_2(\mu\text{-}C_2PPh)(CO)_4(Tp^*)_2]$ with excess $[AuCl(SMe_2)]$ suggested formation of the P-coordinated complex $[Mo_2(\mu\text{-}C_2PPhAuCl)(CO)_4(Tp^*)_2]$.[220]

When a CH_2Cl_2 solution of **33** was treated with one equivalent of $[AuCl(SMe_2)]$ a mixture of products was obtained (Scheme 5.8). The $^{31}P\{^1H\}$ NMR spectrum contained three resonances with ^{183}W satellites at δ_P 49.4 ($^2J_{WP}$ 143.7 Hz, 62%), 63.1 ($^2J_{WP}$ 118.7 Hz, 25%) and 75.7 ($^2J_{WP}$ 88.8 Hz, 3%).* Addition of a second equivalent of $[AuCl(SMe_2)]$ altered the proportions of these three peaks to 16%, 46% and 34%, respectively. Addition of a third $[AuCl(SMe_2)]$ equivalent gave exclusively δ_P 75.7.

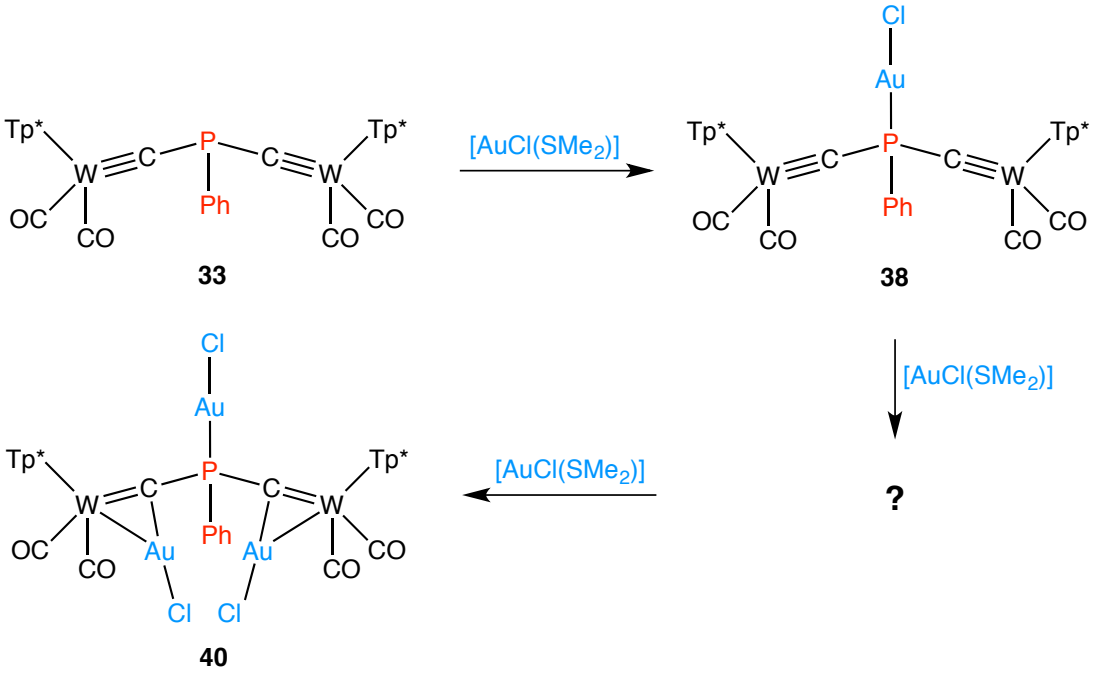

Scheme 5.8. Addition of $[AuCl(SMe_2)]$ to **33**.

Treatment of **33** with 1.1 equivalents of $[AuCl(SMe_2)]$ followed by chromatography allowed isolation of the complex which corresponded to δ_P 49.4 in 24% yield, which was found to be the product of P-coordination $[W_2(\mu\text{-}C_2PPhAuCl)(CO)_4(Tp^*)_2]$ (**38**). The $^{31}P\{^1H\}$ NMR spectrum of **38** comprises a singlet resonance at δ_P 49.4 with $^2J_{WP}$ 143.7 Hz, shifted 30 ppm upfield from that of the precursor **33**. In contrast to this, the

* Percentages quoted represent the % by $^{31}P\{^1H\}$ NMR spectroscopy. The percentage values do not sum to 100% as three other small peaks were present in the spectra.

monometallic complex **2** shifts 5 ppm downfield upon P-complexation of AuCl to give [W(≡CPPh$_2$AuCl)(CO)$_2$(Tp*)] (**8**) (δ_P 32.0 *cf.* 37.5). However, similar coupling constants are seen for **38** ($^2J_{WP}$ 143.7 Hz) and **8** ($^2J_{WP}$ 139.3 Hz), illustrating the recurrent theme throughout this work that the coupling constants are more diagnostic than the chemical shifts. A comparable upfield shift of 39 ppm was observed for the molybdenum analogue [Mo$_2$(μ-C$_2$PPhAuCl)(CO)$_4$(Tp*)$_2$] (δ_P 41.2) compared to the precursor [Mo$_2$(μ-C$_2$PPh)(CO)$_4$(Tp*)$_2$] (δ_P 80.2).[220]

In the $^{13}C\{^1H\}$ NMR spectrum both the chemical shift and couplings of **38** (δ_C 262.5, $^1J_{PC}$ 25.9, $^1J_{WC}$ 203.2 Hz) closely match those of **8** (δ_C 263.3, $^1J_{PC}$ 22.1, $^1J_{WC}$ 199.9 Hz), and resemble the data obtained for [Mo$_2$(μ-C$_2$PPhAuCl)(CO)$_4$(Tp*)$_2$] (δ_C 273.2, $^1J_{PC}$ 42),[220] although larger $^1J_{PC}$ values have been observed for the molybdenum analogues compared to their tungsten counterparts. The carbyne resonance appears 20 ppm upfield with respect to that of the precursor **33**, along with a considerable reduction in the $^1J_{PC}$ value. The ^1H and $^{13}C\{^1H\}$ NMR spectra indicate that the pyrazolyl rings and carbonyl ligands at each tungsten centre are inequivalent, a consequence of their prochiral nature. The carbonyl absorption bands in the IR spectrum show the expected shift to higher frequency due to the withdrawal of electron density from the tungsten centres that accompanies complexation of the phosphine. The ESI(+) mass spectrum clearly demonstrates the presence of one AuCl moiety through the observation of [M + MeCN]$^+$ and [M + H]$^+$ peaks.

Crystals of **38** were obtained from a solution of **38** in Et$_2$O at −20°C. The results of an X-ray crystallographic study are shown in Figure 5.6. Unfortunately the crystals obtained were of low quality, providing poor data that limited the precision of the structural model. Nevertheless, the structure substantiates the proposed formulation of **38** based on spectroscopic data. The two W−C−P angles are comparable (W1−C1−P1 170.3(13)°, W2−C4−P1 173.2(16)°), in contrast to what was seen in **33** and **34**, although the low precision of the structure must be taken into account.

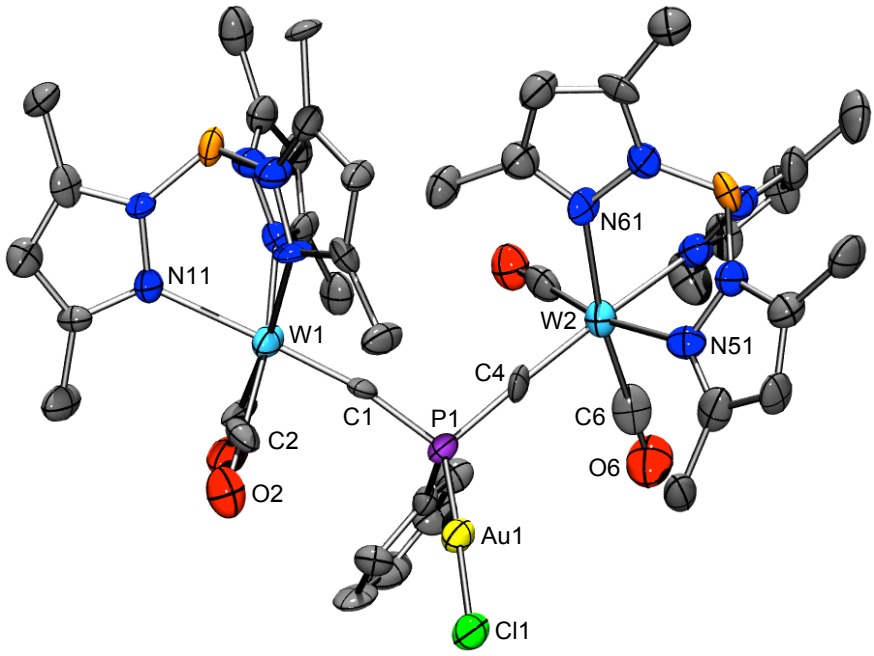

Figure 5.6. Molecular structure of **38** in a crystal of **38**·Et_2O (50% displacement ellipsoids, hydrogen atoms omitted). Selected bond lengths (Å) and angles (°): W1−C1 1.84(2), W2−C4 1.89(2), C1−P1 1.75(2), C4−P1 1.73(2), P1−Au1 2.235(7), W1−C1−P1 170.3(13), W2−C4−P1 173.2(16), C1−P1−C4 106.8(10), P1−Au1−Cl1 178.4(2).

The reaction of **33** with three equivalents of [AuCl(SMe_2)] gave the pentametallic complex [W_2{μ-(η^2-CAuCl)$_2$PPhAuCl}$(CO)_4(Tp^*)_2$] (**40**) in which addition to the phosphine and both W≡C bonds has occurred. The phosphorus resonance is shifted downfield compared to **38** to δ_P 75.7. The $^1J_{WP}$ coupling of 88.8 Hz is comparable to that of [W{η^2-C(AuCl)PPh_2AuCl}$(CO)_2(Tp^*)$] (**9**) ($^1J_{WP}$ 84.3 Hz). The carbyne resonance appears at δ_C 252.0 with no resolvable $^1J_{PC}$ coupling and considerably reduced $^1J_{WC}$ coupling (99.9 Hz) akin to what was seen for **9** (δ_C 253.6, $^1J_{PC}$ 1.5 Hz, $^1J_{WC}$ 99.6 Hz). The carbonyl absorption bands are again shifted to higher frequency compared to **33** and **38** as a result of decreased electron density at the tungsten centres. As seen for **38**, ^{1}H and ^{13}C{^{1}H} NMR data demonstrate the prochiral nature of the carbonyl and pyrazolyl ligands.

Crystals of **40** suitable for X-ray diffraction were obtained from a CH_2Cl_2/hexane solution, and the results of a crystallographic study are shown in Figure 5.7. The solid state structure revealed an Au···Au interaction exists between the two carbyne-bound gold moieties. The Au1···Au2 distance of 3.0318(8) Å falls within the typical range for

aurophilic bonding (2.8 – 3.3 Å),[427] and well within the sum of the van der Waals radii (3.32 Å). The geometric features of **40** mirror those observed in the monotungsten complex **28**, and related literature complexes.[260,275-277,284] As has been seen previously,[267] the carbyne ligands bridge the W−Au linkages unsymmetrically (W1−C1 1.874(15), W2−C4 1.884(14) *cf.* C1−Au1 2.038(17), C4−Au2 2.020(15) Å), consistent with retained W−C multiple bonding. The two C−Au−Cl angles are significantly different, with C4−Au2−Cl2 being almost linear (178.4(4)°) while C1−Au1−Cl1 is considerably distorted from linearity (164.6(4)°). Both Cl1 and Cl2 show interactions with neighbouring dimethylpyrazolyl groups, and Cl1 also interacts with the CH_2Cl_2 solvent molecule, and the cumulative effect of these interactions may be the observed distortion of the C1−Au1−Cl1 angle.

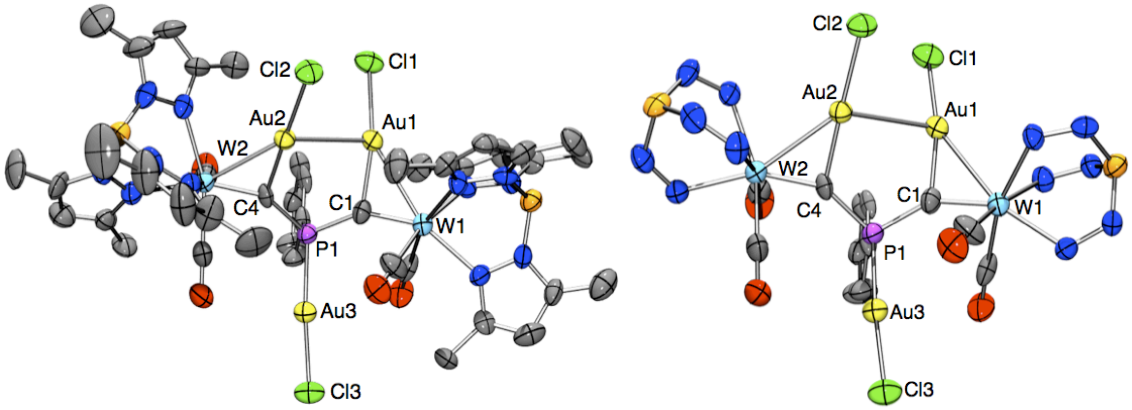

Figure 5.7. Full view (left) and simplified view (right) of the molecular structure of **40** in a crystal of **40**·CH_2Cl_2 (50% displacement ellipsoids, hydrogen atoms omitted). Selected bond lengths (Å) and angles (°): W1−C1 1.874(15), W2−C4 1.884(14), C1−P1 1.804(16), C4−P1 1.831(15), C1−Au1 2.038(17), C4−Au2 2.020(15), W1−Au1 2.8275(9), W2−Au2 2.7691(9), Au1−Au2 3.0318(8), P1−Au3 2.237(4), W1−C1−P1 148.6(10), W2−C4−P1 148.8(9), C1−P1−C4 107.0(7), W1−C1−Au1 92.5(7), W2−C4−Au2 90.3(6), C1−W1−Au1 46.1(5), C4−W2−Au2 46.8(5), C1−Au1−Cl1 164.6(4), C4−Au2−Cl2 178.4(4).

Unfortunately, chromatography did not lead to clean isolation of the complex corresponding to δ_P 63.1, denoted **39**. Instead it was obtained contaminated with considerable quantities of **38**, or both **38** and **40**. The complex **39** was anticipated to

correspond to addition of AuCl to the phosphine and/or W≡C bonds, for which three structures appeared plausible, outlined in Figure 5.8.

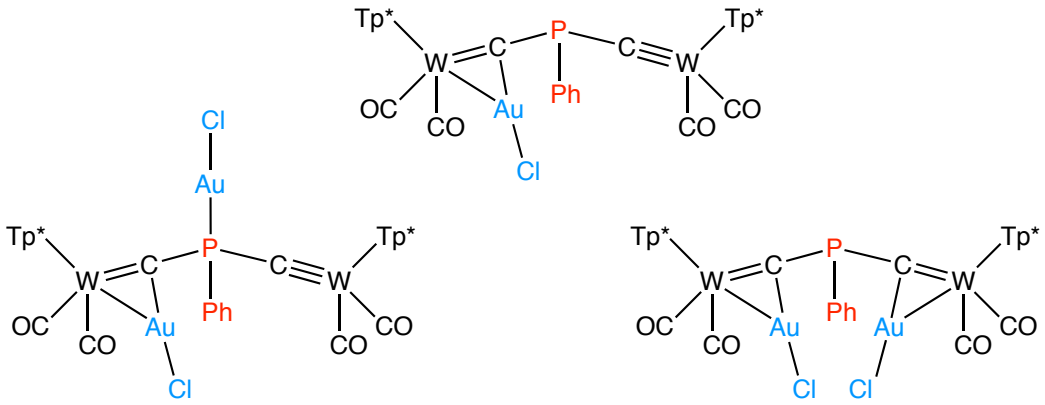

Figure 5.8. Possible structures of **39**.

The asymmetric W_2Au_1 complex $[W_2\{\mu{:}\eta^1\text{-}C;\eta^2\text{-}C,Au\text{-}CP(Ph)C(AuCl)\}(CO)_4(Tp^*)_2]$ was disfavoured as the structure because addition of a second equivalent of $[AuCl(SMe_2)]$ to a mixture of the three products increased the proportion of **39** and decreased the proportion of **38**. Additionally, the proportions of **38**, **39** and **40** obtained are consistent with addition of one, two and three AuCl moieties, respectively, based on the amount of $[AuCl(SMe_2)]$ added. Mass spectrometry of a sample containing **39** and **38** contained peaks consistent with addition of two AuCl moieties, suggesting that **39** does correspond to a di-aurated complex.

We anticipated that the asymmetric complex $[W_2\{\mu{:}\eta^1\text{-}C;\eta^2\text{-}C,Au\text{-}CP(Ph)(AuCl)C(AuCl)\}(CO)_4(Tp^*)_2]$ was the most likely structure as this would correspond to the direct addition of AuCl to one W≡C bond of **38**. However, inspection of the spectroscopic data obtained, outlined in Table 5.1, suggested that **39** actually possessed a symmetric structure in solution (further discounting the asymmetric W_2Au_1 complex as **39**). The $^{31}P\{^1H\}$ NMR spectrum comprised a singlet resonance at δ_P 63.1, for which the tungsten-183 satellite resonance was a doublet ($^2J_{WP}$ 118.7 Hz). The chemical shift is not diagnostic, but the tungsten-phosphorus coupling provides useful structural information. The proposed asymmetric structure contains two inequivalent tungsten atoms; hence it would produce two sets of ^{183}W satellites with different coupling constants (e.g. $^2J_{WP}$ 139.3 Hz in $[W(\equiv CPPh_2AuCl)(CO)_2(Tp^*)]$ *cf.* 84.3 Hz in $[W\{\eta^2\text{-}C(AuCl)PPh_2AuCl\}(CO)_2(Tp^*)]$). The magnitude of the coupling in **39** falls

between these values, indicating either that rapid exchange of the AuCl moieties is occurring on the NMR timescale, or the compound possesses a symmetric structure such as $[W_2\{\mu\text{-}(\eta^2\text{-}CAuCl)_2PPh\}(CO)_4(Tp^*)_2]$.

Table 5.1. Selected spectroscopic data for **33** and AuCl adducts.

Complex	δ_P	$^2J_{WP}$ (Hz)	ν_{CO} (cm^{-1})
$[W_2(\mu\text{-}C_2PPh)(CO)_4(Tp^*)_2]$ (**33**)	79.5	77.2	1986, 1975, 1892
$[W_2(\mu\text{-}C_2PPhAuCl)(CO)_4(Tp^*)_2]$ (**38**)	49.4	143.7	1998, 1913
$[W_2\{\mu\text{-}(CAuCl)_2PPh\}(CO)_4(Tp^*)_2]$ (**39**)	63.1	118.7	2004, 1916[a]
$[W_2\{\mu\text{-}(CAuCl)_2PPhAuCl\}(CO)_4(Tp^*)_2]$ (**40**)	75.7	88.8	2029, 1951

NMR spectra were recorded in $CDCl_3$. IR spectra were recorded in CH_2Cl_2. [a] Tentative assignment as the spectrum also contains bands due to **38** and **40**.

As the infrared timescale is fast, we would expect that the number of carbonyl absorption bands in the IR spectrum should be diagnostic of a symmetric or an asymmetric structure. Because a clean sample of **39** could not be obtained, tentative assignments were made at 2004 and 1916 cm^{-1} (CH_2Cl_2) of a solution also containing **40** and small quantities of **38**. Thus the possibility that additional ν_{CO} bands were masked by the bands of **40** or **38** could not be excluded. Furthermore, as indicated above for the complexes $[W_2(\mu\text{-}C_2PR)(CO)_4(Tp^*)_2]$, the CO oscillators on adjacent tungsten centres may couple, affecting both the frequencies and relative intensities of different modes. The inability to obtain a clean sample of **39** meant that the ^1H NMR spectrum could not be utilised to deduce structural information.

Based on the $^{31}P\{^1H\}$ NMR spectra, scrambling of the three species does occur to a small extent. A mixture containing 16.6% **38**, 47.8% **39** and 35.6% **40** was found to contain the three species in 23.5%, 39.9% and 36.6%, respectively, after 22 hours in $CDCl_3$ at room temperature. The inability to obtain a clean sample of **39** is thus likely hampered by the conversion of **39** to **38** and **40** over time.

The absence of peaks attributable to the asymmetric W_2Au_2 complex $[W_2\{\mu{:}\eta^1\text{-}C;\eta^2\text{-}C,Au\text{-}CP(Ph)(AuCl)C(AuCl)\}(CO)_4(Tp^*)_2]$ or the asymmetric W_2Au_1 complex $[W_2(\mu{:}\eta^1\text{-}C;\eta^2\text{-}C,Au\text{-}CP(Ph)C(AuCl)\}(CO)_4(Tp^*)_2]$ suggests that coordination of AuCl

to one W≡C group affects the donor strength of the remaining ligation sites. In order to form the eventual product **40** these complexes must form, but are perhaps too short lived to be observed (Scheme 5.9). Notably, free **33** is not detected in the reaction after addition of [AuCl(SMe$_2$)].

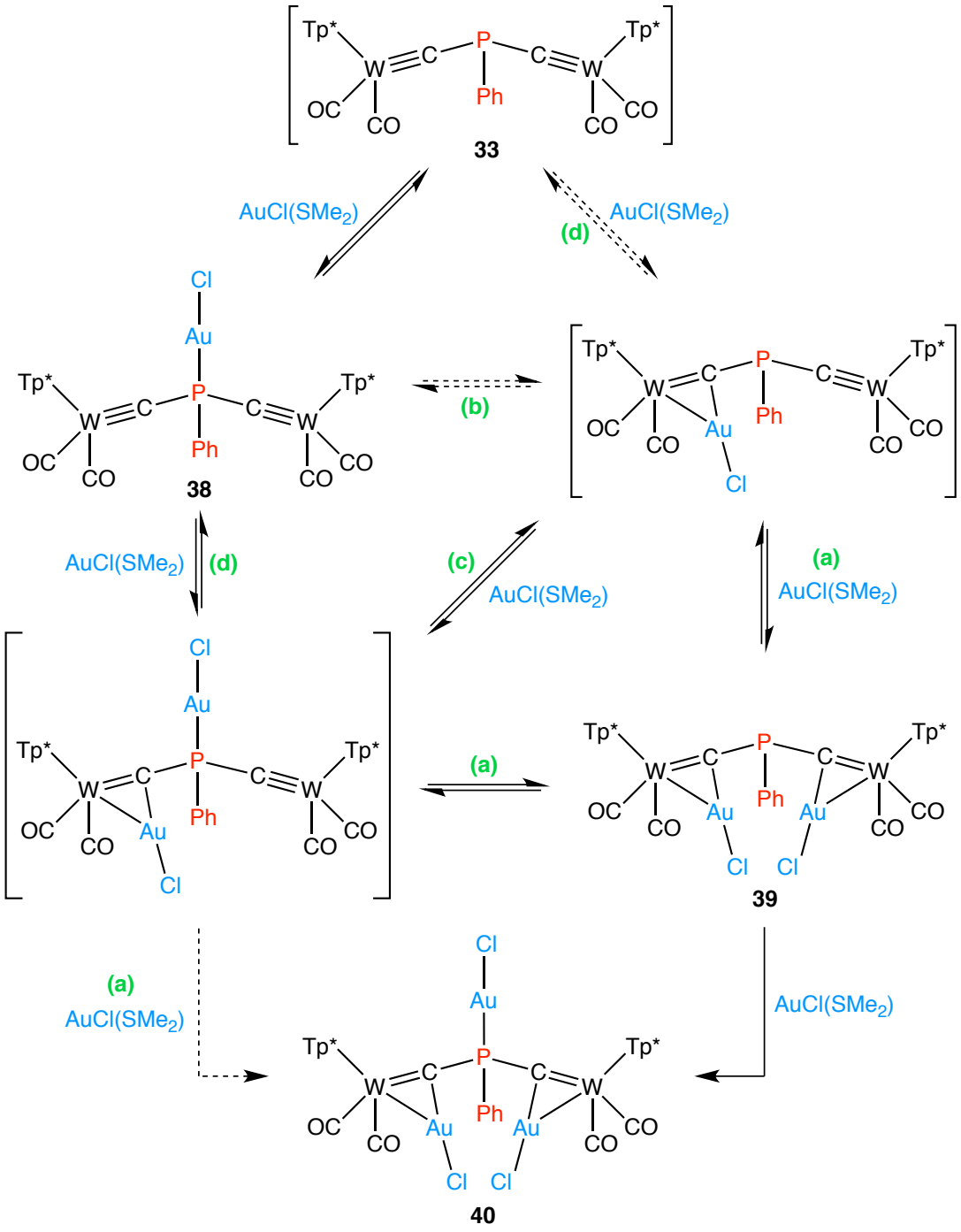

Scheme 5.9. Sequence of AuCl addition to **33**. Complexes depicted in brackets are not detected in the reaction.

There are a number of plausible pathways through which we can rationalise these observations (Scheme 5.9):
(a) complexation of AuCl to W≡C increases the nucleophilicity of the second W≡C bond such that migration or coordination of an AuCl group occurs to give the symmetric complexes;
(b) complexation of AuCl to W≡C increases the nucleophilicity of the phosphorus such that migration of AuCl to phosphorus occurs;
(c) complexation of AuCl to W≡C decreases the nucleophilicity of the phosphorus such that dissociation of the P-coordinated AuCl occurs;
(d) W≡C is not sufficiently nucleophilic and only weakly coordinates AuCl, which subsequently dissociates.

The most plausible explanation would appear to be (c). In the free phosphine **33** the phosphorus is clearly the most nucleophilic site as established by the formation of the 1:1 adduct **38** in which AuCl is bound to phosphorus. Coordination of a second AuCl to one W≡C bond electronically reduces the nucleophilicity of the phosphorus, as well as introducing a degree of proximal steric congestion, which is relieved when the AuCl originally bound to phosphorus migrates (or dissociate/recoordinates) to the second W≡C bond. The observation of an aurophilic interaction in the tris-AuCl adduct **40** points towards a similar interaction being present in the symmetrical bis-AuCl adduct, whilst such an interaction would be precluded for the asymmetrical bis-AuCl adduct, as indicated by the geometry adopted by the complex [W{η^2-C(AuCl)PPh_2AuCl}$(CO)_2$(Tp*)]. Aurophilic interactions have been suggested to span the range 25 – 50 kJ/mol and accordingly could be expected to play a role here.[428] Finally, addition of the third AuCl group to the revealed phosphine occurs in the last step.

In the monometallic complex [W(≡CPPh_2)$(CO)_2$(Tp*)] (**2**), electrophilic addition to the phosphine was found to decrease the nucleophilicity of the W≡C bond, consistent with pathway (d). It appears that in **33** the nucleophilicities of the three competing sites are also linked, wherein complexation to one site alters the nucleophilicity of the other two sites, but in a more complex manner than in **2**, potentially due to the additional driving force of aurophilic interactions.

5.3 Synthesis of a trimetallic phosphinocarbyne complex [$W_3(\mu$-$C_3P)(CO)_6(Tp^*)_3$]

Attempts to extend the lithiocarbyne protocol to the synthesis of a trimetallic, triscarbyne-substituted phosphine were somewhat inconclusive. Treating a THF solution of **1** with ^{n}butyllithium and 0.3 equivalents of trichlorophosphine generated a brown solution, the infrared spectrum of which contained carbonyl bands at 1981, 1970 and 1889 cm^{-1} suggestive of formation of the desired product [$W_3(\mu$-$C_3P)(CO)_6(Tp^*)_3$] (**41**) (Scheme 5.10). The $^{31}P\{^1H\}$ NMR spectrum of the crude product contained a singlet at δ_P 70.1 with tungsten-183 satellites ($^2J_{WP}$ 68.6 Hz). The ^1H NMR spectrum indicated a 2:1 ratio of pyazolyl environments, consistent with formulation of the desired product.

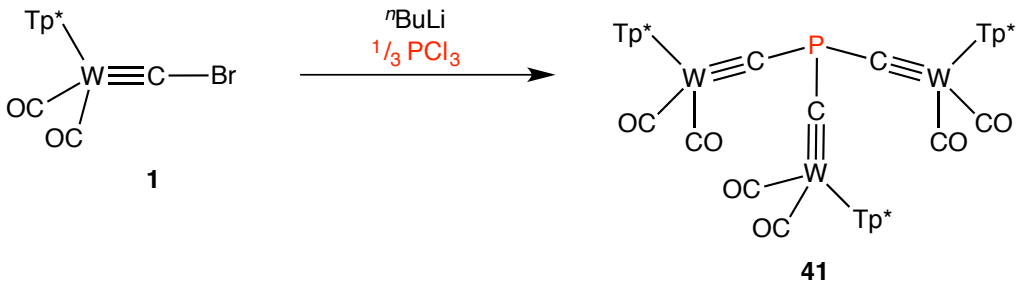

Scheme 5.10. Synthesis of [$W_3(\mu$-$C_3P)(CO)_6(Tp^*)_3$] (**41**).

The complex **41** was not as stable as expected towards chromatographic purification considering the absence of reactive bonds within the molecule (e.g. P–Cl, P–O), whereas previous results have shown that P–C(carbyne) bonds are stable towards chromatography. Two-dimensional thin layer chromatography of crude **41** indicated that decomposition occurred, which is perhaps due to the steric strain of having three [$W(\equiv C)(CO)_2(Tp^*)$] moieties surrounding the phosphorus atom. The ESI(+) mass spectrum of **41** in acetonitrile did not contain any peaks that were identified as belonging to [$W_3(\mu$-$C_3P)(CO)_6(Tp^*)_3$], or fragments or adducts thereof. This might indicate that the isolated product is not the anticipated [$W_3(\mu$-$C_3P)(CO)_6(Tp^*)_3$] complex. Alternatively, the isolated product could be the trimetallic complex but the stability is insufficient to survive the ESI mass spectrometry conditions. This would not be an unreasonable conclusion to draw given the extreme steric requirements of having three bulky [$W(C)(CO)_2(Tp^*)$] fragments surrounding a single phosphorus atom, as illustrated in Figure 5.9. If steric congestion was the destabilising factor, then it may

follow that if the type of rearrangement observed for $[W_2(\mu\text{-}C_2PR)(CO)_4(Tp^*)_2]$ (R = Cl, Ph) to the phosphirenes $[W_2\{\mu:\eta^1\text{-}C;\eta^2\text{-}C,P\text{-}CC(PR)\}(CO)_4(Tp^*)_2]$ were to occur for $[W_3(\mu\text{-}C_3P)(CO)_6(Tp^*)_3]$, this might well alleviate unfavourable intramolecular interactions.

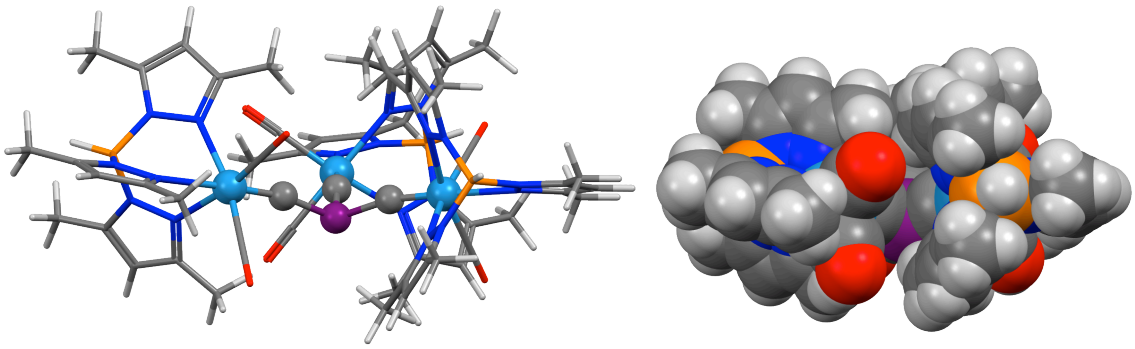

Figure 5.9. Calculated[†] molecular geometry (left) and space-filling representation (right) of **41**. Colours: W light blue, P purple, C grey, N blue, O red, B orange, H white.

In order to substantiate the formulation of **41**, a series of phosphines with varying degrees of carbyne-substitution at the phosphorus were considered, as presented in Table 5.2. Comparing the phosphorus chemical shifts in the series PCl_3 to **41** shows an upfield shift with increasing numbers of carbyne substituents at the phosphorus. However, comparing the δ_P data for the series PPh_3 to **41** indicates a downfield shift with inclusion of one and then two carbyne substituents, but **41** does not conform to this trend, lying upfield of the bis-substituted complex $[W_2(\mu\text{-}C_2PPh)(CO)_4(Tp^*)_2]$. Comparing the infrared data shows that the carbonyl absorptions shift to lower frequency in the chloro-substituted series with increasing numbers of carbyne substituents, again substantiating the formulation of **41** as the trimetallic complex. Significant shifts in the carbonyl absorption stretches are not observed for the phenyl derivatives.

[†] Calculated using Spartan 14 at the semi-empirical PM3 level of theory to qualitatively illustrate the molecular topology of **41**.

Table 5.2. Selected spectroscopic data for mono-, bi- and trimetallic phosphinocarbyne complexes and the relevant free phosphines.

Compound	δ_P	$^2J_{WP}$ (Hz)	ν_{CO} (cm^{-1})
PCl_3	219.9	-	-
$[W(\equiv CPCl_2)(CO)_2(Tp^*)]$ (**17**)	136.2	80.5	2005, 1920
$[W_2(\mu\text{-}C_2PCl)(CO)_4(Tp^*)_2]$ (**35**)	124.9	66.4	1996, 1986, 1906
$[W_3(\mu\text{-}C_3P)(CO)_6(Tp^*)_3]$ (**41**)	71.6	69.7	1981, 1970, 1889
$[W_2(\mu\text{-}C_2PPh)(CO)_4(Tp^*)_2]$ (**33**)	80.4	76.2	1984, 1974, 1892
$[W(\equiv CPPh_2)(CO)_2(Tp^*)]$ (**2**)	32.2	66.2	1981, 1893
PPh_3[429]	−4.7	-	-

NMR spectra were recorded in C_6D_6. IR spectra were recorded in THF.

While most data obtained are strongly suggestive of the formulation of **41** as the trimetallic phosphine $[W_3(\mu\text{-}C_3P)(CO)_6(Tp^*)_3]$, unfortunately this assignment cannot be definitively confirmed without further evidence.

5.4 Summary

The synthetic routes to mononuclear phosphinocarbyne complexes developed in the previous chapters are applicable to the syntheses of bimetallic phosphinocarbyne complexes bearing halo, alkyl or aryl substituents, as depicted in Scheme 5.11. Attempts to extend this to amino-functionalised phosphines were unsuccessful, yielding either the mono-substitution product $[W\{\equiv CPCl(NR_2)\}(CO)_2(Tp^*)]$ or a mixture of compounds. These bimetallic phosphinocarbynes were found to undergo a thermal rearrangement to give the unprecedented carbyne-metallaphosphirene complexes $[W_2\{\mu:\eta^1\text{-}C;\eta^2\text{-}C,P\text{-}CC(PR)\}(CO)_4(Tp^*)_2]$. Using a 3:1 stoichiometry of the lithiocarbyne:trichlorophosphine appears to form the somewhat unstable trimeric complex $[W_3(\mu\text{-}C_3P)(CO)_6(Tp^*)_3]$.

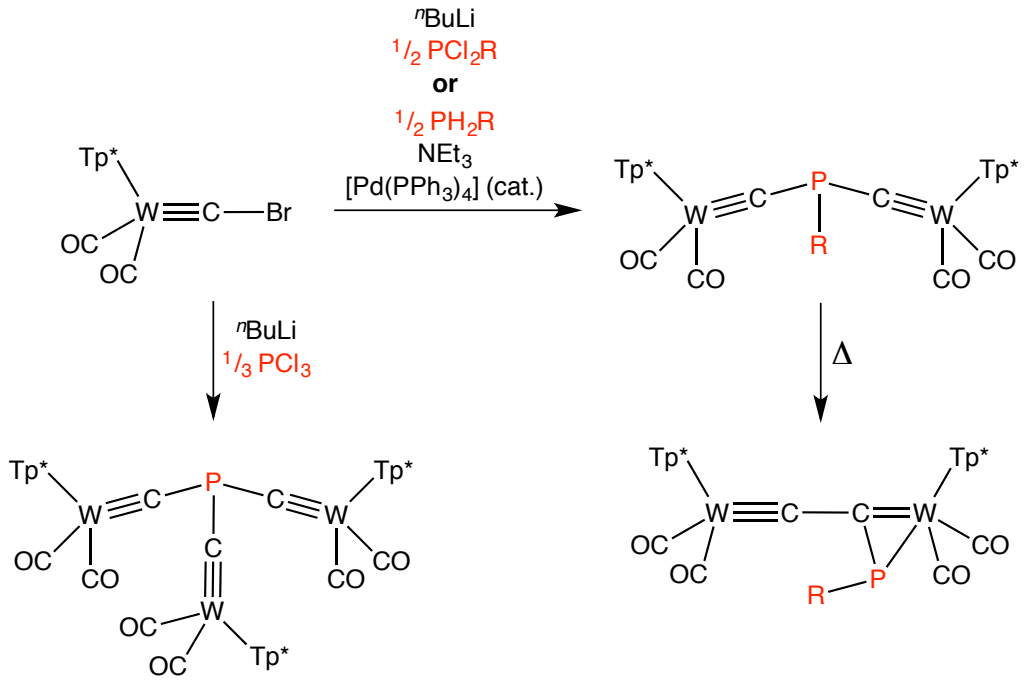

Scheme 5.11. Syntheses of bi- and trimetallic phosphinocarbyne complexes.

While electrophilic addition to the monometallic complex $[W(\equiv CPPh_2)(CO)_2(Tp^*)]$ was found to occur preferentially at the phosphine, in the bimetallic complex $[W_2(\mu\text{-}C_2PPh)(CO)_4(Tp^*)_2]$ the W≡C bond competes effectively with the phosphine as the preferred site for electrophilic attack. Reactions with $[AuCl(SMe_2)]$ resulted in mixtures of products of both P-coordination and carbyne-coordination (Scheme 5.12), although unambiguous characterisation of the di-aurated complex could not be obtained. Addition of excess $[AuCl(SMe_2)]$ pushes the reaction all the way to the pentametallic

complex $[W_2\{\mu\text{-}(\eta^2\text{-}CAuCl)_2PPhAuCl\}(CO)_4(Tp^*)_2]$, the crystal structure of which demonstrates the presence of aurophilic bonding between the two carbyne-bound gold atoms.

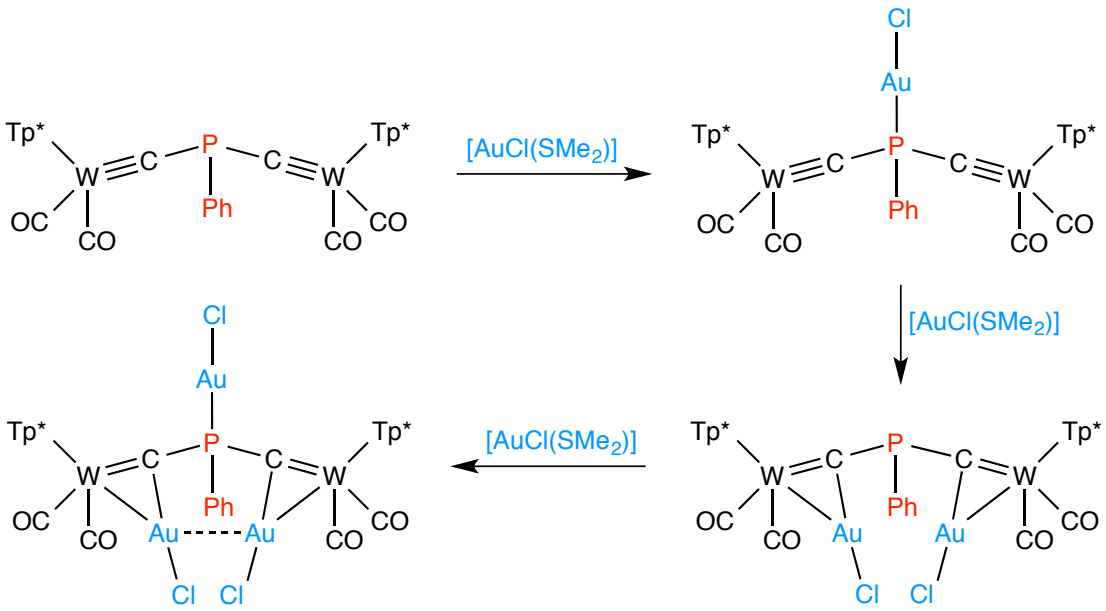

Scheme 5.12. Electrophilic addition of $[AuCl(SMe_2)]$ to $[W_2(\mu\text{-}C_2PPh)(CO)_4(Tp^*)_2]$.

CHAPTER 6.
Conclusions

CHAPTER 6: Conclusions

A library of new phosphinocarbyne complexes has been prepared, including the first syntheses of terminal secondary phosphinocarbynes. The development of two general strategies has provided access to a range of phosphinocarbyne complexes bearing alkyl, aryl, amino, halo and hydro substituents. The utility of these synthetic strategies has been exemplified by extension to the synthesis of bi- and trimetallic phosphinocarbyne complexes, the existence of which was previously unknown. The $[W(CO)_2(Tp^*)]$ moiety has been shown to be a robust and versatile functional group, found to be chemically inert in all experiments undertaken, enabling targeted reactivity at the carbyne and phosphorus centres.

Reactions of tungsten phosphinocarbyne complexes with electrophiles, nucleophiles, acids and bases demonstrate the versatility of these complexes as synthetic precursors. In the monometallic complex $[W(\equiv CPPh_2)(CO)_2(Tp^*)]$ the phosphorus was found to be the most nucleophilic site, although in some cases reactivity at the carbyne carbon atom or the tungsten-carbon bond was observed. Replacement of hydro, halo and amino substituents at phosphorus has delivered further-functionalised complexes, including the salts $[W\{\equiv CP(N^iPr_2)\}(CO)_2(Tp^*)]^+$ and $[W(CPR)(CO)_2(Tp^*)]^-$, which feature, respectively, electrophilic or nucleophilic two-coordinate phosphorus centres. The latter of these has been shown spectroscopically and crystallographically to possess significant phosphaisocyanide character and represents the first example of a terminal phosphaisocyanide complex. The reactivity of the bimetallic phosphinocarbyne complexes differs from what was seen in the monometallic examples, highlighted by the novel thermal rearrangement to the bridging carbyne-tungstaphosphirene complexes $[W_2\{\mu{:}\eta^1\text{-}C;\eta^2\text{-}C,P\text{-}CC(PR)\}(CO)_4(Tp^*)_2]$. Together, these results establish both the viability and the versatility of a wide range of novel unsaturated 'C_1' organophosphorus ligand classes.

Looking forward from this point, the future of C_1P_1 coordination chemistry appears bright. This work has demonstrated that, in many cases, conventional organophosphorus chemistry is applicable to organometallic systems, and the late-stage functionalisation of such systems highlights their value in the broader chemical world. There are several areas stemming from this work that offer significant potential, and some future visions for this chemistry are presented here.

Of particular importance is extension of the preliminary results obtained with regard to the synthesis of carbyne complexes bearing two-coordinate phosphorus moieties. Ideally this could lead to the isolation of phosphenium cations such as $[W\{\equiv CP(N^{i}Pr_2)\}(CO)_2(Tp^*)]^+$, which are especially interesting in comparison to the phosphaisocyanide anions $[W(CPR)(CO)_2(Tp^*)]^-$. The conceptually simple preparative route used to access terminal phosphaisocyanide complexes – involving palladium-catalysed phosphination followed by deprotonation – is likely to be applicable to other systems, and hence elaboration of this methodology could enable preparation of a range of phosphaisocyanide complexes.

Most of the research described in this thesis was conducted using mononuclear carbyne complexes. However, Chapter 5 details studies of the synthesis and reactivity of bis- and triscarbynyl complexes. What is particularly interesting here is that these species were found to possess both similarities (e.g. the synthesis of $[W_2(\mu\text{-}C_2PPh)(CO)_4(Tp^*)_2]$ and its tri-auration) and differences (e.g. the failed synthesis of $[W_2\{\mu\text{-}C_2P(NR_2)\}(CO)_4(Tp^*)_2]$, and the thermal rearrangement and partial auration of $[W_2(\mu\text{-}C_2PPh)(CO)_4(Tp^*)_2]$) to the mononuclear chemistry. In light of these findings, further explorations into such chemistry are expected to yield additional intriguing and potentially unpredictable outcomes.

Although the results presented herein demonstrate that considerable variability is feasible in terms of the nature of the phosphorus substituent, an obvious limitation is that all of this work is restricted to the use of '$W(CO)_2(Tp^*)$' as the metal and co-ligand set. Unfortunately, this is an artefact of the dearth of preparative routes to carbyne complexes bearing halide (or pseudohalide) substituents. However, the outlook is not so bleak since, in the case of phosphorus installation via nucleophilic substitution of halophosphines, this protocol can be applied to other anionic carbynes prepared, for example, by deprotonation of methylidyne complexes (e.g. Cummins' precursor to phosphinocarbynes $[Mo(\equiv CH)\{N^{t}Bu(3,5\text{-}C_6H_3Me_2)\}_3]_2)$[40,41] or fluoride-mediated desilylation of silylcarbynes (e.g. Templeton's $[Mo(\equiv CSiMe_2Ph)(CO)_2(Tp^*)]$).[65] Despite this, for this field to flourish in the future access to a broader array of suitable precursors is essential.

Of interest to the broader research community is the fact that much of the methodology presented in this thesis should be applicable to carbene complexes and more exotic $MC_1P_1R_n$ systems, which could greatly enhance the scope of this work. Since much of the chemistry presented in this thesis is general in nature, it is anticipated that these ideas may contribute to many fertile areas of research in the future.

CHAPTER 7.
Experimental

CHAPTER 7: Experimental

General considerations

Unless otherwise stated, experimental work involving metal complexes was carried out at room temperature under a dry and oxygen-free nitrogen atmosphere using standard Schlenk, vacuum line and inert atmosphere (argon) drybox techniques with dried and degassed solvents. Solvents were dried over sodium/benzophenone (benzene, diethyl ether, dimethoxyethane, hexane, pentane, tetrahydrofuran, toluene) or calcium hydride (acetonitrile, chloroform, dichloromethane) and distilled under N_2. Chromatography was carried out using silica gel (40 − 63 μm) or neutral alumina (activity I, 63 − 200 μm) as specified and degassed where required. Compounds containing four-coordinate phosphorus were generally air stable once isolated, excluding complexes [**5**]BF_4, [**6**]BF_4 and [**26**]$AlCl_4$.

NMR spectra were obtained at 25°C on Varian Mercury 300 (^{1}H at 300.1 MHz, ^{13}C at 75.47 MHz, ^{31}P at 121.5 MHz), Varian Inova 300 (^{1}H at 299.9 MHz, ^{11}B at 96.23 MHz, ^{13}C at 75.42 MHz, ^{31}P at 121.4 MHz), Varian MR 400 (^{1}H at 399.9 MHz, ^{13}C at 100.5 MHz, ^{31}P at 161.9 MHz), Bruker Avance 400 (^{1}H at 400.1 MHz, ^{31}P at 162.0 MHz), Varian Inova 500 (^{1}H at 500.0 MHz, ^{13}C at 125.7 MHz), Bruker Avance 600 (^{1}H at 600.0 MHz, ^{13}C at 150.9 MHz) or Bruker Avance 800 (^{1}H at 800.1 MHz, ^{13}C at 201.2 MHz) spectrometers. Chemical shifts (δ) are reported in ppm and referenced to the residual protonated solvent peak (^{1}H, ^{13}C), external 85% H_3PO_4 (^{31}P) or external $BF_3{\cdot}Et_2O$ (^{11}B) with coupling constants given in Hz. The multiplicities of NMR resonances are denoted by the abbreviations s (singlet), d (doublet), t (triplet), m (multiplet), br (broad) and combinations thereof for more highly coupled systems. Where applicable, the stated multiplicity refers to that of the primary resonance exclusive of ^{183}W satellites. Whilst $^{13}C\{^1H\}$ signals for carbon nuclei of PPh and PCy groups could be routinely observed, their narrow spectral range and comparable J_{PC} values often precluded unequivocal assignment, in which case they are designated as '$C^{2,3,5,6}$(PPh)' or '$C^{2,3,5,6}$(Cy)'. In some cases, distinct peaks were observed in the ^{1}H and $^{13}C\{^1H\}$ NMR spectra, but to the level of accuracy that is reportable (i.e. 2 decimal places for ^{1}H NMR, 1 decimal place for ^{13}C NMR) they are reported as having the same chemical shift.

Infrared spectra were obtained using a Perkin-Elmer Spectrum One FT-IR spectrometer. The strengths of IR absorptions are denoted by the abbreviations vs (very strong), s (strong), m (medium), w (weak), sh (shoulder) and br (broad). Elemental microanalytical data were obtained from the ANU Research School of Chemistry microanalytical service. Electrospray ionisation mass spectrometry (ESI-MS) was performed by the ANU Research School of Chemistry mass spectrometry service with acetonitrile as the matrix. For compounds containing P−Cl functionalities no interpretable mass spectrometry data was obtained due to the hydrolytic sensitivity of the P−Cl bond. Data for X-ray crystallography were collected with a Nonius Kappa CCD, Agilent Xcalibur CCD or Agilent SuperNova CCD diffractometer and structures solved with the assistance of Dr Tony Willis and Mr Jas Ward, whose help is gratefully acknowledged.

The following compounds were prepared according to published procedures: KTp*,[430] [AuCl(L)] (L = SMe_2, THT),[431] $[Cp^*RhCl_2]_2$,[432] KOPh,[336] LiCCPh[433,434] and $[Pd(PPh_3)_4]$.[435] All other reagents were obtained from commercial sources and purified as required.

Synthesis of [W(≡CBr)(CO)$_2$(Tp*)] (1)

Synthesised using a modification of the literature procedure.[196]

A suspension of $[W(CO)_6]$ (20.80 g, 58.11 mmol) and KTp* (24.70 g, 73.45 mmol) in 1,2−dimethoxyethane (150 mL) was heated to reflux under N_2. After five days the reaction mixture was allowed to cool and concentrated under reduced pressure to ca. 100 mL. Bromoform (12 mL, 137 mmol) was added and the reaction mixture was treated with freshly prepared $[MesN_2]BF_4$ (synthesised as per below and used when damp, 17.515 g) in portions resulting in heat and gas evolution. The brown suspension was then connected to N_2 with an oil bubbler to allow effluent gases to escape and stirred overnight. The solvent was removed under reduced pressure (accompanied by sublimation of residual $[W(CO)_6]$ in the cold trap). The brown residue was dissolved in CH_2Cl_2 and filtered to remove the insoluble material and the solvent was removed on the rotary evaporator. The residue was chromatographed (silica gel) using petroleum spirits (40-60) as the eluent and gradually increasing to 6:1 petroleum spirits:CH_2Cl_2. The initial colourless fraction containing residual $[W(CO)_6]$ was discarded. The first yellow band was collected and the solvent removed on the rotary evaporator to afford **1**

as a yellow powder. Yield 10.127 g (16.101 mmol, 28% from $W(CO)_6$). Spectroscopic data conform to those previously reported.[55]

Note: Commercially available $CHBr_3$ contains EtOH as a stabiliser to prevent radical reactions. The $CHBr_3$ was purified by washing with H_2O (5 × 15 mL) to remove the EtOH, then dried over $MgSO_4$ and used without distillation or degassing.

Mesityldiazonium tetrafluoroborate $[MesN_2]BF_4$

To a 2 L conical flask containing $MesNH_2$ (30.0 mL, 214 mmol) was added HCl (37%, 89 mL, 1.1 mol) in H_2O (400 mL) with stirring to provide a yellow suspension. The reaction mixture was cooled to 0°C and treated with $NaNO_2$ (14.75 g, 213.8 mmol) in the minimum H_2O (40 mL) resulting in a slightly cloudy yellow solution. $NaBF_4$ (23.48 g, 213.9 mmol) in the minimum H_2O (50 mL) was added to provide a white precipitate. The suspension was stirred at 0°C for 40 minutes then the white precipitate was collected by filtration and washed with Et_2O and dried under vacuum. Damp weight 40.19 g. Caution! Diazonium salts are potentially explosive when dry! The use of metal spatulas is discouraged. The isolated $[MesN_2]BF_4$ can be used while still damp for the synthesis of $[W(\equiv CBr)(CO)_2(Tp^*)]$.

CHAPTER 2. Tertiary phosphinocarbyne complexes

Synthesis of [W(≡CPPh$_2$)(CO)$_2$(Tp*)] (2)

Synthesised according to the literature procedure for [Mo(≡CPPh$_2$)(CO)$_2$(Tp*)].[54]

A solution of [W(≡CBr)(CO)$_2$(Tp*)] (5.001 g, 7.951 mmol) in THF (100 mL) was cooled to –78°C in a dry ice/acetone bath and treated with ^{n}BuLi (4.7 mL, 1.7 M in hexanes, 8.0 mmol). The resulting light brown solution was stirred for 45 minutes and then treated with PClPh$_2$ (1.45 mL, 8.08 mmol). The solution instantly turned dark red and was left in the dry ice/acetone bath to warm to room temperature overnight. The solvent was removed on the rotary evaporator and the residue was chromatographed on silica gel using CH_2Cl_2 as the eluent. The first orange band (containing the product) was collected. Ethanol was added and the solution was concentrated on the rotary evaporator to afford **2** as an orange powder which was isolated by filtration. Crystals suitable for crystallographic analysis were obtained by slow diffusion of ^{n}hexane into a solution of **2** in CH_2Cl_2. Yield 5.228 g (7.120 mmol, 90%). IR (Nujol) ν/cm^{-1}: 2548 w (BH), 2001 m, 1974 s, 1957 w, 1912 m, 1883 s, 1858 w (CO). IR (CH_2Cl_2) ν/cm^{-1}: 2554 w (BH), 1982 vs, 1891 vs (CO). IR (THF) ν/cm^{-1}: 2550 w (BH), 2000 w, 1981 s, 1914 w, 1893 vs (CO). ^{1}H NMR ($CDCl_3$) δ/ppm: 7.62 – 7.56 (m, 4 H, C_6H_5), 7.36 – 7.31 (m, 6 H, C_6H_5), 5.85 (s, 2 H, pzH), 5.74 (s, 1 H, pzH), 2.38 (s, 3 H, pzCH_3), 2.37 (s, 6 H, pzCH_3), 2.31 (s, 3 H, pzCH_3), 2.26 (s, 6 H, pzCH_3). ^{13}C{^{1}H} NMR ($CDCl_3$) δ/ppm: 292.6 (d, W≡C, $^1J_{PC}$ = 74.5, $^1J_{WC}$ = 187.9), 225.3 (CO, $^1J_{WC}$ = 168.9), 152.6 (1 C), 152.2 (2 C), 145.3 (1 C), 144.6 (2 C) [C^{3,5}(pz)], 136.5 [d, C^1(C_6H_5), $^1J_{PC}$ = 9.4], 133.5 [d, C^{2,3,5,6}(C_6H_5), J_{PC} = 19.7], 128.6 [C^4(C_6H_5)], 128.5 [d, C^{2,3,5,6}(C_6H_5), J_{PC} = 7.2], 106.8 (1 C), 106.6 (2 C) [C^4(pz)], 16.6 (2 C), 15.3 (1 C), 12.9 (2 C), 12.7 (1 C) (pzCH_3). ^{31}P{^{1}H} NMR ($CDCl_3$) δ/ppm: 32.0 ($^2J_{WP}$ = 69.0). MS-ESI(+): *m/z* 734.7 [M]$^+$, 619.8 [M – 2CO + MeCN]$^+$, 679.5 [M – 2CO + H]$^+$. Accurate mass: found 735.2006 [M + H]$^+$. Calcd. for $C_{30}H_{33}{}^{11}BN_6O_2P^{184}W$: 735.2005. Anal. found: C, 48.48; H, 4.65; N, 11.42%. Calcd. for $C_{30}H_{32}BN_6O_2PW$: C, 49.07; H, 4.39; N, 11.45%. Crystal data for $C_{30}H_{32}BN_6O_2PW$: M_w = 734.26, triclinic, *P*−1 (No. 2), *a* = 8.1714(1) Å, *b* = 10.1587(1) Å, *c* = 18.9544(2) Å, *α* = 76.1227(8)°, *β* = 87.1138(8)°, *γ* = 81.0287(7)°, *V* = 1508.67(3) Å^3, *Z* = 2, ρ_{calcd} = 1.616 Mg m^{-3}, *μ*(Mo Kα) = 3.92 mm^{-1}, *T* = 200(2) K, orange plate, 0.23 × 0.14 × 0.05 mm, 8792 independent reflections. F^2 refinement, *R* = 0.025, *wR* = 0.055 for 7926 reflections ($I > 2\sigma(I)$, $2\theta_{max}$ = 60°), 371 parameters.

Synthesis of [W(≡CPMePh$_2$)(CO)$_2$(Tp*)]I ([3]I)

Methyl iodide (7 drops, excess) was added to a solution of [W(≡CPPh$_2$)(CO)$_2$(Tp*)] (0.300 g, 0.409 mmol) in CH_2Cl_2 (20 mL) and stirred for three days. The orange solution gradually became red and IR monitoring showed the formation of the product. The solution was filtered through diatomaceous earth and then chromatographed on neutral alumina using 2:1 CH_2Cl_2:MeCN as the eluent. The bright pink band was collected and the solvent removed by rotary evaporation affording the product as a red solid. Yield 0.268 g (0.306 mmol, 75%). IR (Nujol) ν/cm^{-1}: 2556 w (BH), 2015 s, 1925 s (CO). IR (CH_2Cl_2) ν/cm^{-1}: 2560 w (BH), 2022 s, 1937 vs (CO). IR (THF) ν/cm^{-1}: 2557 w (BH), 2018 vs, 1932 vs (CO). ^{1}H NMR ($CDCl_3$) δ/ppm: 7.90 – 7.83 (m, 4 H, C_6H_5), 7.77 – 7.73 (m, 2 H, C_6H_5), 7.69 – 7.62 (m, 4 H, C_6H_5), 6.00 (s, 2 H, pzH), 5.82 (s, 1 H, pzH), 2.79 (d, 3 H, PCH_3, $^2J_{PH}$ = 12.9), 2.41 (s, 6 H, $pzCH_3$), 2.35 (s, 3 H, $pzCH_3$), 2.31 (s, 3 H, $pzCH_3$), 2.18 (s, 6 H, $pzCH_3$). ^{13}C{^{1}H} NMR ($CDCl_3$) δ/ppm: 242.8 (W≡C, $^1J_{WC}$ = 206.2), 221.8 (d, CO, $^3J_{PC}$ = 2.8, $^1J_{WC}$ = 158.3), 152.1 (1 C), 150.2 (2 C), 146.1 (1 C), 145.3 (2 C) [C^{3,5}(pz)], 133.8 [d, C^4(C_6H_5), $^4J_{PC}$ = 1.9], 131.4 [d, C^{2,3,5,6}(C_6H_5), J_{PC} = 11.1], 129.4 [d, C^{2,3,5,6}(C_6H_5), J_{PC} = 12.8], 120.1 [d, C^1(C_6H_5), $^1J_{PC}$ = 89.3], 107.1 (1 C), 106.6 (2 C) [C^4(pz)], 16.0 (2 C), 14.4 (1 C), 12.0 (1 C), 11.9 (2 C) ($pzCH_3$), 11.1 (d, PCH_3, $^1J_{PC}$ = 57.0). ^{31}P{^{1}H} NMR ($CDCl_3$) δ/ppm: 12.2 ($^2J_{WP}$ = 161.6). MS-ESI(+): *m/z* 762.6 [M + MeCN – CO – I]$^+$, 749.5 [M – I]$^+$, 721.5 [M – CO – I]$^+$, 693.6 [M – 2CO – I]$^+$. Accurate mass: found 749.2168 [M – I]$^+$. Calcd. for $C_{31}H_{35}{}^{11}BN_6O_2P^{184}W$: 749.2162. Anal. found: C, 42.28; H, 4.20; N, 9.63%. Calcd. for $C_{31}H_{35}BIN_6O_2PW$: C, 42.49; H, 4.03; N, 9.59%.

Synthesis of [W(≡CPPh$_2$BH$_3$)(CO)$_2$(Tp*)] (4)

$BH_3{\cdot}SMe_2$ (0.05 mL, 0.5 mmol) was added to a solution of [W(≡CPPh$_2$)(CO)$_2$(Tp*)] (0.300 g, 0.409 mmol) in toluene (10 mL) and the reaction mixture was stirred overnight. The brown suspension was allowed to settle and the solution was filtered off. The precipitate was washed with 2 × 2mL toluene and the washings were combined with the filtrate. The solution was filtered through diatomaceous earth and the solvent removed under reduced pressure. The residue was triturated in Et_2O to provide the product as a brown powder, which was collected by vacuum filtration. Crystals suitable for crystallographic analysis were obtained by slow diffusion of ^{n}hexane into a solution of **4** in $CHCl_3$. Yield 0.178 g (0.238 mmol, 58%). IR (Nujol) ν/cm^{-1}: 2557 w (pzBH), 2359 m, br (BH_3), 2001 s, 1911 s (CO). IR (CH_2Cl_2) ν/cm^{-1}: 2556 w (pzBH), 2359 m,

br (BH_3), 2003 s, 1915 s (CO). IR (THF) ν/cm^{-1}: 2552 w (pzBH), 2375 m, br (BH_3), 2003 s, 1916 s (CO). ^{1}H NMR ($CDCl_3$) δ/ppm: 7.84 – 7.77 (m, 4 H, C_6H_5), 7.47 – 7.41 (m, 6 H, C_6H_5), 5.89 (s, 2 H, pzH), 5.76 (s, 1 H, pzH), 2.38 (s, 9 H, $pzCH_3$), 2.31 (s, 3 H, $pzCH_3$), 2.23 (s, 6 H, $pzCH_3$). $^{13}C\{^1H\}$ NMR ($CDCl_3$) δ/ppm: 271.2 (d, W≡C, $^1J_{PC}$ = 21.1, $^1J_{WC}$ = 199.2), 224.2 (CO, $^1J_{WC}$ = 164.5), 152.8 (1 C), 152.1 (2 C), 145.6 (1 C), 145.0 (2 C) [$C^{3,5}$(pz)], 132.8 [d, $C^{2,3,5,6}(C_6H_5)$, J_{PC} = 10.6], 130.8 [$C^4(C_6H_5)$], 130.3 [d, $C^1(C_6H_5)$, $^1J_{PC}$ = 57.3], 128.6 [d, $C^{2,3,5,6}(C_6H_5)$, J_{PC} = 10.6], 107.2 (1 C), 106.8 (2 C) [C^4(pz)], 16.9 (2 C), 15.2 (1 C), 12.8 (2 C), 12.7 (1 C) ($pzCH_3$). $^{31}P\{^1H\}$ NMR ($CDCl_3$) δ/ppm: 32.0 (br). $^{11}B\{^1H\}$ NMR ($CDCl_3$) δ/ppm: −10.1 (Tp*), −37.8 (BH_3). MS-ESI(+): *m/z* 789.9 $[M + MeCN + H]^+$, 770.8 $[M + Na]^+$, 749.4 $[M + H]^+$, 735.3 $[M - BH_2]^+$. Accurate mass: found 790.2601 $[M + MeCN + H]^+$. Calcd. for $C_{32}H_{39}{}^{11}B_2N_7O_2P^{184}W$: 790.2599. Found 771.2151 $[M + Na]^+$. Calcd. for $C_{30}H_{35}{}^{11}B_2N_6O_2NaP^{184}W$: 771.2152. Anal. found: C, 47.88; H, 4.68; N, 11.35%. Calcd. for $C_{30}H_{35}B_2N_6O_2PW$: C, 48.17; H, 4.72; N, 11.23%. Crystal data for $C_{30}H_{35}B_2N_6O_2PW{\cdot}CHCl_3$: M_w = 867.47, triclinic, *P*−1 (No. 2), *a* = 10.2173(2) Å, *b* = 10.4412(2) Å, *c* = 17.5622(3) Å, *α* = 90.0224(10)°, *β* = 92.6882(10)°, *γ* = 105.8832(10)°, *V* = 1799.87(6) $Å^3$, *Z* = 2, ρ_{calcd} = 1.601 Mg m^{-3}, *μ*(Mo Kα) = 3.51 mm^{-1}, *T* = 200(2) K, orange block, 0.22 × 0.15 × 0.11 mm, 10526 independent reflections. F^2 refinement, *R* = 0.040, *wR* = 0.089 for 8636 reflections ($I > 2\sigma(I)$, $2\theta_{max}$ = 60°), 415 parameters.

Synthesis of $[W(\equiv CPHPh_2)(CO)_2(Tp^*)]BF_4$ ([5]BF_4) and $[W\{\eta^2\text{-}C(H)PPh_2\}(CO)_2(Tp^*)]BF_4$ ([6]BF_4)

A suspension of $[W(\equiv CPPh_2)(CO)_2(Tp^*)]$ (0.200 g, 0.272 mmol) in Et_2O (12 mL) was cooled to –78°C and treated with $HBF_4{\cdot}Et_2O$ (0.06 mL, 0.4 mmol) dropwise. The orange suspension was stirred at –78°C for one hour then allowed to warm to room temperature and stirred for a further 45 minutes. Upon warming the mixture became a pink suspension. The mixture was filtered and the pink precipitate was washed with Et_2O (2 × 3 mL) and ^{n}pentane (2 × 3 mL) and dried under vacuum. IR spectroscopy revealed the precipitate is [**5**]BF_4. Dissolution in CH_3CN, $CHCl_3$ or CH_2Cl_2 affords a dark purple solution, and removal of the solvent gives [**6**]BF_4 as a purple solid.

$[W(\equiv CPHPh_2)(CO)_2(Tp^*)]BF_4$ ([5]BF_4)

IR (Nujol) ν/cm^{-1}: 2578 w (BH), 2459 vw (PH, tentative assignment), 2022 s, 1937 s (CO). IR (CH_2Cl_2) ν/cm^{-1}: 2022 s, 1937 s (CO). The spectrum contains absorptions

attributable to $[W\{\eta^2\text{-}C(H)PPh_2\}(CO)_2(Tp^*)]BF_4$ and $[W(\equiv CPPh_2)(CO)_2(Tp^*)]$ so the BH and PH absorptions cannot be conclusively identified. The mode assigned to ν_{PH} was reproduced computationally.

$[W\{\eta^2\text{-}C(H)PPh_2\}(CO)_2(Tp^*)]BF_4$ ([6]BF_4)

Yield 0.179 g (0.218 mmol, 80%). IR (Nujol) ν/cm^{-1}: 2563 w (BH), 2055 s, 1979 vs, br 1926 m, br (CO). IR (CH_2Cl_2) ν/cm^{-1}: 2567 w (BH), 2054 s, 1982 vs (CO). The IR spectrum could not be obtained in THF as [**6**]BF_4 is not stable in THF. ^{1}H NMR ($CDCl_3$) δ/ppm: 14.78 (d, 1 H, WCH, $^2J_{PH}$ = 4.8, $^2J_{WH}$ = 13.8), 7.45 – 7.40 (m, 2 H, C_6H_5), 7.34 – 7.26 (m, 4 H, C_6H_5), 7.09 – 7.02 (m, 4 H, C_6H_5), 6.06 (s, 1 H, pzH), 5.89 (s, 2 H, pzH), 2.60 (s, 3 H, $pzCH_3$), 2.51 (s, 6 H, $pzCH_3$), 2.35 (s, 3 H, $pzCH_3$), 1.42 (s, 6 H, $pzCH_3$). ^{13}C{^{1}H} NMR ($CDCl_3$) δ/ppm: 237.1 (d, W=C, $^1J_{PC}$ = 46.3, $^1J_{WC}$ = 21.5), 214.8 (CO, $^1J_{WC}$ = 134.3), 154.7 (1 C), 153.5 (2 C), 148.1 (1 C), 146.9 (2 C) [$C^{3,5}$(pz)], 133.2 [d, $C^{2,3,5,6}(C_6H_5)$, J_{PC} = 12.1], 132.2 [$C^4(C_6H_5)$], 129.5 [d, $C^{2,3,5,6}(C_6H_5)$, J_{PC} = 13.6], 128.8 [d, $C^1(C_6H_5)$, $^1J_{PC}$ = 64.9], 109.6 (1 C), 109.0 (2 C) [C^4(pz)], 16.3 (1 C), 15.5 (2 C), 13.1 (1 C), 12.8 (2 C) ($pzCH_3$). ^{13}C NMR ($CDCl_3$) δ/ppm: 237.1 (dd, W=C, $^1J_{PC}$ = 46.3, $^1J_{CH}$ = 199.0, $^1J_{WC}$ = 21.5). ^{31}P{^{1}H} NMR ($CDCl_3$) δ/ppm: –101.3 ($^1J_{WP}$ = 138.5). MS-ESI(+): *m/z* 735.2 $[M - BF_4]^+$. Accurate mass: found 735.2005 $[M - BF_4]^+$. Calcd. for $C_{30}H_{33}{}^{11}BN_6O_2P^{184}W$: 735.2005. Anal. found: C, 44.16; H, 4.34; N, 9.96%. Calcd. for $C_{30}H_{33}B_2F_4N_6O_2PW$: C, 43.83; H, 4.05; N, 10.22%.

Synthesis of $[W\{\equiv CPPh_2RhCl_2(Cp^*)\}(CO)_2(Tp^*)]$ (7)

A solution of $[W(\equiv CPPh_2)(CO)_2(Tp^*)]$ (0.350 g, 0.477 mmol) and $[RhCl_2(Cp^*)]_2$ (0.147 g, 0.239 mmol) in CH_2Cl_2 (20 mL) was stirred overnight. The solvent was removed in vacuo and the residue was dissolved in CH_2Cl_2 and chromatographed on silica gel. Elution with CH_2Cl_2 gave an initial yellow fraction containing $[W(\equiv CPPh_2)(CO)_2(Tp^*)]$. Subsequent elution with THF gave a red fraction, which was collected and the solvent removed under reduced pressure. The residue was dissolved in CH_2Cl_2 and EtOH then concentrated under reduced pressure to afford the product as a red precipitate, which was collected by filtration. Crystals suitable for crystallographic and microanalytical analysis were obtained by slow diffusion of ^{n}hexane into a solution of **7** in CH_2Cl_2. Yield 0.219 g (0.210 mmol, 44%). IR (Nujol) ν/cm^{-1}: 2552 w (BH), 2004 s, 1913 s (CO). IR (CH_2Cl_2) ν/cm^{-1}: 2554 w (BH), 2008 vs, 1916 vs (CO). IR (THF) ν/cm^{-1}: 2012 vs, 1919 vs (CO), ν_{BH} not visible. ^{1}H NMR ($CDCl_3$) δ/ppm: 7.93 –

7.87 (m, 4 H, C_6H_5), 7.39 – 7.36 (m, 6 H, C_6H_5), 5.65 (s, 3 H, pzH, coincident), 2.41 (s, 3 H, $pzCH_3$), 2.28 (s, 6 H, $pzCH_3$), 2.23 (s, 3 H, $pzCH_3$), 1.69 (s, 6 H, $pzCH_3$), 1.35 (d, 15 H, $^3J_{RhH}$ = 3.6). $^{13}C\{^1H\}$ NMR ($CDCl_3$) δ/ppm: 273.0 (d, W≡C, $^1J_{PC}$ = 28.7, $^1J_{WC}$ = 208.2), 226.3 (CO, $^1J_{WC}$ = 170.5), 152.8 (3 C, coincident), 144.8 (1 C), 144.3 (2 C) [$C^{3,5}$(pz)], 134.7 [d, $C^{2,3,5,6}(C_6H_5)$, J_{PC} = 9.1], 132.5 [d, $C^1(C_6H_5)$, $^1J_{PC}$ = 45.3], 130.0 [$C^4(C_6H_5)$], 128.1 [d, $C^{2,3,5,6}(C_6H_5)$, J_{PC} = 9.1], 106.9 (1 C), 106.1 (2 C) [C^4(pz)], 98.5 (C_5Me_5), 15.8 (2 C), 15.2 (1 C), 12.8 (2 C), 12.6 (1 C) ($pzCH_3$), 8.9 (C_5Me_5). $^{31}P\{^1H\}$ NMR ($CDCl_3$) δ/ppm: 37.0 (d, $^1J_{RhP}$ = 139.2, $^2J_{WP}$ = 122.0). MS-ESI(+): *m/z* 1007.8 [M – Cl]$^+$. Accurate mass: found 1007.1848 [M – Cl]$^+$. Calcd. for $C_{40}H_{47}{}^{11}B^{35}ClN_6O_2P^{103}Rh^{184}W$: 1007.1844. Anal. found: C, 41.41; H, 4.32; N, 6.94%. Calcd. for $C_{40}H_{47}BCl_2N_6O_2PRhW\cdot(CH_2Cl_2)_2$: C, 41.58; H, 4.24; N, 6.93%. Crystal data for $C_{40}H_{47}BCl_2N_6O_2PRhW\cdot(CH_2Cl_2)_2$: M_w = 1213.16, orthorhombic, *Pbca*, *a* = 20.9517(2) Å, *b* = 21.1340(2) Å, *c* = 22.1261(1) Å, *V* = 9797.29(14) Å^3, *Z* = 8, ρ_{calcd} = 1.645 Mg m^{-3}, μ(Mo Kα) = 3.08 mm^{-1}, *T* = 200(2) K, red block, 0.27 × 0.20 × 0.14 mm, 14324 independent reflections. F^2 refinement, *R* = 0.040, *wR* = 0.106 for 11541 reflections ($I > 2\sigma(I)$, $2\theta_{max}$ = 60°), 541 parameters.

Synthesis of [W(≡CPPh$_2$AuCl)(CO)$_2$(Tp*)] (8)

A mixture of [W(≡CPPh$_2$)(CO)$_2$(Tp*)] (0.352 g, 0.479 mmol) and [AuCl(SMe$_2$)] (0.143 g, 0.485 mmol) was dissolved in THF (15 mL) resulting in a red solution. The solution was stirred for 18 hours and a small amount of gold precipitate was observed. The solution was filtered through diatomaceous earth and the volatiles were removed in vacuo to afford the product as a red powder. Crystals suitable for crystallographic analysis were obtained by slow diffusion of EtOH into a solution of **8** in CH_2Cl_2. Yield 0.374 g (0.387 mmol, 81%). IR (Nujol) ν/cm^{-1}: 2552 w (BH), 2001 s, 1907 s (CO). IR (CH_2Cl_2) ν/cm^{-1}: 2556 w (BH), 2003 vs, 1916 vs (CO). IR (THF) ν/cm^{-1}: 2553 w (BH), 2002 vs, 1917 vs (CO). ^1H NMR ($CDCl_3$) δ/ppm: 7.81 – 7.73 (m, 4 H, C_6H_5), 7.48 – 7.43 (m, 6 H, C_6H_5), 5.90 (s, 2 H, pzH), 5.77 (s, 1 H, pzH), 2.38 (s, 6 H, $pzCH_3$), 2.36 (s, 3 H, $pzCH_3$), 2.31 (s, 3 H, $pzCH_3$), 2.24 (s, 6 H, $pzCH_3$). $^{13}C\{^1H\}$ NMR ($CDCl_3$) δ/ppm: 263.3 (d, W≡C, $^1J_{PC}$ = 22.1, $^1J_{WC}$ = 199.9), 223.6 (d, CO, $^3J_{PC}$ = 2.8, $^1J_{WC}$ = 163.4), 152.7 (1 C), 151.8 (2 C), 145.9 (1 C), 145.2 (2 C) [$C^{3,5}$(pz)], 133.7 [d, $C^{2,3,5,6}(C_6H_5)$, J_{PC} = 13.8], 131.4 [d, $C^4(C_6H_5)$, $^4J_{PC}$ = 2.0], 129.7 [d, $C^1(C_6H_5)$, $^1J_{PC}$ = 64.3], 129.0 [d, $C^{2,3,5,6}(C_6H_5)$, J_{PC} = 12.4], 107.3 (1 C), 106.9 (2 C) [C^4(pz)], 16.9 (2 C), 15.2 (1 C), 12.7 (3 C, coincident) ($pzCH_3$). $^{31}P\{^1H\}$ NMR ($CDCl_3$) δ/ppm: 37.5 ($^2J_{WP}$ =

139.3). MS-ESI(+): *m/z* 989.6 $[M + Na]^+$, 911.6 $[M – 2CO + H]^+$, 701.7 $[M – 2CO – Au + Na]^+$, 679.8 $[M – 2CO – Au + H]^+$. Accurate mass: found 991.1151 $[M + Na]^+$. Calcd. for $C_{30}H_{32}Au^{11}B^{37}ClN_6NaO_2P^{184}W$: 991.1149. Anal. found: C, 37.24; H, 3.30; N, 8.42%. Calcd. for $C_{30}H_{32}AuBClN_6O_2PW$: C, 37.28; H, 3.34; N, 8.69%. Crystal data for $C_{30}H_{32}AuBClN_6O_2PW$: M_w = 966.68, monoclinic, $P2_1/n$, a = 10.3172(1) Å, b = 13.5659(2) Å, c = 25.2039(3) Å, β = 98.3693(5)°, V = 3490.02(7) Å^3, Z = 4, ρ_{calcd} = 1.840 Mg m^{-3}, μ(Mo Kα) = 7.65 mm^{-1}, T = 200(2) K, orange plate, 0.38 × 0.28 × 0.05 mm, 10247 independent reflections. F^2 refinement, R = 0.030, wR = 0.067 for 8112 reflections ($I > 2\sigma(I)$, $2\theta_{max}$ = 60°), 388 parameters.

Synthesis of [W{η^2-C(AuCl)PPh$_2$AuCl}(CO)$_2$(Tp*)] (9)

A mixture of [W(≡CPPh$_2$)(CO)$_2$(Tp*)] (0.351 g, 0.478 mmol) and [AuCl(SMe$_2$)] (0.428 g, 1.45 mmol) was dissolved in THF (15 mL) resulting in a red solution. The solution was stirred for four days and a small amount of gold precipitate was observed. The solution was decanted by cannula filtration and concentrated to approximately 5 mL in vacuo resulting in precipitation of the product as a peach powder, which was isolated by filtration. Crystals suitable for crystallographic analysis were obtained by slow diffusion of EtOH into a solution of **9** in CH_2Cl_2. Yield 0.240 g (0.200 mmol, 55%). IR (Nujol) ν/cm^{-1}: 2563 w (BH), 2022 vs, 1936 vs (CO). IR (THF) ν/cm^{-1}: 2562 w (BH), 2022 vs, 1944 vs (CO). ^{1}H NMR ($CDCl_3$) δ/ppm: 8.09 – 8.02 (m, 4 H, C_6H_5), 7.61 – 7.49 (m, 6 H, C_6H_5), 5.96 (s, 1 H, pzH), 5.93 (s, 2 H, pzH), 2.50 (s, 3 H, pzCH_3), 2.36 (s, 6 H, pzCH_3), 2.32 (s, 3 H, pzCH_3), 2.25 (s, 6 H, pzCH_3). ^{13}C{^{1}H} NMR ($CDCl_3$) δ/ppm: 253.6 (d, WC, $^1J_{PC}$ = 1.5, $^1J_{WC}$ = 99.6), 216.6 (d, CO, $^3J_{PC}$ = 7.8, $^1J_{WC}$ = 154.2), 154.4 (1 C), 152.5 (2 C), 146.9 (1 C), 146.4 (2 C) [C^{3,5}(pz)], 134.4 [d, C^{2,3,5,6}(C_6H_5), J_{PC} = 13.6], 132.5 [d, C^4(C_6H_5), $^4J_{PC}$ = 3.0], 129.5 [d, C^{2,3,5,6}(C_6H_5), J_{PC} = 12.1], 129.4 [d, C^1(C_6H_5), $^1J_{PC}$ = 61.9], 109.1 (1 C), 108.2 (2 C) [C^4(pz)], 17.4 (2 C), 16.0 (1 C), 13.2 (1 C), 12.7 (2 C) (pzCH_3). ^{31}P{^{1}H} NMR ($CDCl_3$) δ/ppm: 53.6 ($^2J_{WP}$ = 84.3). MS-ESI(+): *m/z* 1220.8 $[M + Na]^+$, 1162.7 $[M – Cl]^+$. Accurate mass: found 1221.0532 $[M + Na]^+$. Calcd. for $C_{30}H_{32}Au_2{}^{11}B^{35}Cl_2N_6NaO_2P^{184}W$: 1221.0533. Anal. found: C, 30.11; H, 2.88; N, 7.04%. Calcd. for $C_{30}H_{32}Au_2BCl_2N_6O_2PW$: C, 30.05; H, 2.69; N, 7.01%. Crystal data for $C_{30}H_{32}Au_2BCl_2N_6O_2PW$: M_w = 1199.10, monoclinic, $P2_1/n$, a = 16.5513(2) Å, b = 12.9890(2) Å, c = 17.7921(2) Å, β = 113.5027(7)°, V = 3507.71(8) Å^3, Z = 4, ρ_{calcd} = 2.270 Mg m^{-3}, μ(Mo Kα) = 11.85 mm^{-1}, T = 200(2) K, red block, 0.36 × 0.29 × 0.26

mm, 10263 independent reflections. F^2 refinement, R = 0.034, wR = 0.080 for 8079 reflections ($I > 2\sigma(I)$, $2\theta_{max}$ = 60°), 406 parameters.

Synthesis of [W{≡CP(=S)Ph$_2$}(CO)$_2$(Tp*)] (10) and [W{η^2-SCP(=S)Ph$_2$}(CO)$_2$(Tp*)] (11)

A solution of [W(≡CPPh$_2$)(CO)$_2$(Tp*)] (0.500 g, 0.681 mmol) and elemental sulfur (0.022 g, 0.686 mg-atom) in THF (30 mL) was stirred overnight. The volatiles were removed in vacuo and the residue was chromatographed on silica gel at –30°C with CH_2Cl_2 as the eluent. The initial faint grey fraction was discarded, and the second (purple, minor) and third (orange, major) fractions were collected, containing [W{η^2-SCP(=S)Ph$_2$}(CO)$_2$(Tp*)] and [W{≡CP(=S)Ph$_2$}(CO)$_2$(Tp*)], respectively. [W{≡CP(=S)Ph$_2$}(CO)$_2$(Tp*)] was isolated by concentration of a CH_2Cl_2/EtOH solution in vacuo to afford the product as an orange powder. Crystals suitable for crystallographic analysis were obtained from CH_2Cl_2/^{n}hexane (**10**) and CH_2Cl_2/MeOH (**11**).

N.B. When the reaction is carried out in toluene it gives 16% **11** and 80% **10**. If the reaction is carried out with an excess of sulphur ($^{10}/_8$ equivalents of S_8) then **10** is obtained in 98% yield.

[W{≡CP(=S)Ph$_2$}(CO)$_2$(Tp*)] (10)

Yield 0.422 g (0.551 mmol, 81%). IR (Nujol) ν/cm^{-1}: 2560 w, 2550 w (BH), 1996 s, 1924 s, 1909 s (CO). IR (CH_2Cl_2) ν/cm^{-1}: 2556 w (BH), 2004 s, 1916 s, br (CO). IR (THF) ν/cm^{-1}: 2552 w (BH), 2004 s, 1997 sh, 1918 s, 1908 sh (CO). ^{1}H NMR ($CDCl_3$) δ/ppm: 8.00 – 7.95 (m, 4 H, C_6H_5), 7.47 – 7.43 (m, 6 H, C_6H_5), 5.88 (s, 2 H, pzH), 5.76 (s, 1 H, pzH), 2.38 (s, 9 H, pzCH_3), 2.31 (s, 3 H, pzCH_3), 2.27 (s, 6 H, pzCH_3). ^{13}C{^{1}H} NMR ($CDCl_3$) δ/ppm: 270.1 (d, W≡C, $^1J_{PC}$ = 4.9, $^1J_{WC}$ = 198.4), 224.0 (CO, $^1J_{WC}$ = 162.5), 152.8 (1 C), 152.4 (2 C), 145.7 (1 C), 145.0 (2 C) [C^{3,5}(pz)], 134.3 [d, C^1(C_6H_5), $^1J_{PC}$ = 86.7], 131.9 [d, C^{2,3,5,6}(C_6H_5), J_{PC} = 11.0], 131.1 [d, C^4(C_6H_5), $^3J_{PC}$ = 2.4], 128.5 [d, C^{2,3,5,6}(C_6H_5), J_{PC} = 12.2], 107.2 (1 C), 106.9 (2 C) [C^4(pz)], 17.0 (2 C), 15.3 (1 C), 12.8 (2 C), 12.8 (1 C) (pzCH_3). ^{31}P{^{1}H} NMR ($CDCl_3$) δ/ppm: 41.0 ($^2J_{WP}$ = 152.5). MS-ESI(+): *m/z* 789.5 [M + Na]$^+$, 710.7 [M – 2CO]$^+$, 454.6 [M – 2CO – Tp* + MeCN]$^+$, 413.5 [M – 2CO – Tp*]$^+$. Accurate mass: found 789.1545 [M + Na]$^+$. Calcd. for $C_{30}H_{32}{}^{11}BN_6O_2NaPS^{184}W$: 789.1545. Anal. found: C, 47.19; H, 4.47; N, 10.84%. Calcd. for $C_{30}H_{32}BN_6O_2PSW$: C, 47.02; H, 4.21; N, 10.97%. Crystal data for

$C_{30}H_{32}BN_6O_2PSW$: M_w = 766.32, triclinic, P – 1 (No. 2), a = 10.2968(2) Å, b = 10.4179(2) Å, c = 17.2038(4) Å, α = 98.7173(12)°, β = 106.0368(13)°, γ = 106.6702(11)°, V = 1644.85(6) Å^3, Z = 2, ρ_{calcd} = 1.547 Mg m^{-3}, μ(Mo Kα) = 3.66 mm^{-1}, T = 200(2) K, orange block, 0.20 × 0.18 × 0.11 mm, 9625 independent reflections. F^2 refinement, R = 0.042, wR = 0.089 for 7233 reflections ($I > 2\sigma(I)$, $2\theta_{max}$ = 60°), 379 parameters.

[W{η^2-SCP(=S)Ph$_2$}(CO)$_2$(Tp*)] (11)

Yield 0.047 g (0.059 mmol, 9%). IR (Nujol) ν/cm^{-1}: 2552 w (BH), 1992 s, 1902 s, 1892 s (CO). IR (CH_2Cl_2) ν/cm^{-1}: 2559 w (BH), 1995 s, 1907 s (CO). IR (THF) ν/cm^{-1}: 1993 s, 1908 s (CO), ν_{BH} not unambiguously identifiable. ^{1}H NMR ($CDCl_3$) δ/ppm: 8.09 – 8.02 (m, 4 H, C_6H_5), 7.51 – 7.42 (m, 6 H, C_6H_5), 5.91 (s, 1 H, pzH), 5.80 (s, 2 H, pzH), 2.55 (s, 3 H, pzCH_3), 2.37 (s, 6 H, pzCH_3), 2.32 (s, 3 H, pzCH_3), 1.93 (s, 6 H, pzCH_3). ^{13}C{^{1}H} NMR ($CDCl_3$) δ/ppm: 250.1 (d, WC, $^1J_{PC}$ = 42.0, $^1J_{WC}$ = 42.8), 224.5 (CO, $^1J_{WC}$ = 76.3), 153.8 (1 C), 152.9 (2 C), 145.3 (1 C), 144.4 (2 C) [C^{3,5}(pz)], 132.7 [d, C^1(C_6H_5), $^1J_{PC}$ = 87.3], 132.5 [d, C^{2,3,5,6}(C_6H_5), J_{PC} = 11.0], 131.5 [C^4(C_6H_5)], 128.3 [d, C^{2,3,5,6}(C_6H_5), J_{PC} = 13.3], 108.2 (1 C), 107.5 (2 C) [C^4(pz)], 16.3 (1 C), 13.7 (2 C), 13.2 (1 C), 12.6 (2 C) (pzCH_3). ^{31}P{^{1}H} NMR ($CDCl_3$) δ/ppm: 52.9 (s). MS-ESI(+): *m/z* 821.6 [M + Na]$^+$, 798.7 [M]$^+$, 743.4 [M – 2CO + H]$^+$. Accurate mass: found 821.1268 [M + Na]$^+$. Calcd. for $C_{30}H_{32}{}^{11}BN_6O_2NaPS_2{}^{184}W$: 821.1266. Anal. found: C, 44.41; H, 4.20; N, 10.42%. Calcd. for $C_{30}H_{32}BN_6O_2PS_2W$: C, 45.13; H, 4.04; N, 10.53%. Crystal data for $C_{30}H_{32}BN_6O_2PS_2W$: M_w = 798.39, monoclinic, $P2_1/c$, a = 9.9675(2) Å, b = 15.4834(4) Å, c = 23.6677(6) Å, β = 92.4264(15)°, V = 3649.38(15) Å^3, Z = 4, ρ_{calcd} = 1.453 Mg m^{-3}, μ(Mo Kα) = 3.36 mm^{-1}, T = 200(2) K, purple lath, 0.30 × 0.09 × 0.04 mm, 8407 independent reflections. F^2 refinement, R = 0.095, wR = 0.217 for 6295 reflections ($I > 2\sigma(I)$, $2\theta_{max}$ = 55°), 388 parameters.

Synthesis of [W{≡CP(=Se)Ph$_2$}(CO)$_2$(Tp*)] (12)

A mixture of [W(≡CPPh$_2$)(CO)$_2$(Tp*)] (0.306 g, 0.417 mmol) and grey selenium (0.033 g, 0.418 mg-atom) was stirred overnight in CH_2Cl_2 (15 mL). The solvent was removed in vacuo. The red residue was chromatographed on silica (3.6 × 10 cm) with 1:1 CH_2Cl_2:^{n}pentane as the eluent. The first yellow band to elute was discarded and the polarity increased to 3:1 CH_2Cl_2:^{n}pentane. The red fraction containing the product was collected and the solvent was removed in vacuo. The orange residue was redissolved in

CH_2Cl_2 and EtOH was added and the solution concentrated in vacuo to afford the product as an orange powder. Crystals suitable for crystallographic analysis were obtained from a solution of **12** in $CHCl_3$. Yield 0.313 g (0.385 mmol, 92%). IR (Nujol) ν/cm^{-1}: 2553 w (BH), 2002 s, 1912 s, br (CO). IR (CH_2Cl_2) ν/cm^{-1}: 2556 w (BH), 2005 vs, 1917 vs, br (CO). IR (THF) ν/cm^{-1}: 2552 w (BH), 2004 vs, 1997 vs, 1918 vs, 1907 vs (CO). ^{1}H NMR ($CDCl_3$) δ/ppm: 8.02 – 7.95 (m, 4 H, C_6H_5), 7.44 – 7.41 (m, 6 H, C_6H_5), 5.90 (s, 2 H, pzH), 5.78 (s, 1 H, pzH), 2.40 (s, 6 H, $pzCH_3$), 2.38 (s, 3 H, $pzCH_3$), 2.32 (s, 3 H, $pzCH_3$), 2.27 (s, 6 H, $pzCH_3$). ^{13}C{^{1}H} NMR ($CDCl_3$) δ/ppm: 265.2 (d, W≡C, $^1J_{PC}$ = 13.6, $^1J_{WC}$ = 201.4), 224.0 (d, CO, $^3J_{PC}$ = 3.0, $^1J_{WC}$ = 164.4), 152.8 (1 C), 152.3 (2 C), 145.7 (1 C), 145.0 (2 C) [C^{3,5}(pz)], 133.2 [d, C^1(C_6H_5), $^1J_{PC}$ = 76.9], 132.2 [d, C^{2,3,5,6}(C_6H_5), J_{PC} = 12.1], 131.1 [d, C^4(C_6H_5), $^3J_{PC}$ = 3.0], 128.4 [d, C^{2,3,5,6}(C_6H_5), J_{PC} = 13.6], 107.2 (1 C), 106.8 (2 C) [C^4(pz)], 17.0 (2 C), 15.3 (1 C), 12.8 (2 C), 12.7 (1 C) ($pzCH_3$). ^{31}P{^{1}H} NMR ($CDCl_3$) δ/ppm: 31.9 ($^2J_{WP}$ = 152.6, $^1J_{SeP}$ = 711.8). MS-ESI(+): *m/z* 836.6 [M + Na]$^+$, 813.3 [M – H]$^+$, 787.4 [M – CO + H]$^+$, 759.5 [M – 2CO + H]$^+$. Accurate mass: found 814.1093 [M]$^+$. Calcd. for $C_{30}H_{32}{}^{11}BN_6O_2P^{80}Se^{184}W$: 814.1092. Anal. found: C, 44.59; H, 3.96; N, 10.77%. Calcd. for $C_{30}H_{32}BN_6O_2PSeW$: C, 44.31; H, 3.97; N, 10.33%. Crystal data for $C_{30}H_{32}BN_6O_2PSeW{\cdot}CHCl_3$: M_w = 932.59, triclinic, $P\bar{1}$ (No. 2), a = 10.2609(2) Å, b = 10.4116(1) Å, c = 17.5341(3) Å, α = 90.5897(11)°, β = 91.1982(9)°, γ = 106.3725(10)°, V = 1796.60(5) Å^3, Z = 2, ρ_{calcd} = 1.724 Mg m^{-3}, μ(Mo Kα) = 4.53 mm^{-1}, T = 200(2) K, orange plate, 0.26 × 0.24 × 0.12 mm, 10523 independent reflections. F^2 refinement, R = 0.041, wR = 0.092 for 8432 reflections ($I > 2\sigma(I)$, $2\theta_{max}$ = 60°), 415 parameters.

Synthesis of [W{≡CP(=O)Ph$_2$}(CO)$_2$(Tp*)] (13)

Method A: A solution of [W(≡CPPh$_2$)(CO)$_2$(Tp*)] (0.100 g, 0.136 mmol) in toluene (9 mL) in air was heated to reflux. After eight hours IR spectroscopy indicated all the starting material had been consumed. The solvent was removed under reduced pressure. ^{1}H and ^{31}P{^{1}H} NMR spectroscopy indicated **13** to be the major product (ca. 70% by ^{31}P{^{1}H} NMR).

Method B: A solution of [W(≡CPPh$_2$)(CO)$_2$(Tp*)] (0.200 g, 0.272 mmol) in CH_2Cl_2 (20 mL) in air was treated with 30% aqueous H_2O_2 (1.0 mL, 9.8 mmol) and the mixture was stirred vigorously. After 75 minutes TLC showed the reaction was complete. The organic layer was washed with water (3 × 15 mL) and dried with $MgSO_4$. The solvent was removed to afford crude **13** as an orange oil. The product was chromatographed on

silica gel with 1:1 THF:hexane. An initial yellow band was discarded and the second (major) orange band containing the product was collected. ^{1}H and ^{31}P{^{1}H} NMR spectroscopy showed only a marginal improvement in purity as a result of chromatography (ca. 80% **13** by ^{31}P{^{1}H} NMR). Yield 0.132 g (0.176 mmol, 65%).

Method C: A solution of [W(≡CBr)(CO)$_2$(Tp*)] (0.020 g, 0.032 mmol) in THF (1 mL) was cooled to –78°C and treated with ^{n}BuLi (0.07 mL, 0.45 M in hexanes, 0.03 mmol). The resulting dark yellow solution was stirred for 30 minutes and then treated with P(=O)ClPh$_2$ (0.31 mL, 0.10 M in THF/hexane, 0.032 mmol). The solution instantly turned orange and was stirred 40 minutes then allowed to warm to room temperature and stirred for a further 40 minutes. The volatiles were removed under reduced pressure. ^{1}H and ^{31}P{^{1}H} NMR spectroscopy indicated formation of **13** as the major product.

IR (Nujol) ν/cm^{-1}: 2550 w (BH), 2002 s, 1987 m, 1913 s, br (CO). IR (CH$_2$Cl$_2$) ν/cm^{-1}: 2556 w (BH), 2004 vs, 1983 m, 1915 vs, br (CO). IR (THF) ν/cm^{-1}: 2553 w (BH), 2001 vs, 1975 w, 1911 vs, br (CO). N.B. ν_{PO} was not unambiguously identifiable. ^{1}H NMR (CDCl$_3$) δ/ppm: 7.96 – 7.93 (m, 4 H, C$_6$H$_5$), 7.49 – 7.46 (m, 6 H, C$_6$H$_5$), 5.91 (s, 2 H, pzH), 5.78 (s, 1 H, pzH), 2.40 (s, 6 H, pzCH$_3$), 2.38 (s, 3 H, pzCH$_3$), 2.35 (s, 6 H, pzCH$_3$), 2.33 (s, 3 H, pzCH$_3$). ^{13}C{^{1}H} NMR (CDCl$_3$) δ/ppm: 281.2 (d, W≡C, $^{1}J_{PC}$ = 16.1, $^{1}J_{WC}$ = 190.6), 224.0 (CO, $^{1}J_{WC}$ = 164.4), 152.0 (1 C), 151.7 (2 C), 145.3 (1 C), 144.5 (2 C) [C^{3,5}(pz)], 133.3 [d, C^{1}(C$_6$H$_5$), $^{1}J_{PC}$ = 105.6], 131.0 [d, C^{2,3,5,6}(C$_6$H$_5$), J_{PC} = 10.0], 130.9 [d, C^{4}(C$_6$H$_5$), $^{3}J_{PC}$ = 1.8], 127.9 [d, C^{2,3,5,6}(C$_6$H$_5$), J_{PC} = 12.1], 106.7 (1 C), 106.4 (2 C) [C^{4}(pz)], 16.2 (2 C), 14.7 (1 C), 12.3 (2 C), 12.2 (1 C) (pzCH$_3$). ^{31}P{^{1}H} NMR (CDCl$_3$) δ/ppm: 19.9 ($^{2}J_{WP}$ = 145.2). MS-ESI(+): *m/z* 1523.4 [2M + Na]$^+$, 814.2 [M + Na + MeCN]$^+$, 789.1 [M + K]$^+$, 773.2 [M + Na]$^+$, 751.2 [M + H]$^+$. Accurate mass: found 751.1953 [M + H]$^+$. Calcd. for C$_{30}$H$_{33}$^{11}BN$_6$O$_3$P^{184}W: 751.1954. Found 773.1777 [M + Na]$^+$. Calcd. for C$_{30}$H$_{32}$BN$_6$^{23}NaO$_3$P^{184}W: 773.1774. Anal. found: C, 47.48; H, 4.45; N, 11.06%. Calcd. for C$_{30}$H$_{32}$BN$_6$O$_3$PW: C, 48.03; H, 4.30; N, 11.20%. Calcd. for the hemi-hydrate C$_{30}$H$_{32}$BN$_6$O$_3$PW·(H$_2$O)$_{0.5}$: C, 47.45; H, 4.38; N, 11.06%.

Synthesis of [W{η^2-C(AuCl)P(=S)Ph$_2$}(CO)$_2$(Tp*)] (14)

[W{≡CP(=S)Ph$_2$}(CO)$_2$(Tp*)] (0.095 g, 0.12 mmol) and [AuCl(SMe$_2$)] (0.037 g, 0.12 mmol) were dissolved in CH$_2$Cl$_2$ (6 mL) resulting in a red solution and golden precipitate. The suspension was stirred for two hours after which time IR spectroscopy showed the presence of the starting material (ν_{CO} 2004, 1916 cm^{-1}) and a new compound (ν_{CO} 2031, 1952 cm^{-1}). After 4.5 hours the infrared showed no change, so a

further half equivalent of [AuCl(THT)]* (0.020 g, 0.062 mmol) was added. After six hours of stirring the IR showed almost complete conversion to the product and the reaction was left to sit overnight. The reaction mixture was filtered through diatomaceous earth and washed with CH_2Cl_2 until the washings were colourless. EtOH was added to the filtrate and the solution was concentrated on the rotary evaporator until a bluish precipitate was observed, which was removed by filtration. The crude product was chromatographed on neutral alumina using 2:1 CH_2Cl_2:MeCN as the eluent. An initial orange fraction was collected containing the starting material, followed by a red fraction containing the product. The solvent was removed under reduced pressure to afford **14** as an orange solid. Yield 0.070 g (0.070 mmol, 57%). IR (Nujol) ν/cm^{-1}: 2560 w (BH), 2028 s, 1948 s, br (CO). IR (CH_2Cl_2) ν/cm^{-1}: 2563 w (BH), 2031 s, 1952 vs, br (CO). IR (THF) ν/cm^{-1}: 2563 w (BH), 2031 vs, 1953 vs, br (CO). ^{1}H NMR ($CDCl_3$) δ/ppm: 8.23 – 8.20 (m, 4 H, C_6H_5), 7.55 – 7.50 (m, 6 H, C_6H_5), 5.94 (s, 1 H, pzH), 5.91 (s, 2 H, pzH), 2.54 (s, 3 H, $pzCH_3$), 2.36 (s, 6 H, $pzCH_3$), 2.32 (s, 3 H, $pzCH_3$), 2.20 (s, 6 H, $pzCH_3$). ^{13}C{^{1}H} NMR ($CDCl_3$) δ/ppm: 262.4 (br, WCP), 216.4 (br, CO), 154.3 (1 C), 152.5 (2 C), 146.7 (1 C), 146.1 (2 C) [$C^{3,5}$(pz)], 132.5 [d, $C^{2,3,5,6}(C_6H_5)$, J_{PC} = 10.0], 132.0 [br, $C^{1,4}(C_6H_5)$], 128.8 [d, $C^{2,3,5,6}(C_6H_5)$, J_{PC} = 8.9], 108.8 (1 C), 108.0 (2 C) [C^4(pz)], 17.2 (2 C), 15.9 (1 C), 13.1 (1 C), 12.7 (2 C) ($pzCH_3$). ^{31}P{^{1}H} NMR ($CDCl_3$) δ/ppm: 52.3 (br). MS-ESI(+): *m/z* 1962.4 [2 M – Cl + H]$^+$, 1729.4 [2 M – Au – 2 Cl]$^+$, 1021.1 [M + Na]$^+$, 963.1 [M – Cl]$^+$. Accurate mass: found 1023.0871 [M + Na]$^+$. Calcd. for $C_{30}H_{32}Au^{11}B^{37}ClN_6NaO_2P^{184}W$: 1023.0870. Found 1021.0909 [M + Na]$^+$. Calcd. for $C_{30}H_{32}Au^{11}B^{35}ClN_6NaO_2P^{184}W$: 1021.0900. Anal. found: C, 35.83; H, 3.25; N, 8.20%. Calcd. for $C_{30}H_{32}AuBClN_6O_2PSW$: C, 36.08; H, 3.23; N, 8.41%. Crystal data for $C_{30}H_{32}AuBClN_6O_2PSW$: M_w = 998.74, monoclinic, $P2_1/c$, a = 16.6239(3) Å, b = 12.8664(3) Å, c = 17.4284(3) Å, β = 116.7247(10)°, V = 3329.55(12) Å^3, Z = 4, ρ_{calcd} = 1.992 Mg m^{-3}, μ(Mo Kα) = 8.08 mm^{-1}, T = 200(2) K, orange block, 0.10 × 0.09 × 0.08 mm, 7648 independent reflections. F^2 refinement, R = 0.043, wR = 0.118 for 5693 reflections ($I > 2\sigma(I)$, $2\theta_{max}$ = 55°), 397 parameters.

* [AuCl(THT)] was used because all of the [AuCl(SMe_2)] sample was used up in this reaction, whereas a sample of [AuCl(THT)] was on hand.

CHAPTER 3. Chlorophosphinocarbyne complexes

Synthesis of [W(≡CPClPh)(CO)$_2$(Tp*)] (15)

A solution of [W(≡CBr)(CO)$_2$(Tp*)] (2.999 g, 4.768 mmol) in THF (100 mL) was cooled to −78°C and treated with ^{n}BuLi (3.0 mL, 1.6 M in hexanes, 4.8 mmol). The resulting light brown solution was stirred for 30 minutes and then treated with PCl_2Ph (0.65 mL, 4.8 mmol). The solution instantly turned dark red and was stirred for a further 70 minutes then allowed to warm to room temperature. Volatiles were removed under reduced pressure and the solid residue was extracted with ^{n}pentane (4 × 50 mL) and the solution was collected by cannula filtration. Concentration under reduced pressure then cooling to −15°C resulted in a peach coloured precipitate which was isolated by filtration. The filtrate was concentrated and cooled to provide a second crop. Yield 2.335 g (3.371 mmol, 71%). IR (Nujol) ν/cm^{-1}: 2550 w, 2524 w (BH), 2006 sh, 1987 s, 1970 sh, 1923 sh, 1898 s (CO). IR (THF) ν/cm^{-1}: 2551 w (BH), 1992 vs, 1905 vs (CO). ^{1}H NMR ($CDCl_3$) δ/ppm: 7.85 – 7.79 (m, 2 H, C_6H_5), 7.45 – 7.42 (m, 3 H, C_6H_5), 5.90 (s, 1 H, pzH), 5.89 (s, 1 H, pzH), 5.75 (s, 1 H, pzH), 2.45 (s, 3 H, pzCH_3), 2.37 (s, 3 H, pzCH_3), 2.36 (s, 6 H, pzCH_3, coincident), 2.36 (s, 3 H, pzCH_3), 2.30 (s, 3 H, pzCH_3). ^{1}H NMR (C_6D_6) δ/ppm: 7.96 – 7.91 (m, 2 H, C_6H_5), 7.10 – 6.99 (m, 3 H, C_6H_5), 5.48 (s, 2 H, pzH, coincident), 5.27 (s, 1 H, pzH), 2.55 (s, 3 H, pzCH_3), 2.51 (s, 3 H, pzCH_3), 2.28 (s, 3 H, pzCH_3), 2.02 (s, 3 H, pzCH_3), 2.01 (s, 3 H, pzCH_3), 1.96 (s, 3 H, pzCH_3). ^{13}C{^{1}H} NMR ($CDCl_3$) δ/ppm: 285.2 (d, W≡C, $^1J_{PC}$ = 96.0, $^1J_{WC}$ = 189.0), 224.7 (CO, $^1J_{WC}$ = 165.4), 224.7 (CO, $^1J_{WC}$ = 165.4), 152.6 (1 C), 152.1 (1 C), 152.0 (1 C), 145.6 (1 C), 144.8 (1 C), 144.8 (1 C) [C^{3,5}(pz)], 138.7 [d, C^1(C_6H_5), $^1J_{PC}$ = 33.2], 132.2 [d, C^{2,3,5,6}(C_6H_5), J_{PC} = 27.2], 130.3 [C^4(C_6H_5)], 128.7 [d, C^{2,3,5,6}(C_6H_5), J_{PC} = 7.5], 107.0 (1 C), 106.7 (2 C, coincident) [C^4(pz)], 16.9 (2 C, coincident), 15.2 (1 C), 12.7 (2 C, coincident), 12.7 (1 C) (pzCH_3). ^{13}C{^{1}H} NMR (C_6D_6) δ/ppm: 286.6 (d, W≡C, $^1J_{PC}$ = 95.5, $^1J_{WC}$ = 189.3), 225.7 (CO, $^1J_{WC}$ = 164.6), 225.5 (CO, $^1J_{WC}$ = 165.4), 152.8 (1 C), 152.2 (1 C), 152.2 (1 C), 145.3 (1 C), 144.5 (1 C), 144.5 (1 C) [C^{3,5}(pz)], 139.5 [d, C^1(C_6H_5), $^1J_{PC}$ = 33.3], 132.7 [d, C^{2,3,5,6}(C_6H_5), J_{PC} = 26.3], 130.5 [C^4(C_6H_5)], 129.0 [d, C^{2,3,5,6}(C_6H_5), J_{PC} = 8.1], 107.3 (1 C), 107.1 (2 C, coincident) [C^4(pz)], 17.2 (1 C), 17.1 (1 C), 15.1(1 C), 12.4 (3 C, coincident) (pzCH_3). ^{31}P{^{1}H} NMR ($CDCl_3$) δ/ppm: 91.2 ($^2J_{WP}$ = 77.9). ^{31}P{^{1}H} NMR (C_6D_6) δ/ppm: 91.2 ($^2J_{WP}$ = 74.9). Anal. found: C, 41.58; H, 4.11; N, 12.17%. Calcd. for $C_{24}H_{27}BClN_6O_2PW$: C, 41.62; H, 3.93; N, 12.13%.

Synthesis of [W(≡CPClCy)(CO)$_2$(Tp*)] (16)

A solution of [W(≡CBr)(CO)$_2$(Tp*)] (2.500 g, 3.975 mmol) in THF (80 mL) was cooled to –78°C and treated with ^{n}BuLi (2.35 mL, 1.7 M in hexanes, 4.0 mmol). The resulting light brown solution was stirred for 45 minutes and then treated with PCl_2Cy (0.61 mL, 4.0 mmol). The solution instantly turned dark red and was stirred for a further 60 minutes then allowed to warm to room temperature. Volatiles were removed under reduced pressure and the solid residue was extracted with ^{n}pentane (4 × 30 mL) and the solution was collected by cannula filtration. Concentration under reduced pressure then cooling to −15°C resulted in an orange coloured precipitate which was isolated by filtration. Yield 1.814 g (2.596 mmol, 65%). IR (Nujol) ν/cm^{-1}: 2552 w, 2528 w (BH), 2006 s, 1987 s, 1967 m, 1917 s, 1897 s (CO). IR (THF) ν/cm^{-1}: 2550 w (BH), 1989 s, 1969 m, 1901 s (CO). ^{1}H NMR ($CDCl_3$) δ/ppm: 5.97 (s, 2 H, pzH, coincident), 5.80 (s, 1 H, pzH), 2.64 (s, 6 H, pzCH_3, coincident), 2.42 (s, 9 H, pzCH_3, coincident), 2.36 (s, 3 H, pzCH_3), 2.20 – 1.31 (m, 11 H, Cy). ^{1}H NMR (C_6D_6) δ/ppm: 5.53 (s, 2 H, pzH, coincident), 5.32 (s, 1 H, pzH), 2.74 (s, 3 H, pzCH_3), 2.70 (s, 3 H, pzCH_3), 2.32 (s, 3 H, pzCH_3), 2.28 – 2.17 (m, 2 H, Cy), 2.05 (s, 6 H, pzCH_3, coincident), 2.00 (s, 3 H, pzCH_3), 1.68 – 1.10 (m, 9 H, Cy). ^{13}C{^{1}H} NMR (C_6D_6) δ/ppm: 292.2 (d, W≡C, $^1J_{PC}$ = 99.9, $^1J_{WC}$ = 193.6), 227.2 (CO, $^1J_{WC}$ = 165.7), 225.8 (CO, $^1J_{WC}$ = 166.9), 152.7 (1 C), 152.2 (2 C, coincident), 145.3 (1 C), 144.7 (1 C), 144.5 (1 C) [C^{3,5}(pz)], 107.3 (1 C), 107.1 (2 C, coincident) [C^4(pz)], 46.1 [d, C^1(Cy), $^1J_{PC}$ = 30.2], 29.0 [d, C^{2,3,5,6}(Cy), J_{PC} = 16.7], 28.7 [d, C^{2,3,5,6}(Cy), J_{PC} = 10.4], 27.1 [d, C^{2,3,5,6}(Cy), J_{PC} = 12.6], 27.0 [d, C^{2,3,5,6}(Cy), J_{PC} = 8.8], 26.3 [C^4(Cy)], 17.5 (1 C), 17.4 (1 C), 15.2 (1 C), 12.5 (2 C, coincident), 12.5 (1 C) (pzCH_3). ^{31}P{^{1}H} NMR ($CDCl_3$) δ/ppm: 121.1 ($^2J_{WP}$ = 69.0). ^{31}P{^{1}H} NMR (C_6D_6) δ/ppm: 120.2 ($^2J_{WP}$ = 67.9). Anal. found: C, 41.79; H, 5.12; N, 11.61%. Calcd. for $C_{24}H_{33}BClN_6O_2PW$: C, 41.26; H, 4.76; N, 12.03%.

Synthesis of [W(≡CPCl$_2$)(CO)$_2$(Tp*)] (17)

A solution of [W(≡CBr)(CO)$_2$(Tp*)] (0.150 g, 0.238 mmol) in THF (20 mL) was cooled to –78°C and treated with ^{n}BuLi (0.53 mL, 0.45 M in hexanes, 0.24 mmol). The resulting light brown solution was stirred for 20 minutes and then treated with PCl_3 (0.79 mL, 0.30 M in hexanes, 0.24 mmol). The solution instantly turned red and was stirred for a further 30 minutes then allowed to warm to room temperature. Volatiles were removed under reduced pressure. The product was extracted with benzene and the solvent was removed under reduced pressure to afford crude **17** as a dark red solid (ca.

90% **17** by $^{31}P\{^{1}H\}$ NMR spectroscopy). Yield 0.121 g (0.186 mmol, 78%). Limited spectroscopic data for the crude product are given here. IR (THF) ν/cm^{-1}: 2552 w (BH), 2005 s, 1920 vs (CO). ^{1}H NMR (C_6D_6) δ/ppm: 5.48 (s, 2 H, pzH), 5.30 (s, 1 H, pzH), 2.58 (s, 6 H, pzCH_3), 2.22 (s, 3 H, pzCH_3), 2.04 (s, 6 H, pzCH_3), 1.96 (s, 3 H, pzCH_3). $^{31}P\{^{1}H\}$ NMR (C_6D_6) δ/ppm: 136.2 ($^{2}J_{WP}$ = 80.5).

Synthesis of [W{≡CPCl(NEt$_2$)}(CO)$_2$(Tp*)] (18)

A solution of [W(≡CBr)(CO)$_2$(Tp*)] (174 mg, 0.277 mmol) in THF (10 mL) was cooled to −78°C and treated with ^{n}BuLi (0.16 mL, 1.7 M in hexanes, 0.27 mmol). The resulting light brown solution was stirred for one hour and then treated with $PCl_2(NEt_2)$ (0.04 mL, 0.3 mmol). The solution instantly turned dark red and was stirred for a further 60 minutes then allowed to warm to room temperature. Volatiles were removed under reduced pressure and the solid residue was extracted with ^{n}pentane (25 mL, then 3 × 10 mL) and the solution was collected by cannula filtration. Concentration under reduced pressure then cooling to −78°C did not result in precipitation of the product. Limited spectroscopic data for the crude product (ca. 80% by $^{31}P\{^{1}H\}$ NMR spectroscopy) are given here. IR (THF) ν/cm^{-1}: 2551 w (BH), 1993 vs, 1904 vs (CO). ^{1}H NMR (C_6D_6) δ/ppm: 5.56 (s, 1 H, pzH), 5.55 (s, 1 H, pzH), 5.31 (s, 3 H, pzH), 2.82 (s, 3 H, pzCH_3), 2.71 (s, 3 H, pzCH_3), 2.32 (s, 3 H, pzCH_3), 2.05 (s, 3 H, pzCH_3), 2.03 (s, 3 H, pzCH_3), 1.99 (s, 3 H, pzCH_3), 0.96 (t, 6 H, N($CH_2C\mathit{H}_3$)$_2$, $^{3}J_{HH}$ = 15.0). Unfortunately, the ^{1}H NMR spectrum of the crude product was too complex to confidently assign the resonance attributed to N($C\mathit{H}_2CH_3$)$_2$. $^{31}P\{^{1}H\}$ NMR (C_6D_6) δ/ppm: 136.7 ($^{2}J_{WP}$ = 76.4).

Synthesis of [W{≡CPCl(N^{i}Pr$_2$)}(CO)$_2$(Tp*)] (19)

A solution of [W(≡CBr)(CO)$_2$(Tp*)] (2.000 g, 3.180 mmol) in THF (60 mL) was cooled to −78°C and treated with ^{n}BuLi (1.3 mL, 2.5 M in hexanes, 3.3 mmol). The resulting light brown solution was stirred for 20 minutes and then treated with $PCl_2(N^{i}Pr_2)$ (0.59 mL, 3.2 mmol). The solution instantly turned dark red and was stirred for a further 30 minutes then allowed to warm to room temperature. Volatiles were removed under reduced pressure. The solid residue was suspended in hexane and filtered through diatomaceous earth and the filter pad was washed with hexane and benzene until the washings were colourless. The solvent was removed under reduced pressure to afford **19** as a brown solid. Yield 2.193 g (3.102 mmol, 96%). IR (Nujol) ν/cm^{-1}: 2547 w (BH), 1988 vs, 1909 sh, 1900 vs (CO). IR (THF) ν/cm^{-1}: 2551 w (BH), 1992 vs, 1904

vs (CO). ^{1}H NMR (C_6D_6) δ/ppm: 5.57 (s, 1 H, pzH), 5.56 (s, 1 H, pzH), 5.33 (s, 1 H, pzH), 4.83 (s, br, 1 H, NCH), 3.06 (s, br, 1 H, NCH), 2.82 (s, 3 H, pzCH_3), 2.77 (s, 3 H, pzCH_3), 2.33 (s, 3 H, pzCH_3), 2.07 (s, 3 H, pzCH_3), 2.05 (s, 3 H, pzCH_3), 2.01 (s, 3 H, pzCH_3), 1.32 (m, br, 3 H, NCH(CH_3)$_2$), 1.20 (m, br, 6 H, NCH(CH_3)$_2$), 1.01 (m, br, 3 H, NCH(CH_3)$_2$). ^{1}H NMR (toluene-d_8, −60°C) δ/ppm: 5.45 (s, 1 H, pzH), 5.43 (s, 1 H, pzH), 5.19 (s, 1 H, pzH), 4.85 (m, 1 H, NCH), 2.85 (s, 3 H, pzCH_3), 2.80 (s, 3 H, pzCH_3), 2.34 (s, 3 H, pzCH_3), 1.99 (s, 3 H, pzCH_3), 1.95 (s, 3 H, pzCH_3), 1.92 (s, 3 H, pzCH_3), 1.31 (d, 3 H, NCH(CH_3)$_2$, $^{3}J_{HH}$ = 6.5), 1.20 (d, 3 H, NCH(CH_3)$_2$, $^{3}J_{HH}$ = 7.5), 1.19 (d, 3 H, NCH(CH_3)$_2$, $^{3}J_{HH}$ = 7.5), 1.00 (d, 3 H, NCH(CH_3)$_2$, $^{3}J_{HH}$ = 6.5). The other NCH resonance was obscured by the pzCH_3 resonance (ca. 2.85 ppm). ^{13}C{^{1}H} NMR (C_6D_6) δ/ppm: 291.3 (d, W≡C, $^{1}J_{PC}$ = 93.5, $^{1}J_{WC}$ = 187.2), 226.3 (CO, $^{1}J_{WC}$ = 166.9), 226.0 (CO, $^{1}J_{WC}$ = 165.5), 152.6 (1 C), 152.3 (1 C), 152.3 (1 C), 145.2 (1 C), 144.6 (1 C), 144.6 (1 C) [C^{3,5}(pz)], 107.3 (1 C), 107.1 (1 C), 107.1 (1 C) [C^{4}(pz)], 54.5 (br, NCH), 45.9 (d, br, NCH, $^{2}J_{PC}$ = 23.4), 26.9 (br, NCH(*C*H$_3$)$_2$), 24.9 (d, br, NCH(*C*H$_3$)$_2$, $^{3}J_{PC}$ = 21.9), 22.1 (br, NCH(*C*H$_3$)$_2$), 21.8 (br, NCH(*C*H$_3$)$_2$), 17.5 (1 C), 17.4 (1 C), 15.1 (1 C), 12.5 (2 C, coincident), 12.4 (1 C) (pzCH_3). ^{31}P{^{1}H} NMR (C_6D_6) δ/ppm: 130.3 ($^{2}J_{WP}$ = 81.2). Anal. found: C, 39.93; H, 4.77; N, 13.41%. Calcd. for $C_{24}H_{36}BClN_7O_2PW$: C, 40.28; H, 5.07; N, 13.70%.

Synthesis of [W(≡CPMePh)(CO)$_2$(Tp*)] (20)

A suspension of [W(≡CPClPh)(CO)$_2$(Tp*)] (0.167 g, 0.241 mmol) in Et_2O (20 mL) was cooled to –78°C and treated with MeLi (0.16 mL, 1.6 M in Et_2O, 0.26 mmol). The resulting brown suspension was stirred for one hour then allowed to warm to room temperature. The reaction mixture was chromatographed on silica using 2:1 hexane:THF as the eluent. The first yellow band containing the product was collected and the solvent removed under reduced pressure to afford **20** as a yellow powder. Yield 0.080 g (0.12 mmol, 49%). IR (Nujol) ν/cm^{-1}: 2548 w (BH), 1996 m, 1968 s, 1907 m, 1879 s (CO). IR (THF) ν/cm^{-1}: 2550 w (BH), 1995 w, 1977 s, 1905 w, sh, 1888 vs (CO). ^{1}H NMR ($CDCl_3$) δ/ppm: 7.68 – 7.62 (m, 2 H, C_6H_5), 7.40 – 7.32 (m, 3 H, C_6H_5), 5.89 (s, 1 H, pzH), 5.84 (s, 1 H, pzH), 5.74 (s, 1 H, pzH), 2.51 (s, 3 H, pzCH_3), 2.39 (s, 3 H, pzCH_3), 2.35 (s, 3 H, pzCH_3), 2.34 (s, 3 H, pzCH_3), 2.30 (s, 3 H, pzCH_3), 2.28 (s, 3 H, pzCH_3), 1.70 (d, 3 H, PCH_3, $^{2}J_{PH}$ = 3.3). ^{1}H NMR (C_6D_6) δ/ppm: 7.76 – 7.70 (m, 2 H, C_6H_5), 7.12 – 7.02 (m, 3 H, C_6H_5), 5.52 (s, 1 H, pzH), 5.48 (s, 1 H, pzH), 5.32 (s, 1 H, pzH), 2.62 (s, 3 H, pzCH_3), 2.41 (s, 3 H, pzCH_3), 2.40 (s, 3 H, pzCH_3), 2.03 (s, 3 H,

$pzCH_3$), 2.02 (s, 3 H, $pzCH_3$), 1.99 (s, 3 H, $pzCH_3$), 1.67 (d, 3 H, PCH_3, $^2J_{PH}$ = 3.6). $^{13}C\{^1H\}$ NMR ($CDCl_3$) δ/ppm: 299.3 (d, W≡C, $^1J_{PC}$ = 75.6, $^1J_{WC}$ = 184.0), 225.3 (CO, $^1J_{WC}$ = 168.2), 225.3 (CO, $^1J_{WC}$ = 168.4), 152.5 (1 C), 152.0 (1 C), 152.0 (1 C), 145.2 (1 C), 144.6 (1 C), 144.6 (1 C) [$C^{3,5}$(pz)], 137.3 [d, $C^1(C_6H_5)$, $^1J_{PC}$ = 10.3], 132.5 [d, $C^{2,3,5,6}(C_6H_5)$, J_{PC} = 19.5], 128.7 [$C^4(C_6H_5)$], 128.5 [d, $C^{2,3,5,6}(C_6H_5)$, J_{PC} = 7.5], 107.0 (1 C), 106.8 (1 C), 106.7 (1 C) [C^4(pz)], 17.0 (1 C), 16.8 (1 C), 15.2 (1 C), 12.8 (2 C, coincident), 12.7 (1 C) ($pzCH_3$), 11.5 (d, PCH_3, $^1J_{PC}$ = 13.6). $^{13}C\{^1H\}$ NMR (C_6D_6) δ/ppm: 300.9 (d, W≡C, $^1J_{PC}$ = 75.4, $^1J_{WC}$ = 184.9), 226.3 (CO, $^1J_{WC}$ = 169.0), 226.0 (CO, $^1J_{WC}$ = 169.0), 152.5 (1 C), 152.0 (1 C), 151.9 (1 C), 144.9 (1 C), 144.3 (1 C), 144.2 (1 C) [$C^{3,5}$(pz)], 138.3 [d, $C^1(C_6H_5)$, $^1J_{PC}$ = 10.6], 132.6 [d, $C^{2,3,5,6}(C_6H_5)$, J_{PC} = 19.6], 128.7 [d, $C^{2,3,5,6}(C_6H_5)$, J_{PC} = 9.1], 128.7 [$C^4(C_6H_5)$], 107.0 (1 C), 106.8 (1 C), 106.7 (1 C) [C^4(pz)], 17.0 (1 C), 17.0 (1 C), 16.9 (1 C), 12.4 (2 C, coincident), 12.3 (1 C) ($pzCH_3$), 11.6 (d, PCH_3, $^1J_{PC}$ = 15.1). $^{31}P\{^1H\}$ NMR ($CDCl_3$) δ/ppm: 9.5 ($^2J_{WP}$ = 74.0). $^{31}P\{^1H\}$ NMR (C_6D_6) δ/ppm: 9.8 ($^2J_{WP}$ = 71.2). MS-ESI(+): *m/z* 673.2 $[M + H]^+$. Accurate mass: found 673.1852 $[M + H]^+$. Calcd. for $C_{25}H_{31}{}^{11}BN_6O_2P^{184}W$: 673.1849. Anal. found: C, 44.20; H, 4.60; N, 11.75%. Calcd. for $C_{25}H_{30}BN_6O_2PW$: C, 44.67; H, 4.50; N, 12.50%.

Synthesis of $Tp^*(CO)_2W{\equiv}CP(=O)MePh$ (21)

Exposure of a C_6D_6 solution of $Tp^*(CO)_2W{\equiv}CPMePh$ to air for three days resulted in conversion to the oxide **21** as the major product (ca. 70% by $^{31}P\{^1H\}$ NMR spectroscopy). Limited spectroscopic data for the crude product are given here. ^1H NMR (C_6D_6) δ/ppm: 8.04 – 7.98 (m, 2 H, C_6H_5), 5.49 (s, 1 H, pzH), 5.40 (s, 1 H, pzH), 5.29 (s, 1 H, pzH), 2.72 (s, 3 H, $pzCH_3$), 2.30 (s, 3 H, $pzCH_3$), 2.26 (s, 3 H, $pzCH_3$), 2.03 (s, 3 H, $pzCH_3$), 2.00 (s, 3 H, $pzCH_3$), 1.95 (s, 3 H, $pzCH_3$), 1.68 (d, 3 H, PCH_3, $^2J_{PH}$ = 13.2). The other C_6H_5 resonances could not be identified as they were obscured by the C_6H_6 solvent peak. $^{31}P\{^1H\}$ NMR (C_6D_6) δ/ppm: 24.7 ($^2J_{WP}$ = 141.2). MS-ESI(+): *m/z* 689.2 $[M + H]^+$. Accurate mass: found 689.1795 $[M + H]^+$. Calcd. for $C_{25}H_{31}{}^{11}BN_6O_3P^{184}W$: 689.1789.

Synthesis of $[W\{{\equiv}CP(C{\equiv}CPh)Ph\}(CO)_2(Tp^*)]$ (22)

A solution of $[W({\equiv}CPClPh)(CO)_2(Tp^*)]$ (0.200 g, 0.289 mmol) in THF (10 mL) was cooled to –78°C and treated with LiC≡CPh (1.6 mL, 0.18 M in THF, 0.29 mmol). The resulting orange solution was stirred for 40 minutes then allowed to warm to room

temperature and stirred for a further hour. The volatiles were removed under reduced pressure. The residue was chromatographed on silica using hexane as the eluent and increasing the polarity to 1:1 CH_2Cl_2:hexane. The first orange fraction was collected and the solvent was removed under reduced pressure to afford **22** as an orange powder. Crystals suitable for crystallographic analysis were grown from a solution of **22** in benzene/hexane. Yield 0.196 g (0.258 mmol, 90%). IR (Nujol) ν/cm^{-1}: 2549 w (BH), 2162 w (C≡C), 1981 s, 1890 s, br (CO). IR (THF) ν/cm^{-1}: 2550 w (BH), 2160 w (C≡C), 1983 s, 1896 vs (CO). ^{1}H NMR ($CDCl_3$) δ/ppm: 7.90 (m, 2 H, C_6H_5), 7.60 (m, 2 H, C_6H_5), 7.42 (m, 3 H, C_6H_5), 7.37 (m, 3 H, C_6H_5), 5.92 (s, 1 H, pzH), 5.90 (s, 1 H, pzH), 5.78 (s, 1 H, pzH), 2.54 (s, 3 H, $pzCH_3$), 2.48 (s, 3 H, $pzCH_3$), 2.43 (s, 3 H, $pzCH_3$), 2.39 (s, 6 H, $pzCH_3$), 2.35 (s, 3 H, $pzCH_3$). ^{13}C{^{1}H} NMR ($CDCl_3$) δ/ppm: 281.5 (d, W≡C, $^1J_{PC}$ = 75.9, $^1J_{WC}$ = 192.1), 224.4 (CO, $^1J_{WC}$ = 166.9), 224.3 (CO, $^1J_{WC}$ = 167.0), 152.6 (1 C), 152.2 (2 C, coincident), 145.4 (1 C), 144.6 (1 C), 144.6 (1 C) [$C^{3,5}$(pz)], 133.9 [d, C^1{P(C_6H_5)}, $^1J_{PC}$ = 3.0], 133.2 [d, $C^{2,3,5,6}${P(C_6H_5)}, J_{PC} = 22.0], 131.9 [$C^{2,3,5,6}${CC(C_6H_5)}], 129.2 [C^4(C_6H_5)], 128.7 [d, $C^{2,3,5,6}${P(C_6H_5)}, J_{PC} = 8.0], 128.7 [C^4(C_6H_5)], 128.4 [$C^{2,3,5,6}${CC(C_6H_5)}], 123.3 [C^1{CC(C_6H_5)}], 107.4 (d, PC≡*C*Ph, $^2J_{PC}$ = 3.5), 106.9 (1 C), 106.6 (1 C), 106.6 (1 C) [C^4(pz)], 82.6 (d, P*C*≡CPh, $^1J_{PC}$ = 7.5), 16.9 (1 C), 16.8 (1 C), 15.2 (1 C), 12.7 (2 C, coincident), 12.7 (1 C) ($pzCH_3$). N.B. The C^4(C_6H_5) resonances could not be unambiguously assigned. ^{31}P{^{1}H} NMR ($CDCl_3$) δ/ppm: –4.0 ($^2J_{WP}$ = 82.5). MS-ESI(+): *m/z* 797.0 [M + K]$^+$, 781.5 [M + Na]$^+$, 759.5 [M + H]$^+$, 731.5 [M – CO + H]$^+$, 701.9 [M – 2 CO]$^+$. Accurate mass: found 797.1568 [M + K]$^+$. Calcd. for $C_{32}H_{32}{}^{11}BN_6O_2{}^{39}KP^{184}W$: 797.1564. Found 759.2010 [M + H]$^+$. Calcd. for $C_{32}H_{33}{}^{11}BN_6O_2P^{184}W$: 759.2005. Anal. found: C, 50.46; H, 4.46; N, 11.14%. Calcd. for $C_{32}H_{32}BN_6O_2PW$: C, 50.69; H, 4.25; N, 11.08%. Crystal data for $C_{32}H_{32}BN_6O_2PW$: M_w = 836.39, triclinic, *P*−1 (No. 2), *a* = 12.2295(5) Å, *b* = 12.8837(5) Å, *c* = 13.0374(6) Å, *α* = 66.331(2)°, *β* = 78.549(3)°, *γ* = 77.752(3)°, *V* = 1823.77(14) Å^3, *Z* = 2, ρ_{calcd} = 1.523 Mg m^{-3}, *μ*(Mo Kα) = 3.25 mm^{-1}, *T* = 200(2) K, orange prism, 0.16 × 0.07 × 0.06 mm, 6448 independent reflections. F^2 refinement, *R* = 0.041, *wR* = 0.082 for 5307 reflections ($I > 2\sigma(I)$, $2\theta_{max}$ = 50°), 442 parameters.

Synthesis of [W{≡CP(OPh)Ph}(CO)$_2$(Tp*)] (23)

A solution of [W(≡CPClPh)(CO)$_2$(Tp*)] (0.099 g, 0.14 mmol) in THF (2 mL) was cooled to 0°C and treated with KOPh (0.020 g, 0.15 mmol) in THF (1 mL). The resulting orange-brown solution was stirred for 30 minutes then allowed to warm to

room temperature and stirred for a further 30 minutes. The solvent was removed under reduced pressure. The residue was dissolved in benzene, filtered through diatomaceous earth and washed through with benzene until the washings were colourless. The filtrate was concentrated to ca. 0.5 mL and hexane (2 mL) was added with stirring. The orange suspension was cooled to –50°C and filtered to yield a bright orange solution. The solvent was removed under reduced pressure to afford **23** as an orange solid. Yield 47 mg (0.063 mmol, 44%). IR (Nujol) ν/cm^{-1}: 2551 w (BH), 2004 s, 1984 s, 1915 s, 1893 s (CO). IR (THF) ν/cm^{-1}: 2550 w (BH), 1987 s, 1900 vs (CO). ^{1}H NMR (C_6D_6) δ/ppm: 7.94 (m, 2 H, C_6H_5), 7.33 – 6.80 (m, 8 H, C_6H_5), 5.51 (s, 1 H, pzH), 5.49 (s, 1 H, pzH), 5.30 (s, 1 H, pzH), 2.62 (s, 3 H, pzCH_3), 2.52 (s, 3 H, pzCH_3), 2.31 (s, 3 H, pzCH_3), 2.04 (s, 3 H, pzCH_3), 2.03 (s, 3 H, pzCH_3), 1.98 (s, 3 H, pzCH_3). ^{1}H NMR ($CDCl_3$) δ/ppm: 7.75 – 6.81 (m, 10 H, C_6H_5), 5.86 (s, 1 H, pzH), 5.83 (s, 1 H, pzH), 5.71 (s, 1 H, pzH), 2.44 (s, 3 H, pzCH_3), 2.35 (s, 3 H, pzCH_3), 2.33 (s, 9 H, pzCH_3), 2.23 (s, 3 H, pzCH_3). ^{13}C{^{1}H} NMR (C_6D_6) δ/ppm:[†] 294.8 (d, W≡C, $^{1}J_{PC}$ = 42.5, $^{1}J_{WC}$ = 185.1), 225.8 (CO, $^{1}J_{WC}$ = 167.0), 225.6 (CO, $^{1}J_{WC}$ = 167.0), 152.7 (1 C), 152.2 (1 C), 152.1 (1 C), 145.1 (1 C), 144.4 (1 C), 144.3 (1 C) [$C^{3,5}$(pz)], 158.0 [d, C^{1}(POC_6H_5), $^{1}J_{PC}$ = 10.1], 141.0 [d, C^{1}(PC_6H_5), $^{1}J_{PC}$ = 16.1], 130.9 [d, $C^{2,3,5,6}$(PC_6H_5), J_{PC} = 22.1], 129.7 [$C^{3,5}$(POC_6H_5)], 129.7 [C^{4}(PC_6H_5)], 128.8 [d, $C^{2,3,5,6}$(C_6H_5), J_{PC} = 8.0], 122.6 [C^{4}(POC_6H_5)], 119.3 [d, $C^{2,6}$(POC_6H_5), J_{PC} = 10.1], 107.2 (1 C), 106.9 (1 C), 106.9 (1 C) [C^{4}(pz)], 17.1 (1 C), 16.9 (1 C), 15.1 (1 C), 12.4 (2 C, coincident), 12.4 (1 C) (pzCH_3). ^{31}P{^{1}H} NMR (C_6D_6) δ/ppm: 127.3 ($^{2}J_{WP}$ = 74.0). ^{31}P{^{1}H} NMR ($CDCl_3$) δ/ppm: 126.4 ($^{2}J_{WP}$ = 76.2). MS-ESI(+): *m/z* 807.7 [M + O + MeCN]$^{+}$, 789.6 [M + O + Na]$^{+}$, 767.6 [M + O + H]$^{+}$. Accurate mass: found 789.1725 [M + O + Na]$^{+}$. Calcd. for $C_{30}H_{32}{}^{11}BN_6O_4{}^{23}NaP^{184}W$: 789.1723. Found 807.2098 [M + O + MeCN]$^{+}$. Calcd. for $C_{32}H_{35}{}^{11}BN_7O_4P^{184}W$: 807.2091. Anal. found: C, 48.02; H, 4.32; N, 11.24%. Calcd. for $C_{30}H_{32}BN_6O_3PW$: C, 48.03; H, 4.30; N, 11.20%.

Synthesis of [W{≡CPMe(N^{i}Pr$_2$)}(CO)$_2$(Tp*)] (24)

A solution of [W{≡CPCl(N^{i}Pr$_2$)}(CO)$_2$(Tp*)] (0.150 g, 0.210 mmol) in THF (8 mL) was cooled to –78°C and treated with MeLi (0.17 mL, 1.6 M in Et_2O, 0.27 mmol). The resulting brown was stirred for two hours then allowed to warm to room temperature. The volatiles were removed under reduced pressure. The residue was chromatographed

[†] ^{13}C PC_6H_5 and POC_6H_5 resonances assigned by comparison with $P(OPh)Ph_2$[436,437] and MeOPh.[438]

on alumina using hexane as the eluent and increasing the polarity to 5:1 hexane:THF. The first yellow fraction was collected and the solvent was removed under reduced pressure to afford **24** as a yellow powder. Yield 83 mg (0.12 mmol, 57%). IR (Nujol) ν/cm^{-1}: 2542 w, (BH), 1987 m, 1972 s, 1957 sh, 1902 m, 1883 s, 1862 m (CO). IR (THF) ν/cm^{-1}: 2551 w (BH), 1974 vs, 1884 vs (CO). ^{1}H NMR (C_6D_6) δ/ppm: 5.56 (s, 1 H, pzH), 5.55 (s, 1 H, pzH), 5.36 (s, 1 H, pzH), 3.60 (m, 2 H, NCH), 2.85 (s, 3 H, pzCH_3), 2.71 (s, 3 H, pzCH_3), 2.43 (s, 3 H, pzCH_3), 2.09 (s, 3 H, pzCH_3), 2.07 (s, 3 H, pzCH_3), 2.03 (s, 3 H, pzCH_3), 1.52 (d, 3 H, PCH_3, $^{2}J_{PH}$ = 6.4), 1.40 (d, 6 H, NCH(CH_3)$_2$, $^{3}J_{HH}$ = 6.8), 1.05 (d, 6 H, NCH(CH_3)$_2$, $^{3}J_{HH}$ = 6.8). ^{13}C{^{1}H} NMR (C_6D_6) δ/ppm: 312.8 (d, W≡C, $^{1}J_{PC}$ = 80.5, $^{1}J_{WC}$ = 178.1), 227.5 (CO, $^{1}J_{WC}$ = 171.0), 227.0 (CO, $^{1}J_{WC}$ = 171.0), 152.5 (1 C), 152.2 (1 C), 152.0 (1 C), 144.7 (1 C), 144.3 (1 C), 144.2 (1 C) [C^{3,5}(pz)], 107.0 (1 C), 106.8 (1 C), 106.7 (1 C) [C^{4}(pz)], 48.6 (br, NCH), 24.7 (d, NCH(*C*H$_3$)$_2$, $^{3}J_{PC}$ = 7.6), 24.4 (d, NCH(*C*H$_3$)$_2$, $^{3}J_{PC}$ = 5.6), 17.5 (d, pzCH_3, $^{5}J_{PC}$ = 1.4), 17.4 (d, pzCH_3, $^{5}J_{PC}$ = 4.4), 15.4 (d, PCH_3, $^{1}J_{PC}$ = 18.5), 15.2 (1 C), 12.5 (1 C), 12.5 (1 C), 12.4 (pzCH_3). ^{31}P{^{1}H} NMR (C_6D_6) δ/ppm: 54.0 ($^{2}J_{WP}$ = 77.5). MS-ESI(+): *m/z* 696.3 [M + H]$^{+}$. Accurate mass: found 696.2589 [M + H]$^{+}$. Calcd. for $C_{25}H_{40}{}^{11}BN_7O_2P^{184}W$: 696.2584. Anal. found: C, 43.17; H, 5.80; N, 13.98%. Calcd. for $C_{25}H_{39}BN_7O_2PW$: C, 43.19; H, 5.65; N, 14.10%.

Synthesis of [W{≡CP(N^{i}Pr$_2$)}(CO)$_2$(Tp*)]AlCl$_4$ ([25]AlCl$_4$)

In a glove box [W{≡CPCl(N^{i}Pr$_2$)}(CO)$_2$(Tp*)] (0.030 g, 0.042 mmol) and freshly sublimed $AlCl_3$ (0.016 g, 0.12 mmol) were dissolved in CD_2Cl_2 (0.5 mL) in an NMR tube, resulting in a brown solution. After 45 minutes the ^{31}P{^{1}H} NMR spectrum indicated that [**25**]$AlCl_4$ was the major product (ca. 82% by ^{31}P{^{1}H} NMR spectroscopy). Unfortunately, the ^{1}H NMR spectrum of the crude product was too complex for resonances attributed to [**25**]$AlCl_4$ to be confidently assigned. ^{31}P{^{1}H} NMR (C_6D_6) δ/ppm: 54.0 ($^{2}J_{WP}$ = 77.5).

Synthesis of [W{≡CP(N^{i}Pr$_2$)(CPhCPh)}(CO)$_2$(Tp*)]AlCl$_4$ ([26]AlCl$_4$)

In a glove box [W{≡CPCl(N^{i}Pr$_2$)}(CO)$_2$(Tp*)] (0.030 g, 0.042 mmol), freshly sublimed $AlCl_3$ (8 mg, 0.06 mmol) and diphenylacetylene (8 mg, 0.05 mmol) were dissolved in CD_2Cl_2 (0.5 mL). The resultant brown solution was transferred to an NMR tube. After two days ^{1}H and ^{31}P{^{1}H} NMR spectroscopy indicated formation of [**26**]$AlCl_4$ as the major product (ca. 80%). ^{1}H NMR (CD_2Cl_2) δ/ppm: 6.10 (s, 2 H, pzH), 5.83 (s, 1 H,

pzH), 3.72 (m, br, 2 H, NCH), 2.58 (s, 6 H, $pzCH_3$), 2.44 (s, 6 H, $pzCH_3$), 2.33 (s, 3 H, $pzCH_3$), 2.26 (s, 3 H, $pzCH_3$), 1.50 (d, 6 H, $NCH(CH_3)_2$, $^3J_{HH}$ = 6.4), 1.28 (d, 6 H, $NCH(CH_3)_2$, $^3J_{HH}$ = 6.8). The Ph resonances could not be unambiguously identified (probably due to the presence of unreacted diphenylacetylene). $^{31}P\{^1H\}$ NMR (CD_2Cl_2) δ/ppm: −77.3 ($^2J_{WP}$ = 219.9).

CHAPTER 4. Secondary phosphinocarbyne complexes

Synthesis of [W(≡CPHPh)(CO)$_2$(Tp*)] (27)

A solution of [W(≡CBr)(CO)$_2$(Tp*)] (1.000 g, 1.590 mmol) in THF (50 mL) was cooled to –78°C and treated with ^{n}BuLi (0.64 mL, 2.5 M in hexanes, 1.6 mmol). The resulting light brown solution was stirred for 30 minutes and then treated with PCl_2Ph (1.6 mL, 0.99 M in THF, 1.6 mmol). The solution instantly turned dark red and was stirred for a further 25 minutes then allowed to warm to room temperature and stirred for 20 minutes. The solution was cooled to –78°C and treated with Li[$BHEt_3$] (1.6 mL, 1.0 M in THF, 1.6 mmol). The resultant orange-brown solution was stirred for 20 minutes then allowed to warm to room temperature. Volatiles were removed under reduced pressure. The residue was suspended in toluene and filtered through diatomaceous earth. The filter pad was washed with toluene until the washings were colourless. The solvent was removed under reduced pressure to afford crude **27** as a dark red powder. $^{31}P\{^1H\}$ NMR spectroscopy indicated that the crude product contained 89% **27**. Crude yield 0.965 g (1.47 mmol, 92%).

Further purification may be achieved by cryostatic chromatography, but significant losses of product are encountered during chromatography. A sample of crude **27** (1.5 mmol, containing 61% **27** by $^{31}P\{^1H\}$ NMR spectroscopy) was chromatographed on silica gel at –40°C using hexane as the initial eluent then increasing the polarity to 2:1 toluene:hexane. The first yellow fraction (containing the product) was collected and the solvent was removed under reduced pressure to afford **27** as a yellow powder. A second orange fraction was collected which contained a mixture of **27** (15.4%), [W(μ-C_2PPh)(CO)$_2$(Tp*)] (30.9%) and an unidentified species (δ_P 22.8, J_{WP} = 68.5 Hz, 53.7%). Removal of the solvent from fraction one under reduced pressure afforded **27** as a yellow powder. Yield 0.198 g (0.301 mmol, 20%).

IR (Nujol) ν/cm^{-1}: 2547 w, 2531 sh (BH), 2269 vw, 2244 vw, 2222 vw (PH), 2000 m, 1977 vs, 1911 m, 1895 vs, 1879 vs, 1865 sh (CO). IR (THF) ν/cm^{-1}: 2549 w (BH), 2257 vw (PH), 1980 s, 1892 vs (CO). ^{1}H NMR (C_6D_6) δ/ppm: 7.67 – 7.63 (m, 2 H, C_6H_5), 7.10 – 7.02 (m, 3 H, C_6H_5), 5.81 (d, 1 H, PH, $^1J_{PH}$ = 222.7, $^3J_{WH}$ = 7.8), 5.51 (s, 1 H, pzH), 5.50 (s, 1 H, pzH), 5.31 (s, 1 H, pzH), 2.52 (s, 3 H, pzCH_3), 2.49 (s, 3 H, pzCH_3), 2.36 (s, 3 H, pzCH_3), 2.04 (s, 6 H, pzCH_3, coincident), 1.99 (s, 3 H, pzCH_3). $^{13}C\{^1H\}$ NMR (C_6D_6) δ/ppm: 289.5 (d, W≡C, $^1J_{PC}$ = 74.2, $^1J_{WC}$ = 187.8), 225.6 (CO, $^1J_{WC}$ = 167.2), 225.3 (CO, $^1J_{WC}$ = 167.6), 152.7 (1 C), 152.2 (1 C), 152.1 (1 C), 145.0 (1

C), 144.3 (1 C), 144.3 (1 C) [$C^{3,5}$(pz)], 134.6 [d, $C^{2,3,5,6}(C_6H_5)$, J_{PC} = 17.1], 132.6 [d, $C^1(C_6H_5)$, $^1J_{PC}$ = 8.9], 129.9 [d, $C^{2,3,5,6}(C_6H_5)$, J_{PC} = 6.6], 128.6 [$C^4(C_6H_5)$], 107.1 (1 C), 106.9 (1 C), 106.8 (1 C) [C^4(pz)], 16.7 (1 C), 16.7 (1 C), 15.2 (1 C), 12.4 (2 C, coincident), 12.4 (1 C) ($pzCH_3$). $^{31}P\{^1H\}$ NMR (C_6D_6) δ/ppm: −12.8 ($^2J_{WP}$ = 67.3). MS-ESI(+): *m/z* 697.1 $[M + K]^+$, 659.2 $[M + H]^+$. Accurate mass: found 697.1251 $[M + K]^+$. Calcd. for $C_{24}H_{28}{}^{11}BKN_6O_2P^{184}W$: 697.1251. Found 659.1693 $[M + H]^+$. Calcd. for $C_{24}H_{29}{}^{11}BN_6O_2P^{184}W$: 659.1692. Anal. found: C, 45.17; H, 4.38; N, 12.45%. Calcd. for $C_{24}H_{28}BN_6O_2PW$: C, 43.80; H, 4.29; N, 12.77%.

Synthesis of [W(≡CPHCy)(CO)$_2$(Tp*)] (28)

A solution of [W(≡CBr)(CO)$_2$(Tp*)] (0.400 g, 0.636 mmol) and [Pd(PPh$_3$)$_4$] (0.037 g, 0.032 mmol) in toluene (15 mL) was treated with NEt_3 (0.11 mL, 0.79 mmol) and PH_2Cy (0.94 M in hexane, 0.82 mL, 0.77 mmol). The brown solution was heated to 80°C for one hour after which time IR spectroscopy indicated complete consumption of the starting material [W(≡CBr)(CO)$_2$(Tp*)]. The mixture was allowed to cool and volatiles were removed under reduced pressure. $^{31}P\{^1H\}$ NMR spectroscopy indicated that the crude product contained ca. 88% **28**.

Further purification may be achieved by cryostatic chromatography, but significant losses of product are encountered during chromatography. The crude residue was chromatographed on silica gel at –40°C using hexane as the initial eluent before increasing the polarity to 3:2 hexane:CH_2Cl_2. An initial faint green fraction was discarded, and the second yellow fraction (containing the product) was collected. A third orange fraction was collected which contained a mixture of [W(μ-C_2PCy)(CO)$_2$(Tp*)] and PPh_3. Removal of the solvent from fraction two under reduced pressure afforded **28** as a yellow powder. Crystals suitable for crystallographic analysis were grown from a solution of **28** in a mixture of Et_2O and pentane at –24°C. Yield 0.183 g (0.276 mmol, 43%).

IR (Nujol) ν/cm^{-1}: 2547 w, 2527 w (BH), 2283 vw, 2244 vw (PH), 2000 s, 1977 s, 1911 s, 1888 s (CO). IR (THF) ν/cm^{-1}: 2550 w (BH), 2243 vw (PH), 1976 vs, 1887 vs (CO). ^1H NMR (C_6D_6) δ/ppm: 5.56 (s, 1 H, pzH), 5.54 (s, 1 H, pzH), 5.35 (s, 1 H, pzH), 4.71 (dd, 1 H, PH, $^1J_{PH}$ = 210.0, $^3J_{HH}$ = 6.0, $^3J_{WH}$ = 8.4 Hz), 2.73 (s, 3 H, $pzCH_3$), 2.68 (s, 3 H, $pzCH_3$), 2.41 (s, 3 H, $pzCH_3$), 2.23 (m, 1 H, PCH), 2.14 (m, 2 H, Cy), 2.08 (s, 3 H, $pzCH_3$), 2.07 (s, 3 H, $pzCH_3$), 2.03 (s, 3 H, $pzCH_3$), 1.66 (m, 2 H, Cy), 1.51 (m, 2 H, Cy), 1.41 (m, 1 H, Cy), 1.23 (m, 2 H, Cy), 1.15 (m, 1 H, Cy). $^{13}C\{^1H\}$ NMR (C_6D_6)

δ/ppm: 298.3 (d, W≡C, $^{1}J_{PC}$ = 76.9, $^{1}J_{WC}$ = 184.1), 227.1 (CO, $^{1}J_{WC}$ = 168.4), 225.7 (CO, $^{1}J_{WC}$ = 169.1), 152.6 (1 C), 152.3 (1 C), 152.0 (1 C), 144.9 (1 C), 144.2 (1 C), 144.1 (1 C) [$C^{3,5}$(pz)], 107.0 (1 C), 106.8 (1 C), 106.8 (1 C) [C^{4}(pz)], 35.3 [d, $C^{2,3,5,6}$(Cy), J_{PC} = 7.5], 33.5 [d, $C^{2,3,5,6}$(Cy), J_{PC} = 6.0], 32.9 [d, $C^{2,3,5,6}$(Cy), J_{PC} = 15.9], 27.4 [$C^{3,4,5}$(Cy)], 27.3 [d, C^{1}(Cy), J_{PC} = 19.6], 26.3 [$C^{3,4,5}$(Cy)], 17.0 (1 C), 16.8 (1 C), 15.2 (1 C), 12.5 (2 C, coincident), 12.4 (1 C) ($pzCH_3$). $^{31}P\{^{1}H\}$ NMR (C_6D_6) δ/ppm: −4.6 ($^{2}J_{WP}$ = 64.7). ^{31}P NMR (C_6D_6) δ/ppm: −4.5 (d, $^{1}J_{PH}$ = 209.8). MS-ESI(+): *m/z* 1327.4 $[2M - H]^+$, 665.2 $[M + H]^+$. Accurate mass: found 665.2151 $[M + H]^+$. Calcd. for $C_{24}H_{35}{}^{11}BN_6O_2P^{184}W$: 665.2162. Anal. found: C, 45.70; H, 5.20; N, 11.96%. Calcd. for $C_{24}H_{34}BN_6O_2PW$: C, 43.40; H, 5.16; N, 12.65%. Crystal data for $C_{24}H_{34}BN_6O_2PW$: M_w = 664.21, monoclinic, $P2_1/n$, a = 10.6309(2) Å, b = 14.6523(3) Å, c = 18.3905(4) Å, β = 104.4069(11)°, V = 2774.55(10) Å^3, Z = 4, ρ_{calcd} = 1.590 Mg m^{-3}, μ(Mo Kα) = 4.25 mm^{-1}, T = 200(2) K, orange block, 0.12 × 0.07 × 0.06 mm, 6380 independent reflections. F^2 refinement, R = 0.058, wR = 0.161 for 4658 reflections ($I > 2\sigma(I)$, $2\theta_{max}$ = 55°), 317 parameters.

Synthesis of [W{≡CPH(N^{i}Pr$_2$)}(CO)$_2$(Tp*)] (29) and [W{≡CPEt(N^{i}Pr$_2$)}(CO)$_2$(Tp*)] (30)

A solution of [W{≡CPCl(N^{i}Pr$_2$)}(CO)$_2$(Tp*)] (0.028 g, 0.039 mmol) in THF (1 mL) was cooled to –78°C and treated with Li[BHEt$_3$] (0.08 mL, 1.0 M in THF, 0.08 mmol). The resulting orange-brown solution was stirred for 60 minutes then allowed to warm to room temperature. Volatiles were removed under reduced pressure to afford crude **29** as a brown solid. $^{31}P\{^{1}H\}$ NMR spectroscopy indicated that the crude product contained 75% **29** and 15% **30**. Attempts to scale up the procedure (0.150 g **19**) gave **29** and **30** in 25% and 38% spectroscopic yield, respectively. As samples of reasonable purity of **29** and **30** were not obtained, only very limited spectroscopic data are available.

[W{≡CPH(N^{i}Pr$_2$)}(CO)$_2$(Tp*)] (29)

IR (THF) ν/cm^{-1}: 2550 w (BH), 1976 s, 1886 vs (CO), (ν_{PH} not unambiguously identifiable). ^{1}H NMR (C_6D_6) δ/ppm: 6.46 (d, 1 H, PH, $^{1}J_{PH}$ = 228.1), 5.55 (s, 2 H, pzH), 5.34 (s, 1 H, pzH). The pz-CH_3 and ^{i}Pr resonances could not be unambiguously identified. $^{31}P\{^{1}H\}$ NMR (C_6D_6) δ/ppm: 22.6 ($^{2}J_{WP}$ = 77.6). ^{31}P NMR (C_6D_6) δ/ppm: 22.6 (dt, $^{1}J_{PH}$ = 229.5, $^{3}J_{PH}$ = 20.8).

[W{≡CPEt(N^{i}Pr$_2$)}(CO)$_2$(Tp*)] (30)

^{31}P{^{1}H} NMR (C_6D_6) δ/ppm: 68.8 ($^2J_{WP}$ = 71.2), *cf*. 54.0 ($^2J_{WP}$ = 77.5) for [W{≡CPMe(N^{i}Pr$_2$)}(CO)$_2$(Tp*)]. ^{31}P NMR (C_6D_6) δ/ppm: 68.9 (m, br). MS-ESI(+): *m/z* 710.3 $[M + H]^+$, 726.3 $[M + H + O]^+$. Accurate mass: found 710.2739 $[M + H]^+$. Calcd. for $C_{26}H_{42}{}^{11}BN_7O_2P^{184}W$: 710.2740.

Synthesis of K[Tp*(CO)$_2$W≡CPCy] (K[31])

In a glove box [W(≡CPHCy)(CO)$_2$(Tp*)] (0.025 g, 0.038 mmol) and potassium hydride (4 mg, 0.1 mmol) were dissolved in THF to form a brown solution with visible effervescence. After five hours ^{31}P{^{1}H} NMR spectroscopy indicated formation of K[**31**] as the major product (ca. 90% by ^{31}P{^{1}H} NMR spectroscopy). Limited spectroscopic data are given below. Unfortunately, the extreme sensitivity of K[**31**] made acquisition of more complete spectroscopic data difficult due to the persistent formation of **28**. IR (THF) ν/cm^{-1}: 1862 vs, 1753 vs (CO), (ν_{BH} not unambiguously identifiable). ^{31}P{^{1}H} NMR (THF-d_8) δ/ppm: 115.3 (br).

Synthesis of K[W(CPPh)(CO)$_2$(Tp*)] (K[32])

In a glove box [W(≡CPHPh)(CO)$_2$(Tp*)] (0.050 g, 0.076 mmol) and potassium hydride (8 mg, 0.2 mmol) were dissolved in THF-d_8 to form a dark red solution with visible effervescence. After 15 minutes the solution was transferred to an NMR tube. After 2.5 hours, ^{1}H and ^{31}P{^{1}H} NMR spectroscopy indicated quantitative formation of K[**32**]. IR (THF) ν/cm^{-1}: 1889 vs, 1877 s, 1771 vs (CO), (ν_{BH} not unambiguously identifiable). ^{1}H NMR (THF-d_8) δ/ppm: 7.50 (m, 2 H, C_6H_5), 6.91 (m, 2 H, C_6H_5), 6.69 (m, 1 H, C_6H_5), 5.72 (s, 2 H, pzH), 5.66 (s, 1 H, pzH), 2.53 (s, 6 H, pzCH_3), 2.41 (s, 3 H, pzCH_3), 2.36 (s, 6 H, pzCH_3), 2.31 (s, 3 H, pzCH_3). ^{13}C{^{1}H} NMR (THF-d_8) δ/ppm: 358.9 (d, W≡C, $^1J_{PC}$ = 100.6, $^1J_{WC}$ = 183.1), 234.7 (CO, $^1J_{WC}$ = 175.1), 152.4 (2 C), 143.4 (1 C) [$C^{3,5}$(pz)], 147.5 [d, $C^1(C_6H_5)$, $^1J_{PC}$ = 58.4], 130.9 [d, $C^{2,3,5,6}(C_6H_5)$, J_{PC} = 16.1], 128.8 [$C^{2,3,5,6}(C_6H_5)$], 127.2 [$C^4(C_6H_5)$], 106.0 (3 C, coincident) [C^4(pz)], 17.3 (2 C), 15.7 (1 C), 12.5 (2 C), 12.3 (1 C) (pzCH_3). ^{31}P{^{1}H} NMR (THF-d_8) δ/ppm: 81.9 ($^2J_{WP}$ = 47.0).

Synthesis of [K(2.2.2-cryptand)][W(CPPh)(CO)$_2$(Tp*)] ([K(2.2.2-cryptand)][32])

In a glove box excess 2.2.2-cryptand was added to a solution of K[**32**] in THF. The dark red solution was filtered, layered with Et_2O and stored at −25°C to provide dark purple crystals of [K(2.2.2-cryptand)][W(CPPh)(CO)$_2$(Tp*)] suitable for crystallographic

analysis. Crystal data for $C_{24}H_{27}BN_6O_2PW \cdot KC_{18}H_{36}N_2O_6$: M_w = 1072.74, monoclinic, $P2_1/n$, a = 14.6929(3) Å, b = 23.4328(5) Å, c = 15.9038(3) Å, β = 95.3960(18)°, V = 5451.35(19) Å^3, Z = 4, ρ_{calcd} = 1.307 Mg m^{-3}, μ(Cu Kα) = 5.30 mm^{-1}, T = 150(2) K, dark purple needle, 0.13 × 0.07 × 0.06 mm, 10683 independent reflections. F^2 refinement, R = 0.061, wR = 0.112 for 9566 reflections ($I > 2\sigma(I)$, $2\theta_{max}$ = 144°), 559 parameters.

CHAPTER 5. Bi- and polymetallic phosphinocarbyne complexes

Synthesis of $[W_2(\mu\text{-}C_2PPh)(CO)_4(Tp^*)_2]$ (33)

A solution of $[W(\equiv CBr)(CO)_2(Tp^*)]$ (1.000 g, 1.596 mmol) and $[Pd(PPh_3)_4]$ (0.088 g, 0.076 mmol, 5 mol% - not optimised) in benzene (40 mL) was treated with triethylamine (0.26 mL, 1.9 mmol) and phenylphosphine (1.25 mL, 0.63 M in hexane, 0.788 mmol) and the reaction mixture was heated to reflux. After 18 hours the dark brown solution was allowed to cool and the solvent was removed under reduced pressure. The crude mixture was chromatographed on silica gel using hexane as the eluent initially, then increasing the polarity to 2:1 toluene:hexane. The initial yellow and brown fractions were collected and discarded, and the following major red-orange band containing the product was collected. The solvent was removed under reduced pressure and the residue was dissolved in CH_2Cl_2. EtOH was added and the solution was concentrated on the rotary evaporator to afford **33** as an orange powder. Crystals suitable for crystallographic analysis were grown from a solution of **33** in benzene/Et_2O/pentane at –20°C. Yield 0.640 g (0.531 mmol, 67%). IR (Nujol) ν/cm^{-1}: 2549 w (BH), 2010 sh, 1997 s, 1980 s, 1970 s, 1913 s, br 1887 s (CO). IR (THF) ν/cm^{-1}: 2548 w (BH), 1984 vs, 1974 vs, 1892 vs (CO). ^{1}H NMR (C_6D_6) δ/ppm: 8.09 (m, 2 H, C_6H_5), 7.22 (m, 2 H, C_6H_5), 7.08 (m, 1 H, C_6H_5), 5.50 (s, 4 H, pzH), 5.33 (s, 2 H, pzH), 2.51 (s, 12 H, pzCH_3), 2.34 (s, 6 H, pzCH_3), 2.07 (s, 12 H, pzCH_3), 2.01 (s, 6 H, pzCH_3). ^{13}C{^{1}H} NMR (C_6D_6) δ/ppm: 285.0 (d, W≡C, $^1J_{PC}$ = 78.6, $^1J_{WC}$ = 192.4), 226.4 (br, CO, $^1J_{WC}$ = 161.1), 152.7 (4 C), 152.5 (2 C), 144.8 (2 C), 143.9 (4 C) [C^{3,5}(pz)], 133.4 (d, J_{PC} = 19.6, C_6H_5), 128.8, 128.7 (C_6H_5, multiplicities and couplings unknown as the rest of the C_6H_5 peaks are obscured by the C_6D_6 peak), 107.0 (2 C), 106.7 (4 C) [C^4(pz)], 16.9 (4 C), 15.1 (2 C), 12.4 (2 C), 12.3 (4 C) (pzCH_3). ^{31}P{^{1}H} NMR (C_6D_6) δ/ppm: 80.4 ($^2J_{WP}$ = 76.2). MS-ESI(+): *m/z* 1245.3 $[M + K]^+$, 1222.3 $[M + O]^+$. Accurate mass: found 1245.2579 $[M + K]^+$. Calcd. for $C_{42}H_{49}{}^{11}B_2{}^{39}KN_{12}O_4P^{184}W_2$: 1245.2580. Anal. found: C, 42.10; H, 4.06; N, 13.93%. Calcd. for $C_{42}H_{49}B_2N_{12}O_4PW_2$: C, 41.82; H, 4.09; N, 13.93%. Calcd. for $C_{42}H_{49}B_2N_{12}O_4PW_2\cdot(C_5H_{12})_{0.25}$: C, 42.43; H, 4.28; N, 13.73%. Crystal data for $C_{42}H_{49}B_2N_{12}O_4PW_2\cdot(C_5H_{12})_{0.25}$: M_w = 1224.27, triclinic, P – 1 (No. 2), a = 10.5139(4) Å, b = 21.4625(9) Å, c = 24.2130(9) Å, α = 66.375(4)°, β = 88.740(3)°, γ = 84.806(3)°, V = 4984.6(4) Å^3, Z = 4, ρ_{calcd} = 1.631 Mg m^{-3}, μ(Mo Kα) = 4.70 mm^{-1}, T = 150(2) K, orange block, 0.24 × 0.12 × 0.07 mm,

23071 independent reflections. F^2 refinement, R = 0.065, wR = 0.141 for 13731 reflections ($I > 2\sigma(I)$, $2\theta_{max}$ = 59.5°), 1180 parameters.

Synthesis of [W$_2$(μ-C$_2$PCy)(CO)$_4$(Tp*)$_2$] (34)

A solution of [W(≡CBr)(CO)$_2$(Tp*)] (0.250 g, 0.397 mmol) in THF (10 mL) was cooled to –78°C and treated with ^{n}BuLi (2.5 M in hexanes, 0.16 mL, 0.40 mmol). The resulting light brown solution was stirred for 50 minutes and then treated with PCl$_2$Cy (1.0 M in THF, 0.20 mL, 0.20 mmol). The solution instantly turned red and was stirred for a further 30 minutes then allowed to warm to room temperature. Volatiles were removed under reduced pressure. The residue was chromatographed on silica using hexane as the eluent. The polarity was gradually increased to 2:1 hexane:THF. The first yellow band (containing [W(≡CBr)(CO)$_2$(Tp*)]) was discarded, and the second (orange) band containing the product was collected. The solvent was removed under reduced pressure to afford **34** as a red-orange powder. Crystals suitable for crystallographic analysis were grown from a solution of **34** in benzene/hexane at –12°C. Yield 0.136 g (0.121 mmol, 57%). IR (Nujol) ν/cm^{-1}: 2546 w (BH), 2000 sh, 1990 s, 1981 s, 1967 s, 1905 s, 1883 s (CO). IR (THF) ν/cm^{-1}: 2548 w (BH), 1980 m, 1969 s, 1888 vs (CO). ^{1}H NMR (C$_6$D$_6$) δ/ppm: 5.45 (s, 4 H, pzH), 5.32 (s, 2 H, pzH), 2.63 (s, 12 H, pzCH$_3$), 2.37 (s, 6 H, pzCH$_3$), 2.26 – 2.11 (m, 2 H, Cy), 2.08 (s, 12 H, pzCH$_3$), 2.01 (s, 6 H, pzCH$_3$), 1.68 – 1.13 (m, 9 H, Cy). ^{13}C{^{1}H} NMR (C$_6$D$_6$) δ/ppm: 291.1 (d, W≡C, $^1J_{PC}$ = 80.3, $^1J_{WC}$ = 190.1), 227.1 (br, CO), 152.6 (4 C), 152.5 (2 C), 144.8 (2 C), 143.7 (4 C) [C^{3,5}(pz)], 107.0 (2 C), 106.7 (4 C) [C^4(pz)], 41.2 [d, C^{1,2,3,5,6}(Cy), J_{PC} = 11.2], 31.3 [d, C^{1,2,3,5,6}(Cy), J_{PC} = 12.2], 27.4 [d, C^{1,2,3,5,6}(Cy), J_{PC} = 11.8], 26.6 [C^4(Cy)], 17.0 (4 C), 15.2 (2 C), 12.5 (4 C), 12.3 (2 C) (pzCH$_3$). ^{31}P{^{1}H} NMR (C$_6$D$_6$) δ/ppm: 89.9 ($^2J_{WP}$ = 67.5). ^{31}P{^{1}H} NMR (CDCl$_3$) δ/ppm: 87.8 ($^2J_{WP}$ = 68.0). MS-ESI(+): *m/z* 1213.3 [M + H]$^+$. Accurate mass: found 1213.3494 [M + H]$^+$. Calcd. for C$_{42}$H$_{56}$^{11}B$_2$N$_{12}$O$_4$P^{184}W$_2$: 1213.3490. Anal. found: C, 41.79; H, 4.67; N, 13.62%. Calcd. for C$_{42}$H$_{55}$B$_2$N$_{12}$O$_4$PW$_2$: C, 41.61; H, 4.57; N, 13.86%. Crystal data for C$_{42}$H$_{55}$B$_2$N$_{12}$O$_4$PW$_2$·C$_6$H$_6$: M_w = 1290.39, monoclinic, $P2_1/c$, a = 24.2055(3) Å, b = 10.4092(1) Å, c = 25.5107(3) Å, β = 105.9841(6)°, V = 6179.17(12) Å^3, Z = 4, ρ_{calcd} = 1.387 Mg m^{-3}, μ(Mo Kα) = 3.79 mm^{-1}, T = 200(2) K, orange plate, 0.19 × 0.18 × 0.09 mm, 14148 independent reflections. F^2 refinement, R = 0.038, wR = 0.100 for 10493 reflections ($I > 2\sigma(I)$, $2\theta_{max}$ = 55°), 622 parameters.

Synthesis of $[W_2(\mu\text{-}C_2PCl)(CO)_4(Tp^*)_2]$ (35)

A solution of $[W(\equiv CBr)(CO)_2(Tp^*)]$ (0.100 g, 0.159 mmol) in THF (5 mL) was cooled to –78°C and treated with ^{n}BuLi (0.45 M in hexanes, 0.42 mL, 0.19 mmol). The resulting light brown solution was stirred for 30 minutes and then treated with PCl_3 (0.30 M in hexane, 0.27 mL, 0.081 mmol). The solution instantly turned dark red and was stirred for a further 30 minutes then allowed to warm to room temperature. Volatiles were removed under reduced pressure. The residue was extracted with benzene (5 mL), filtered and the solvent was removed under reduced pressure to afford crude **35** as a dark red solid (ca. 72% **35** and ca. 12% **36** by $^{31}P\{^1H\}$ NMR spectroscopy). Yield 0.083 g (0.071 mmol, 90%). IR (THF) ν/cm^{-1}: 2550 w (BH), 1996 s, 1986 s, 1906 vs (CO). ^1H NMR (C_6D_6) δ/ppm: 5.48 (s, 4 H, pzH), 5.32 (s, 2 H, pzH), 2.69 (s, 6 H, pzCH_3), 2.54 (s, 6 H, pzCH_3), 2.31 (s, 6 H, pzCH_3), 2.09 (s, 12 H, pzCH_3), 2.02 (s, 6 H, pzCH_3). $^{13}C\{^1H\}$ NMR (C_6D_6) δ/ppm: 280.0 (d, W≡C, $^1J_{PC}$ = 97.9, $^1J_{WC}$ = 194.0), 226.4 (CO, $^1J_{WC}$ = 164.5), 225.0 (CO, $^1J_{WC}$ = 166.0), 152.8 (2 C), 152.6 (2 C), 152.2 (2 C), 145.4 (2 C), 144.4 (2 C), 144.3 (2 C) [$C^{3,5}$(pz)], 107.4 (2 C), 106.9 (4 C) [C^4(pz)], 17.3 (2 C), 17.0 (2 C), 15.2 (2 C), 12.6 (4 C), 12.5 (2 C) (pzCH_3). $^{31}P\{^1H\}$ NMR (C_6D_6) δ/ppm: 124.9 ($^2J_{WP}$ = 66.4).

Synthesis of $[W_2\{\mu\text{:}\eta^1\text{-}C;\eta^2\text{-}C,P\text{-}CC(PCl)\}(CO)_4(Tp^*)_2]$ (36)

A solution of $[W_2(\mu\text{-}C_2PCl)(CO)_4(Tp^*)_2]$ (0.083 g, 0.071 mmol) in C_6D_6 (0.5 mL) was heated to 50°C. After 13 hours $^{31}P\{^1H\}$ NMR spectroscopy of the dark magenta solution indicated formation of **36** as the major product (ca. 75% by $^{31}P\{^1H\}$ NMR spectroscopy). Crystals suitable for crystallographic analysis were grown by slow diffusion of ^{n}pentane into a solution of **36** in CH_2Cl_2 at –15°C. Unfortunately, the ^1H NMR spectra obtained of samples of **36** were either too complex (due to the impure nature of the sample), or the peaks were significantly broadened (presumably due to the presence of the insoluble side-products that form during the conversion of **35** to **36**) such that analysis was not possible. $^{31}P\{^1H\}$ NMR (C_6D_6) δ/ppm: 92.7 (br). Crystal data for $C_{36}H_{44}B_2ClN_{12}O_4PW_2\cdot(CH_2Cl_2)_2$: M_w = 1334.44, monoclinic, $P2_1/c$, a = 22.1833(6) Å, b = 10.5501(3) Å, c = 23.1940(4) Å, β = 114.4551(14)°, V = 4941.2(2) Å^3, Z = 4, ρ_{calcd} = 1.794 Mg m^{-3}, μ(Mo Kα) = 5.01 mm^{-1}, T = 200(2) K, dark red block, 0.09 × 0.06 × 0.04 mm, 8702 independent reflections. F^2 refinement, R = 0.096, wR = 0.242 for 6928 reflections ($I > 2\sigma(I)$, $2\theta_{max}$ = 50°), 576 parameters.

Synthesis of $[W_2\{\mu:\eta^1\text{-}C;\eta^2\text{-}C,P\text{-}CC(PPh)\}(CO)_4(Tp^*)_2]$ (37)

A solution of $[W_2(\mu\text{-}C_2PPh)(CO)_4(Tp^*)_2]$ (0.192 g, 0.16 mmol) in toluene (15 mL) was heated to reflux for 42 hours. The dark purple suspension was filtered and the volatiles were removed under reduced pressure. The solid was extracted with benzene (5 mL) and filtered, then layered with hexane (5 mL) and cooled to 4°C. The resulting purple precipitate was isolated by filtration and found to contain **37** as the major product (ca. 65% by $^{31}P\{^1H\}$ NMR spectroscopy). Crystals suitable for crystallographic analysis were grown from a solution of **37** in a mixture of benzene and hexane at −12°C. IR (toluene) ν/cm^{-1}: 2548 vw (BH), 1941 vs, 1876 vs (CO). The IR spectra obtained all contain some unreacted **33** (toluene: ν_{CO} 1985, 1974, 1893 cm^{-1}) so additional weak bands due to **37** may be present but obscured by the residual **33** bands. ^1H NMR (C_6D_6) δ/ppm: 8.19 (m, 2 H, C_6H_5), 7.34 (m, 3 H, C_6H_5), 5.66 (s, 1 H, pzH), 5.46 (s, 2 H, pzH), 5.24 (s, 1 H, pzH), 5.22 (s, 2 H, pzH), 2.67 (s, 3 H, $pzCH_3$), 2.62 (s, broad, 3 H, $pzCH_3$), 2.53 (s, 3 H, $pzCH_3$), 2.26 (s, 3 H, $pzCH_3$), 2.24 (s, 3 H, $pzCH_3$), 2.17 (s, 6 H, $pzCH_3$), 2.15 (s, 3 H, $pzCH_3$), 2.13 (s, 3 H, $pzCH_3$), 2.01 (s, 3 H, $pzCH_3$), 1.94 (s, 3 H, $pzCH_3$), 1.72 (s, broad, 3 H, $pzCH_3$). $^{31}P\{^1H\}$ NMR (C_6D_6) δ/ppm: −74.5 (br). MS-ESI(+): *m/z* 1207.3 $[M + H]^+$. Accurate mass: found 1207.3021 $[M + H]^+$. Calcd. for $C_{42}H_{50}{}^{11}B_2N_{12}O_4P^{184}W_2$: 1207.3021. Crystal data for $C_{42}H_{49}B_2N_{12}O_4PW_2\cdot C_6H_6$: M_w = 1284.34, orthorhombic, $Pca2_1$, a = 24.8643(5) Å, b = 10.7400(2) Å, c = 19.2900(4) Å, V = 5151.25(18) $Å^3$, Z = 4, ρ_{calcd} = 1.656 Mg m^{-3}, μ(Mo Kα) = 4.55 mm^{-1}, T = 200(2) K, dark purple block, 0.10 × 0.07 × 0.06 mm, 8997 independent reflections. F^2 refinement, R = 0.043, wR = 0.089 for 6669 reflections ($I > 2\sigma(I)$, $2\theta_{max}$ = 50°), 623 parameters.

Synthesis of $[W_2(\mu\text{-}C_2PPhAuCl)(CO)_4(Tp^*)_2]$ (38)

A solution of $[W_2(\mu\text{-}C_2PPh)(CO)_4(Tp^*)_2]$ (0.050 g, 0.041 mmol) and $[AuCl(SMe_2)]$ (0.013 g, 0.044 mmol) in CH_2Cl_2 (3 mL) was stirred at room temperature for 30 minutes. The volatiles were removed under reduced pressure. The residue was chromatographed on silica gel using CH_2Cl_2 as the eluent. A small initial grey band and yellow band were collected and discarded, and the first orange band (containing the product) was collected. The solvent was removed on the rotary evaporator to afford **38** as a red solid. The remaining two red-orange bands contain a mixture of **38**, **39** and **40**. Crystals suitable for crystallographic analysis were grown from a solution of **38** in Et_2O at −20°C. Yield 0.014 g (0.010 mmol, 24%). IR (Nujol) ν/cm^{-1}: 2553 w (BH), 2000 sh,

1995 s, 1911 s (CO). IR (THF) ν/cm^{-1}: 2553 vw (BH), 1996 s, 1914 vs (CO). ^{1}H NMR ($CDCl_3$) δ/ppm: 8.02 (m, 2 H, C_6H_5), 7.48 (m, 3 H, C_6H_5), 5.82 (s, 4H, pzH), 5.74 (s, 2 H, pzH), 2.37 (s, 18 H, $pzCH_3$), 2.35 (s, 6 H, $pzCH_3$), 2.34 (s, 6 H, $pzCH_3$), 2.29 (s, 6 H, $pzCH_3$). $^{13}C\{^{1}H\}$ NMR ($CDCl_3$) δ/ppm: 262.5 (d, W≡C, $^{1}J_{PC}$ = 25.9, $^{1}J_{WC}$ = 203.2), 225.1 (CO, $^{1}J_{WC}$ = 164.0), 223.7 (CO, $^{1}J_{WC}$ = 164.3), 152.6 (2 C), 152.5 (2 C), 152.2 (2 C), 145.6 (2 C), 144.7 (2 C), 144.7 (2 C) [$C^{3,5}$(pz)], 134.4 [d, $C^{2,3,5,6}(C_6H_5)$, J_{PC} = 14.6], 131.1 [$C^{4}(C_6H_5)$], 130.3 [d, $C^{1}(C_6H_5)$, $^{1}J_{PC}$ = 65.3], 128.8 [d, $C^{2,3,5,6}(C_6H_5)$, J_{PC} = 12.5], 107.1 (2 C), 106.7 (2 C), 106.6 (2 C) [C^{4}(pz)], 17.5 (4 C), 15.2 (2 C), 12.7 (6 C) ($pzCH_3$). $^{31}P\{^{1}H\}$ NMR ($CDCl_3$) δ/ppm: 49.4 ($^{2}J_{WP}$ = 143.7). MS-ESI(+): *m/z* 1479.3 $[M + MeCN]^+$, 1460.2 $[M + Na - H]^+$, 1439.2 $[M + H]^+$. Accurate mass: found 1463.2169 $[M + Na]^+$. Calcd. for $C_{42}H_{49}Au^{11}B_2{}^{37}ClN_{12}NaO_4P^{184}W_2$: 1463.2165. Found 1461.2184 $[M + Na]^+$. Calcd. for $C_{42}H_{49}Au^{11}B_2{}^{35}ClN_{12}NaO_4P^{184}W_2$: 1461.2194. Anal. found: C, 34.83; H, 3.63; N, 11.30%. Calcd. for $C_{42}H_{49}AuB_2ClN_{12}O_4PW_2$: C, 35.07; H, 3.43; N, 11.68%. Crystal data for $C_{42}H_{49}AuB_2ClN_{12}O_4PW_2 \cdot C_4H_{10}O$: M_w = 1512.77, triclinic, *P* – 1 (No. 2), *a* = 12.5001(13) Å, *b* = 14.7647(14) Å, *c* = 17.4599(10) Å, *α* = 66.723(7)°, *β* = 69.805(7)°, *γ* = 73.373(9)°, *V* = 2735.9(5) Å^3, *Z* = 2, ρ_{calcd} = 1.836 Mg m^{-3}, *μ*(Mo Kα) = 7.00 mm^{-1}, *T* = 150(2) K, red prism, 0.19 × 0.08 × 0.07 mm, 11228 independent reflections. F^2 refinement, *R* = 0.081, *wR* = 0.175 for 5382 reflections (*I* > *2σ(I)*, $2\theta_{max}$ = 52°), 631 parameters.

Synthesis of $[W_2\{\mu\text{-}(CAuCl)_2PPh\}(CO)_4(Tp^*)_2]$ (39)

$[W_2(\mu\text{-}C_2PPh)(CO)_4(Tp^*)_2]$ (0.020 g, 0.017 mmol) and $[AuCl(SMe_2)]$ (0.010 g, 0.034 mmol) were dissolved in $CDCl_3$ (0.5 mL) in an NMR tube. After 15 minutes, $^{31}P\{^{1}H\}$ NMR spectroscopy indicated the solution contained a mixture of **38** (16.0%), **39** (45.8%) and **40** (34.2%), as well as two small singlets without resolvable ^{183}W satellites at δ_P 37.5 (0.5%) and 30.2 (3.6%). Attempts to chromatograph mixtures containing **39** did not lead to isolation of pure **39**; instead it was isolated contaminated with **38**, or both **38** and **40**. Limited spectroscopic data for the crude product are given here. IR (CH_2Cl_2) ν/cm^{-1}: 2004 s, 1916 vs (CO) (tentative assignments as the spectrum also contains bands due to **38** and **40**). $^{31}P\{^{1}H\}$ NMR ($CDCl_3$) δ/ppm: 63.1 ($^{2}J_{WP}$ = 118.7). MS-ESI(+): *m/z* 1693.2 $[M + MeCN]^+$. Accurate mass: found 1693.1543 $[M + Na]^+$. Calcd. for $C_{42}H_{49}Au_2{}^{11}B_2{}^{35}Cl_2N_{12}NaO_4P^{184}W_2$: 1693.1548.

Synthesis of $[W_2\{\mu\text{-}(CAuCl)_2PPhAuCl\}(CO)_4(Tp^*)_2]$ (40)

A solution of $[W_2(\mu\text{-}C_2PPh)(CO)_4(Tp^*)_2]$ (0.020 g, 0.017 mmol) and $[AuCl(SMe_2)]$ (0.015 g, 0.051 mmol) in CH_2Cl_2 (2 mL) was stirred at room temperature for 20 minutes. The red solution was decanted into a round bottom flask to which hexane (ca. 1 mL) was added and volatiles removed on the rotary evaporator to afford **40** as a pink powder. Crystals suitable for crystallographic analysis were grown from a solution of **40** in CH_2Cl_2 layered with hexane. Yield 0.031 g (0.016 mmol, 96%). IR (Nujol) ν/cm^{-1}: 2560 w (BH), 2024 s, 1943 s, br, 1914 sh (CO). IR (THF) ν/cm^{-1}: 2060 vw (BH), 2026 s, 1948 vs (CO). ^1H NMR ($CDCl_3$) δ/ppm: 8.60 (m, 2 H, C_6H_5), 7.60 (m, 1 H, C_6H_5), 7.57 (m, 2 H, C_6H_5), 5.99 (s, 2 H, pzH), 5.94 (s, 2 H, pzH), 5.89 (s, 2 H, pzH), 2.76 (s, 6 H, $pzCH_3$), 2.45 (s, 6 H, $pzCH_3$), 2.38 (s, 6 H, $pzCH_3$), 2.36 (s, 6 H, $pzCH_3$), 2.32 (s, 6 H, $pzCH_3$), 2.15 (s, 6 H, $pzCH_3$). $^{13}C\{^1H\}$ NMR ($CDCl_3$) δ/ppm: 252.0 (WC, $^1J_{WC}$ = 99.9), 217.5 (d, CO, $^3J_{PC}$ = 8.0, $^1J_{WC}$ = 153.4), 216.2 (d, CO, $^3J_{PC}$ = 8.1, $^1J_{WC}$ = 153.4), 154.3 (2 C), 153.5 (2 C), 152.9 (2 C), 146.8 (2 C), 146.3 (2 C), 146.2 (2 C) [$C^{3,5}$(pz)], 136.7 [d, br, $C^{2,3,5,6}(C_6H_5)$, J_{PC} = 15.4], 133.1 [$C^4(C_6H_5)$], 129.1 [d, $C^{2,3,5,6}(C_6H_5)$, J_{PC} = 12.4], 129.0 [d, $C^1(C_6H_5)$, $^1J_{PC}$ = 59.3], 109.0 (2 C), 108.1 (2 C), 108.0 (2 C) [C^4(pz)], 19.4 (2 C), 17.9 (2 C), 16.0 (2 C), 13.2 (2 C), 12.8 (2 C), 12.7 (2 C) ($pzCH_3$). $^{31}P\{^1H\}$ NMR ($CDCl_3$) δ/ppm: 75.7 ($^2J_{WP}$ = 88.8). MS-ESI(+): *m/z* 1943.1 $[M + K]^+$, 1927.1 $[M + Na]^+$. Accurate mass: found 1929.0847 $[M + Na]^+$. Calcd. for $C_{42}H_{49}Au_3{}^{11}B_2{}^{35}Cl^{37}Cl_2N_{12}NaO_4P^{184}W_2$: 1929.0844. Found 1927.0875 $[M + Na]^+$. Calcd. for $C_{42}H_{49}Au_3{}^{11}B_2{}^{35}Cl_2{}^{37}ClN_{12}NaO_4P^{184}W_2$: 1927.0873. Anal. found: C, 26.51; H, 2.58; N, 8.71%. Calcd. for $C_{42}H_{49}Au_3B_2Cl_3N_{12}O_4PW_2$: C, 26.50; H, 2.59; N, 8.83%. Crystal data for $C_{42}H_{49}Au_3B_2Cl_3N_{12}O_4PW_2\cdot CH_2Cl_2$: M_w = 1988.42, monoclinic, $P2_1/c$, a = 23.7948(4) Å, b = 10.6312(2) Å, c = 24.9238(5) Å, β = 116.0601(9)°, V = 5663.91(19) Å^3, Z = 4, ρ_{calcd} = 2.332 Mg m^{-3}, μ(Mo Kα) = 12.11 mm^{-1}, T = 200(2) K, red prism, 0.17 × 0.04 × 0.03 mm, 9980 independent reflections. F^2 refinement, R = 0.056, wR = 0.160 for 7173 reflections ($I > 2\sigma(I)$, $2\theta_{max}$ = 50°), 649 parameters.

Synthesis of $[W_3(\mu\text{-}C_3P)(CO)_6(Tp^*)_3]$ (41)

A solution of $[W(\equiv CBr)(CO)_2(Tp^*)]$ (0.216 g, 0.343 mmol) in THF (10 mL) was cooled to –78°C and treated with ^{n}BuLi (1.7 M in hexanes, 0.20 mL, 0.34 mmol). The resulting light brown solution was stirred for 60 minutes and then treated with PCl_3 (0.01 mL, 0.1 mmol). The solution instantly turned dark brown and was allowed to warm to room temperature gradually over five hours. Volatiles were removed under reduced pressure.

The residue was extracted with pentane (3 × 10 mL), filtered and the solvent was removed under reduced pressure to afford crude **41** as a brown solid (ca. 87% **41** by $^{31}P\{^{1}H\}$ NMR spectroscopy, accompanied by peaks at δ_P 19.0 (5%) and 17.5 (8%)). Limited spectroscopic data for the crude product are given here. IR (THF) ν/cm^{-1}: 2548 w (BH), 1981 s, 1970 s, 1889 vs (CO). ^{1}H NMR ($CDCl_3$) δ/ppm: 5.74 (s, 3 H, pzH), 5.69 (s, 6 H, pzH), 2.37 (s, 27 H, $pzCH_3$), 2.31 (s, 27 H, $pzCH_3$). $^{31}P\{^{1}H\}$ NMR ($CDCl_3$) δ/ppm: 70.1 ($^{2}J_{WP}$ = 68.6). $^{31}P\{^{1}H\}$ NMR (C_6D_6) δ/ppm: 71.6 ($^{2}J_{WP}$ = 69.7). ESI mass spectrometry did not yield any identifiable peaks, presumably due to the high sensitivity of **41**.

CHAPTER 8.

References

CHAPTER 8: References

(1) Fischer, E. O.; Kreis, G.; Kreiter, C. G.; Müller, J.; Huttner, G.; Lorenz, H. *Angew. Chem., Int. Ed. Engl.* **1973**, *12*, 564.
(2) Fischer, E. O.; Maasböl, A. *Angew. Chem., Int. Ed. Engl.* **1964**, *3*, 580.
(3) Doering, W. v. E.; Buttery, R. G.; Laughlin, R. G.; Chaudhuri, N. *J. Am. Chem. Soc.* **1956**, *78*, 3224.
(4) Skell, P. S.; Woodworth, R. C. *J. Am. Chem. Soc.* **1956**, *78*, 4496.
(5) Haszeldine, R. N.; Young, J. C. *Proc. Chem. Soc., London* **1959**, 394.
(6) Do Minh, T.; Gunning, H. E.; Strausz, O. P. *J. Am. Chem. Soc.* **1967**, *89*, 6785.
(7) Font, J.; Serratosa, F.; Vilarrasa, L. *Tetrahedron Lett.* **1969**, 4743.
(8) Mayr, A.; McDermott, G. A.; Dorries, A. M. *Organometallics* **1985**, *4*, 608.
(9) McDermott, G. A.; Dorries, A. M.; Mayr, A. *Organometallics* **1987**, *6*, 925.
(10) Kim, H. P.; Angelici, R. J. *Adv. Organomet. Chem.* **1987**, *27*, 51.
(11) Mayr, A.; Hoffmeister, H. *Adv. Organomet. Chem.* **1991**, *32*, 227.
(12) Pombeiro, A. J. L.; Hughes, D. L.; Pickett, C. J.; Richards, R. L. *J. Chem. Soc., Chem. Commun.* **1986**, 246.
(13) Pombeiro, A. J. L.; Fátima, M.; Silva, C. G. d.; Michelin, R. A. *Coord. Chem. Rev.* **2001**, *218*, 43.
(14) Murdzek, J. S.; Schrock, R. R., High Oxidation State Alkylidyne Complexes. In *Carbyne Complexes*, Fischer, H.; Fischer, E. O., Eds. VCH: Weinheim, 1988; pp 147.
(15) Schrock, R. R. *Acc. Chem. Res.* **1986**, *19*, 342.
(16) Schrock, R. R. *Chem. Rev.* **2002**, *102*, 145.
(17) Schrock, R. R. *Chem. Commun.* **2005**, 2773.
(18) Kreissl, F. R., *Transition Metal Carbyne Complexes*. Kluwer Academic: Dordrecht, 1993.
(19) Gallop, M. A.; Roper, W. R. *Adv. Organomet. Chem.* **1986**, *25*, 121.
(20) Roper, W. R. *J. Organomet. Chem.* **1986**, *300*, 167.
(21) Caldwell, L. M. *Adv. Organomet. Chem.* **2008**, *56*, 1.
(22) Schrock, R. R. *Chem. Commun.* **2013**, *49*, 5529.
(23) Herndon, J. W. *Coord. Chem. Rev.* **2012**, *256*, 1281.
(24) Herndon, J. W. *Coord. Chem. Rev.* **2013**, *257*, 2899.
(25) Jia, G. *Coord. Chem. Rev.* **2007**, *251*, 2167.
(26) Shi, C.; Jia, G. *Coord. Chem. Rev.* **2013**, *257*, 666.
(27) Yang, H.; Jin, Y.; Du, Y.; Zhang, W. *J. Mater. Chem. A* **2014**, *2*, 5986.
(28) Schrock, R. R.; Czekelius, C. *Adv. Synth. Catal.* **2007**, *349*, 55.
(29) Schrock, R. R. *J. Am. Chem. Soc.* **1974**, *96*, 6796.
(30) Shortland, A. J.; Wilkinson, G. *J. Chem. Soc., Dalton Trans.* **1973**, 872.
(31) Guggenberger, L. J.; Schrock, R. R. *J. Am. Chem. Soc.* **1975**, *97*, 2935.
(32) Sharp, P. R.; Holmes, S. J.; Schrock, R. R.; Churchill, M. R.; Wasserman, H. J. *J. Am. Chem. Soc.* **1981**, *103*, 965.
(33) Fischer, E. O.; Frank, A. *Chem. Ber.* **1978**, *111*, 3740.
(34) Mayr, A.; McDermott, G. A. *J. Am. Chem. Soc.* **1986**, *108*, 548.
(35) Clark, G. R.; Marsden, K.; Roper, W. R.; Wright, L. J. *J. Am. Chem. Soc.* **1980**, *102*, 6570.

(36) Hill, A. F.; Roper, W. R.; Waters, J. M.; Wright, A. H. *J. Am. Chem. Soc.* **1983**, *105*, 5939.
(37) Segawa, Y.; Yamashita, M.; Nozaki, K. *Science* **2006**, *314*, 113.
(38) Dombek, B. D.; Angelici, R. J. *Inorg. Chem.* **1976**, *15*, 2397.
(39) Dillon, K. B.; Nixon, J. F.; Mathey, F., *Phosphorus: The Carbon Copy*. John Wiley & Sons: Chichester, 1998.
(40) Agapie, T.; Diaconescu, P. L.; Cummins, C. C. *J. Am. Chem. Soc.* **2002**, *124*, 2412.
(41) Greco, J. B.; Peters, J. C.; Baker, T. A.; Davis, W. M.; Cummins, C. C.; Wu, G. *J. Am. Chem. Soc.* **2001**, *123*, 5003.
(42) Cummins, C. C. *Chem. Commun.* **1998**, 1777.
(43) Cummins, C. C. *Angew. Chem., Int. Ed.* **2006**, *45*, 862.
(44) Peters, J. C.; Odom, A. L.; Cummins, C. C. *Chem. Commun.* **1997**, 1995.
(45) Cherry, J.-P. F.; Johnson, A. R.; Baraldo, L. M.; Tsai, Y.-C.; Cummins, C. C.; Kryatov, S. V.; Rybak-Akimova, E. V.; Capps, K. B.; Hoff, C. D.; Haar, C. M.; Nolan, S. P. *J. Am. Chem. Soc.* **2001**, *123*, 7271.
(46) Curley, J. J.; Cook, T. R.; Reece, S. Y.; Muller, P.; Cummins, C. C. *J. Am. Chem. Soc.* **2008**, *130*, 9394.
(47) Curley, J. J.; Cozzolino, A. F.; Cummins, C. C. *Dalton Trans.* **2011**, *40*, 2429.
(48) Curley, J. J.; Piro, N. A.; Cummins, C. C. *Inorg. Chem.* **2009**, *48*, 9599.
(49) Johnson, A. R.; Davis, W. M.; Cummins, C. C.; Serron, S.; Nolan, S. P.; Musaev, D. G.; Morokuma, K. *J. Am. Chem. Soc.* **1998**, *120*, 2071.
(50) Laplaza, C. E.; Cummins, C. C. *Science* **1995**, *268*, 861.
(51) Laplaza, C. E.; Davis, W. M.; Cummins, C. C. *Angew. Chem., Int. Ed. Engl.* **1995**, *34*, 2042.
(52) Laplaza, C. E.; Johnson, M. J. A.; Peters, J.; Odom, A. L.; Kim, E.; Cummins, C. C.; George, G. N.; Pickering, I. J. *J. Am. Chem. Soc.* **1996**, *118*, 8623.
(53) Mindiola, D. J.; Tsai, Y.-C.; Hara, R.; Chen, Q.; Meyer, K.; Cummins, C. C. *Chem. Commun.* **2001**, 125.
(54) Cordiner, R. L.; Gugger, P. A.; Hill, A. F.; Willis, A. C. *Organometallics* **2009**, *28*, 6632.
(55) Lalor, F. J.; Desmond, T. J.; Cotter, G. M.; Shanahan, C. A.; Ferguson, G.; Parvez, M.; Ruhl, B. *J. Chem. Soc., Dalton Trans.* **1995**, 1709.
(56) Schmidbaur, H.; Pichl, R.; Müller, G. *Angew. Chem., Int. Ed. Engl.* **1986**, *25*, 574.
(57) Hughes, K. A.; Dopico, P. G.; Sabat, M.; Finn, M. G. *Angew. Chem., Int. Ed. Engl.* **1993**, *32*, 554.
(58) Holmes, S. J.; Schrock, R. R.; Churchill, M. R.; Wasserman, H. J. *Organometallics* **1984**, *3*, 476.
(59) List, A. K.; Hillhouse, G. L.; Rheingold, A. L. *J. Am. Chem. Soc.* **1988**, *110*, 6926.
(60) List, A. K.; Hillhouse, G. L.; Rheingold, A. L. *J. Am. Chem. Soc.* **1988**, *110*, 4855.
(61) List, A. K.; Hillhouse, G. L.; Rheingold, A. L. *Organometallics* **1989**, *8*, 2010.
(62) Bruce, A. E.; Gamble, A. S.; Tonker, T. L.; Templeton, J. L. *Organometallics* **1987**, *6*, 1350.
(63) Enriquez, A. E.; Templeton, J. L. *Organometallics* **2002**, *21*, 852.
(64) Enriquez, A. E.; White, P. S.; Templeton, J. L. *J. Am. Chem. Soc.* **2001**, *123*, 4992.
(65) Jamison, G. M.; Bruce, A. E.; White, P. S.; Templeton, J. L. *J. Am. Chem. Soc.* **1991**, *113*, 5057.
(66) Jamison, G. M.; White, P. S.; Templeton, J. L. *Organometallics* **1991**, *10*, 1954.

(67) Stone, K. C.; Jamison, G. M.; White, P. S.; Templeton, J. L. *Inorg. Chim. Acta* **2002**, *330*, 161.
(68) Weber, L.; Dembeck, G.; Boese, R.; Bläser, D. *Chem. Ber.* **1997**, *130*, 1305.
(69) Weber, L.; Dembeck, G.; Stammler, H.-G.; Neumann, B.; Schmidtmann, M.; Müller, A. *Organometallics* **1998**, *17*, 5254.
(70) Weber, L.; Dembeck, G.; Stammler, H. G.; Neumann, B. *Eur. J. Inorg. Chem.* **1998**, 579.
(71) Weber, L.; Dembeck, G.; Boese, R.; Bläser, D. *Organometallics* **1999**, *18*, 4603.
(72) Weber, L.; Dembeck, G.; Lönneke, P.; Stammler, H.-G.; Neumann, B. *Organometallics* **2001**, *20*, 2288.
(73) Li, X.; Schopf, M.; Stephan, J.; Harms, K.; Sundermeyer, J. *Organometallics* **2002**, *21*, 2356.
(74) Li, X.; Schopf, M.; Stephan, J.; Kippe, J.; Harms, K.; Sundermeyer, J. *J. Am. Chem. Soc.* **2004**, *126*, 8660.
(75) Li, X.; Stephan, J.; Harms, K.; Sundermeyer, J. *Organometallics* **2004**, *23*, 3359.
(76) Li, X.; Sun, H.; Harms, K.; Sundermeyer, J. *Organometallics* **2005**, *24*, 4699.
(77) Li, X.; Schopf, M.; Stephan, J.; Kipke, J.; Harms, K.; Sundermeyer, J. *Organometallics* **2006**, *25*, 528.
(78) Li, X.; Wang, A.; Sun, H.; Wang, L.; Schmidt, S.; Harms, K.; Sundermeyer, J. *Organometallics* **2007**, *26*, 3456.
(79) Li, X.; Wang, A.; Wang, L.; Sun, H.; Harms, K.; Sundermeyer, J. *Organometallics* **2007**, *26*, 1411.
(80) Mayr, A.; Bastos, C. M. *Prog. Inorg. Chem.* **1992**, *40*, 1.
(81) Bertani, R.; Casarin, M.; Pandolfo, L. *Coord. Chem. Rev.* **2003**, *236*, 15.
(82) Belluco, U.; Michelin, R. A.; Mozzon, M.; Bertani, R.; Facchin, G.; Zanotto, L.; Pandolfo, L. *J. Organomet. Chem.* **1998**, *557*, 37.
(83) Herd, O.; Hessler, A.; Hingst, M.; Tepper, M.; Stelzer, O. *J. Organomet. Chem.* **1996**, *522*, 69.
(84) Liek, C.; Machnitzki, P.; Nickel, T.; Schenk, S.; Tepper, M.; Stelzer, O. *Z. Naturforsch. B* **1999**, *54*, 1532.
(85) Hirao, T.; Masunaga, T.; N, Y.; Ohshiro, Y.; Agawa, T. *Bull. Chem. Soc. Jpn.* **1982**, *55*, 909.
(86) Angelici, R. J. *Angew. Chem., Int. Ed.* **2007**, *46*, 330.
(87) Jun, H.; Young, V. G.; Angelici, R. J. *J. Am. Chem. Soc.* **1992**, *114*, 10064.
(88) Jun, H.; Angelici, R. J. *Organometallics* **1994**, *13*, 2454.
(89) Laurent, J. C. T. R. B.-S.; Hitchcock, P. B.; Kroto, H. W.; Nixon, J. F. *J. Chem. Soc., Chem. Commun.* **1981**, 1141.
(90) Konze, W. V.; Young, V. G.; Angelici, R. J. *Organometallics* **1999**, *18*, 258.
(91) Cordaro, J. G.; Stein, D.; Rüegger, H.; Grützmacher, H. *Angew. Chem., Int. Ed.* **2006**, *45*, 6159.
(92) Trathen, N.; Leech, M. C.; Crossley, I. R.; Greenacre, V. K.; Roe, S. M. *Dalton Trans.* **2014**, *43*, 9004.
(93) Mansell, S. M.; Green, M.; Russell, C. A. *Dalton Trans.* **2012**, *41*, 14360.
(94) Lucas, M. F.; Michelini, M. C.; Russo, N.; Sicilia, E. *J. Chem. Theory Comput.* **2008**, *4*, 397.
(95) Weber, L. *Eur. J. Inorg. Chem.* **2003**, 1843.
(96) Appel, R.; Immenkeppel, M. *Z. Anorg. Allg. Chem.* **1987**, *553*, 7.

(97) Ito, S.; Sugiyama, H.; Yoshifuji, M. *Angew. Chem., Int. Ed.* **2000**, *39*, 2781.
(98) Ito, S.; Toyota, K.; Yoshifuji, M. *Chem. Commun.* **1997**, 1637.
(99) Niecke, E.; Nieger, M.; Schmidt, O.; Gudat, D.; Schoeller, W. W. *J. Am. Chem. Soc.* **1999**, *121*, 519.
(100) Yoshifuji, M.; Kawanami, H.; Kawai, Y.; Toyota, K.; Yasunami, M.; Niitsu, T.; Inamoto, N. *Chem. Lett.* **1992**, 1053.
(101) Yoshifuji, M.; Niitsu, T.; Inamoto, N. *Chem. Lett.* **1988**, 1733.
(102) Goede, S. J.; Bickelhaupt, F. *Chem. Ber.* **1991**, *124*, 2677.
(103) Jun, H.; Young, V. G., Jr.; Angelici, R. J. *J. Am. Chem. Soc.* **1991**, *113*, 9379.
(104) Jun, H.; Angelici, R. J. *Organometallics* **1993**, *12*, 4265.
(105) Jun, H.; Young, V. G., Jr.; Angelici, R. J. *Organometallics* **1994**, *13*, 2444.
(106) Weber, L.; Schumann, I.; Schmidt, T.; Stammler, H. G.; Neumann, B. *Z. Anorg. Allg. Chem.* **1993**, *619*, 1759.
(107) Weber, L.; Schumann, I.; Stammler, H.-G.; Neumann, B. *Chem. Ber.* **1994**, *127*, 1349.
(108) Weber, L.; Schumann, I.; Scheffer, M. H.; Stammler, H. G.; Neumann, B. *Z. Naturforsch. B* **1997**, *52*, 655.
(109) Bourissou, D.; Bertrand, G. *Adv. Organomet. Chem.* **1999**, *44*, 175.
(110) Jones, N. D.; Cavell, R. G. *J. Organomet. Chem.* **2005**, *690*, 5485.
(111) Cantat, T.; Mezailles, N.; Auffrant, A.; Le Floch, P. *Dalton Trans.* **2008**, 1957.
(112) Liddle, S. T.; Mills, D. P.; Wooles, A. J. *Chem. Soc. Rev.* **2011**, *40*, 2164.
(113) Fischer, E. O.; Reitmeier, R. *Z. Naturforsch. B* **1983**, *38*, 582.
(114) Kreissl, F. R.; Wolfgruber, M.; Sieber, W. J. *J. Organomet. Chem.* **1984**, *270*, C4.
(115) Kreissl, F. R.; Ostermeier, J.; Ogric, C. *Chem. Ber.* **1995**, *128*, 289.
(116) Lehotkay, T.; Wurst, K.; Jaitner, P.; Kreissl, F. R. *J. Organomet. Chem.* **1996**, *523*, 105.
(117) Ogric, C.; Ostermeier, J.; Heckel, M.; Hiller, W.; Kreissl, F. R. *Inorg. Chim. Acta* **1994**, *222*, 77.
(118) Sattler, A.; Parkin, G. *Chem. Commun.* **2011**, *47*, 12828.
(119) Fischer, E. O.; Reitmeier, R.; Ackermann, K. *Angew. Chem., Int. Ed. Engl.* **1983**, *22*, 411.
(120) Gibson, V. C.; Grebenik, P. D.; Green, M. L. H. *J. Chem. Soc., Chem. Commun.* **1983**, 1101.
(121) Gibson, V. C.; Graimann, C. E.; Hare, P. M.; Green, M. L. H.; Bandy, J. A.; Grebenik, P. D.; Prout, K. *J. Chem. Soc., Dalton Trans.* **1985**, 2025.
(122) Kee, T. P.; Gibson, V. C.; Clegg, W. *J. Organomet. Chem.* **1987**, *325*, C14.
(123) Green, M. L. H.; Hare, P. M.; Bandy, J. A. *J. Organomet. Chem.* **1987**, *330*, 61.
(124) Dovesi, S.; Solari, E.; Scopelliti, R.; Floriani, C. *Angew. Chem., Int. Ed.* **1999**, *38*, 2388.
(125) Merceron-Saffon, N.; Gornitzka, H.; Baceiredo, A.; Bertrand, G. *J. Organomet. Chem.* **2004**, *689*, 1431.
(126) Huy, N. H. T.; Fischer, J.; Mathey, F. *Organometallics* **1988**, *7*, 240.
(127) Yu, I.; Wallis, C. J.; Patrick, B. O.; Mehrkhodavandi, P. *Organometallics* **2009**, *28*, 6370.
(128) Townsend, E. M.; Kilyanek, S. M.; Schrock, R. R.; Müller, P.; Smith, S. J.; Hoveyda, A. H. *Organometallics* **2013**, *32*, 4612.
(129) Vignolle, J.; Cattoën, X.; Bourissou, D. *Chem. Rev.* **2009**, *109*, 3333.

(130) Igau, A.; Grutzmacher, H.; Baceiredo, A.; Bertrand, G. *J. Am. Chem. Soc.* **1988**, *110*, 6463.
(131) Despagnet, E.; Miqueu, K.; Gornitzka, H.; Dyer, P. W.; Bourissou, D.; Bertrand, G. *J. Am. Chem. Soc.* **2002**, *124*, 11834.
(132) Valyaev, D. A.; Lugan, N.; Lavigne, G.; Ustynyuk, N. A. *Organometallics* **2008**, *27*, 5180.
(133) Valyaev, D. A.; Lugan, N. l.; Lavigne, G.; Ustynyuk, N. A. *Organometallics* **2011**, *30*, 2318.
(134) Kreissl, F. R.; Stückler, P.; Meineke, E. W. *Chem. Ber.* **1977**, *110*, 3040.
(135) Kreissl, F. R.; Uedelhoven, W.; Kreis, G. *Chem. Ber.* **1978**, *111*, 3283.
(136) Kreissl, F. R. *J. Organomet. Chem.* **1975**, *99*, 305.
(137) Romero, P. E.; Piers, W. E.; McDonald, R. *Angew. Chem., Int. Ed.* **2004**, *43*, 6161.
(138) Leitao, E. M.; van der Eide, E. F.; Romero, P. E.; Piers, W. E.; McDonald, R. *J. Am. Chem. Soc.* **2010**, *132*, 2784.
(139) Khalimon, A. Y.; Leitao, E. M.; Piers, W. E. *Organometallics* **2012**, *31*, 5634.
(140) Leitao, E. M.; Piers, W. E.; Parvez, M. *Can. J. Chem.* **2013**, *91*, 935.
(141) Fischer, E. O.; Huttner, G.; Kleine, W.; Frank, A. *Angew. Chem.* **1975**, *87*, 781.
(142) Fischer, E. O.; Kleine, W.; Kreis, G.; Kreissl, F. R. *Chem. Ber.* **1978**, *111*, 3542.
(143) Himmelreich, D.; Fischer, E. O. *Z. Naturforsch. B* **1982**, *37*, 1218.
(144) Fischer, E. O.; Schneider, J.; Neugebauer, D. *Angew. Chem., Int. Ed. Engl.* **1984**, *23*, 820.
(145) Chatt, J.; Pombeiro, A. J. L.; Richards, R. L.; Royston, G. H. D.; Muir, K. W.; Walker, R. *J. Chem. Soc., Chem. Commun.* **1975**, 708.
(146) Filippou, A. C.; Gruenleitner, W.; Fischer, E. O. *J. Organomet. Chem.* **1992**, *428*, C37.
(147) Filippou, A. C.; Wagner, C.; Fischer, E. O.; Völkl, C. *J. Organomet. Chem.* **1992**, *438*, C15.
(148) Greaves, W. W.; Angelici, R. J. *Inorg. Chem.* **1981**, *20*, 2983.
(149) Chatt, J.; Pombeiro, A. J. L.; Richards, R. L. *J. Chem. Soc., Dalton Trans.* **1979**, 1585.
(150) Pombeiro, A. J. L.; Richards, R. L.; Dilworth, J. R. *J. Organomet. Chem.* **1979**, *175*, C17.
(151) Pombeiro, A. L.; Richards, R. *Transition Met. Chem.* **1980**, *5*, 55.
(152) Chatt, J.; Pombeiro, A. J. L.; Richards, R. L. *J. Chem. Soc., Dalton Trans.* **1980**, 492.
(153) Chatt, J.; Pombeiro, A. J. L.; Richards, R. L. *J. Organomet. Chem.* **1980**, *184*, 357.
(154) Pombeiro, A. J. L.; Carvalho, M. F. N. N.; Hitchcock, P. B.; Richards, R. L. *J. Chem. Soc., Dalton Trans.* **1981**, 1629.
(155) da Silva, M. F. C. G.; Lemos, M. A. N. D. A.; da Silva, J. J. R. F.; Pombeiro, A. J. L.; Pellinghelli, M. A.; Tiripicchio, A. *J. Chem. Soc., Dalton Trans.* **2000**, 373.
(156) Pombeiro, A. J. L.; Fátima, M.; Guedes da Silva, C. *J. Organomet. Chem.* **2001**, *617–618*, 65.
(157) Filippou, A. C.; Wanninger, K.; Mehnert, C. *J. Organomet. Chem.* **1993**, *461*, 99.
(158) Lungwitz, B.; Filippou, A. C. *J. Organomet. Chem.* **1995**, *498*, 91.
(159) Anderson, S.; Hill, A. F. *J. Organomet. Chem.* **1990**, *394*, c24.
(160) Anderson, S.; Cook, D. J.; Hill, A. F. *J. Organomet. Chem.* **1993**, *463*, C3.
(161) Anderson, S.; Cook, D. J.; Hill, A. F. *Organometallics* **1997**, *16*, 5595.

(162) Anderson, S.; Hill, A. F. *Organometallics* **1995**, *14*, 1562.
(163) Anderson, S.; Hill, A. F.; Ng, Y. T. *Organometallics* **2000**, *19*, 15.
(164) Chiu, K. W.; Howard, C. G.; Wilkinson, G.; Galas, A. M. R.; Hursthouse, M. B. *Polyhedron* **1982**, *1*, 803.
(165) Seino, H.; Nonokawa, D.; Nakamura, G.; Mizobe, Y.; Hidai, M. *Organometallics* **2000**, *19*, 2002.
(166) Filippou, A. C.; Grünleitner, W.; Völkl, C.; Kiprof, P. *Angew. Chem., Int. Ed. Engl.* **1991**, *30*, 1167.
(167) Wang, Y.; Da Silva, J. J. R. F.; Pombeiro, A. J. L.; Pellinghelli, M. A.; Tiripicchio, A.; Henderson, R. A.; Richards, R. L. *J. Chem. Soc., Dalton Trans.* **1995**, 1183.
(168) Filippou, A. C.; Hofmann, P.; Kiprof, P.; Schmidt, H. R.; Wagner, C. *J. Organomet. Chem.* **1993**, *459*, 233.
(169) Filippou, A. C.; Völkl, C.; Grünleitner, W.; Kiprof, P. *J. Organomet. Chem.* **1992**, *434*, 201.
(170) da Silva, J. J. R. F.; Pellinghelli, M. A.; Pombeiro, A. J. L.; Richards, R. L.; Tiripicchio, A.; Wang, Y. *J. Organomet. Chem.* **1993**, *454*, C8.
(171) Filippou, A. C.; Gruenleitner, W. *Z. Naturforsch. B* **1989**, *44*, 1023.
(172) Filippou, A. C.; Gruenleitner, W. *Z. Naturforsch. B* **1991**, *46*, 216.
(173) Filippou, A. C.; Gruenleitner, W. *J. Organomet. Chem.* **1990**, *393*, C10.
(174) Marchetti, F.; Zacchini, S.; Zanotti, V. *Organometallics* **2014**, *33*, 3990.
(175) Filippou, A. C.; Gruenleitner, W. *Z. Naturforsch. B* **1989**, *44*, 1572.
(176) Filippou, A. C.; Gruenleitner, W. *J. Organomet. Chem.* **1990**, *398*, 99.
(177) Filippou, A. C.; Gruenleitner, W.; Fischer, E. O. *J. Organomet. Chem.* **1991**, *411*, C21.
(178) Filippou, A. C.; Gruenleitner, W.; Fischer, E. O.; Imhof, W.; Huttner, G. *J. Organomet. Chem.* **1991**, *413*, 165.
(179) Filippou, A. C.; Fischer, E. O. *J. Organomet. Chem.* **1990**, *382*, 143.
(180) Filippou, A. C.; Gruenleitner, W.; Fischer, E. O. *J. Organomet. Chem.* **1991**, *401*, C37.
(181) Filippou, A. C.; Mehnert, C.; Wanninger, K. M. A.; Kleine, M. *J. Organomet. Chem.* **1995**, *491*, 47.
(182) Filippou, A. C.; Lungwitz, B.; Kociok-Köhn, G. *Eur. J. Inorg. Chem.* **1999**, 1905.
(183) Filippou, A. C.; Portius, P.; Jankowski, C. *J. Organomet. Chem.* **2001**, *617-618*, 656.
(184) Filippou, A. C.; Portius, P.; Winter, J. G.; Kociok-Köhn, G. *J. Organomet. Chem.* **2001**, *628*, 11.
(185) Filippou, A. C.; Fischer, E. O. *J. Organomet. Chem.* **1988**, *352*, 149.
(186) Filippou, A. C. *Polyhedron* **1989**, *8*, 1285.
(187) Filippou, A. C.; Fischer, E. O. *J. Organomet. Chem.* **1989**, *365*, 317.
(188) Filippou, A. C.; Woessner, D.; Kociok-Koehn, G.; Hinz, I.; Gruber, L. *J. Organomet. Chem.* **1997**, *532*, 207.
(189) Brothers, P. J.; Roper, W. R. *Chem. Rev.* **1988**, *88*, 1293.
(190) Hartshorn, A. J.; Lappert, M. F. *J. Chem. Soc., Chem. Commun.* **1976**, 761.
(191) Fischer, H.; Motsch, A.; Maerkl, R.; Ackermann, K. *Organometallics* **1985**, *4*, 726.
(192) Fischer, H.; Reindl, D.; Hofmann, J.; Troll, C. *J. Organomet. Chem.* **1994**, *472*, 163.
(193) Fischer, H.; Reindl, D.; Troll, C. *J. Organomet. Chem.* **1994**, *480*, 221.
(194) Cordiner, R. L.; Hill, A. F.; Wagler, J. *Organometallics* **2008**, *27*, 4532.

(195) Desmond, T.; Lalor, F. J.; Ferguson, G.; Parvez, M. *J. Chem. Soc., Chem. Commun.* **1983**, 457.
(196) Cordiner, R. L.; Hill, A. F.; Wagler, J. *Organometallics* **2008**, *27*, 5177.
(197) Trofimenko, S.; Calabrese, J. C.; Thompson, J. S. *Inorg. Chem.* **1987**, *26*, 1507.
(198) Shiu, K.-B.; Lee, L.-Y. *J. Organomet. Chem.* **1988**, *348*, 357.
(199) Woodworth, B. E.; Frohnapfel, D. S.; White, P. S.; Templeton, J. L. *Organometallics* **1998**, *17*, 1655.
(200) Woodworth, B. E.; Templeton, J. L. *J. Am. Chem. Soc.* **1996**, *118*, 7418.
(201) Desmond, T.; Lalor, F. J.; Ferguson, G.; Parvez, M. *J. Chem. Soc., Chem. Commun.* **1984**, 75.
(202) Caldwell, L. M.; Hill, A. F.; Rae, A. D.; Willis, A. C. *Organometallics* **2008**, *27*, 341.
(203) Etienne, M.; White, P. S.; Templeton, J. L. *J. Am. Chem. Soc.* **1991**, *113*, 2324.
(204) Colebatch, A. L.; Hill, A. F.; Shang, R.; Willis, A. C. *Organometallics* **2010**, *29*, 6482.
(205) Colebatch, A. L.; Cordiner, R. L.; Hill, A. F.; Nguyen, K. T. H. D.; Shang, R.; Willis, A. C. *Organometallics* **2009**, *28*, 4394.
(206) Cordiner, R. L.; Hill, A. F.; Shang, R.; Willis, A. C. *Organometallics* **2011**, *30*, 139.
(207) Hill, A. F.; Shang, R.; Willis, A. C. *Organometallics* **2011**, *30*, 3237.
(208) Hill, A. F.; Shang, R. *Organometallics* **2012**, *31*, 4635.
(209) Hill, A. F.; Sharma, M.; Willis, A. C. *Organometallics* **2012**, *31*, 2538.
(210) Colebatch, A. L.; Hill, A. F.; Sharma, M. *Organometallics* **2014**, DOI: 10.1021/om500833n.
(211) Borren, E. S.; Hill, A. F.; Shang, R.; Sharma, M.; Willis, A. C. *J. Am. Chem. Soc.* **2013**, *135*, 4942.
(212) Cotton, F. A., *Chemical Applications of Group Theory*. Wiley-Interscience: New York, U.S.A., 1963.
(213) Bennett, M. A.; Kwan, L.; Rae, A. D.; Wenger, E.; Willis, A. C. *J. Chem. Soc., Dalton Trans.* **2002**, 226.
(214) Desmond, T. J.; Lalor, F. J.; Ferguson, G.; Parvez, M.; Wieckowski, T. *Acta Cryst.* **1990**, *C46*, 59.
(215) Kazul'kin, D. N.; Ryabov, A. N.; Izmer, V. V.; Churakov, A. V.; Beletskaya, I. P.; Burns, C. J.; Voskoboynikov, A. Z. *Organometallics* **2005**, *24*, 3024.
(216) Brauer, D. J.; Hingst, M.; Kottsieper, K. W.; Liek, C.; Nickel, T.; Tepper, M.; Stelzer, O.; Sheldrick, W. S. *J. Organomet. Chem.* **2002**, *2002*, 14.
(217) Murata, M.; Buchwald, S. L. *Tetrahedron* **2004**, *60*, 7397.
(218) Kwong, F. Y.; Chan, K. S. *Chem. Commun.* **2000**, 1069.
(219) Berger, O.; Petit, C.; Deal, E. L.; Montchamp, J.-L. *Adv. Synth. Catal.* **2013**, *355*, 1361.
(220) Shang, R. Ph.D. Thesis, Australian National University, 2012.
(221) Cetinkaya, B.; Lappert, M. F.; McMeeking, J.; Palmer, D. *J. Organomet. Chem.* **1972**, *34*, C37.
(222) Verkade, J. G.; Quin, L. D., *Phosphorus-31 NMR Spectroscopy in Stereochemical Analysis*. VCH Publishers: Florida, USA, 1987.
(223) Balcı, M., *Basic ^{1}H- and ^{13}C-NMR Spectroscopy*. Elsevier: Amsterdam, Netherlands, 2005.

(224) Staubitz, A.; Robertson, A. P. M.; Sloan, M. E.; Manners, I. *Chem. Rev.* **2010**, *110*, 4023.
(225) Brunel, J. M.; Faure, B.; Maffei, M. *Coord. Chem. Rev.* **1998**, *178-180*, 665.
(226) Kubo, K.; Kanemitsu, I.; Murakami, E.; Mizuta, T.; Nakazawa, H.; Miyoshi, K. *J. Organomet. Chem.* **2004**, *689*, 2425.
(227) Barratt, D.; Davies, S. J.; Elliott, G. P.; Howard, J. A. K.; Lewis, D. B.; Stone, F. G. A. *J. Organomet. Chem.* **1987**, *325*, 185.
(228) Carriedo, G. A.; Elliott, G. P.; Howard, J. A. K.; Lewis, D. B.; Stone, F. G. A. *J. Chem. Soc., Chem. Commun.* **1984**, 1585.
(229) Wadepohl, H.; Arnold, U.; Kohl, U.; Pritzkow, H.; Wolf, A. *J. Chem. Soc., Dalton Trans.* **2000**, 3554.
(230) Wadepohl, H.; Arnold, U.; Pritzkow, H. *Angew. Chem., Int. Ed. Engl.* **1997**, *36*, 974.
(231) Imamoto, T.; Saitoh, Y.; Koide, A.; Ogura, T.; Yoshida, K. *Angew. Chem., Int. Ed.* **2007**, *46*, 8636.
(232) Huffman, J. C.; Skupinski, W. A.; Caulton, K. G. *Cryst. Struct. Commun.* **1982**, *11*, 1435.
(233) Haav, K.; Saame, J.; Kütt, A.; Leito, I. *Eur. J. Org. Chem.* **2012**, *2012*, 2167.
(234) Coetzee, J. F.; Padmanabhan, G. R. *J. Am. Chem. Soc.* **1965**, *87*, 5005.
(235) Henderson, R. A. *Angew. Chem., Int. Ed. Engl.* **1996**, *35*, 946.
(236) Torraca, K. E.; Ghiviriga, I.; McElwee-White, L. *Organometallics* **1999**, *18*, 2262.
(237) Holmes, S. J.; Clark, D. N.; Turner, H. W.; Schrock, R. R. *J. Am. Chem. Soc.* **1982**, *104*, 6322.
(238) Holmes, S. J.; Schrock, R. R. *J. Am. Chem. Soc.* **1981**, *103*, 4599.
(239) Kostic, N.; Fenske, R. *J. Am. Chem. Soc.* **1981**, *103*, 4677.
(240) Kostic, N. M.; Fenske, R. F. *Organometallics* **1982**, *1*, 489.
(241) Green, M.; Orpen, A. G.; Williams, I. D. *J. Chem. Soc., Chem. Commun.* **1982**, 493.
(242) Baudler, M. *Pure Appl. Chem.* **1980**, *52*, 755.
(243) Baudler, M. *Angew. Chem., Int. Ed. Engl.* **1982**, *21*, 492.
(244) Kim, H. P.; Kim, S.; Jacobson, R. A.; Angelici, R. J. *Organometallics* **1984**, *3*, 1124.
(245) Doyle, R. A.; Angelici, R. J. *Organometallics* **1989**, *8*, 2207.
(246) Nelson, G. O.; Brookhart, M. *J. Am. Chem. Soc.* **1977**, *99*, 6099.
(247) Tafipolsky, M.; Scherer, W.; Öfele, K.; Artus, G.; Pedersen, B.; Herrmann, W. A.; McGrady, G. S. *J. Am. Chem. Soc.* **2002**, *124*, 5865.
(248) Frey, G. D.; Herdtweck, E.; Herrmann, W. A. *J. Organomet. Chem.* **2006**, *691*, 2465.
(249) Cook, D. J.; Hill, A. F. *Organometallics* **1997**, *16*, 5616.
(250) Kramarz, K. W.; Norton, J. R., Slow Proton-Transfer Reactions in Chemistry. In *Progress in Inorganic Chemistry*, Karlin, K. D., Ed. John Wiley & Sons: Hoboken, NJ, USA, 1994; Vol. 42, pp 1.
(251) Kersting, M.; Friebel, C.; Dehnicke, K.; Krestel, M.; Allmann, R. *Z. Anorg. Allg. Chem.* **1988**, *563*, 70.
(252) Herbowski, A.; Lis, T. *Polyhedron* **1985**, *4*, 127.
(253) Walker, B. J., *Organophosphorus Chemistry*. Penguin: Harmondsworth, England, 1972.
(254) Kim, H. P.; Angelici, R. J. *Organometallics* **1986**, *5*, 2489.

(255) Cook, D. J.; Hill, A. F. *Chem. Commun.* **1997**, 955.
(256) Ostermeier, J.; Hiller, W.; Kreissl, F. R. *J. Organomet. Chem.* **1995**, *491*, 283.
(257) Bermudez, M. D.; Brown, F. P. E.; Stone, F. G. A. *J. Chem. Soc., Dalton Trans.* **1988**, 1139.
(258) Bermudez, M. D.; Delgado, E.; Elliott, G. P.; Ngoc, H. T. H.; Mayor-Real, F.; Stone, F. G. A.; Winter, M. J. *J. Chem. Soc., Dalton Trans.* **1987**, 1235.
(259) Byers, P. K.; Carr, N.; Stone, F. G. A. *J. Chem. Soc., Dalton Trans.* **1990**, 3701.
(260) Carr, N.; Gimeno, M. C.; Goldberg, J. E.; Pilotti, M. U.; Stone, F. G. A.; Topaloglu, I. *J. Chem. Soc., Dalton Trans.* **1990**, 2253.
(261) Carriedo, G. A.; Howard, J. A. K.; Marsden, K.; Stone, F. G. A.; Woodward, P. *J. Chem. Soc., Dalton Trans.* **1984**, 1589.
(262) Carriedo, G. A.; Howard, J. A. K.; Stone, F. G. A. *J. Chem. Soc., Dalton Trans.* **1984**, 1555.
(263) Carriedo, G. A.; Howard, J. A. K.; Stone, F. G. A.; Went, M. J. *J. Chem. Soc., Dalton Trans.* **1984**, 2545.
(264) Delgado, E.; Hein, J.; Jeffery, J. C.; Ratermann, A. L.; Stone, F. G. A.; Farrugia, L. J. *J. Chem. Soc., Dalton Trans.* **1987**, 1191.
(265) Dossett, S. J.; Hill, A. F.; Jeffery, J. C.; Marken, F.; Sherwood, P.; Stone, F. G. A. *J. Chem. Soc., Dalton Trans.* **1988**, 2453.
(266) Etches, S. J.; Hart, I. J.; Stone, F. G. A. *J. Chem. Soc., Dalton Trans.* **1989**, 2281.
(267) Green, M.; Howard, J. A. K.; James, A. P.; Nunn, C. M.; Stone, F. G. A. *J. Chem. Soc., Dalton Trans.* **1987**, 61.
(268) Hoskins, S. V.; James, A. P.; Jeffery, J. C.; Stone, F. G. A. *J. Chem. Soc., Dalton Trans.* **1986**, 1709.
(269) Jeffery, J. C.; Marsden, C.; Stone, F. G. A. *J. Chem. Soc., Dalton Trans.* **1985**, 1315.
(270) Jeffery, J. C.; Ruiz, M. A.; Stone, F. G. A. *J. Chem. Soc., Dalton Trans.* **1988**, 1131.
(271) Berenguer, J. R.; Bernechea, M.; Forniés, J.; Gómez, J.; Lalinde, E. *Organometallics* **2002**, *21*, 2314.
(272) Jones, W. D.; Kuykendall, V. L. *Inorg. Chem.* **1991**, *30*, 2615.
(273) Paz-Michel, B. A.; González-Bravo, F. J.; Hernández-Muñoz, L. S.; Paz-Sandoval, M. A. *Organometallics* **2010**, *29*, 3709.
(274) Abad, J. A.; Delgado, E.; Garcia, M. E.; Grosse-Ophoff, M. J.; Hart, I. J.; Jeffery, J. C.; Simmons, M. S.; Stone, F. G. A. *J. Chem. Soc., Dalton Trans.* **1987**, 41.
(275) Strasser, C. E.; Cronje, S.; Raubenheimer, H. G. *New J. Chem.* **2010**, *34*, 458.
(276) Albano, V. G.; Busetto, L.; Cassani, M. C.; Sabatino, P.; Schmitz, A.; Zanotti, V. *J. Chem. Soc., Dalton Trans.* **1995**, 2087.
(277) Carriedo, G. A.; Riera, V.; Sanchez, G.; Solans, X. *J. Chem. Soc., Dalton Trans.* **1988**, 1957.
(278) Carriedo, G. A.; Riera, V.; Sanchez, G.; Solans, X.; Labrador, M. *J. Organomet. Chem.* **1990**, *391*, 431.
(279) Jeffery, J. C.; Jelliss, P. A.; Stone, F. G. A. *Organometallics* **1994**, *13*, 2651.
(280) Green, M.; Howard, J. A. K.; James, A. P.; Nunn, C. M.; Stone, F. G. A. *J. Chem. Soc., Chem. Commun.* **1984**, 1113.
(281) Clark, G. R.; Cochrane, C. M.; Roper, W. R.; Wright, L. J. *J. Organomet. Chem.* **1980**, *199*, C35.

(282) Schier, A.; Grohmann, A.; López-de-Luzuriaga, J. M.; Schmidbaur, H. *Inorg. Chem.* **2000**, *39*, 547.
(283) Schneider, D.; Schier, A.; Schmidbaur, H. *Dalton Trans.* **2004**, 1995.
(284) Kim, H. P.; Kim, S.; Jacobson, R. A.; Angelici, R. J. *J. Am. Chem. Soc.* **1986**, *108*, 5154.
(285) Bruno, I. J.; Cole, J. C.; Edgington, P. R.; Kessler, M.; Macrae, C. F.; McCabe, P.; Pearson, J.; Taylor, R. *Acta Cryst.* **2002**, *B58*, 389.
(286) Clark, G. R.; Cochrane, C. M.; Marsden, K.; Roper, W. R.; Wright, L. J. *J. Organomet. Chem.* **1986**, *315*, 211.
(287) Gill, D. S.; Green, M.; Marsden, K.; Moore, I.; Orpen, A. G.; Stone, F. G. A.; Williams, I. D.; Woodward, P. *J. Chem. Soc., Dalton Trans.* **1984**, 1343.
(288) Huy, N. H. T.; Donnadieu, B.; Bertrand, G.; Mathey, F. *Chem. Asian J.* **2009**, *4*, 1225.
(289) Antiñolo, A.; García-Yuste, S.; Otero, A.; Pérez-Flores, J. C.; Reguillo-Carmona, R.; Rodríguez, A. M.; Villaseñor, E. *Organometallics* **2006**, *25*, 1310.
(290) Hey, E.; Lappert, M. F.; Atwood, J. L.; Bott, S. G. *J. Chem. Soc., Chem. Commun.* **1987**, 421.
(291) Anderson, S.; Cook, D. J.; Hill, A. F. *Organometallics* **2001**, *20*, 2468.
(292) Mayr, A.; McDermott, G. A.; Dorries, A. M.; Holder, A. K.; Fultz, W. C.; Rheingold, A. L. *J. Am. Chem. Soc.* **1986**, *108*, 311.
(293) Lim, P. J.; Slizys, D. A.; White, J. M.; Young, C. G.; Tiekink, E. R. T. *Organometallics* **2003**, *22*, 4853.
(294) Aitken, R. A.; Dawson, G.; Keddie, N. S.; Kraus, H.; Slawin, A. M. Z.; Wheatley, J.; Woollins, J. D. *Chem. Commun.* **2009**, 7381.
(295) Adiwidjaja, G.; Günther, H.; Voß, J. *Liebigs Ann. Chem.* **1983**, *1983*, 1116.
(296) Clark, G. R.; Collins, T. J.; Marsden, K.; Roper, W. R. *J. Organomet. Chem.* **1978**, *157*, C23.
(297) Clark, G. R.; Collins, T. J.; Marsden, K.; Roper, W. R. *J. Organomet. Chem.* **1983**, *259*, 215.
(298) Rickard, C. E. F.; Roper, W. R.; Woodgate, S. D.; Wright, L. J. *J. Organomet. Chem.* **2001**, *623*, 109.
(299) Rickard, C. E. F.; Roper, W. R.; Woodgate, S. D.; Wright, L. J. *J. Organomet. Chem.* **2000**, *607*, 27.
(300) Cowley, A. R.; Hector, A. L.; Hill, A. F.; White, A. J. P.; Williams, D. J.; Wilton-Ely, J. D. E. T. *Organometallics* **2007**, *26*, 6114.
(301) Bedford, R. B.; Hill, A. F.; White, A. J. P.; Williams, D. J. *Angew. Chem., Int. Ed. Engl.* **1996**, *35*, 95.
(302) Drews, R.; Edelmann, F.; Behrens, U. *J. Organomet. Chem.* **1986**, *315*, 369.
(303) Ando, W.; Ohtaki, T.; Suzuki, T.; Kabe, Y. *J. Am. Chem. Soc.* **1991**, *113*, 7782.
(304) Zhu, C.; Li, S.; Luo, M.; Zhou, X.; Niu, Y.; Lin, M.; Zhu, J.; Cao, Z.; Lu, X.; Wen, T.; Xie, Z.; Schleyer, P. v. R.; Xia, H. *Nat. Chem.* **2013**, *5*, 698.
(305) Dalebrook, A. F.; Wright, L. J. *Organometallics* **2009**, *28*, 5536.
(306) Bartlett, P. D.; Meguerian, G. *J. Am. Chem. Soc.* **1956**, *78*, 3710.
(307) Lloyd, J. R.; Lowther, N.; Zsabo, G.; Hall, C. D. *J. Chem. Soc., Perkin Trans. 2* **1985**, 1813.
(308) Cook, D. J.; Hill, A. F. *Organometallics* **2003**, *22*, 3502.
(309) Kreissl, F. R.; Ullrich, N. *J. Organomet. Chem.* **1989**, *361*, C30.

(310) Caldwell, L. M.; Hill, A. F.; Willis, A. C. *Chem. Commun.* **2005**, 2615.
(311) Kimura, T.; Murai, T.; Mizuhata, N. *Heteroat. Chem.* **2005**, *16*, 185.
(312) Beckmann, U.; Süslüyan, D.; Kunz, P. C. *Phosphorus, Sulfur Silicon Relat. Elem.* **2011**, *186*, 2061.
(313) Quin, L. D., *A Guide to Organophosphorus Chemistry*. John Wiley and Sons: New York, USA, 2000.
(314) Wilke, G.; Schott, H.; Heimbach, P. *Angew. Chem., Int. Ed. Engl.* **1967**, *6*, 92.
(315) Li, Y.; Lu, L.-Q.; Das, S.; Pisiewicz, S.; Junge, K.; Beller, M. *J. Am. Chem. Soc.* **2012**, *134*, 18325.
(316) Moussa, S.; Aloui, F.; Hassine, B. B. *Synth. Commun.* **2013**, *43*, 268.
(317) Miller, A. D.; Johnson, S. A.; Tupper, K. A.; McBee, J. L.; Tilley, T. D. *Organometallics* **2009**, *28*, 1252.
(318) Hu, J.; Zhao, N.; Yang, B.; Wang, G.; Guo, L.-N.; Liang, Y.-M.; Yang, S.-D. *Chem. Eur. J.* **2011**, *17*, 5516.
(319) Michaelis, A. *Ber. Dtsch. Chem. Ges.* **1879**, *12*, 1009.
(320) Tanimoto, Y.; Ishizu, Y.; Kubo, K.; Miyoshi, K.; Mizuta, T. *J. Organomet. Chem.* **2012**, *713*, 80.
(321) Do, L. H.; Labinger, J. A.; Bercaw, J. E. *ACS Catal.* **2013**, *3*, 2582.
(322) Khiri-Meribout, N.; Bertrand, E.; Bayardon, J.; Eymin, M.-J.; Rousselin, Y.; Cattey, H.; Fortin, D.; Harvey, P. D.; Juge, S. *Organometallics* **2013**, *32*, 2827.
(323) Mueller, D.; Guenee, L.; Alexakis, A. *Eur. J. Org. Chem.* **2013**, *2013*, 6335.
(324) Zakharov, A. V.; Vishnevskiy, Y. V.; Allefeld, N.; Bader, J.; Kurscheid, B.; Steinhauer, S.; Hoge, B.; Neumann, B.; Stammler, H.-G.; Berger, R. J. F.; Mitzel, N. W. *Eur. J. Inorg. Chem.* **2013**, *2013*, 3392.
(325) Salomon, C.; Fortin, D.; Khiri, N.; Juge, S.; Harvey, P. D. *Eur. J. Inorg. Chem.* **2011**, 2597.
(326) Tay, M. Q. Y.; Lu, Y.; Ganguly, R.; Vidović, D. *Angew. Chem., Int. Ed.* **2013**, *52*, 3132.
(327) Marchenko, A. P.; Koidan, G. N.; Baram, G. O.; Chernega, A. N.; Pinchuk, A. M.; Romanenko, E. A. *Zh. Obshch. Khim.* **1994**, *64*, 913.
(328) Stadlbauer, S.; Frank, R.; Maulana, I.; Lönnecke, P.; Kirchner, B.; Hey-Hawkins, E. *Inorg. Chem.* **2009**, *48*, 6072.
(329) Baba, G.; Pilard, J.-F.; Tantaoui, K.; Gaumont, A.-C.; Denis, J.-M. *Tetrahedron Lett.* **1995**, *36*, 4421.
(330) Huang, C.; Tang, X.; Fu, H.; Jiang, Y.; Zhao, Y. *J. Org. Chem.* **2006**, *71*, 5020.
(331) Espinosa-Jalapa, N. Á.; Hernández-Ortega, S.; Le Goff, X.-F.; Morales-Morales, D.; Djukic, J.-P.; Le Lagadec, R. *Organometallics* **2013**, *32*, 2661.
(332) Kozlov, V. A.; Aleksanyan, D. V.; Nelyubina, Y. V.; Lyssenko, K. A.; Petrovskii, P. V.; Vasil'ev, A. A.; Odinets, I. L. *Organometallics* **2011**, *30*, 2920.
(333) Zang, Y.; Ojima, I. *J. Org. Chem.* **2013**, *78*, 4013.
(334) Jia, X.; Wang, Z.; Xia, C.; Ding, K. *Chem. Eur. J.* **2012**, *18*, 15288.
(335) Elma, D.; Durap, F.; Aydemir, M.; Baysal, A.; Meric, N.; Ak, B.; Turgut, Y.; Gümgüm, B. *J. Organomet. Chem.* **2013**, *729*, 46.
(336) Liang, L.-C.; Chien, P.-S.; Lee, P.-Y.; Lin, J.-M.; Huang, Y.-L. *Dalton Trans.* **2008**, 3320.
(337) Bedford, R. B.; Hazelwood, S. L.; Horton, P. N.; Hursthouse, M. B. *Dalton Trans.* **2003**, 4164.

(338) Neu, R. C.; Ouyang, E. Y.; Geier, S. J.; Zhao, X.; Ramos, A.; Stephan, D. W. *Dalton Trans.* **2010**, *39*, 4285.
(339) Peng, W.; Shreeve, J. n. M. *J. Fluorine Chem.* **2005**, *126*, 1054.
(340) Angerer, W.; Sheldrick, W. S.; Malisch, W. *Chem. Ber.* **1985**, *118*, 1261.
(341) Appel, R.; Schuhn, W.; Knoch, F. *Angew. Chem.* **1985**, *97*, 421.
(342) Maisch, R.; Barth, M.; Malisch, W. *J. Organomet. Chem.* **1984**, *260*, C35.
(343) Malisch, W.; Alsmann, R. *Angew. Chem.* **1976**, *88*, 809.
(344) Malisch, W.; Angerer, W.; Cowley, A. H.; Norman, N. C. *J. Chem. Soc., Chem. Commun.* **1985**, 1811.
(345) Malisch, W.; Maisch, R.; Colquhoun, I. J.; McFarlane, W. *J. Organomet. Chem.* **1981**, *220*, C1.
(346) Gröer, T.; Scheer, M. *Z. Anorg. Allg. Chem.* **2000**, *626*, 1211.
(347) Liu, Y.-Y.; Mar, A.; Rettig, S. J.; Storr, A.; Trotter, J. *Can. J. Chem.* **1988**, *66*, 1997.
(348) King, R. B. *Acc. Chem. Res.* **1970**, *3*, 417.
(349) Gladysz, J. A.; Williams, G. M.; Tam, W.; Johnson, D. L.; Parker, D. W.; Selover, J. C. *Inorg. Chem.* **1979**, *18*, 553.
(350) Ohishi, T.; Shiotani, Y.; Yamashita, M. *J. Org. Chem.* **1994**, *59*, 250.
(351) Sanchez-Nieves, J.; Sterenberg, B. T.; Udachin, K. A.; Carty, A. J. *J. Am. Chem. Soc.* **2003**, *125*, 2404.
(352) Dimroth, K. *Top. Curr. Chem.* **1973**, *38*, 1.
(353) Nakazawa, H. *J. Organomet. Chem.* **2000**, *611*, 349.
(354) Nakazawa, H. *Adv. Organomet. Chem.* **2004**, *50*, 107.
(355) Rosenberg, L. *Coord. Chem. Rev.* **2012**, *256*, 606.
(356) Cowley, A. H.; Kemp, R. A. *Chem. Rev.* **1985**, *85*, 367.
(357) Jayaraman, A.; Sterenberg, B. T. *Organometallics* **2013**, *32*, 745.
(358) Jayaraman, A.; Sterenberg, B. T. *Organometallics* **2014**, *33*, 522.
(359) Rajagopalan, R. A.; Jayaraman, A.; Sterenberg, B. T. *J. Organomet. Chem.* **2014**, *761*, 84.
(360) Rajagopalan, R. A.; Sterenberg, B. T. *Organometallics* **2011**, *30*, 2933.
(361) Sterenberg, B. T.; Udachin, K. A.; Carty, A. J. *Organometallics* **2001**, *20*, 2657.
(362) Sterenberg, B. T.; Udachin, K. A.; Carty, A. J. *Organometallics* **2003**, *22*, 3927.
(363) Vaheesar, K.; Bolton, T. M.; East, A. L. L.; Sterenberg, B. T. *Organometallics* **2010**, *29*, 484.
(364) Graham, T. W.; Cariou, R. P.-Y.; Sánchez-Nieves, J.; Allen, A. E.; Udachin, K. A.; Regragui, R.; Carty, A. J. *Organometallics* **2005**, *24*, 2023.
(365) Reed, R. W.; Xie, Z.; Reed, C. A. *Organometallics* **1995**, *14*, 5002.
(366) Schrödel, H.-P.; Schmidpeter, A.; Nöth, H. *Heteroat. Chem.* **1996**, *7*, 355.
(367) Wiacek, R. J.; Macdonald, C. L. B.; Jones, J. N.; Pietryga, J. M.; Cowley, A. H. *Chem. Commun.* **2003**, 430.
(368) Spinney, H. A.; Korobkov, I.; DiLabio, G. A.; Yap, G. P. A.; Richeson, D. S. *Organometallics* **2007**, *26*, 4972.
(369) Spinney, H. A.; Yap, G. P. A.; Korobkov, I.; DiLabio, G.; Richeson, D. S. *Organometallics* **2006**, *25*, 3541.
(370) Burford, N.; Ragogna, P. J.; McDonald, R.; Ferguson, M. J. *J. Am. Chem. Soc.* **2003**, *125*, 14404.

(371) Vaheesar, K.; Kuntz, C. M.; Sterenberg, B. T. *J. Organomet. Chem.* **2013**, *745–746*, 347.
(372) Brasch, N. E.; Hamilton, I. G.; Krenske, E. H.; Wild, S. B. *Organometallics* **2004**, *23*, 299.
(373) Conrad, E.; Burford, N.; McDonald, R.; Ferguson, M. J. *Inorg. Chem.* **2008**, *47*, 2952.
(374) Hockless, D. C. R.; McDonald, M. A.; Pabel, M.; Wild, S. B. *J. Organomet. Chem.* **1997**, *529*, 189.
(375) Fongers, K. S.; Hogeveen, H.; Kingma, R. F. *Tetrahedron Lett.* **1983**, *24*, 643.
(376) Breslow, R.; Deuring, L. A. *Tetrahedron Lett.* **1984**, *25*, 1345.
(377) Sterenberg, B. T.; Udachin, K. A.; Carty, A. J. *Organometallics* **2001**, *20*, 4463.
(378) Sterenberg, B. T.; Carty, A. J. *J. Organomet. Chem.* **2001**, *617-618*, 696.
(379) Gamble, A. S.; White, P. S.; Templeton, J. L. *Organometallics* **1991**, *10*, 693.
(380) Warner, S.; Lippard, S. J. *Organometallics* **1989**, *8*, 228.
(381) Vrtis, R. N.; Rao, C. P.; Warner, S.; Lippard, S. J. *J. Am. Chem. Soc.* **1988**, *110*, 2669.
(382) Ishii, Y.; Kawaguchi, M.; Hidai, M. *Chem. Lett.* **1995**, *24*, 983.
(383) Hughes, D. L.; Ibrahim, S. K.; Ali, H. M. d.; Pickett, C. J. *J. Chem. Soc., Chem. Commun.* **1994**, 425.
(384) Hughes, D. L.; Mohammed, M. Y.; Pickett, C. J. *J. Chem. Soc., Chem. Commun.* **1989**, 1399.
(385) Busacca, C. A.; Bartholomeyzik, T.; Cheekoori, S.; Raju, R.; Eriksson, M.; Kapadia, S.; Saha, A.; Zeng, X.; Senanayake, C. H. *Synlett* **2009**, *2*, 287.
(386) Frew, J. J. R.; Damian, K.; Van, R. H.; Slawin, A. M. Z.; Tooze, R. P.; Clarke, M. L. *Chem. Eur. J.* **2009**, *15*, 10504.
(387) Meiners, J.; Friedrich, A.; Herdtweck, E.; Schneider, S. *Organometallics* **2009**, *28*, 6331.
(388) Gaumont, A.-C.; Bourumeau, K.; Denis, J.-M.; Guenot, P. *J. Organomet. Chem.* **1994**, *484*, 9.
(389) Mercier, F.; Hugel-Le Goff, C.; Mathey, F. *Organometallics* **1988**, *7*, 955.
(390) Baccolini, G.; Boga, C.; Mazzacurati, M.; Sangirardi, F. *Org. Lett.* **2006**, *8*, 1677.
(391) Ito, S.; Miyake, H.; Yoshifuji, M. *ARKIVOC* **2012**, *ii*, 6.
(392) Ohff, M.; Holz, J.; Quirmbach, M.; Börner, A. *Synthesis* **1998**, *1998*, 1391.
(393) Vaughan, G. A.; Hillhouse, G. L.; Rheingold, A. L. *Organometallics* **1989**, *8*, 1760.
(394) Herd, O.; Hessler, A.; Hingst, M.; Machnitzki, P.; Tepper, M.; Stelzer, O. *Catal. Today* **1998**, *42*, 413.
(395) Schwan, A. L. *Chem. Soc. Rev.* **2004**, *33*, 218.
(396) Tappe, F. M. J.; Trepohl, V. T.; Oestreich, M. *Synthesis* **2010**, *2010*, 3037.
(397) Armitt, D. J.; Bruce, M. I.; Gaudio, M.; Zaitseva, N. N.; Skelton, B. W.; White, A. H.; Le, G. B.; Halet, J.-F.; Fox, M. A.; Roberts, R. L.; Hartl, F.; Low, P. J. *Dalton Trans.* **2008**, 6763.
(398) Bruce, M. I.; Cole, M. L.; Gaudio, M.; Skelton, B. W.; White, A. H. *J. Organomet. Chem.* **2006**, *691*, 4601.
(399) Niecke, E.; Rueger, R.; Gueth, W. *Z. Naturforsch. B* **1985**, *40B*, 1049.
(400) Xie, Z.-M.; Neilson, R. H. *Organometallics* **1983**, *2*, 921.
(401) O'Neal, H. R.; Neilson, R. H. *Inorg. Chem.* **1983**, *22*, 814.

(402) Duan, L.; Schnakenburg, G.; Daniels, J.; Streubel, R. *Eur. J. Inorg. Chem.* **2012**, *2012*, 2314.
(403) Grobe, J.; Le, V. D.; Martin, S.; Szameitat, J. *Z. Naturforsch. B* **1992**, *47*, 321.
(404) Cowley, A. H.; Gabbai, F.; Schluter, R.; Atwood, D. *J. Am. Chem. Soc.* **1992**, *114*, 3142.
(405) Mikhailine, A. A.; Lagaditis, P. O.; Sues, P. E.; Lough, A. J.; Morris, R. H. *J. Organomet. Chem.* **2010**, *695*, 1824.
(406) Landau, S. E.; Groh, K. E.; Lough, A. J.; Morris, R. H. *Inorg. Chem.* **2002**, *41*, 2995.
(407) Stone, K. C.; White, P. S.; Templeton, J. L. *J. Organomet. Chem.* **2003**, *684*, 13.
(408) Carvalho, M. F. N. N.; Duarte, M. T.; Galvão, A. M.; Pombeiro, A. J. L. *J. Organomet. Chem.* **1994**, *469*, 79.
(409) Shaver, A.; Hynes, R. C.; Trojansek, D. *J. Organomet. Chem.* **1994**, *483*, 1.
(410) Woodard, S. S.; Jacobson, R. A.; Angelici, R. J. *J. Organomet. Chem.* **1976**, *117*, C75.
(411) van der Knaap, T. A.; Klebach, T. C.; Visser, F.; Bickelhaupt, F.; Ros, P.; Baerends, E. J.; Stam, C. H.; Konijn, M. *Tetrahedron* **1984**, *40*, 765.
(412) Safronova, A. V.; Bochkarev, L. N.; Stolyarova, N. E.; Grigor'eva, I. K.; Malysheva, I. P.; Basova, G. V.; Fukin, G. K.; Kurskii, Y. A.; Khorshev, S. Y.; Abakumov, G. A. *Russ. Chem. Bull.* **2003**, *52*, 2140.
(413) Brym, M.; Jones, C.; Richards, A. F. *J. Chem. Soc., Dalton Trans.* **2002**, 2800.
(414) Brym, M.; Jones, C.; Waugh, M. *Dalton Trans.* **2003**, 2889.
(415) Brym, M.; Jones, C.; Wilton-Ely, J. D. E. T. *Inorg. Chem.* **2005**, *44*, 3275.
(416) Mathey, F.; Huy, N. H. T.; Marinetti, A. *Helv. Chim. Acta* **2001**, *84*, 2938.
(417) Aktaş, H.; Slootweg, J. C.; Lammertsma, K. *Angew. Chem., Int. Ed.* **2010**, *49*, 2102.
(418) Mathey, F.; Regitz, M., 2.1 - Three-membered Rings: 1. Phosphiranes and Phosphirenes. In *Phosphorus-Carbon Heterocyclic Chemistry*, Mathey, F., Ed. Elsevier Science Ltd: Oxford, 2001; pp 17.
(419) Weber, L. *Eur. J. Inorg. Chem.* **2007**, *2007*, 4095.
(420) Li, X.; Lei, D.; Chiang, M. Y.; Gaspar, P. P. *J. Am. Chem. Soc.* **1992**, *114*, 8526.
(421) Eisch, J. J.; Shafii, B.; Rheingold, A. L. *J. Am. Chem. Soc.* **1987**, *109*, 2526.
(422) Eisch, J. J.; Shafii, B.; Odom, J. D.; Rheingold, A. L. *J. Am. Chem. Soc.* **1990**, *112*, 1847.
(423) Borst, M. L. G.; Bulo, R. E.; Winkel, C. W.; Gibney, D. J.; Ehlers, A. W.; Schakel, M.; Lutz, M.; Spek, A. L.; Lammertsma, K. *J. Am. Chem. Soc.* **2005**, *127*, 5800.
(424) Duffy, M. P.; Mathey, F. *J. Am. Chem. Soc.* **2009**, *131*, 7534.
(425) Cambridge Structural Database: http://www.ccdc.cam.ac.uk (Cambridge Crystallographic Data Centre, 9/10/2014).
(426) Juaid, S. S. A.; Carmichael, D.; Hitchcock, P. B.; Marinetti, A.; Mathey, F.; Nixon, J. F. *J. Chem. Soc., Dalton Trans.* **1991**, 905.
(427) Schmidbaur, H.; Cronje, S.; Djordjevic, B.; Schuster, O. *Chem. Phys.* **2005**, *311*, 151.
(428) Schmidbaur, H. *Gold Bull.* **2000**, *33*, 3.
(429) Schraml, J.; Čapka, M.; Blechta, V. *Magn. Reson. Chem.* **1992**, *30*, 544.
(430) Trofimenko, S. *J. Am. Chem. Soc.* **1967**, *89*, 6288.
(431) Al-Sa'Ady, A. K.; McAuliffe, C. A.; Parish, R. V.; Sandbank, J. A.; Potts, R. A.; Schneider, W. F. *Inorg. Synth.* **1985**, *23*, 191.

(432) White, C.; Yates, A.; Maitlis, P. M.; Heinekey, D. M. *Inorg. Synth.* **1992**, *29*, 228.
(433) Hong, L.; Lin, W.; Zhang, F.; Liu, R.; Zhou, X. *Chem. Commun.* **2013**, *49*, 5589.
(434) Wang, Y.; Zhang, W.-X.; Wang, Z.; Xi, Z. *Angew. Chem., Int. Ed.* **2011**, *50*, 8122.
(435) Coulson, D. R.; Satek, L. C.; Grim, S. O. *Inorg. Synth.* **1990**, *28*, 107.
(436) van der Slot, S. C.; Duran, J.; Luten, J.; Kamer, P. C. J.; van Leeuwen, P. W. N. M. *Organometallics* **2002**, *21*, 3873.
(437) Kuroda, K.; Maruyama, Y.; Hayashi, Y.; Mukaiyama, T. *Bull. Chem. Soc. Jpn.* **2009**, *82*, 381.
(438) SDBSWeb: http://sdbs.riodb.aist.go.jp (National Institute of Advanced Industrial Science and Technology, 16/5/2014).

Appendix

Computational details

All computational works were performed by Dr Manab Sharma using the Gaussian 09 suite of programs.[1] The geometries of all complexes have been optimised at the DFT level of theory using the exchange functional of Becke[2] in conjunction with the correlation functional of Perdew[3,4] (BP86). The Stuttgart basis set in combination with the 60-core-electron relativistic effective core potential (SDD)[5,6] was used for W; 6-31G(d)[7] basis sets were used for all other atoms. This basis set combination is referred to as BS1. Frequency calculations were performed to confirm that optimised structures were minima or saddle points using the BP86/BS1 level of theory. Single-point energy calculations for all the optimised structures were carried out with a larger basis set (BS2). BS2 utilises the quadruple-ζ valence def2-QZVP[8] basis set on W along with the corresponding ECP and the 6-311+G(2d,p) basis set on other atoms. The solvation energies were calculated using BS2 on gas phase optimised geometries with the CPCM solvation model[9] using dichloromethane and acetonitrile as solvents. Single-point calculations were also carried out at the M06/BS2, B97D/BS2 and B3LYP/BS2 level of theories, and found to follow similar trends. For the ionic complexes, optimisations were also carried out in solvent (dichloromethane) medium.

References

(1) Frisch, M. J. *et al.* Gaussian 09, revision A.02; Gaussian, Inc.: Wallingford, CT, 2009.

(2) Becke, A. D. *Phys. Rev. A* **1988**, *38*, 3098.

(3) Perdew, J. P. *Phys. Rev. B* **1986**, *34*, 7406.

(4) Perdew, J. P. *Phys. Rev. B* **1986**, *33*, 8822.

(5) Kuechle, W.; Dolg, M.; Stoll, H.; Preuss, H. *J. Chem. Phys.* **1994**, *100*, 7535.

(6) Dolg, M.; Stoll, H.; Preuss, H.; Pitzer, R. M. *J. Phys. Chem.* **1993**, *97*, 5852.

(7) Hariharan, P. C.; Pople, J. A. *Theor. Chim. Acta* **1973**, *28*, 213.

(8) Weigend, F.; Furche, F.; Ahlrichs, R. *J. Chem. Phys.* **2003**, *119*, 12753.

(9) Barone, V.; Cossi, M. *J. Phys. Chem. A.* **1998**, *102*, 1995.

Numbered compounds

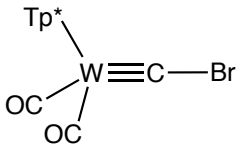

1

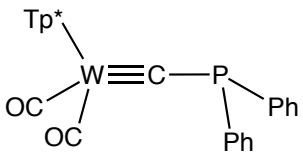

2

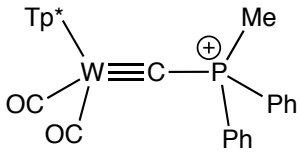

[3]⁺

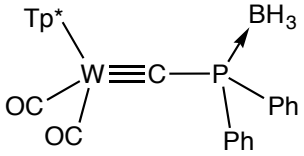

4

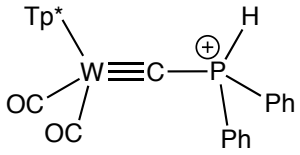

[5]⁺

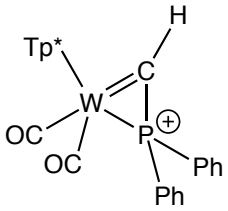

[6]⁺

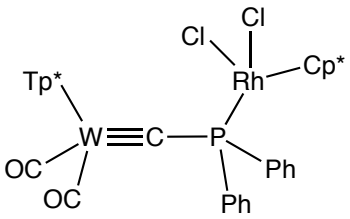

7

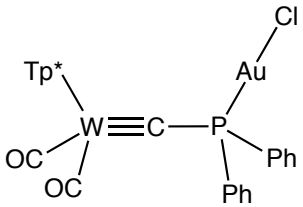

8

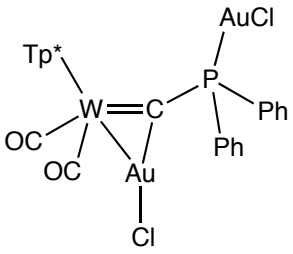

9

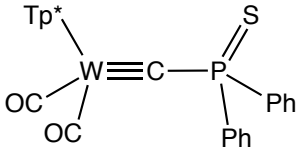

10

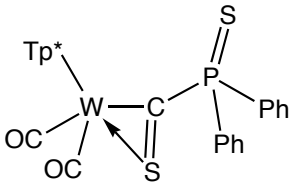

11

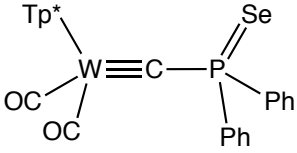

12

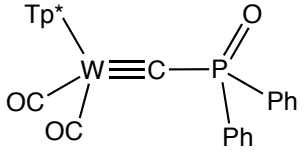

13

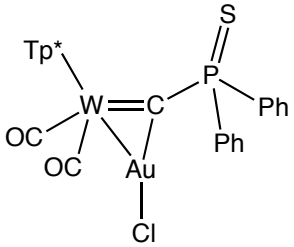

14

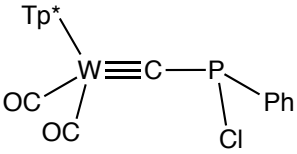

15

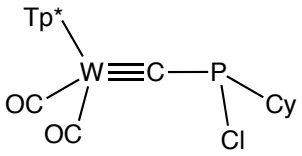

16

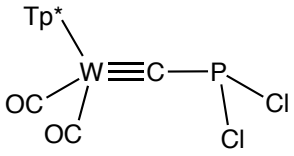

17

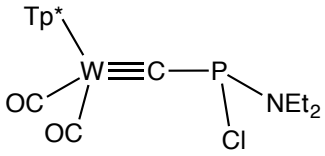

18

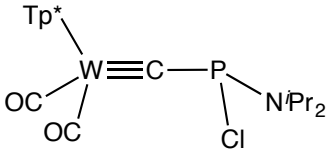

19

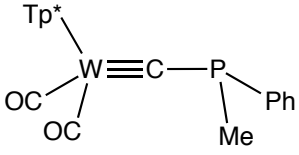

20

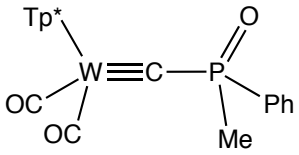

21

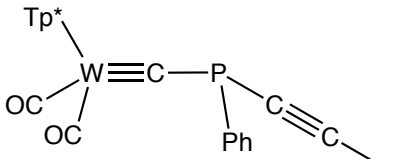

22

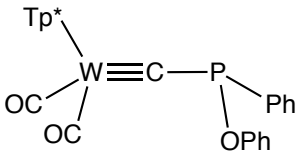

23

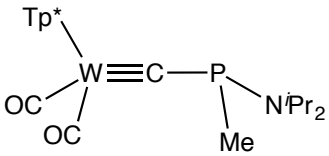

24

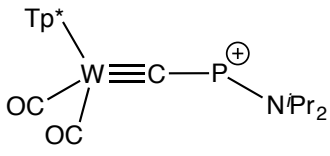

[25]⁺

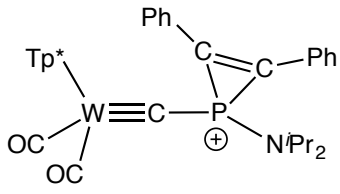

[26]⁺

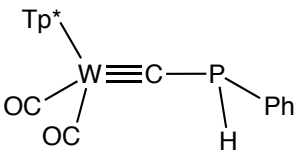

27

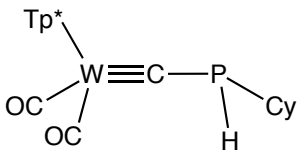

28

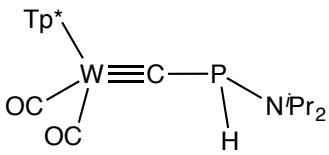

29

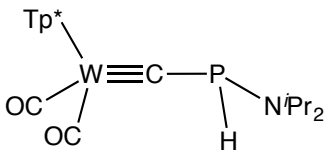

29

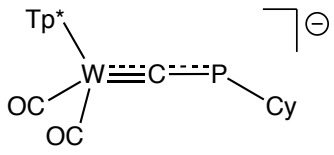

[31]⁻

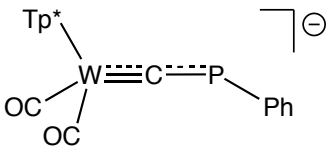

[32]⁻

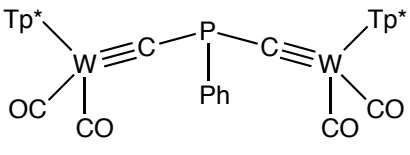

33

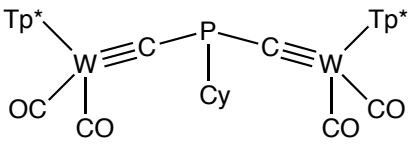

34

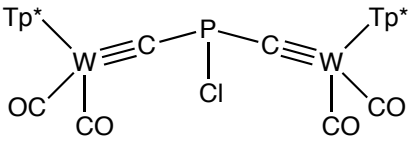

35

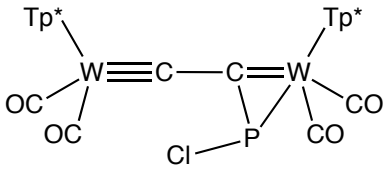

36

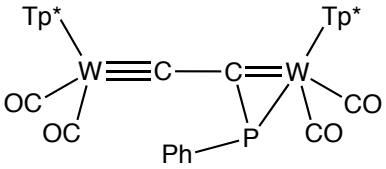

37

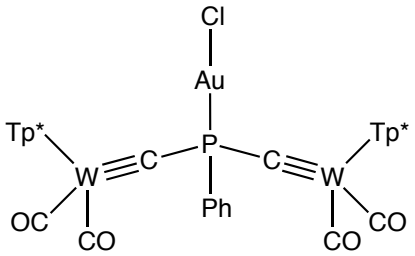

38

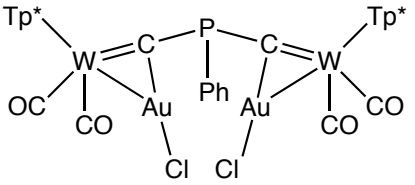

39

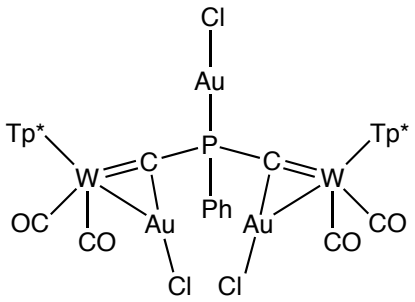

40

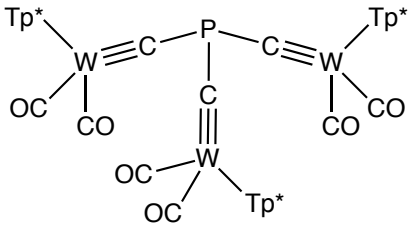

41